

University of Alberta
Department of Civil &
Environmental Engineering



Structural Engineering Report No. 63

A Classical Flexibility Analysis for Gentilly Type Containment Structures

by
D.W. Murray
A.M. Rohardt
and
S.H. Simmonds

June, 1977

University of Alberta
Department of Civil Engineering

A Classical Flexibility Analysis
for Gentilly Type Containment
Structures

by

D. W. Murray,
A. M. Rohardt,
S. H. Simmonds.

Faculty Investigators:

Professor J. G. MacGregor
Professor D. W. Murray
Professor S. H. Simmonds

A Technical Report to the
Atomic Energy Control Board
Nuclear Plant Licensing Directorate

P.O. Box 1046

Ottawa, Canada K1P 5S9

June 1977

Abstract

A computer program, called FLEXSHELL is developed for the analysis of thin shell structures, which consist of branched, axisymmetric segments of shells of revolution. The procedure follows the standard flexibility matrix approach and uses formulae obtained from simple classical elastic shell theory.

Solutions are presented for the stress resultants for a number of typical load conditions for a Gentilly type nuclear containment structure. These results are compared with those obtained from a stiffness analysis based on a numerical integration of an energy finite difference formulation (BOSOR4).

2725048

Acknowledgements

This report was sponsored by the Atomic Energy Control Board of Canada. The authors wish to acknowledge the cooperation of the following agencies which provided technical information for the study.

Atomic Energy of Canada, Limited.

Canatom Limited.

Hydro-Québec.

Ontario Hydro.

The interpretation of technical data and any opinions or conclusions arising in this report are those of the authors only and do not necessarily reflect those of the sponsor or the cooperating agencies.

Table of Contents

	PAGE
Title Page	
Abstract	ii
Acknowledgements	iii
Table of Contents	iv
List of Tables	vii
List of Figures	viii
Nomenclature	
<u>1. Introduction</u>	
1.1 Background to Report	1
1.2 Objective of Report	2
1.3 Structure of Report	4
<u>2. Theory and Organization of FLEXSHELL</u>	
2.1 Introduction	5
2.2 Identification of Variables and Constraint Equations	6
2.3 Matrix Formulation of Solution Procedure	11
2.4 Coding Strategy for Identifying Forces and Connectivity Requirements.	17
<u>3. Segment Response</u>	
3.1 Introduction	19
3.2 Short Cylinder Flexibility Matrix	21

	PAGE
3.3 Spherical Segment Flexibility Matrix	25
3.4 Short Plate in Elastic Foundation Flexibility Matrix	26
3.5 Particular Solutions	29
3.6 Coding Strategy for Assembly and Solution	30
<u>4. Example Applications of FLEXSHELL</u>	
4.1 Introduction to Applications	33
4.2 Analysis for Internal Pressure	34
4.3 Analysis for Prestressing Effects	35
<u>5. Comparison with BOSOR4 Analyses</u>	
5.1 Introduction to Comparison of Results	37
5.2 Comparison of FLEXSHELL and BOSOR4 Results	40
5.2.1 Comparison of Internal Pressure Stress Resultants	41
5.2.2 Comparison of Dead Load Stress Resultants	42
5.2.3 Comparison of Prestress Stress Resultants	43
5.2.4 Comparison of Thermal Effects	43
5.3 Effect of Foundation Modulus	44
5.4 Effect of 'Hinge' Detail	47
5.5 Reference State Rf1	47
<u>6. Stress Computations</u>	
6.1 Introduction to Stress Computations	49
6.2 Stress Plots	50
6.3 Check of Serviceability Conditions (Switched-On Analysis)	50
6.4 Check of Serviceability Conditions (Load Superposition Analysis)	52

	PAGE
<u>7. Summary and Conclusions</u>	
7.1 Summary	54
7.2 Limitations on FLEXSHELL	55
7.3 Conclusions	56
References	57
Tables	59
Figures	65
Appendix A: FLEXSHELL User's Manual	A1
Appendix B: Program Listing	B1
Appendix C: Data Files and Output for Typical Load Conditions	C1
Appendix D: Formulae for Homogeneous and Particular Solutions	D1
Appendix E: Derivation of Short Cylinder B Matrix	E1
Appendix F: Spherical Shell M_2 Stress Resultant	F1
Appendix G: Asymptotic Approximation for Base Segments	G1

List of Tables

TABLE	TITLE	PAGE
2.1	Segment Definition and Connectivity Arrays	59
3.1	Derivatives of Base Segment $\{\phi\}$ Vector	60
4.1	Computation of Prestress Loading	61
5.1	Influence of Foundation Subgrade Coefficient on Stress Resultants	62
6.1	Stresses in Dome Including Thickening	63
6.2	Pressure Factors in Dome Including Thickening	64
C.1	Index of Data Files	C1
D.1	Labeling of Homogeneous and Particular Solution Equations	D2
D.2	Spherical Segment Homogeneous Solutions	D4
D.3	Spherical Segment Particular Solutions	D5
D.4	Cylindrical Segment Particular Solutions	D6
D.5	Special Homogeneous Solutions	D7
D.6	Plate on Elastic Foundation Formulae	D8
E.1	Functions for Short Cylinder Displacements	E4

List of Figures

FIGURE	TITLE	PAGE
2.1	Typical Containment Structure	65
2.2	Sign Convention For Positive End Effects	66
3.1	Subscripting of Segment Arrays	67
4.1	Principle Dimensions of GENTILLY-2	68
4.2	Standard Model for FLEXSHELL GENTILLY-2 Analyses	69
4.3a&b	Details of Standard Model	70
4.3c	Details of Standard Model	71
4.4	Stress Resultant Sign Convention	72
4.5	Prestressing PSF Forces	73
5.1	N1 for Internal Pressure of 1 lb/ft ²	74
5.2	N2 for Internal Pressure of 1 lb/ft ²	75
5.3	M1 for Internal Pressure of 1 lb/ft ²	76
5.4	M2 for Internal Pressure of 1 lb/ft ²	77
5.5	Horizontal Cylinder Displacements for Internal Pressure of 1 lb/ft ²	78
5.6	N1 for Dead Load of 150 lb/ft ³	79
5.7	N2 for Dead Load of 150 lb/ft ³	80
5.8	M1 for Dead Load of 150 lb/ft ³	81
5.9	M2 for Dead Load of 150 lb/ft ³	82
5.10	Horizontal Cylinder Displacement for Dead Load of 150 lb/ft ³	83
5.11	N1 for Simplified Switched-on-Prestress	84
5.12	N2 for Simplified Switched-on-Prestress	85
5.13	M1 for Simplified Switched-on-Prestress	86
5.14	M2 for Simplified Switched-on-Prestress	87
5.15	Horizontal Cylinder Displacements for Simplified Switched-on-Prestress	88

	PAGE	
5.16	N1 for BOSOR4 Switched-on-Prestress	89
5.17	N2 for BOSOR4 Switched-on-Prestress	90
5.18	M1 for BOSOR4 Switched-on-Prestress	91
5.19	M2 for BOSOR4 Switched-on-Prestress	92
5.20	Horizontal Cylinder Displacements for BOSOR4 Switched-on-Prestress	93
5.21	N1 for Winter Operating Temperature (WOT)	94
5.22	N2 for Winter Operating Temperature (WOT)	95
5.23	M1 for Winter Operating Temperature (WOT)	96
5.24	M2 for Winter Operating Temperature (WOT)	97
5.25	Horizontal Cylinder Displacements for Winter Operating Temperature (WOT)	98
5.26	N2 for BOSOR4 Model and WOT	99
5.27	M1 for BOSOR4 Model and WOT	100
5.28	M2 for BOSOR4 Model and WOT	101
5.29	Horizontal Cylinder Displacements for BOSOR4 Model and WOT	102
5.30	Dead Load Base Deflections	103
5.31	Variations of Base Connection Detail	104
5.32	N2 for Dead Load for Various Base Connections	105
5.33	M1 for Dead Load for Various Base Connections	106
5.34	M2 for Dead Load for Various Base Connections	107
5.35	Horizontal Cylinder Displacements for Dead Load for Various Base Connections	108
5.36	N2 for Internal Pressure for Various Base Connections	109
5.37	M1 for Internal Pressure for Various Base Connections	110
5.38	M2 for Internal Pressure for Various Base Connections	111

	PAGE
5.39 Horizontal Cylinder Displacements for Internal Pressure for Various Base Connections	112
5.40 N1 for Reference State Rf1	113
5.41 N2 for Reference State Rf1	114
5.42 M1 for Reference State Rf1	115
5.43 M2 for Reference State Rf1	116
6.1 S1 for Internal Pressure of 18 psi	117
6.2 S2 for Internal Pressure of 18 psi	118
6.3 S1 for Switched-on Reference State	119
6.4 S2 for Switched-on Reference State	120
6.5 P1 for Switched-on Reference State	121
6.6 P1 in Ring Beam Area for Switched-on Reference State	122
6.7 P2 for Switched-on Reference State	123
6.8 S1 for Reference State Rf1	124
6.9 S2 for Reference State Rf1	125
6.10 P1 for Reference State Rf1	126
6.11 P1 in Ring Beam Area for Reference State Rf1	127
6.12 P2 for Reference State Rf1	128
D.1 Notation for Segment Equations	D1

1. INTRODUCTION

1.1 Background to Report

This report is the second technical report in a continuing program, sponsored by the Atomic Energy Control Board of Canada, to investigate the overpressure response of nuclear containment structures. The prototype building for the report is the Gentilly-2 Nuclear Power Station Reactor Building [1], which is considered to be representative of containment buildings to house 600 MW CANDU-PHW type nuclear reactors.

The first report in the series [6,7], entitled 'An Elastic Stress Analysis of a Gentilly Type Containment Structure', contains a description of the prototype building and describes the objectives of the overall study. It also contains the results of an extensive elastic load superposition study, which examines the effects of internal pressure, dead load, prestressing forces, shrinkage and temperature. An assessment of the relative significance of these effects (including the effects of the construction sequence) on the stress resultants predicted throughout the structure was reported.

The analyses in the first report were carried out by employing the BOSOR4 computer code [4,5]. This code is a versatile program, based on an energy finite-difference displacement model, which is generally available for distribution, and is specifically designed to handle complex problems in shells of revolution. However, a linear thin shell analysis of a Gentilly type structure should not require the use of such a complex code and the question arises as to whether satisfactory results could be obtained with a much simpler classical shell analysis.

1.2 Objective of Report

While the objective of the overall study is to assess the response of nuclear containment structures, subjected to internal overpressures up to the point of collapse, detailed design and analysis of the prototype buildings has generally been confined to estimating the elastic response under prescribed factored service load conditions. The analysis of the structure under service loading, which may consist of a number of load combinations of the influences itemized in Sect. 1, therefore plays an important role in the proportioning of the components of the structure which, in turn, influences its overpressure response. It is, therefore, pertinent to investigate simple methods of determining stress resultants which may be sufficiently accurate for design purposes, or preliminary design purposes, or which may serve to verify the validity of the design of important segments of a containment structure. It is also important to be aware of the limits of applicability of any simple analyses which may be employed.

The objective of this report is to develop a simple, but flexible, analytical capability for the elastic analysis of axisymmetric segmented shell containment structures, which can include all of the significant static loading effects which may influence the stress resultants in such structures under service load and design basis accident conditions.

The approach is to use simple idealized classical shell theory, in the context of a matrix flexibility analysis, and to solve for the redundants which establish compatibility at the junctions between shell segments. Once the redundants have been determined, the stress resultants

throughout the shell segments may be determined from the closed form solutions available in the literature.

It was originally anticipated that a simple set of compatibility equations could be set up for a manual solution of the problem. However, in view of the fact that even a 'clean' containment building, such as Gentilly-2, contains six to twelve different shell segments, it was decided to produce a small computer code to perform the analyses. This report discusses the background, development and application of the code, designated as FLEXSHELL, and compares the results obtained from it with similar results obtained from the BOSOR4 analyses of Refs. 6 and 7.

The advantages of the approach are:

- (a) A simple classical shell program, devised to handle all significant load cases, contains approximately 1200 source statements which is about an order of magnitude less than general purpose shell programs. It can, therefore, be used on office mini-computers without difficulty.
- (b) The input to such a program is simple and can be readily understood by engineers who have no specialized knowledge of computer technology.
- (c) Such classical solutions can serve as benchmark solutions to which other solutions can be compared. Since most shell programs, such as BOSOR4, are based on the Love-Kirchhoff hypothesis, and the geometry of the principal shell segments under consideration is such that they may be classified as 'thin', the results of simple classical shell theory may be as acceptable for design and evaluation purposes as those

obtained from more complex analyses.

Factors such as stress concentrations at points of geometric discontinuity, and departures from axial symmetry cannot, of course, be accounted for by either of the approaches under consideration.

1.3 Structure of Report

Chapter 1 has described the objective and background for this report. Chapter 2 considers the theory and organization of the FLEXSHELL program. Chapter 3 considers the formulation and solution of equations for individual shell segments. Chapter 4 consists of a description of the input and output for some simple problems. A comparison of results to those of BOSOR4 for some important load cases is contained in Chapter 5. Chapter 6 introduces a set of stress plots and pressure factor plots which permit an examination of serviceability limit states. Chapter 7 contains a brief summary and conclusions. Detailed derivations, the program listing, user's manual and input data, together with a summary of formulae are contained in the Appendices.

2. THEORY AND ORGANIZATION OF FLEXSHELL

2.1 Introduction

Classical flexibility analysis of shell structures follows the following pattern:

- (a) A 'particular solution' for the membrane stresses in the shell, which will equilibrate the applied loading, is determined. This 'membrane solution' does not contain any bending moments.
- (b) The displacements at the boundaries (i.e. edges) of the shell, consistent with the particular solution, are computed.
- (c) Known boundary forces are applied to each shell segment and the boundary displacements associated with these edge forces are computed. These solutions, referred to as 'homogeneous solutions', necessarily require the inclusion of bending deformations.
- (d) Step (c) permits compatibility equations to be established in terms of unknown boundary forces (i.e. redundants) to express the requirements that the displacements of the boundaries of adjacent shells must coincide at the junctions between shell segments (i.e. to eliminate the incompatibility of the particular solution displacements computed in step (b)).
- (e) The compatibility equations are solved to determine the redundant boundary forces.
- (f) The final solution is obtained for each segment from the superposition of the particular solution from step (a) and the effects of the redundant boundary forces from step (e).

The membrane solutions of step (a) and the boundary force solutions of step (c) are generally available in the literature [2,3,8-12], although usually in a rather disjointed form. Thus the primary problems in constructing a computer code for the flexibility analysis of shell structures are:

- (i) to devise a scheme to automate the assembly and solution of the compatibility equations, and
- (ii) to find in the literature the appropriate solutions to deal with the variety of load conditions required.

This Chapter addresses the first problem itemized above, i.e. it describes the basis for the FLEXSHELL code from a point of view of assembly and solution of equations. The particular and homogeneous solutions, and the element flexibility matrices, required in the solution are presented in Chapter 3.

2.2 Identification of Variables and Constraint Equations

The formulation of the problem and organization of the code can best be explained by example. A sketch of a typical containment structure is shown in Fig. 2.1(a). The structure can be considered to be made up of a number of segments as shown. These segments may be classified as (a) spherical (b) cylindrical or (c) base segments. Each segment may be considered to have a 'top' and a 'bottom'. These terms are defined with reference to a coordinate starting at the line of symmetry at the apex of the structure and traversing the centerline of the shell in a clockwise sense until again reaching the symmetry line at the base of the structure. A coordinate for branches that do

not fall on this primary circuit may be defined in the same manner, starting at the free edge, and increasing in the same sense as the main circuit coordinate at the junction point with the main circuit. The 'top' of a segment may then be defined as that boundary of the segment with the lowest coordinate.

It can be seen from Fig. 2.1(a) that, with the above definitions, the 'bottom' of a segment is always supported by the 'top' of an adjacent segment, except for the last segment in the primary circuit. The segments may now be numbered sequentially in such a way that any segment always has a higher number than any of the segments which it supports. The structure may then be separated into its component segments as shown in Fig. 2.1(b). In carrying out this separation the forces representing the interaction between the segments may be identified. Only those forces which will produce deformations restoring compatibility of deformations between adjacent segments need be identified. In general there will be two forces acting on each segment, at each junction between segments, which will contribute to these deformations, namely, a horizontal force and a moment. These have been designated in Fig. 2.1(b) as V_1^j and M_1^j at the top of segment j , and V_2^j and M_2^j at the bottom of segment j . (The base will be ignored throughout the remainder of this Chapter since it complicates the description without contributing conceptually to the arguments. Hence one may consider the last segment in Fig. 1 to be segment 7).

A displacement may be associated with each of the intersegment forces identified above. These are also shown in Fig. 2.1(b). For each V_i^j the corresponding displacement is designated as Δ_i^j , and for each M_i^j

the corresponding displacement (a rotation) is designated as θ_i^j . The forces V_i^j and M_i^j denote stress resultants per unit of width, while the associated displacements Δ_i^j and θ_i^j denote the corresponding displacements produced by these forces.

The requirements for compatible displacements, down to segment 7, may be written as

$$t_{\Delta_2}^1 - t_{\Delta_1}^3 = 0 \quad (2.2.1a)$$

$$t_{\theta_2}^1 - t_{\theta_1}^3 = 0 \quad (2.2.1b)$$

$$t_{\Delta_2}^2 - t_{\Delta_1}^3 = 0 \quad (2.2.1c)$$

$$t_{\theta_2}^2 - t_{\theta_1}^3 = 0 \quad (2.2.1d)$$

$$t_{\Delta_2}^4 - t_{\Delta_1}^5 = 0 \quad (2.2.1e)$$

$$t_{\theta_2}^4 - t_{\theta_1}^5 = 0 \quad (2.2.1f)$$

$$t_{\Delta_2}^5 - t_{\Delta_1}^6 = 0 \quad (2.2.1g)$$

$$t_{\theta_2}^5 - t_{\theta_1}^6 = 0 \quad (2.2.1h)$$

$$t_{\Delta_2}^3 - t_{\Delta_1}^6 = 0 \quad (2.2.1i)$$

$$t_{\theta_2}^3 - t_{\theta_1}^6 = 0 \quad (2.2.1j)$$

$$t^{\Delta_2^6} - t^{\Delta_1^7} = 0 \quad (2.2.1k)$$

$$t^{\theta_2^6} - t^{\theta_1^7} = 0 \quad (2.2.1l)$$

The leading subscript 't' in these equations denotes that the compatibility requirement is imposed on the total displacements. In general, when this subscript is omitted, the displacements referred to will be those produced by the edge forces, V_i^j and M_i^j .

Equilibrium equations may be written at each junction point. For this purpose it is important to recognize that the centerline of each segment may terminate at a different distance from the axis of symmetry. Let R_i^j denote the horizontal distance from the axis of symmetry to the terminal point of the centerline of segment j at end i as shown in Fig. 2.2. Equilibrium equations must be written at a specifically designated junction point. Since all segments at a junction may not end at the same point, a horizontal eccentricity may be defined to the junction point at each end of each segment. Let this eccentricity at end i of segment j be denoted by E_i^j , as shown in Fig. 2.2.

It is now necessary to introduce an explicit sign convention which has been only implied to this point. The sign convention is illustrated in Fig. 2.2, and consistently follows the following rules:

- (a) The origin of the local centerline coordinate is at the top end of the segment.
- (b) Positive displacements, w , are normal to the segment coordinate and are in a positive sense towards the central axis.
- (c) End forces, end displacements and eccentricities, except for the base segment, are horizontal, and positive in the direction

of the central axis.

- (d) End moments and rotations are positive in a clockwise sense.
- (e) End forces are always referred to a unit width of the shell segment at the end of the segment (i.e. at a distance R_i^j from the central axis).
- (f) For the base segment, positive vertical displacements are downward whereas positive eccentricities are upward.

With these conventions the equilibrium equations at the junction of the segments in Fig. 2.1, down to segment 7, may be written as follows (note that the superscripts are not powers):

$$R_2^1 V_2^1 + R_2^2 V_2^2 + R_1^3 V_1^3 = 0 \quad (2.2.2a)$$

$$R_2^1 M_2^1 + P_2^1 E_2^1 R_2^1 + R_2^2 M_2^2 + P_2^2 E_2^2 R_2^2 + R_1^3 M_1^3 + P_1^3 E_1^3 R_1^3 = 0 \quad (2.2.2b)$$

$$R_2^4 V_2^4 + R_1^5 V_1^5 = 0 \quad (2.2.2c)$$

$$R_2^4 M_2^4 + T_2^4 P_2^4 E_2^4 + R_1^5 M_1^5 + R_1^5 P_1^5 E_1^5 = 0 \quad (2.2.2d)$$

$$R_2^3 V_2^3 + R_2^5 V_2^5 + R_1^6 V_1^6 = 0 \quad (2.2.2e)$$

$$R_2^3 M_2^3 + R_2^3 P_2^3 E_2^3 + R_2^5 M_2^5 + R_2^5 E_2^5 P_2^5 + R_1^6 M_1^6 + R_1^6 E_1^6 P_1^6 = 0 \quad (2.2.2f)$$

$$R_2^6 V_2^6 + R_1^7 V_1^7 = 0 \quad (2.2.2g)$$

$$R_2^6 M_2^6 + R_2^6 E_2^6 P_2^6 + R_2^7 M_2^7 + R_2^7 E_2^7 P_2^7 = 0 \quad (2.2.2h)$$

The portion of the problem in Fig. 2.1 that is described by

Eqs. 2.2.2 contains 20 unknown segment forces, namely, $\langle V_2^1, M_2^1, V_2^2, M_2^2, V_1^3, M_1^3, V_2^4, M_2^4, V_1^5, M_1^5, V_2^5, M_2^5, V_2^3, M_2^3, V_1^6, M_1^6, V_2^6, M_2^6, V_1^7, M_1^7 \rangle$.

However, Eqs. 2.2.2 are eight equilibrium equations expressing constraints between these unknown forces. Hence, there are only twelve (20-8=12) independent forces. These twelve 'redundant' forces may be determined from twelve compatibility equations (Eqs. 2.2.1) which become the governing equations for a flexibility analysis. In the discussion that follows, n_f will denote the number of unknown segment end forces, n_e the numbers of equilibrium equations, n_c the number of compatibility equations, and n_r the number of redundants. Note that, in all cases,

$$n_r = n_c = n_f - n_e \quad (2.2.3)$$

2.3 Matrix Formulation of Solution Procedure

It is assumed that it is possible to form segment flexibility matrices, relating the end forces identified in Fig. 2.1 to the corresponding end displacements which these forces produce. Thus for segment 3 it is possible to write

$$\begin{Bmatrix} \Delta_1^3 \\ \theta_1^3 \\ \Delta_2^3 \\ \theta_2^3 \end{Bmatrix} = [F]_3 \begin{Bmatrix} V_1^3 \\ M_1^3 \\ V_2^3 \\ M_2^3 \end{Bmatrix} \quad (2.3.1)$$

where $[F]_3$ is the flexibility matrix of segment 3. The construction of segment flexibility matrices will be considered in Chapter 3 and need

not concern us now. The force induced displacements of all segments may be assembled into a vector $\{\Delta\}$ and written collectively in the matrix equation

$$\{\Delta\} = [F] \{V\} \quad (2.3.2)$$

where $\langle\Delta\rangle$ and $\langle V\rangle$ are the assembled vectors

$$\begin{aligned} \langle\Delta\rangle = & \langle \Delta_2^1 \ \theta_2^1 \ \Delta_2^2 \ \theta_2^2 \ \Delta_1^3 \ \theta_1^3 \ \Delta_2^3 \ \theta_2^3 \ \Delta_2^4 \ \theta_2^4 \ \Delta_1^5 \ \theta_1^5 \ \Delta_2^5 \ \theta_2^5 \\ & \Delta_1^6 \ \theta_1^6 \ \Delta_2^6 \ \theta_2^6 \ \Delta_1^7 \ \theta_1^7 \rangle \end{aligned} \quad (2.3.3a)$$

$$\begin{aligned} \langle V\rangle = & \langle V_2^1 \ M_2^1 \ V_2^2 \ M_2^2 \ V_1^3 \ M_1^3 \ V_2^3 \ M_2^3 \ V_2^4 \ M_2^4 \ V_1^5 \ M_1^5 \ V_2^5 \ M_2^5 \\ & V_1^6 \ M_1^6 \ V_2^6 \ M_2^6 \ V_2^7 \ M_2^7 \rangle \end{aligned} \quad (2.3.3b)$$

and $[F]$ is a global matrix with segment flexibility matrices assembled down the main diagonal

$$[F] = \text{diag} [F_1, F_2, \dots, F_7] \quad (2.3.3c)$$

Eq. 2.3.2 does not, however, express the total displacements of the segment ends, since these will be also influenced by the primary loading effects on the structure. The displacements produced by primary loads on the structure will be denoted as δ_i^j and $\bar{\theta}_i^j$, with the same subscript notation as applicable to Δ_i^j and θ_i^j . The primary displacements arising from particular solutions for the shell in response to the primary

$$[A] \{\Delta\} + [A] \{\delta\} = \{0\} \quad (2.3.6a)$$

which, upon making use of Eq. 2.3.2 becomes

$$[A] [F] \{V\} = -[A] \{\delta\} \quad (2.3.6b)$$

While Eqs. 2.3.6 represent the compatibility requirements, it is not yet possible to determine the unknown forces $\{V\}$ since there are n_f unknown forces and only $n_r = n_c$ equations.

There is a general theorem of structural analysis that states that if a set of forces $\{V\}$ is associated with a set of displacements $\{v\}$, and if, in another coordinate system, the same set of forces may be described as $\{U\}$ and their associated displacements as $\{u\}$, then the work done by equivalent sets of forces in the two systems must be identical when undergoing equivalent displacements. That is,

$$\langle u \rangle \{U\} = \langle v \rangle \{V\} \quad (2.3.7)$$

If the leading subscript (t) is omitted, the left hand sides of Eqs. 2.2.1 may be considered to define a set of relative displacements $\{q\}$ in terms of the end displacements $\{\Delta\}$, such that

$$\{q\} = [A] \{\Delta\} \quad (2.3.8)$$

The forces associated with $\{\Delta\}$ are the forces $\{V\}$. Therefore the (redundant) forces $\{Q\}$ associated with the relative displacements $\{q\}$ may be determined by making use of Eq. 2.3.7 in the form

$$\langle q \rangle \{Q\} = \langle \Delta \rangle \{V\} \quad (2.3.9a)$$

Substituting for $\langle q \rangle$ from Eq. 2.3.8 yields

$$\langle \Delta \rangle \{[A]^T \{Q\} - \{V\}\} = 0 \quad (2.3.9b)$$

and since this must be true for all $\langle \Delta \rangle$, Eq. 2.3.9b implies that

$$\{V\} = [A]^T \{Q\} \quad (2.3.10)$$

Eq. 2.3.10 is the force transformation consistent with the displacement transformation expressed by Eq. 2.3.8.

Substituting Eq. 2.3.10 into Eq. 2.3.6b yields

$$[A] [F] [A]^T \{Q\} = -[A] \{\delta\} \quad (2.3.11)$$

which can be written as

$$[\hat{F}] \{Q\} = \{q_0\} \quad (2.3.12)$$

where the matrices are defined by identifying corresponding terms between the last two equations.

Eq. 2.3.12 can be solved for the redundant forces $\{Q\}$ that are necessary to restore the lack of compatibility expressed by the relative displacements $\{q_0\}$.

The procedure for a flexibility analysis of a Gentilly type structure may now be described as follows:

- (1) Identify the number of segments and the unknown segment forces $\{V\}$.
- (2) Establish the connectivity matrix $[A]$ of Eqs. 2.3.5.
- (3) Compute the displacements of each segment arising from the particular solution for the segment, assemble them into the vector $\{\delta\}$, and determine the relative displacement vector $\{q_0\}$, of Eq. 2.3.12, from the relation

$$\{q_0\} = -[A] \{\delta\} \quad (2.3.13)$$

- (4) Evaluate the flexibility matrix of each segment, and assemble it into the diagonal flexibility matrix $[F]$ of Eq. 2.3.3c. Compute the structure flexibility matrix $[\hat{F}]$ of Eq. 2.3.12 from the relation

$$[\hat{F}] = [A] [F] [A]^T \quad (2.3.14)$$

- (5) Solve Eq. 2.3.12 for the redundants, $\{Q\}$, and recover the segment end forces, $\{V\}$, that are necessary to restore compatibility, from Eq. 2.3.10.
- (6) Superimpose the stress resultants arising from $\{V\}$ on those associated with the particular solution.

The above procedure has been implemented in the FLEXSHELL program which forms the basis of this report. It should be noted that, with this procedure, explicit use of Eqs. 2.2.2 is not required, nor is

it necessary to physically interpret the meaning of the redundant forces {Q}. The next Section describes the strategy of implementation for this analytical procedure.

2.4 Coding Strategy for Identifying Forces and Connectivity Requirements

One strategy of automating the procedure described in Sect. 2.3 is as follows. Number the segments as described in Sect. 2.1. Associate with each end of each segment a flag which indicates whether the end is attached to another segment. This input information is shown in Table 2.1a, where a segment type of 1 indicates it is spherical, a segment type of 2 indicates it is cylindrical, and 0 and 1 indicate the absence or presence of a connection, respectively, at the top and bottom of the segment as indicated by IR and JR, respectively. The eccentricities are also specified for internal use in the program. It is a matter of simple coding to have the program number the segment end forces as shown in Table 2.1b, which orders the end forces of Fig. 2.1b for assembly into the vector { Δ } of Sect. 2.3.

The segment connectivities are then specified as indicated in Table 1c. Note that the 'top segments' are arranged in order, each segment appearing precisely once. The 'bottom segment' is the segment to which the top segment is attached. Note that the bottom end of a top segment must always connect to the top end of a bottom segment.

The information in Tables 1a and 1c is all that the user must supply in order for the program to identify the end forces and establish the [A] matrix of Sect. 2.3. It is necessary, of course, to also supply information on the geometric and material properties of the segment, and on the type and magnitude of the loads. Details of the requirements for

this input data may be found in Appendix A - FLEXSHELL User's Manual and examples are given in Chapter 4. The only point of significance that may be of interest at this stage is that only one type of loading effect may be treated at a time (e.g. - pressure load, dead load or thermal load), the final results for a load combination being determined by a separate superposition program.

3. SEGMENT RESPONSE

3.1 Introduction

The analysis described in Chapter 2 assumes that segment flexibilities $[F]_i$, as required in Eq. 2.3.1, are available to establish the matrix $[F]$ of Eq. 2.3.3c. It also assumes that particular solution displacements $\{\delta\}$, as required in Eq. 2.3.4, can be evaluated and that the particular solution stress resultants and edge force stress resultants can be determined throughout the segment for the final superposition as required in step (6) of the procedure described in Sect. 2.3.

Although there are many reference books on shell analysis available [2,3,8-12] none of these contains all of the formulae necessary to evaluate the above quantities for the type of structure under consideration. In most shell applications the effect of end forces dies out exponentially with the distance from the end of the shell. Most classical flexibility shell analyses make use of this fact by assuming that the shell is 'long', in which case the forces applied at one end of the shell segment produce negligible displacement effects at the other end of the segment. Under these conditions the off-diagonal submatrices in the segment flexibility matrices reduce to zero and there is no coupling between ends. That is, the segment flexibilities take the form

$$[F]_i = \begin{bmatrix} F_{11} & 0 \\ 0 & F_{22} \end{bmatrix}_i \quad (3.1.1)$$

where $[F]_i$ is a 4x4 matrix, while $[F]_{11}$ and $[F]_{22}$ are 2x2 matrices. It

is quite apparent, however, that for the short cylindrical segments of the idealization shown in Fig. 2.1, this assumption is unwarranted [Ref. 9, pg. 318]. Hence, the investigators have derived a short cylindrical shell flexibility matrix (which, to the authors' knowledge, is not available in the literature). The development of this matrix is described in Sect. 3.2.

For spherical segments the authors have formed a flexibility matrix extracted from the classical shell theory literature. This matrix is described in Sect. 3.3. Because of the limitations on the classical shell solution it is required that the angle subtended by the spherical segment be greater than 20° [2, pg. 76; 8, pg. 341] in order for these equations to be reasonably valid. This means that FLEXSHELL cannot treat an extension of the lower dome on the inside of ring beam 4 (Fig. 2.1a) as a spherical segment because it does not, at this time, have a proper formulation for the flexibility of such an element. The desirability of formulating such a segment flexibility matrix can best be assessed by the sponsoring body, after an assessment of what role a FLEXSHELL type of analysis may be expected to play in future design or regulatory functions associated with containment structures.

A short 'plate on elastic foundation' flexibility matrix is derived, in a manner similar to that for a short cylinder segment, in Sect. 3.4 on the basis of asymptotic solutions to the classical equations. This short plate foundation matrix is only accurate for equivalent radii which are relatively large. However, for the range of arguments encountered in Gentilly type structures it appears to be extremely effective.

The particular solutions required for the evaluation of $\{\delta\}$ are discussed in Sect. 3.5, while the coding strategy for handling flexibility matrices, and transfer of forces is discussed in Sect. 3.6.

3.2 Short Cylinder Flexibility Matrix

The flexibility matrix for the short axisymmetric cylindrical segment implemented in FLEXSHELL is based on the governing differential equation which may be written as [Ref. 3, page 91]

$$\frac{d^4 w}{dy^4} + 4 \beta^4 w = \frac{p_z}{D} \quad (3.2.1)$$

where w is the inward radial displacement; y is the cylinder centerline coordinate; p_z is the radial inward pressure; D is the flexural stiffness of the segment and β is a parameter of the segment properties.

The flexural stiffness of the cylindrical shell segment D , is defined by the expression

$$D = \frac{E}{1 - \nu^2} \frac{t^3}{12} \quad (3.2.2)$$

where E is the elastic modulus, ν is Poisson's ratio and t is the thickness of the segment. The parameter β is defined as

$$\beta^4 = \frac{3(1 - \nu^2)}{r^2 t^2} \quad (3.2.3)$$

where r is the centerline radius of the cylinder.

The solution to the homogeneous form of Eq. 3.2.1 is [Ref. 3, pg. 91]

$$w = e^{\beta y} (C_1 \cos \beta y + C_2 \sin \beta y) + e^{-\beta y} (C_3 \cos \beta y + C_4 \sin \beta y) \quad (3.2.4)$$

The meridional moment and radial shear in the wall may be expressed in terms of derivatives of the displacement w in the form [Ref. 3, pg. 93]

$$M = +D \frac{d^2 w}{dy^2} \quad (3.2.5)$$

and

$$Q = -D \frac{d^3 w}{dy^3} \quad (3.2.6)$$

where moment is positive when it produces compression on the inside of the cylinder and shear is positive acting radially inward on the bottom of the element.

Let us write Eq. 3.2.4 as the vector product

$$w = \langle \phi(y) \rangle \{c\} \quad (3.2.7a)$$

in which

$$\langle \phi(y) \rangle = \langle e^{\beta y} \cos \beta y, e^{\beta y} \sin \beta y, e^{-\beta y} \cos \beta y, \quad (3.2.7b)$$

$$e^{-\beta y} \sin \beta y \rangle$$

and

$$\langle c \rangle = \langle c_1 \quad c_2 \quad c_3 \quad c_4 \rangle \quad (3.2.7c)$$

Evaluating the stress resultants at the ends of the segment, illustrated in Fig. 2.2(b), by making use of Eqs. 3.2.5 and 3.2.6

$$\begin{Bmatrix} V_1 \\ M_1 \\ V_2 \\ M_2 \end{Bmatrix}^j = D \begin{bmatrix} +\langle \phi''''(0) \rangle \\ -\langle \phi''(0) \rangle \\ -\langle \phi''''(\ell) \rangle \\ +\langle \phi''(\ell) \rangle \end{bmatrix} \{c\}^j \quad (3.2.8)$$

where ' indicates d/dy and j is the segment number. Upon evaluating the derivatives of $\langle \phi \rangle$ indicated in Eq. 3.2.8, the vector of coefficients $\{c\}$ can be determined in terms of the end force vector by inverting the matrix in Eq. 3.2.8. Let the inverse of this matrix be designated as $[B]$. Then we may write

$$\{c\}^j = [B] \begin{Bmatrix} V_1 \\ M_1 \\ V_2 \\ M_2 \end{Bmatrix}^j \quad (3.2.9)$$

The boundary displacements of the segment in Fig. 2.2(b) may now be evaluated from Eqs. 3.2.7 as

$$\begin{Bmatrix} \Delta_1 \\ \theta_1 \\ \Delta_2 \\ \theta_2 \end{Bmatrix}^j = \begin{bmatrix} \langle \phi(0) \rangle \\ \langle \phi'(0) \rangle \\ \langle \phi(\ell) \rangle \\ \langle \phi'(\ell) \rangle \end{bmatrix} \{c\}^j \quad (3.2.10)$$

Substituting the value of $\{c\}$, from Eq. 3.2.9, into Eq. 3.2.10 yields

$$\begin{Bmatrix} \Delta_1 \\ \theta_1 \\ \Delta_2 \\ \theta_2 \end{Bmatrix}^j = \begin{bmatrix} \langle \phi(0) \rangle \\ \langle \phi'(0) \rangle \\ \langle \phi(l) \rangle \\ \langle \phi'(l) \rangle \end{bmatrix} [B] \begin{Bmatrix} V_1 \\ M_1 \\ V_2 \\ M_2 \end{Bmatrix}^j \quad (3.2.11)$$

This equation may be written as

$$\begin{Bmatrix} \Delta_1 \\ \theta_1 \\ \Delta_2 \\ \theta_2 \end{Bmatrix}^j = [F]_j \begin{Bmatrix} V_1 \\ M_1 \\ V_2 \\ M_2 \end{Bmatrix}^j \quad (3.2.12)$$

where $[F]_j$ may be identified as the flexibility matrix of the short cylindrical shell segment. The algebraic details of this procedure are presented in Appendix E - Derivation of Short Cylinder B Matrix, where closed form expressions for the elements of the $[B]$ matrix are derived. $[F]_j$ is formed in FLEXSHELL by numerically evaluating the matrix product in Eq. 3.2.11.

The flexibility matrix discussed above is required for the evaluation of $[\hat{F}]$, according to step 4 of the procedure outlined in Sect. 2.3. The end forces on the segment are determined in step 5, and in step 6 it is necessary to evaluate the moment stress resultants throughout the segment arising from the known set of end forces. This latter evaluation is accomplished by substituting the known end forces, of step 5, into Eq. 3.2.9 to determine the $\{c\}$ vector applicable for the

segment, and using this vector to evaluate the equation which results after substituting Eq. 3.2.7a into Eq. 3.2.5. That is, the homogeneous solution for the meridional moment produced by end forces is evaluated as

$$M(y) = D \langle \phi''(y) \rangle \{c\} \quad (3.2.13)$$

where the numerical values of $\{c\}$ are known.

3.3 Spherical Segment Flexibility Matrix

The spherical segment flexibility matrix may be evaluated from the homogeneous solution for a spherical shell segment subjected to edge forces as illustrated on segment 5 of Fig. 2.1. Homogeneous solutions associated with unit values of each of these edge forces are given in Table D.2 of Appendix D. The system of labelling the equations in Appendix D is explained in Table D.1 and the geometric variables appearing in the equations are defined in Fig. D.1. The 4x4 flexibility matrix corresponding to the $[F]$ matrix of Eq. 2.3.1 for a spherical shell segment can be obtained by evaluating Eqs. SHj.i of Table D.2, as

$$F_{kj} = SH_{j.i} \quad j = 1,4; \quad i = 1,2 \quad (3.3.1)$$

for the specified geometry of the segment, and the appropriate value of the argument. When the argument is associated with the upper end of the segment $k = i$. When the argument is associated with the lower end of the segment $k = i + 2$.

It has been pointed out in Sect. 3.1 that there is a limit on the subtended angle of the shell segment below which this matrix is no longer applicable.

3.4 Short 'Plate on Elastic Foundation' Flexibility Matrix

The notation for a 'plate on elastic foundation' segment (which will also be referred to as a base segment) is illustrated in Fig. 2.2, except for the spring foundation elements which are assumed to have a stiffness of k (load/area/height). The governing differential equation for this plate is [11, pg. 260]

$$\left(\frac{d^2}{dr^2} + \frac{1}{r} \frac{d}{dr}\right) \left(\frac{d^2 w}{dr^2} + \frac{1}{r} \frac{dw}{dr}\right) = \frac{q - kw}{D} \quad (3.4.1)$$

and the internal stress resultants may be determined as [11, pg. 52]

$$M_r = -D \left(\frac{d^2 w}{dr^2} + \frac{\nu}{r} \frac{dw}{dr}\right) \quad (3.4.2a)$$

$$M_t = -D \left(\frac{1}{r} \frac{dw}{dr} + \nu \frac{d^2 w}{dr^2}\right) \quad (3.4.2b)$$

$$V = D \left(\frac{d^3 w}{dr^3} + \frac{1}{r} \frac{d^2 w}{dr^2} - \frac{1}{r^2} \frac{dw}{dr}\right) \quad (3.4.2c)$$

Defining a new variable

$$\sigma = r/(\sqrt{2\ell}) \quad (3.4.3a)$$

where

$$\ell = \sqrt[4]{D/k} \quad (3.4.3b)$$

the general solution to Eq. 3.4.1, for large values of σ , may be written as

$$w = \langle \sigma_1 \quad \sigma_2 \quad \sigma_3 \quad \sigma_4 \rangle \begin{pmatrix} c_1 \\ c_2 \\ c_3 \\ c_4 \end{pmatrix} \quad (3.4.4a)$$

or $w = \langle \phi \rangle \{c\}$ (3.4.4b)

where [11, pg. 266]

$$\phi_1 = \left(\frac{e^\sigma}{\eta \sqrt{\sigma}} \right) \cos (\sigma - \pi/8) \quad (3.4.5a)$$

$$\phi_2 = \left(\frac{e^\sigma}{\eta \sqrt{\sigma}} \right) \sin (\sigma - \pi/8) \quad (3.4.5b)$$

$$\phi_3 = \left(\frac{\pi e^{-\sigma}}{\eta \sqrt{\sigma}} \right) \cos (\sigma + \pi/8) \quad (3.4.5c)$$

$$\phi_4 = \left(\frac{\pi e^{-\sigma}}{\eta \sqrt{\sigma}} \right) \sin (\sigma + \pi/8) \quad (3.4.5d)$$

with

$$\eta = 2^{0.75} \pi^{0.5} \quad (3.4.5e)$$

Eqs. 3.4.5 are asymptotic approximations to the Bessel function solutions of Eq. 3.4.1 which introduces some limitations to their range of applicability as discussed in Appendix G.

Evaluating Eqs. 3.4.2a and 3.4.2c at the ends of the plate segment results in

$$\begin{Bmatrix} M_1 \\ V_1 \\ M_2 \\ V_2 \end{Bmatrix}^j = D \begin{bmatrix} [\langle \phi'' \rangle + \frac{\nu}{r} \langle \phi' \rangle]_{r_0} \\ -[\langle \phi''' \rangle + \frac{1}{r} \langle \phi'' \rangle - \frac{1}{r^2} \langle \phi' \rangle]_{r_0} \\ -[\langle \phi'' \rangle + \frac{\nu}{r} \langle \phi' \rangle]_{r_i} \\ [\langle \phi''' \rangle + \frac{1}{r} \langle \phi'' \rangle - \frac{1}{r^2} \langle \phi' \rangle]_{r_i} \end{bmatrix} \{c\}^j \quad (3.4.6a)$$

$$= [B] \{c\}^j \quad (3.4.6b)$$

where M_i and V_i are the boundary forces illustrated in Fig. 2.2c; r_0 and r_i are the outer and inner radii, respectively; and ' indicates d/dr .

Inverting the B matrix of Eqs. 3.4.6 yields

$$\{c\}^j = [B]^{-1} \begin{Bmatrix} M_1 \\ V_1 \\ M_2 \\ V_2 \end{Bmatrix}^j \quad (3.4.7)$$

Evaluating the boundary displacements illustrated in Fig. 2.2c, from Eqs. 3.4.4 and substituting from Eq. 3.4.7 for $\{c\}$, yields

$$\begin{Bmatrix} \theta_1 \\ \delta_1 \\ \theta_2 \\ \delta_2 \end{Bmatrix}^j = \begin{bmatrix} \langle \phi' \rangle_{r_0} \\ \langle \phi \rangle_{r_0} \\ \langle \phi' \rangle_{r_i} \\ \langle \phi \rangle_{r_i} \end{bmatrix} [B]^{-1} \begin{Bmatrix} M_1 \\ V_1 \\ M_2 \\ V_2 \end{Bmatrix}^j \quad (3.4.8)$$

or

$$\begin{Bmatrix} \theta_1 \\ \delta_1 \\ \theta_2 \\ \delta_2 \end{Bmatrix}^j = [F]_j \begin{Bmatrix} M_1 \\ V_1 \\ M_2 \\ V_2 \end{Bmatrix}^j \quad (3.4.9)$$

where $[F]_j$ is a short plate segment 4x4 flexibility matrix.

Expressions for the derivatives of the $\langle \phi \rangle$ vector required in this development are contained in Table 3.1. No attempt has been made to derive closed form solutions for the elements of the $[B]^{-1}$ matrix. The matrix $[B]$ is formed in the program by making use of the derivatives in Table 3.1 and Eq. 3.4.6a, inverted numerically, and the product of Eq. 3.4.8 is evaluated to produce the flexibility matrix of Eq. 3.4.9.

Unlike the other segments in FLEXSHELL, the complete segment flexibility matrix for the base segment is a 6x6 matrix rather than a 4x4. However, the in-plane effects are uncoupled from the transverse effects and, therefore, a 2x2 in-plane flexibility matrix may be combined with the above 4x4 flexibility matrix simply by inserting the two matrices into the complete segment flexibility matrix with a proper ordering of subscripts. The 2x2 in-plane flexibility matrix was obtained from the classical thick cylinder solution, and is formed by evaluating Eqs. PH.1.1 and PH.2.1 of Table D6, Appendix D.

3.5 Particular Solutions

Particular solutions for the various loading cases may, in the main, be extracted directly from the literature. The equations for the particular solutions coded into FLEXSHELL are tabulated in Tables D3, and D4 and D6 of Appendix D. The system of labelling these equations is

also explained in Table D.1. Particular solution displacements at the edges of the elements are obtained for load case ℓ , from Eqs. XP ℓ .i where $i = 1$ indicates a \bar{w} displacement and $i = 2$ indicates a rotation.

3.6 Coding Strategy for Assembly and Solution

The remainder of the coding strategy associated with the solution of Sect. 2.3 may now be described. The technique of identifying the forces and constructing the [A] matrix has been outlined in Sect. 2.4. It should be noted, however, that the connectivity of a base segment with vertical eccentricity introduces an additional element into the [A] matrix to establish horizontal compatibility. Thus, in Fig. 2.1, if segment 7 is considered attached to the top of plate segment 9, and if it is assumed plane sections remain plane in the plate segment, this may be modelled by a rigid eccentricity E_1^9 , of Fig. 2.2c, where E_1^9 has a magnitude of one-half the slab thickness. The horizontal compatibility equations, similar to Eqs. 2.2.1, become

$$t_2^{\Delta 7} - (t_1^{\Delta 9} - E_1^9 t_1^{\theta 9}) = 0 \quad (3.6.1a)$$

and

$$t_2^{\theta 7} - t_1^{\theta 9} = 0 \quad (3.6.1b)$$

Eq. 3.6.1a introduces E_1^9 into the [A] matrix.

The program has the limitation that plate segment vertical eccentricities specifying connections to cylinders or dome must be input as E_1^j values for the segment with the higher segment (ie. plate) number.

Plate segment eccentricities specifying eccentric vertical connections with other plate segments must be input as E_2^j values of the segment with the lower segment number.

The element flexibility matrices are constructed as outlined in Sects. 3.2, 3.3 and 3.4 and the structure flexibility matrix is evaluated according to Eq. 2.3.14.

The segment end forces and displacements are evaluated as follows. An array of 'particular solution basic forces' (PBF) is constructed which contains the edge forces which must be exerted on each segment in order to equilibrate the particular solution for that segment. These forces are obtained from a resolution of the forces evaluated at the ends of the segments by equations $XP_{\ell,j}$ for $j=3$ and 5 , in Tables D3 and D4, where ℓ is the loading effect. The order of PBF subscripts, for each of the segment types is shown in Fig. 3.1. The vertical force applied to the top of the segment and the net vertical force resulting from the applied loading is also stored in this array with subscripts 5 and 6, respectively.

Each segment is treated in turn and the PBF(5) and PBF(6) forces are transferred from any segment to those below it, by making use of the connectivity information illustrated in Table 2.1(c). That is, the PBF(5) forces for the 'lower' elements are augmented by the vertical load on the element under consideration according to the hierarchy specified in the connectivity input.

The array of PBF forces for the segment is then examined to see if the adjacent segments are required to equilibrate any edge forces that are not a part of their particular solution. If so, the edge

forces that will produce displacements in a segment, over and above those displacements produced by its own particular solution, are accumulated in a particular solution force array PSF.

The displacements for each segment are calculated, at the edges of the segments from equations $XP_{\lambda,i}$, for $i=1,2$, of Tables D.3, D.4 and D.6c, as explained in Sect. 3.4, where λ is the loading effect. These 'particular solution displacements' are stored in the segment array PSD. The PSD displacements are then augmented by the homogeneous solution displacements arising from the 'particular solution forces' (PSF) accumulated as described above (as evaluated from Tables D.2, D.5, and D.6a,b, and Eqs. 3.2.12 and 3.4.9) and assembled into the vector $\{\delta\}$ of Eq. 2.3.4. Premultiplying by the $[A]$ matrix produces the right hand side of Eq. 2.3.12.

Eq. 2.3.12 is solved for $\{Q\}$ by a simple Gaussian elimination procedure. The segment forces, $\{V\}$, required to restore compatibility are recovered from Eq. 2.3.10. The internal stress resultants are computed by superimposing the redundants $\{V\}$ onto the segment end forces (PSF) to obtain a 'segment end force' array SF which represents the final end forces, which are applied to the edges of the segment. The final stress resultants are then those produced by the particular solution, which are valued by Eqs. $XP_{\lambda,i}$, of Tables D.3, D.4 and D.6c, $i=3$ to 6, plus those produced by the homogeneous solutions for the SF array of edge forces (computed from Eqs. $XX_{i,j}$, $j=3,6$, of Tables D.2 and D.5, where i identifies the boundary force, or Eq. 3.2.13 or Eqs. 3.4.2).

4. EXAMPLE APPLICATIONS OF FLEXSHELL

4.1 Introduction to Applications

In this Chapter two example solutions are discussed. These examples serve to illustrate the input for, and the output from, the FLEXSHELL program. The first example is an analysis of the effects of internal pressure which requires very simple input. The second solution is for prestressing effects, and is somewhat more complicated. The reader is referred to "Appendix A - FLEXSHELL User's Manual" for a detailed description of all input data required. This Appendix should be read prior to or concurrently with this Chapter.

The principal geometric dimensions of the Gentilly-2 containment structure are shown in Fig. 4.1. The structure has been modelled in this report in a manner similar to the structure illustrated in Fig. 2.1, and the 'standard model' is shown in Fig. 4.2. Details of the model in the area of the ring beam, the inner perimeter beam of the lower dome, and the base are shown in Figs. 4.3a-c. The input files, for the load cases which will be compared with the BOSOR4 stress results in Chapter 5, are listed in Appendix C, on pages C1 to C15. In general, an attempt has been made to keep the input data as consistent as possible to the BOSOR4 model of Ref. 6, except where the influence of loading and geometric variations are being investigated.

The input for any of the analyses on the standard model, which consists of 10 segments, requires only 41 lines, as can be seen on pages C2 to C15, each page containing the complete input for one run. Table C1, on page C1, contains an index to the data files. The input data remains constant for a given model as only the loading information changes from

one run to another. Thus, referring to page C2, lines 3 to 12 contain the type of information illustrated in Table 2.1a (discussed in Sect. 2.4) with an additional column (column 5) specifying at how many locations in a segment the stress resultants are required. The eccentricities specified on these lines are consistent with those shown in Fig. 4.3. Lines 13 to 21 specify the connectivity information illustrated in Table 2.1c (discussed in Sect. 2.4). Lines 22 to 31 specify the geometry and material properties of the segments, as illustrated in Figs. 4.2 and 4.3.

The variation in input is then associated with the loading information which for the pressure example is contained on lines 32 to 41 of page C2, and for the prestress example is contained on lines 35 to 45 of page C4. This is discussed in detail in the following Sections.

4.2 Analysis for Internal Pressure

The input for internal pressure is contained on page C2 where the loading information is contained on lines 32 to 41. This loading condition is identified by the 1 in the second column of figures on these lines. Only segments 1, 3, 6, 7, 8 and 10 are subjected to nonzero pressures. The pressures on these load cards are consistent with 1 psf internal pressure which must be reduced in the ratio of the internal radius to the centerline radius of each segment, and is negative according to the sign conventions of Fig. 2.2, except for the base segment. The nonzero PSF forces to the right of the third column of figures for segment 7 are the result of the internal pressure acting upward on the 0.75 ft. interior overhang of the ring beam as illustrated in Fig. 4.2. The computation of this type of force will be illustrated in Sect. 4.3.

Typical program output for the analysis for internal pressure is reproduced on pages C16 to C22. Pages C16 and C17 contain the echo check of input data and the results of the analysis start at the top of page C18 with a summary of the forces of interaction between segments (the $\{V\}$ vector of Sect. 2.3), identified by segment number and the subscripting order of Fig. 3.1. This is followed on pages C19 to C20 by the typical output for a spherical segment consisting of the total end forces acting on the segment, the $N1$, $N2$, $M1$ and $M2$ stress resultants at stations along the length of the segment, and the horizontal displacements along the segment. The stress resultants, and the sign conventions for them, are illustrated in Fig. 4.4a. Page C21 illustrates output for a typical cylindrical segment. Page C22 illustrates output for a typical base segment. It should be noted that the program does not output values close to the radial centerline for base segments because of the limitation on accuracy as the radius becomes small, which was mentioned in Sect. 3.1.

The form of the output always follows this pattern unless a nonzero IPRINT value is included on line 2 of the input data, in which case considerably more information, such as the $[A]$ matrix, the $[F]$ matrices and the $[\hat{F}]$ matrix, is contained in the output for the problem.

A comparison of these results with the BOSOR4 results is included in Chapter 5.

4.3 Analysis for Prestressing Effects

The input data for two switched-on prestress analyses is reproduced on pages C4 and C7. The ring beam for these models has been subdivided into four and five segments, respectively, rather than the

three of the standard model, in order to accommodate discontinuities in the prestress loading.

The prestress load condition is characterized by a number of concentrated loading effects, in addition to distributed loads, which are input as PSF forces (see Sect. 3.5). These are contained on the loading lines (the last twelve in the file on page C4, and the last thirteen of the file on page C7), in addition to the segment number and the prestress load identification number, i.e. 3. The prestress forces have been computed as equivalent pressure loads except that the vertical wall prestress, and the self-equilibrating forces for the anchorage of the dome prestressing cables must be applied as concentrated (line) loads. The essential computations required to evaluate the prestress loading are shown in Table 4.1 and the resulting PSF forces are shown in Fig. 4.5. The external PSF forces which are applied to segments 2 and 3, according to the sign convention of Fig. 2.2, make it possible to account for concentrated loading conditions arising at the ends of the segments.

The output for the prestress analyses have been omitted but follow the same pattern as that for internal pressure discussed in Sect. 4.2. The results are presented in Chapter 5 where they are discussed in detail.

5. COMPARISON WITH BOSOR4 ANALYSES

5.1 Introduction to Comparison of Result

In order to assess the reliability of the stress resultants obtained from simple shell theory for Gentilly type structures, it is desirable to compare the results from FLEXSHELL with those of more complex analyses. The results from the FLEXSHELL program are compared herein with those obtained from the BOSOR4 analyses of Refs. 6 and 7.

It should be noted that the theoretical basis for BOSOR4 is more 'exact' than that for FLEXSHELL, in that the BOSOR4 formulation accounts for a number of geometric effects which are not included in simple shell theory. In the formulation for BOSOR4 it is possible to retain many geometric effects that are discarded in classical shell theory because the resulting energy expressions are integrated numerically. Classical shell theory attempts to reduce the governing equations to a set of linear partial differential equations which facilitates a solution using classical mathematical techniques. A comparison of the two approaches on a rigorous basis is difficult because simple shell theory discards terms in a rather ad-hoc manner. However, the following gives some indication of the basis for the two approaches.

BOSOR4 develops a consistent energy formulation from the following strain-displacement equations [5].

$$\{\epsilon\} = \begin{Bmatrix} \epsilon_1 \\ \epsilon_2 \\ \chi_1 \\ \chi_2 \end{Bmatrix} = \begin{Bmatrix} u' + w/R_1 + \frac{1}{2}(\xi^2 + \gamma^2) \\ \dot{v}/r + u r'/r + w/R_2 + \frac{1}{2}(\psi^2 + \gamma^2) \\ \xi' \\ \dot{\psi}/r + r' \xi/r \end{Bmatrix} \quad (5.1a)$$

$$\begin{aligned}
 \text{where } \xi &= w' - u/R_1 \\
 \psi &= \dot{w}/r - v/R_2 \\
 \gamma &= \frac{1}{2} (\dot{u}/r - v' - r'v/r)
 \end{aligned}
 \tag{5.1d}$$

and u , v and w are the displacements in the meridional, circumferential and normal directions, respectively; s , and θ are the meridional and (angular) circumferential coordinates, respectively; ' and \cdot indicate differentiation with respect to the meridional and circumferential coordinates, respectively; R_1 , R_2 and r are the meridional, circumferential and radial radii of curvature, respectively; and, ξ , ψ and γ are the rotation of the meridian, rotation about the meridian and rotation around the normal, respectively. The energy associated with these strains is integrated through the shell thickness by dividing the thickness into a number of layers and numerically evaluating the required products. In this manner geometric effects, such as the change in radius through the thickness and product terms in the strain displacement equations, can be accounted for.

In the more classical shell theory, on which FLEXSHELL is based, the formulation starts from essentially the same strain-displacement relations, and derives equilibrium equations, except that all non-linear terms are neglected as they arise. In order to solve the resulting differential equations the solution is separated into a homogeneous part, corresponding to the edge effects arising from the continuity of the shell segments, and a particular solution corresponding to the membrane effects for the applied load condition. These two solutions, and the technique of superposition, have been discussed in Chapters 2 and 3.

The uncoupling of the load and edge effects for cylindrical

segments results in differential equations which can be solved by standard mathematical techniques and solutions obtained, for 'thin' shells, are sufficiently accurate for engineering applications. However, for spherical shell segments a further simplification is required before the differential equation can be solved. If it is assumed that edge effects decay rapidly as one proceeds from the edge then only higher derivatives need be retained in the equilibrium equation and the differential equation reduces to a simple form resembling that of the cylindrical shell segment. This assumption is reasonable if the angle from the central axis of symmetry is large, say in the order of 30 degrees. The effect of this simplification (first introduced by Geckler [10, pg. 63], and used in FLEXSHELL) on the stress resultants is generally small, except for the M_2 stress resultant, for which one of the neglected terms becomes significant, and for small angles from the axis of symmetry. The approximate theory for M_2 retains only the term corresponding to $\sqrt{M_1}$. This approximation has been found to be completely inadequate and the authors have adapted an equation recommended by Pflüger [10, pg. 66], as described in Appendix F, for the computation of the M_2 stress resultant. All formulae in Appendix D, and results presented herein, include this modification.

In view of the above differences between the two approaches it should not be expected that the results from the two would precisely correspond. Where discrepancies occur it must be assumed, for the present, that the BOSOR4 analyses are the more reliable. This is particularly true in the upper regions of the lower dome where the opening occurs at a small angle from the axis of symmetry.

It is also questionable whether the stress resultants computed within the ring beam are accurate. The ring beam has a depth to thickness ratio of 2 to 1, and contains junctions with the spherical segments along its length. For this type of geometry the 'plane sections remain plane' assumption, upon which both programs are based, is questionable and finite element analyses are probably required to determine stresses within this region. Such studies are presently underway and a comparison of finite element results with those contained herein will be the subject of a subsequent report.

5.2 Comparison of FLEXSHELL and BOSOR4 Results

The N_1 , N_2 , M_1 and M_2 stress resultants, and the horizontal displacements, for four load conditions are compared with the BOSOR4 results of Ref. 6 in Figs. 5.1 to 5.29. The load cases are internal pressure, dead load, total ('switched-on') prestressing and winter operating temperature (WOT). Each of these load cases is discussed separately in the following sub-sections. The analyses will generally be carried out on the standard model for which a foundation modulus of 450000 lb/ft³ is used. The effects of varying this foundation modulus will be considered in Sect. 5.3 and discussion of comparisons at the base connection will be undertaken in that section.

The discussion of Sect. 5.1 has alluded to the fact that the computation of the M_2 stress resultant presents a source of difficulty in a classical shell approach. The result is that the FLEXSHELL M_2 predictions are generally 15-25% lower than those of BOSOR4 at the interior maximum moment location. This must be regarded as a deficiency in the classical shell theory and will receive little further attention.

The sign convention for the comparison of stress resultants is that of BOSOR4, illustrated in Fig. 4.4b. In all plots the solid lines are the BOSOR4 results while the x's represent FLEXSHELL results. The linear coordinate against which the stress resultants are plotted is that of the BOSOR4 analyses of Ref. 6.

The reader is cautioned to check the scale of each drawing since the vertical scale varies from plot to plot and the relative significance of the stress resultants cannot always be judged without referring to the absolute values.

5.2.1 Comparison of Internal Pressure Stress Resultants

A comparison between the N_1 , N_2 , M_1 and M_2 stress resultants, and horizontal displacement, for an internal pressure of 1 psf, as predicted by FLEXSHELL and BOSOR4, is presented on Figs. 5.1 to 5.5, respectively. Except for the perturbation at the crown the N_1 stress resultants (Fig. 5.1) differ by less than 3%. It should be noted that the classical shell theory gives a singular value at this point if the boundary effects are retained (Eqs. SH3.3 and SH4.3). The N_2 stress resultants (Fig. 5.2) show excellent agreement. The M_1 stress resultants (Fig. 5.3) also show excellent agreement. The M_2 stress resultant (Fig. 5.4) displays a 15% discrepancy for the peak interior moment in the spherical shell, as discussed in Sect. 5.2, and a small perturbation at the apex of the shell for the same reason as the N_1 stress resultant (Eq. SH4.6).

The discrepancies in the ring beam at the junction with the upper dome in Figs. 5.3 and 5.4 result from the facts that there is a very high gradient in this area and the FLEXSHELL model had slightly

different geometry than the BOSOR4 model. The FLEXSHELL results are probably 'theoretically' more correct at this junction than the BOSOR4 results. The discrepancy is also influenced by the finite element mesh size in the BOSOR4 model.

The horizontal displacements in the cylindrical segments are compared in Fig. 5.5. Since BOSOR4 outputs normal displacements for the spherical segments, and these are not available from a classical analysis, the FLEXSHELL spherical segment displacements have been set to zero. No further reference to spherical segment displacements will be made in subsequent comparisons.

5.2.2 Comparison of Dead Load Stress Resultants

The comparison between the N_1 , N_2 , M_1 and M_2 stress resultants, and horizontal cylinder displacements, for switched-on dead load is presented on Figs. 5.6 to 5.10, respectively. Excellent correspondence for the N_1 stress resultant (Fig. 5.6) is obtained except at the inner opening of the lower dome. Excellent correspondence for the N_2 stress resultant (Fig. 5.7) is obtained except at the same location and at the base junction. The difficulty in the lower dome relates to the Geckler approximation and the small angle of the opening, as discussed in Sect. 5.1 and Appendix F. The base connection is discussed in Sect. 5.3. The correspondence of the M_1 moment (Fig. 5.8) is considered good, while the M_2 stress resultant (Fig. 5.9) exhibits the characteristic discrepancy (23%) for the interior maximum moment in the upper spherical shell. Horizontal cylinder displacements show good agreement (Fig. 5.10).

5.2.3 Comparison of Prestress Stress Resultants

Two prestressing analyses are presented herein, the difference in the analyses being in the way the anchorage loads for the dome prestressing are treated. The computation of these forces was discussed in Sect. 4.3 and summarized in Table 4.1 and Fig. 4.5. A comparison for both the 'simplified model' and the 'BOSOR4 model' follows.

The N_1 , N_2 , M_1 and M_2 stress resultants, and the horizontal cylinder displacements, are shown in Figs. 5.11 to 5.15, respectively, for the switched-on simplified prestress. Except in the region of the prestress anchorages, and the usual discrepancy of M_2 internal moment (in this case 26%), the correspondence with BOSOR4 results is excellent throughout.

Introducing an additional segment to the model, as illustrated in Fig. 4.5b, allows a simulation of force effects more consistent with the BOSOR4 model of Ref. 6. The N_1 , N_2 , M_1 and M_2 stress resultants, and the horizontal displacements, are shown in Figs. 5.16 to 5.20, respectively, for the switched-on BOSOR4 prestress loading. The agreement between the two sets of results is now excellent even in the areas of abrupt discontinuity where concentrated force effects are applied.

5.2.4 Comparison of Thermal Effects

Two sets of thermal stress resultants are presented herein. The first set is for the standard model of Fig. 4.2. The N_1 , N_2 , M_1 and M_2 stress resultants, and the horizontal cylinder displacements, for the winter operating temperature (WOT) thermal conditions of Ref. 6, are shown on Figs. 5.21 to 5.25, respectively. These stress resultants are obtained by superimposing the results from the thermal gradient input,

on page C6, and those from the constant temperature change input, on page C5. The maximum N_1 stress resultants on Fig. 5.21 correspond closely with those of BOSOR4. There is, however, a discrepancy with the BOSOR4 results in the upper part of the outer dome. The BOSOR4 output predicts a force at the apex of 2000 lb. while the FLEXSHELL results reduce to zero. However, it should be noted that the BOSOR4 force is small in magnitude, producing an average stress of 7 psi, and that the classical particular solution used for FLEXSHELL requires this force to vanish. Because of the low forces generated the discrepancy is not considered to be serious. The remaining stress resultants (Figs. 5.22 to 5.24) and the horizontal cylinder displacements (Fig. 5.25) generally show good agreement except in the vicinity of the base connection. Hence, a thermal model more closely resembling the BOSOR4 model at the base was analyzed.

The BOSOR4 model did not have the outer perimeter base ring, namely, segment 9 of Fig. 4.2. The thermal input files, similar to those on pages C5 and C6, but omitting this base segment are contained on pages C8 and C9. Results from this input are shown in Figs. 5.26 to 5.29 (the N_1 stress resultant is identical to that in Fig. 5.21). It can be seen from these plots that the discrepancy with the BOSOR4 results in the lower portion of the cylinder wall has disappeared and, indeed, the correspondence is quite remarkable.

5.3 Effect of Foundation Modulus

One area of weakness in the BOSOR4 analyses of Ref. 6 was the simulation of the foundation stiffness. The base was supported by 5 vertical springs whose stiffnesses were made proportional to their distance from the axis of symmetry and were adjusted to reproduce the field

measurement of deflection (0.15 inches) observed on the outer perimeter of the Gentilly 1 Powerhouse under dead load.

The current 'base-on-elastic foundation' segment in the FLEXSHELL code has continuous elastic support whose stiffness is expressed as the subgrade modulus, k , of Eq. 3.4.1, but is subject to the deficiency that the support is of the Winkler type. This type of support is a common simplification for structural analysts but is not regarded favourably by soils engineers who consider it to be an oversimplification. There does not appear to be any rational technique for determining an equivalent subgrade modulus from the properties of the foundation. Stress resultants are, however, relatively insensitive to the precise subgrade modulus selected and recourse is generally made to tabulated recommendations, giving approximate values based on verbal descriptions of the subgrade, such as those on pg. 259 of Ref. 11.

The subgrade modulus selected for the standard model of this report was 450000 lb/ft^3 . The base deflection under dead load for this modulus is shown as line A on fig. 5.30. In addition, deflections for a subgrade modulus of 900000 lb/ft^3 are shown as line B, from the BOSOR4 analysis are shown as line D, and from preliminary finite element studies are shown as line C. It is quite apparent that by adjusting the foundation modulus a FLEXSHELL analysis could be made to precisely reproduce the BOSOR4 deflection at the wall centerline. However, this would be a rather pointless exercise. It appears that the angular rotation at the base of the wall is more significant than deflection and that the chosen subgrade modulus closely approximates the rotation for the BOSOR4 model.

The analyses for self-equilibrating forces (prestressing and thermal effects) shown in Figs. 5.11 to 5.20, and Figs. 5.26 to 5.29,

are relatively unaffected by the subgrade modulus and exhibit excellent correspondence in the area of the hinge. The analyses which require base slab participation (internal pressure and dead load), shown on Figs. 5.1 to 5.5, and Figs. 5.6 to 5.10, do not exhibit as good a correspondence in the hinge area. Nevertheless, the correspondence is still quite reasonable in view of the discrete nature of the support associated with the BOSOR4 model and the omission of the outer perimeter base ring from the BOSOR4 model (as discussed in Sect. 5.2.4).

The effect of doubling the foundation modulus (from 450000 lb/ft³ to 900000 lb/ft³) on the stress resultants at the bottom of the cylinder wall is shown, for the standard model, in Table 5.1 for three load cases. The large variations in N_2 for dead load and internal pressure are not considered significant since the effects of these load cases are an order of magnitude less than the prestressing effect. The moment stress resultants for dead load are the most sensitive to changes in foundation modulus while those for prestressing are the least sensitive. Magnitudes of moments decrease for both dead load and internal pressure as the foundation modulus increases.

In view of the fact that the Winkler type foundation appears to give rather different rotation characteristics than a finite element model (compare curves A and C in Fig. 5.30) and that the nature of the structural model in the area of the 'hinge' also has an effect on stress resultants (see Sect. 5.2.6), it was considered inappropriate to 'tune' a foundation modulus to produce closer correspondence of FLEXSHELL stress resultants with those of BOSOR4. Effort is more appropriately directed at determining an effective foundation modulus to simulate finite element results.

5.4 Effect of 'Hinge' Detail

The 'hinge' detail for the standard model used in this report is shown in Fig. 4.3c. Stress resultants at the base junction are influenced by the type of connection contained in the model. For comparison purposes, three variations of base detail from the standard model have been considered. These are shown in Fig. 5.31. The details in Figs. 5.31a, b and c are all 'rigid link models', with a variation of detail at the base of the cylinder wall. For Fig. 5.31d the wall was assumed to extend through the base to the slab center-line, thus eliminating the rigid link.

The results for N_2 , M_1 and M_2 , and the horizontal cylinder displacement, are shown in Figs. 5.32 to 5.35, respectively, for the effect of dead load. It is apparent that the short segment of flexible cylinder inserted at the connection in the standard model has a significant effect. A similar conclusion arises from a consideration of the effects of internal pressure shown in Figs. 5.36 to 5.39, inclusive.

In view of the sensitivity of results in this area to the modelling of the base connection and the differences between the FLEXSHELL and BOSOR4 models, the discrepancies adjacent to the connection in Figs. 5.2 to 5.4 and in Figs. 5.7 to 5.9 appear to be very reasonable.

5.5 Reference State Rf1

The N_1 , N_2 , M_1 and M_2 stress resultants, for the reference state Rf1 of Ref. 6, are shown in Figs. 5.40 to 5.43, respectively. This reference state is obtained by sequencing the application of dead load and prestressing forces to partial structures in such a manner as to simulate the site construction procedure. Details are given in Ref. 6,

and the necessary data files to simulate the partial structure loadings for reference state Rf1 are included in Appendix C.

It is quite apparent that since FLEXSHELL exhibits good correlation with BOSOR4 for individual load cases it should also correlate well with any set of load combinations. The results on Figs. 5.40 to 5.43 exhibit this excellent correlation (the FLEXSHELL analysis presented is for the simplified prestressed loading).

6. STRESS COMPUTATIONS

6.1 Introduction to Stress Computations

Chapter 5 has established that a simple classical shell flexibility analysis gives results for Gentilly type structures which are essentially the same as those from more sophisticated displacement analyses, except in clearly definable regions. The results appear to be suitable for most aspects of preliminary design and for checking the adequacy of a given structure in meeting serviceability requirements. However, for determining first cracking pressures and regions subjected to tensile stresses in a specified serviceability state it is much more convenient to examine stresses rather than stress resultants. This Chapter illustrates a convenient method of examining stress states in a Gentilly type structure, excluding the effects of stress concentrations.

Stresses may be computed with reasonable accuracy from the previously determined stress resultants by the simple flexure formula, namely,

$$\sigma = \frac{N}{A} \pm \frac{My}{I} \quad (6.1)$$

where N is the membrane force per unit width; M is the moment per unit of width; A and I are the section properties per unit width; and, y is the distance from the middle surface. In the following S_1 refers to the extreme fibre stress arising from a combination of N_1 and M_1 , while S_2 refers to the extreme fibre stresses arising from a combination of N_2 and M_2 , at any point in the structure.

6.2 Stress Plots

The stress plots for S_1 resulting from an internal pressure of 18 psi are shown on Fig. 6.1. The plot shows the variation of stress on the internal and external faces of the structure. The effect of moment is exhibited by the spread between the two stress points at the same section. The average of the two stress points at any section indicates the effect of axial force. Clearly the critical section for uniform thickness of dome is at the springing line of the dome and this has lead the designers to thicken the structure in this area.

In the absence of a more exact analysis a common technique of design is to compute stress resultants on the basis of a dome of uniform thickness (ie. carry out the analysis for uniform thickness) but to vary the thickness during the design phase to produce acceptable stresses. The effect of thickening the structure at the springing line, using the above technique, is shown by the solid lines in Fig. 6.1. The reduction in stress at the springing line is very significant. A similar plot for the circumferential stresses, S_2 , is shown in Fig. 6.2.

Stress plots for a 'switched-on reference' state are shown in Figs. 6.3 and 6.4. Stresses for the FLEXSHELL simulation of the Rf1 reference state of Ref. 6 (partial structure load superposition) are shown in Figs. 6.8 and 6.9.

A summary of the stresses at the springing line of the dome, in the region of dome thickening, is given in Table 6.1 for the three load cases discussed above.

6.3 Check of Serviceability Conditions (Switched-on Analysis)

Given the stress ordinates for the reference states and internal

pressure, it is straightforward to compute the pressure to produce any desired stress at any specified point on the faces of the structure. Thus, if s is the stress at any point due to a unit internal pressure, σ is the reference state stress, f is the desired stress and p is the internal pressure producing the desired stress, then

$$p s + \sigma = f \quad (6.2)$$

or

$$p = (f - \sigma)/s \quad (6.3)$$

In general, for serviceability requirements f is either zero (a no tension state) or f_t (the tensile strength of the concrete).

Using Eq. 6.2, the internal pressure required to produce zero stress ($f = 0$) and the cracking stress ($f = f_t = 450$ psi) at all points on the exterior and interior faces of the structure have been determined. The results are shown in Figs. 6.5, 6.6 and 6.7.

Fig 6.7 indicates that for a 'switched-on' reference state no circumferential tension is predicted until the internal pressure exceeds 30 psi.

In contrast, Fig. 6.5 indicates that tensile regions exist, prior to pressurization, on the exterior face of the ring beam, the underside (interior) of the lower dome at the springing line, and the topside (exterior) of the lower dome, over approximately one-half its length. These regions are indicated on Fig. 6.5 by the points plotted at 0 psi

and correspond to the tensile stress regions of the reference state stresses in Fig. 6.3.

Since the lower dome is unstressed and does not act as a part of the containment, no further discussion of this area will be undertaken. Fig. 6.5 also indicates, however, that the exterior of the top of the cylinder wall, and the interior of the (unthickened) dome at the springing line would be subject to tensile stress at pressures below the design basis accident conditions (18 psi). (The horizontal dashed lines on Figs. 6.5 to 6.7 and Figs. 6.10 to 6.12 indicate the design basis accident pressure of 18 psi and the proof test pressure of 20.7 psi). An enlargement of the pressure factor plot of Fig. 6.5 in the region of the ring beam is shown in Fig. 6.6. When the thickening of the upper dome is included it can be seen that the pressure to produce zero tensile stress at the springing line rises above the design basis accident pressure. In addition, it is apparent from Figs. 6.5 and 6.6 that no cracking is indicated at the proof test pressure. The pressurizations, in the region of thickening, that are required to produce the serviceability limit states are tabulated in Table 6.2.

6.4 Check of Serviceability Conditions (Load Superposition Analysis)

One of the objectives of this study is to determine if secondary effects, such as the construction sequence, have a significant effect on serviceability limit states. It was for this reason that Ref. 6 undertook to simulate the effects of construction sequence which requires a considerably more detailed analysis than the 'switched-on' type of analysis. The stress resultants arising from the more detailed analysis are reflected in reference state Rf1. The plots in Figs. 5.40

to 5.43, discussed in Sect. 5.5, indicate that this reference state can be accurately reproduced by FLEXSHELL.

The Rf1 reference state stresses are shown in Figs. 6.8 and 6.9. The pressure factor plots to produce the serviceability limit states, defined in Sect. 6.3, are shown in Figs. 6.10 to 6.12 for pressurization starting from the Rf1 reference condition. Fig. 6.12 again indicates that serviceability pressure factors relative to the S2 stresses are of no concern.

A comparison of Figs. 6.5 and 6.10 indicates the construction sequence produces somewhat lower pressure factors at the top of the cylinder wall on the exterior face and indicates some cracking may occur, at the same location, during the proof test. However, a comparison of Figs. 6.11 and 6.6 indicates that construction sequence has essentially no effect on serviceability limit states at the dome springing line.

7. SUMMARY AND CONCLUSIONS

7.1 Summary

This report has discussed the development of, and application of, a 'small' program for the analysis of axisymmetric segmented thin-shell structures, based on classical shell solutions generally available in the literature and a matrix flexibility approach. The program has been applied to the analysis of a number of loading cases for a Gentilly type nuclear containment structure and compared with the results of BOSOR4 analyses.

The results, on the whole, show excellent agreement between the two solution techniques. The greatest discrepancies between the two types of analysis are in the determination of the N1 thermal stress resultants in the spherical segments (Fig. 5.21), which are small, and in the maximum interior M2 stress resultants towards the mid-ordinate of the spherical segments (Figs. 5.4, 5.9 and 5.14).

Within the theoretical limitations of a Winkler type of foundation the plate-on-elastic foundation base segments give an effective means of representing the interaction between the foundation and the containment structure. The stress resultants in the base of the wall have been shown to be relatively insensitive to a variation in subgrade modulus (Table 5.1) but considerably more sensitive to the technique of modeling the base connection (Figs. 5.31 to 5.39).

A load superposition construction sequencing analysis can be simply carried out with excellent results (Figs. 5.40 to 5.43). The effect of altering the details of the model in the region of dome pre-stress anchorage has been demonstrated (compare Figs. 5.11 to 5.15 with

Figs. 5.16 to 5.20). The effect of alteration of the base geometry on the thermal stress resultants has also been shown (compare Figs. 5.22 to 5.25 with Figs. 5.26 to 5.27).

Stress plots over the exterior and interior faces of the structure have been presented for a number of loading conditions and these represent a convenient way of presenting the loading influence on the structure. The pressure factors to produce the serviceability limit states of zero tension and of the concrete tensile strength have been presented graphically. A comparison of pressurization factors for a 'switched-in-analysis' (Figs. 6.5 to 6.7) with those for a 'construction sequence analysis' (Figs. 6.10 to 6.12) indicates that the results are substantially the same except on the exterior face of the cylinder wall immediately below the ring beam. A comparison of stress states at the springing line of the dome indicates that, while thickening of the dome has a substantial effect on stresses arising from each load case (see, for example, Figs. 6.1 and 6.3), the effect on serviceability limit states is much more subdued (see, for example, Fig. 6.6). Nevertheless, the change is sufficient to alter the pressurization factors enough to satisfy the design criteria under the conditions of this analysis.

7.2 Limitations on FLEXSHELL

The following limitations on the FLEXSHELL program, as developed herein, have been stated throughout the report but are summarized as follows:

- (a) The program assumes thin shells.
- (b) For spherical segments the program uses a classical solution of simplified thin shell equations which requires the minimum

angle subtended by any shell segment to be in the order of 20° to 30° .

- (c) For spherical segments the M2 stress resultants are less accurate than other stress resultants although they appear to be reliable in all critical areas for Gentilly-type structures.
- (d) The base segments assume a Winkler type of foundation and use asymptotic expansions of the solution of the governing differential equation.

The advantages of a FLEXSHELL approach are stated in Sect. 1.2.

7.3 Conclusions

Within the context of this study, at its present stage of development, it may be concluded that FLEXSHELL is a simple effective tool for use in the prediction of serviceability states for Gentilly-type structures.

REFERENCES

REFERENCES

1. "Safety Report: Gentilly-2 600MW Nuclear Power Station", Atomic Energy of Canada Limited, Report to the Atomic Energy Control Board (for Hydroelectricite de Quebec).
2. Baker, E.H., Kovalevsky, L., Rish, F.L., "Structural Analysis of Shells", McGraw-Hill Book Company Inc., New York, 1972.
3. Billington, D.P., "Thin Shell Concrete Structures", McGraw-Hill Book Company, Inc., New York, 1965.
4. Bushnell, D., "Stress, Stability and Vibration of Complex Branched Shells of Revolution: User's Manual for BOSOR4", Lockheed Missiles and Space Company, Inc., Sunnyvale, California.
5. Bushnell, D., "Analysis of Ring Stiffened Shells of Revolution Under Combined Thermal and Mechanical Loading", Journal of the American Institute of Aeronautics and Astronautics, Vol. 9, No. 3, March 1971, pp. 401-410.
6. Epstein, M., Murray, D.W., "An Elastic Stress Analysis of a Gentilly Type Containment Structure - Volume 1", Structural Engineering Report No. 55, The University of Alberta, Edmonton, April 1976.
7. Epstein, M., Murray, D.W., "An Elastic Stress Analysis of a Gentilly Type Containment Structure - Volume 2, (Appendices B to F)", Structural Engineering Report No. 56, The University of Alberta, Edmonton, April 1976.
8. Flügge, W., "Stresses in Shells", 2nd Edition, Springer-Verlag, New York - Berlin, 1973.
9. Markus, G., "Theorie und Berechnung Rotations Symmetrischer Bauwerke", (Theory and Analysis of Axisymmetrical Structures), 2nd Edition, Werner-Verlag, Düsseldorf, 1976.
10. Pflüger, A., "Elementare Schalenstatik" (Elementary Shell Analysis), 4th Edition, Springer-Verlag, Berlin - New York, 1967. (An English Edition of an earlier version of this book is "Elementary Statics of Shells", 2nd Edition, F. W. Dodge Corporation, New York, 1961. This edition does not contain the homogeneous solutions.)
11. Timoshenko, S., and Woinowsky-Krieger, S., "Theory of Plates and Shells", 2nd Edition, McGraw-Hill Book Company, Inc., 1959.
12. Tsui, E.Y.W., "Stresses in Shells of Revolution" Pacific Coast Publishers, Menlo Park, California, 1968.
13. Jahnke, E., Emde, F., "Tables of Functions", Dover Publications, New York, 1945.

14. Stiglat, Wipple, "Platten", Wilhelm Ernst & Sohn, Berlin, 1973.

TABLES

Segment	Segment Type	IR (Top End)	JR (Bottom End)	ECI	ECJ
1	2	0	1		-3.5
2	1	0	1		
3	1	1	1		
4	1	0	1		
5	2	1	1		-3.5
6	1	1	1		
7	1	1	0	-1.0	

(a) Segment Types, Redundant Flags and Eccentricities (INPUT)

Segment	Top Forces		Bottom Forces	
1	0	0	1	2
2	0	0	3	4
3	5	6	7	8
4	0	0	9	10
5	11	12	13	14
6	15	16	17	18
7	19	20	0	0

(b) Identification of Segment End Forces (GENERATED)

Top Segment	Bottom Segment
1	3
2	3
3	6
4	5
5	6
6	7

(c) Segment Connectivities (INPUT)

TABLE 2.1 - SEGMENT DEFINITION AND CONNECTIVITY ARRAYS

TABLE 3.1 - DERIVATIVES OF BASE SEGMENT
{ ϕ } VECTOR

ϕ_1	$e^\sigma \sigma^{-1/2} \eta^{-1} \cos(\sigma - \beta)$
$\dot{\phi}_1$	$(1 - 1/(2\sigma))\phi_1 - \phi_2$
$\ddot{\phi}_1$	$\phi_1/(2\sigma^2) + (1 - 1/(2\sigma))\dot{\phi}_1 - \dot{\phi}_2$
$\overset{\circ}{\phi}_1$	$-\phi_1/\sigma^3 + \dot{\phi}_1/\sigma^2 + (1 - 1/(2\sigma))\ddot{\phi}_1 - \ddot{\phi}_2$
ϕ_2	$e^\sigma \sigma^{-1/2} \eta^{-1} \sin(\sigma - \beta)$
$\dot{\phi}_2$	$(1 - 1/(2\sigma))\phi_2 + \phi_1$
$\ddot{\phi}_2$	$\phi_2/(2\sigma^2) + (1 - 1/(2\sigma))\dot{\phi}_2 + \dot{\phi}_1$
$\overset{\circ}{\phi}_2$	$-\phi_2/\sigma^3 + \dot{\phi}_2/\sigma^2 + (1 - 1/(2\sigma))\ddot{\phi}_2 + \ddot{\phi}_1$
ϕ_3	$\pi e^{-\sigma} \sigma^{-1/2} \eta^{-1} \cos(\sigma + \beta)$
$\dot{\phi}_3$	$-(1 + 1/(2\sigma))\phi_3 - \phi_4$
$\ddot{\phi}_3$	$\phi_3/(2\sigma^2) - (1 + 1/(2\sigma))\dot{\phi}_3 - \dot{\phi}_4$
$\overset{\circ}{\phi}_3$	$-\phi_3/\sigma^3 + \dot{\phi}_3/\sigma^2 - (1 + 1/(2\sigma))\ddot{\phi}_3 - \ddot{\phi}_4$
ϕ_4	$\pi e^{-\sigma} \sigma^{-1/2} \eta^{-1} \sin(\sigma + \beta)$
$\dot{\phi}_4$	$-(1 + 1/(2\sigma))\phi_4 + \phi_3$
$\ddot{\phi}_4$	$\phi_4/(2\sigma^2) - (1 + 1/(2\sigma))\dot{\phi}_4 + \dot{\phi}_3$
$\overset{\circ}{\phi}_4$	$-\phi_4/\sigma^3 + \dot{\phi}_4/\sigma^2 - (1 + 1/(2\sigma))\ddot{\phi}_4 + \ddot{\phi}_3$

- Notation:
1. $(\dot{}) = d()/d\sigma$
 2. $\frac{d()}{d r} = \frac{1}{\sqrt{2}l} \frac{d()}{d \sigma}$
 3. $\eta = 2^{0.75} \pi^{0.5}$
 4. $\beta = \pi/8$

TABLE 4.1 - COMPUTATION OF PRESTRESS LOADING

a. Distributed Cylinder Wall Pressure (Horizontal Cables)

$$p = 2.41 \frac{\text{in}^2}{\text{ft}} \times \frac{153 \text{ ksi}}{69.75 \text{ ft}} = 5286 \text{ psf}$$

b. Distributed Ring Beam Prestress Pressures

Lower Ring Beam (4.5 ft: 4 cables)

$$p = \frac{4 \text{ cables} \times 150.8 \text{ ksi} \times 5.08 \text{ in}^2}{70.75 \text{ ft} \times 4.5 \text{ ft} \text{ cable}} = 9625 \text{ psf}$$

Upper Ring Beam (9.5 ft: 4 cables)

$$p = \frac{4 \text{ cables} \times 150.8 \text{ ksi} \times 5.08 \text{ in}^2}{70.75 \text{ ft} \times 9.5 \text{ ft} \text{ cable}} = 4559 \text{ psf}$$

c. Distributed Dome Prestress Pressures

$$p = \frac{712 \text{ k}}{\text{cable}} \times \frac{3 \text{ layers}}{3 \text{ ft/cable}} \times \frac{1}{137 \text{ ft}} = 5197 \text{ psf}$$

d. Vertical Wall Prestressing

$$\text{Load/ft} = 1.30 \frac{\text{in}^2}{\text{ft}} \times 153.5 \text{ ksi} = 199.5 \text{ k/ft}$$

$$\text{PSF Load/ft} = 199.5 \text{ k/ft} \times 69.75/70.75 = 196.68 \text{ k/ft}$$

$$\text{PSF Moment} = 199.5 \text{ k/ft} \times 1 \text{ ft} \times 69.75/70.75 = 196.68 \text{ 'k/ft}$$

e. Anchorage Forces for Dome Prestressing

$$P = 5197 \text{ psf} \times \frac{137}{2} \text{ ft} = 356 \text{ k/ft}$$

$$H = 356 \text{ k/ft} \times \cos 29.398 \times 67.25/70.75 = 294.82 \text{ k/ft}$$

$$V = 356 \text{ k/ft} \times \sin 29.398 \times 67.25/70.75 = 166.11 \text{ k/ft}$$

$$M = H \cdot e = 294.82 \text{ k/ft} \times 1.972 \text{ ft} = 581.39 \text{ 'k/ft}$$

TABLE 5.1 - INFLUENCE OF THE FOUNDATION SUBGRADE COEFFICIENT ON STRESS RESULTANTS

STRESS RESULTANT	INT. PRESSURE (1 PSF)			PRESTRESS			DEAD LOAD		
	k= 450000 p/ft ³	k= 900000 p/ft ³	Change %	k= 450000 p/ft ³	k= 900000 p/ft ³	Change %	k= 450000 p/ft ³	k= 900000 p/ft ³	Change %
N1 (1b/ft)	32.94	32.94	0	-202350	-202350	0	-104600	-104600	0
N2 (1b/ft)	1.683	5.907	251%	-200290	-197590	-1.3%	10939	-841	
M1 ($\frac{\text{ft-lb}}{\text{ft}}$)	-50.66	-38.71	-23.6%	51992	59641	14.7%	65550	32223	-50.8%
M2 ($\frac{\text{ft-lb}}{\text{ft}}$)	-7.598	-5.806	-23.6%	7799	8946	14.7%	9832	4833	-50.8%

TABLE 6.1 - STRESSES (SI) IN DOME INCLUDING THE EFFECT OF ACTUAL THICKNESS (in psi)

1	2	3	4	5	6	7	8	9
POINT	COORD.	THICKNESS	INT. PRESSURE (1 PSF) SI I SI E	"SWITCHED-ON" D.L. & PRESTRESS SI I SI E	RF1 SI I SI E			
35	24.988	2.0	32.80	27.73	-1223	-1334	-1181	-1378
36	25.723	2.09	40.00	16.20	-1248	-1182	-1208	-1223
37	26.458	2.20	47.49	4.132	-1274	-1016	-1236	-1054
38	27.193	2.34	54.49	-7.67	-1292	-844	-1259	-875
39	27.928	2.52	59.35	-18.27	-1293	-672	-1266	-697
40	28.663	2.95	56.40	-22.07	-1161	-503	-1144	-517
41	29.398	3.87	42.57	-17.38	-890	-367	-882	-372

TABLE 6.2 - PRESSURES (P1) FOR ZERO TENSION AND CRACKING IN THE DOME (INCLUDING THICKENING)

10	11	12	13	14	15	16	17	18	19	20
POINT	COORD.	THICKNESS	TENSION PRESSURE FACTOR (SWITCHED-ON-RF1) P1 I P1 E	TENSION PRESSURE FACTOR (SWITCHED-ON-RF1) P1 I P1 E	CRACKING PRESSURE FACTOR (SWITCHED-ON-RF1) P1 I P1 E	TENSION PRESSURE FACTOR (RF1) P1 I P1 E	TENSION PRESSURE FACTOR (RF1) P1 I P1 E	CRACKING PRESSURE FACTOR (RF1) P1 I P1 E	CRACKING PRESSURE FACTOR (RF1) P1 I P1 E	CRACKING PRESSURE FACTOR (RF1) P1 I P1 E
			6/4	7/5	450-6/4	450-7/5	8/4	9/5	450-8/4	450-9/5
35	24.988	2.0	37.29	48.11	51.0	64.33	36.00	49.69	49.7	65.92
36	25.732	2.09	31.20	72.96	42.45	100.7	30.20	75.49	41.45	103.3
37	26.458	2.20	26.83	245.8	36.30	354.8	26.03	255.1	35.50	364.0
38	27.193	2.34	23.71	-110.0	31.97	-168.7	23.10	-114.1	31.36	-172.7
39	27.928	2.52	21.79	-36.78	29.37	-61.4	31.33	-38.15	28.91	-62.78
40	48.663	2.95	20.58	-22.79	28.56	-43.1	20.28	-23.42	28.26	-43.81
41	29.398	3.87	20.91	-21.12	31.48	-47.0	20.71	-21.40	31.29	-47.29

FIGURES

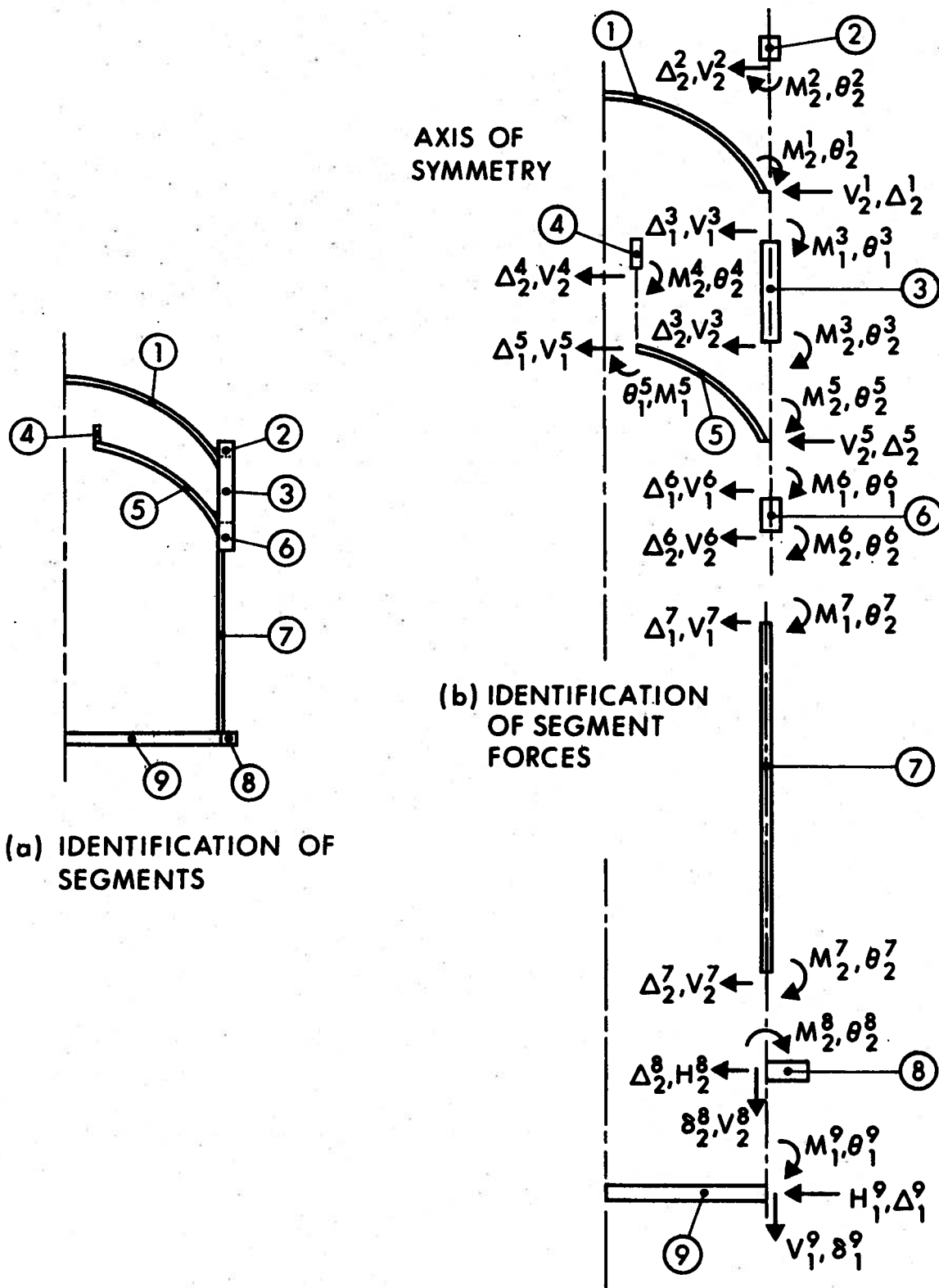


FIGURE 2.1 Typical Containment Structure

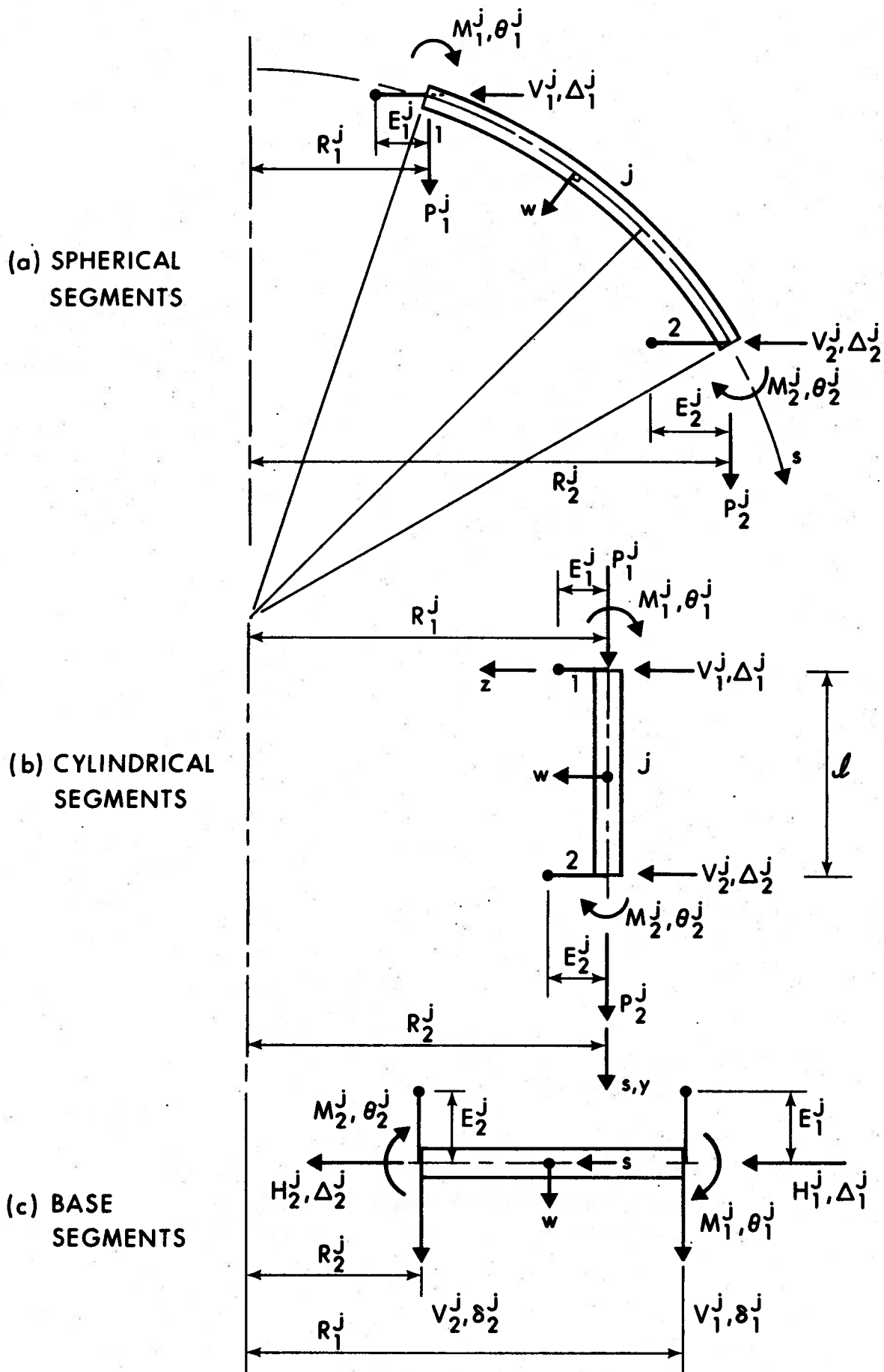
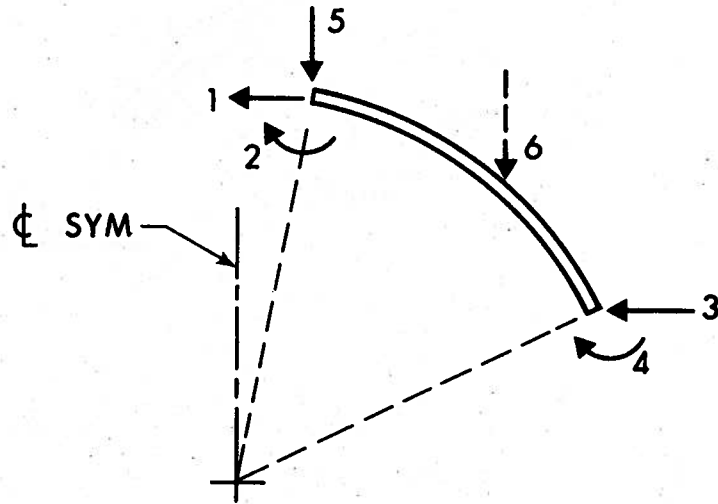
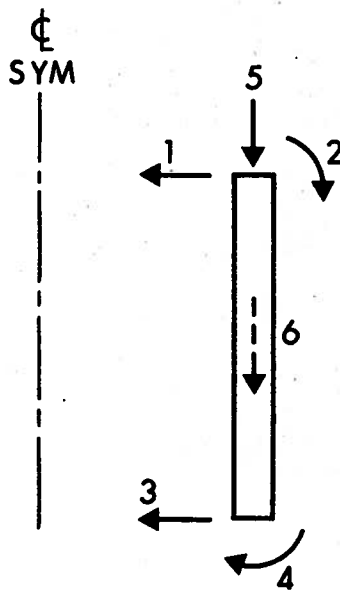


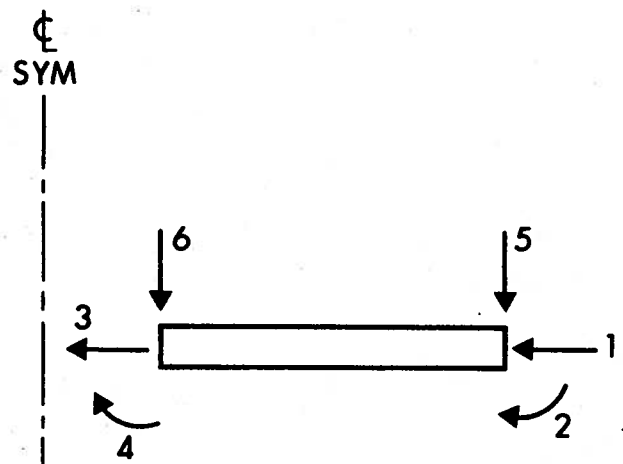
FIGURE 2.2 Sign Convention For Positive End Effects



(a) SPHERICAL SEGMENT



(b) CYLINDRICAL SEGMENTS



(c) BASE SEGMENTS

ARRAYS : PBF - PARTICULAR SOLUTION BASIC FORCES
 PSD - PARTICULAR SOLUTION DISPLACEMENTS
 PSF - PARTICULAR SOLUTION SEGMENT FORCES
 SF - SEGMENT FORCES

FIGURE 3.1 Subscripting of Segment Arrays

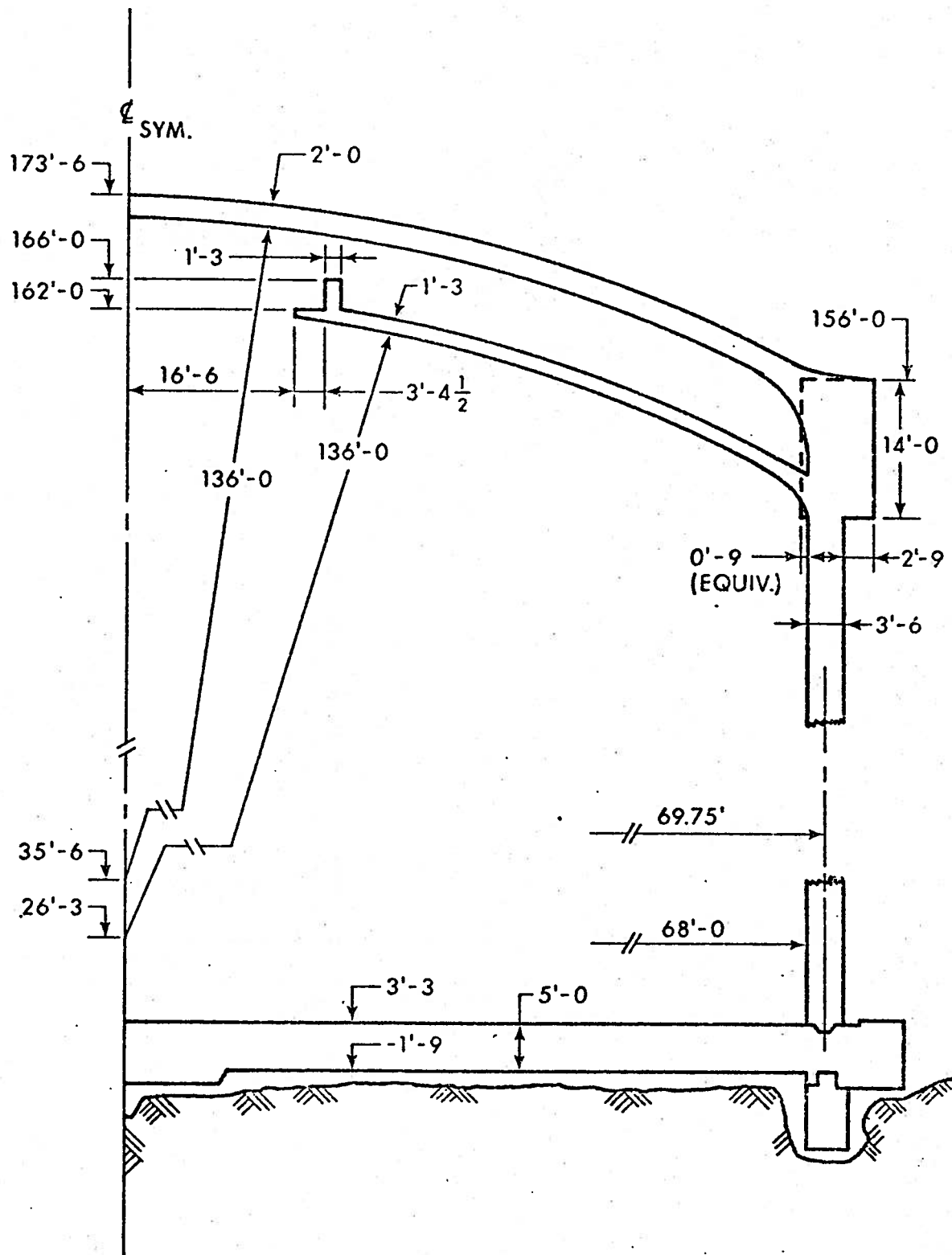


FIGURE 4.1 Principal Dimensions of GENTILLY-2

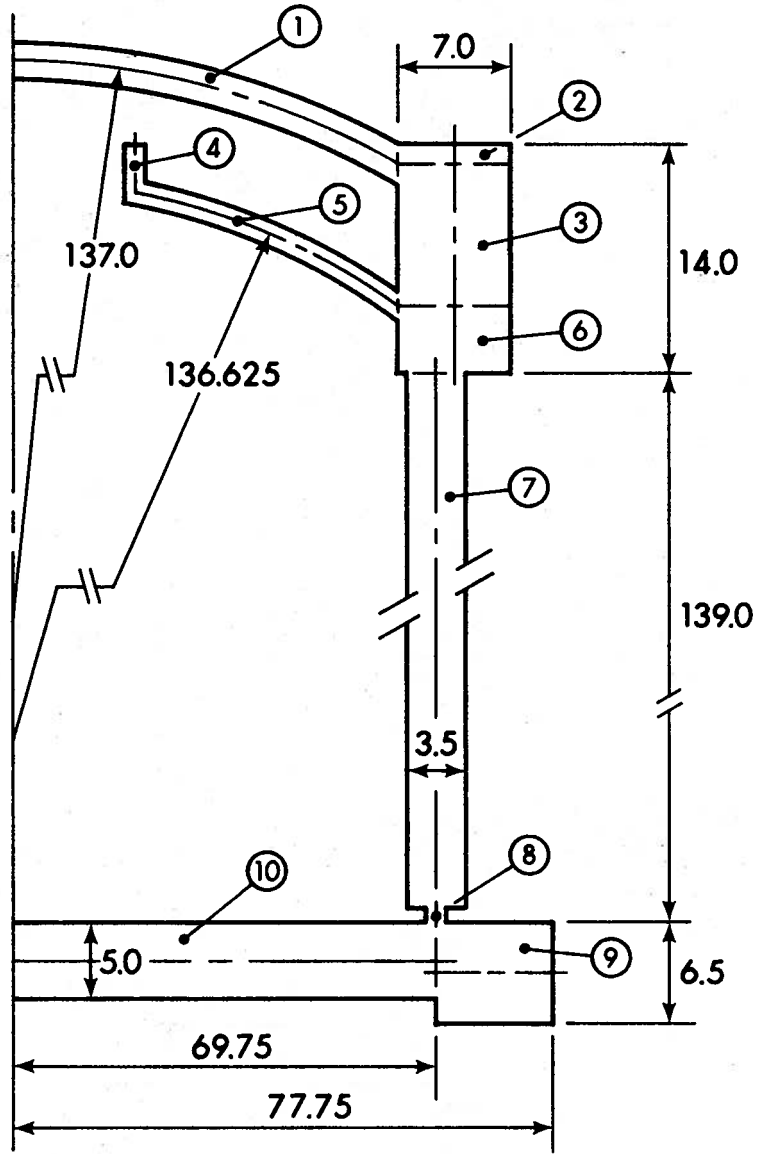


FIGURE 4.2 Standard Model for FLEXSHELL GENTILLY-2 Analyses

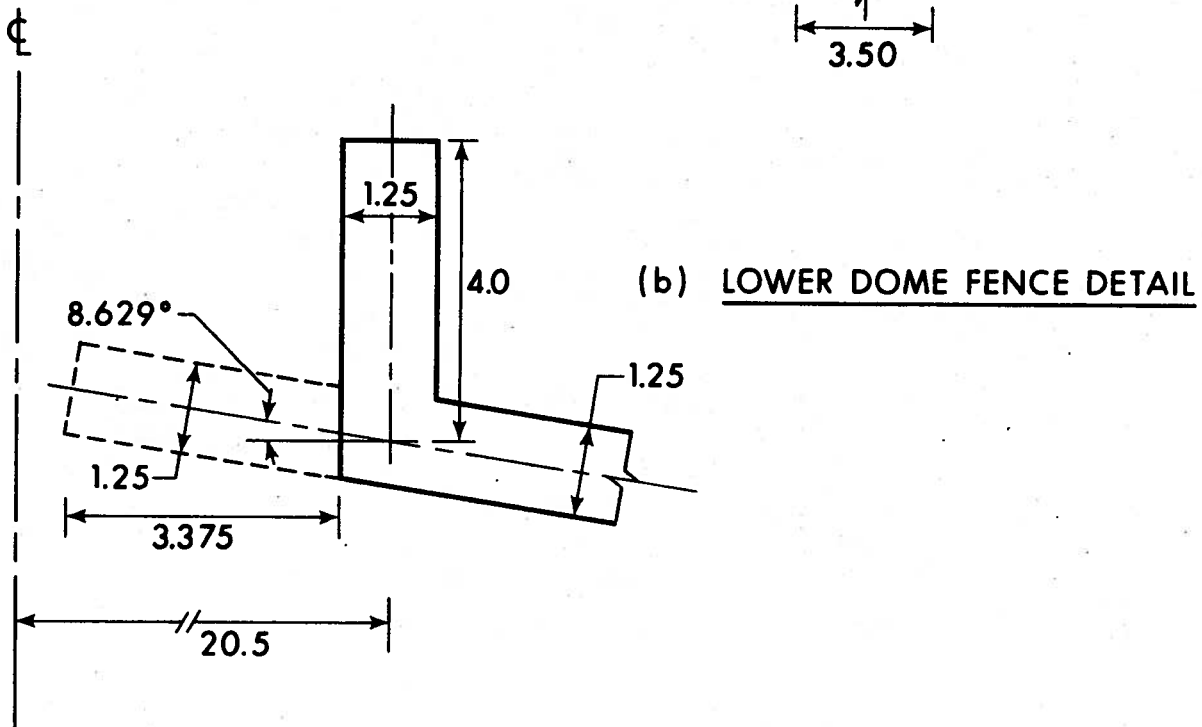
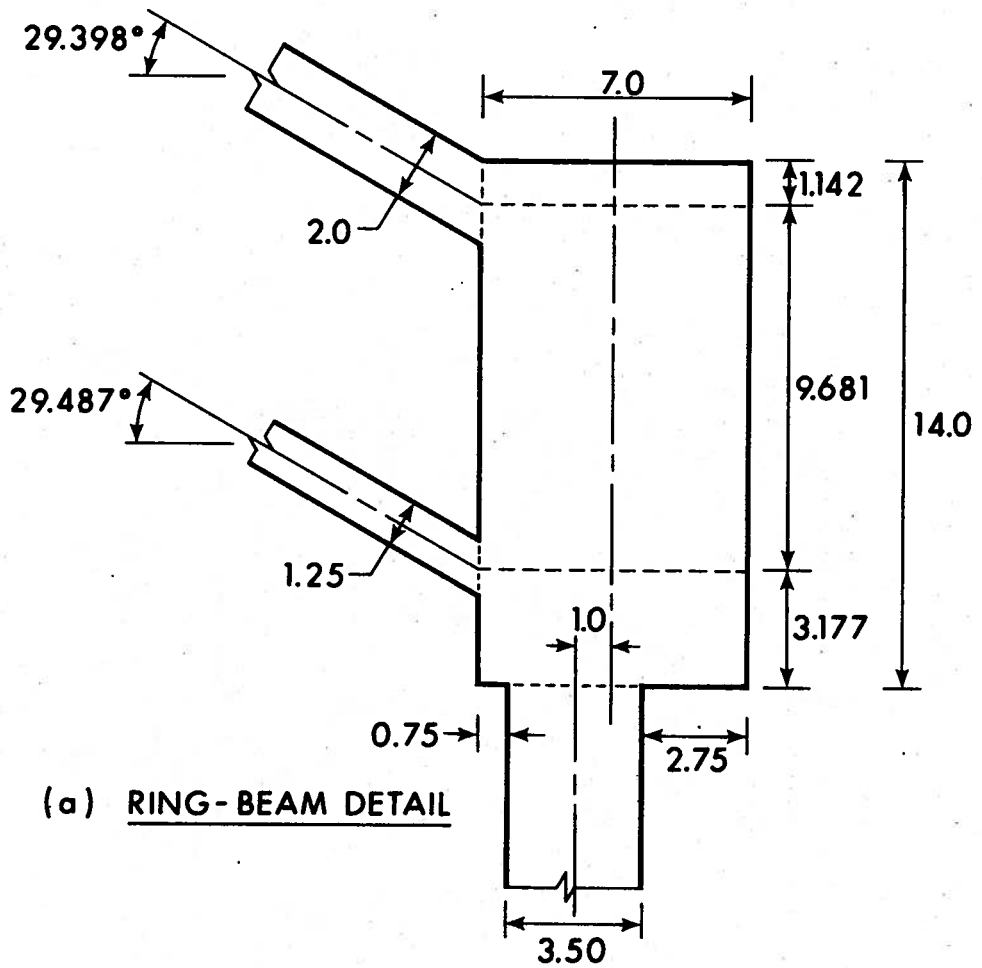
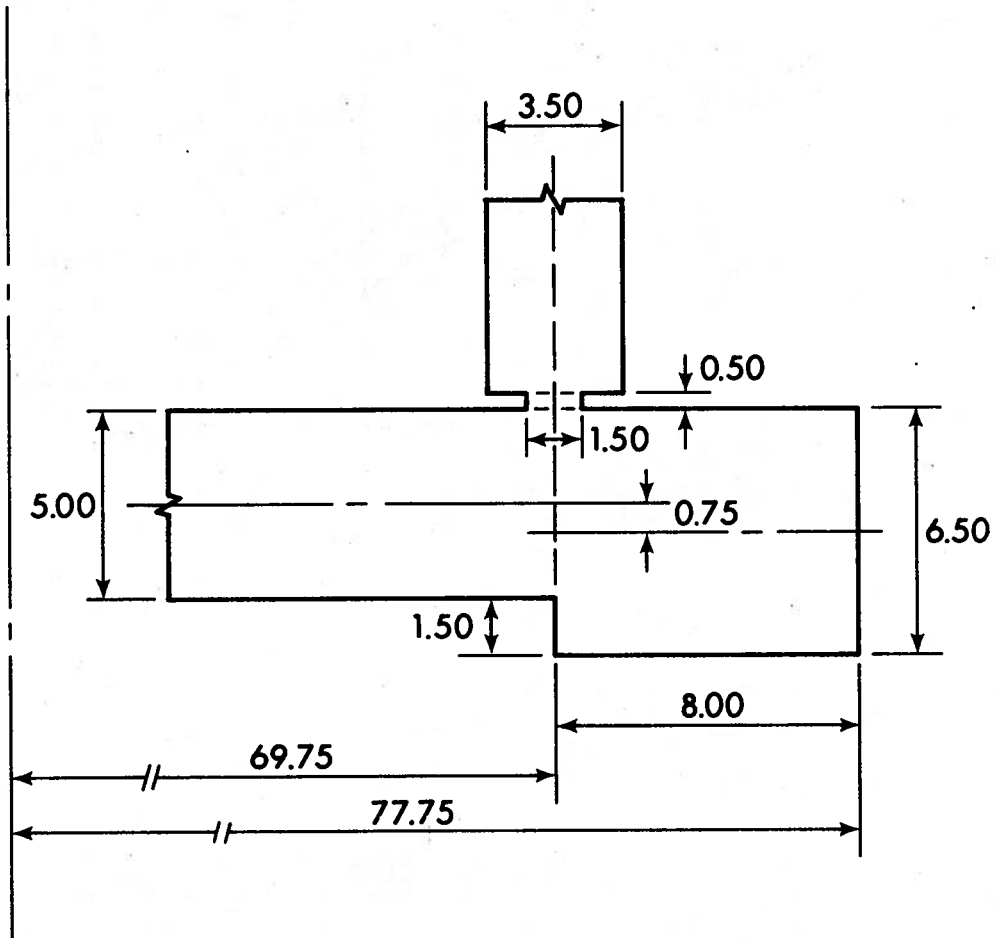


FIGURE 4.3a&b Details of Model



(c) WALL - BASE DETAIL

FIGURE 4.3c Details of Model

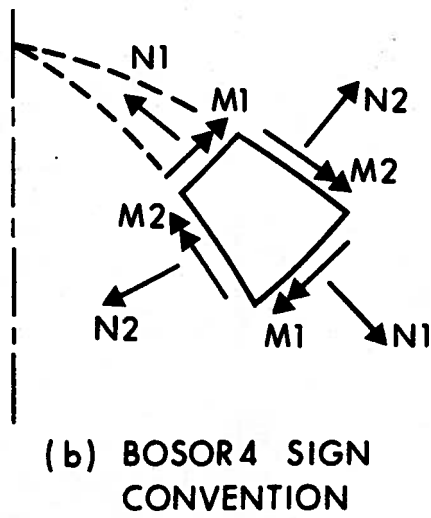
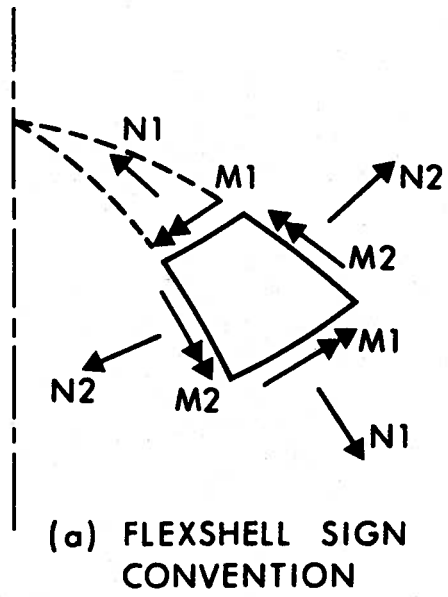
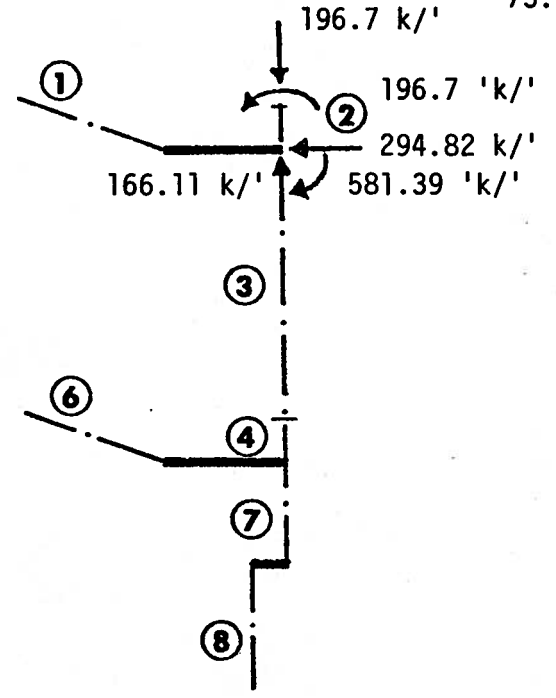
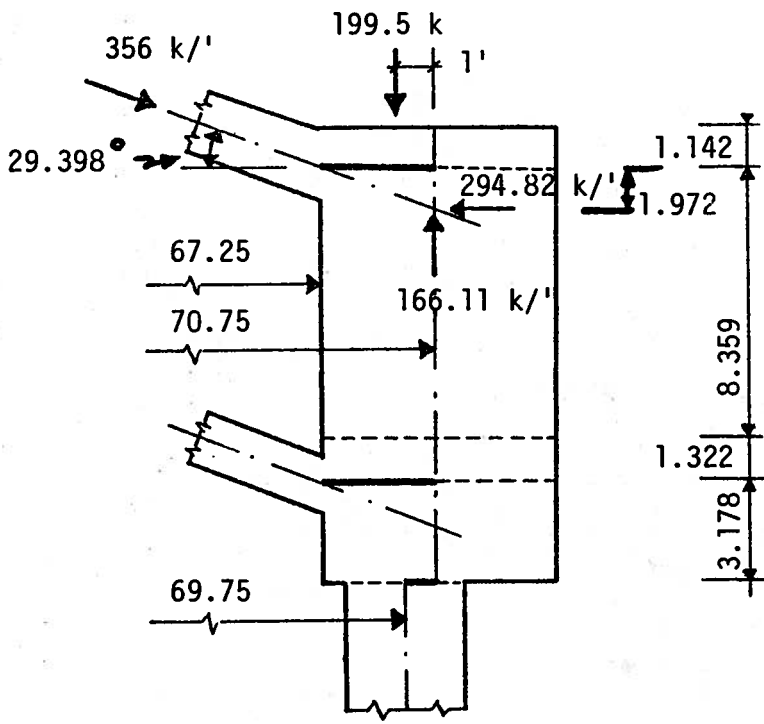
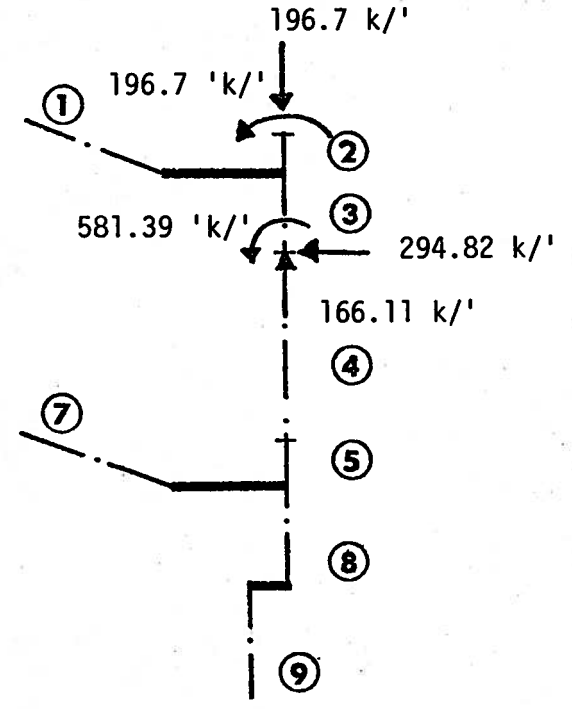
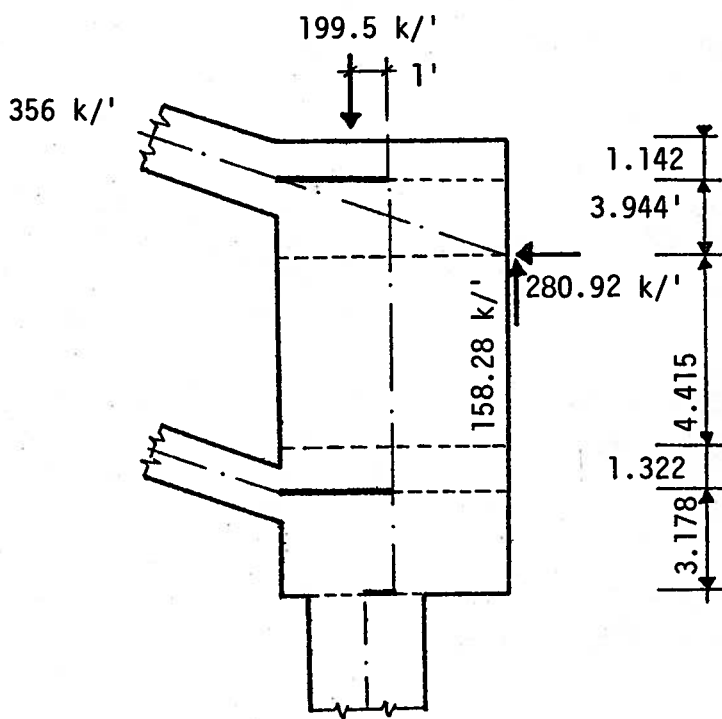


FIGURE 4.4 Stress Resultant Sign Convention



(a) PSF FORCES FOR SIMPLIFIED PRESTRESS



(b) PSF FORCES FOR BOSOR4 PRESTRESS

FIGURE 4.5 Prestressing PSF Forces

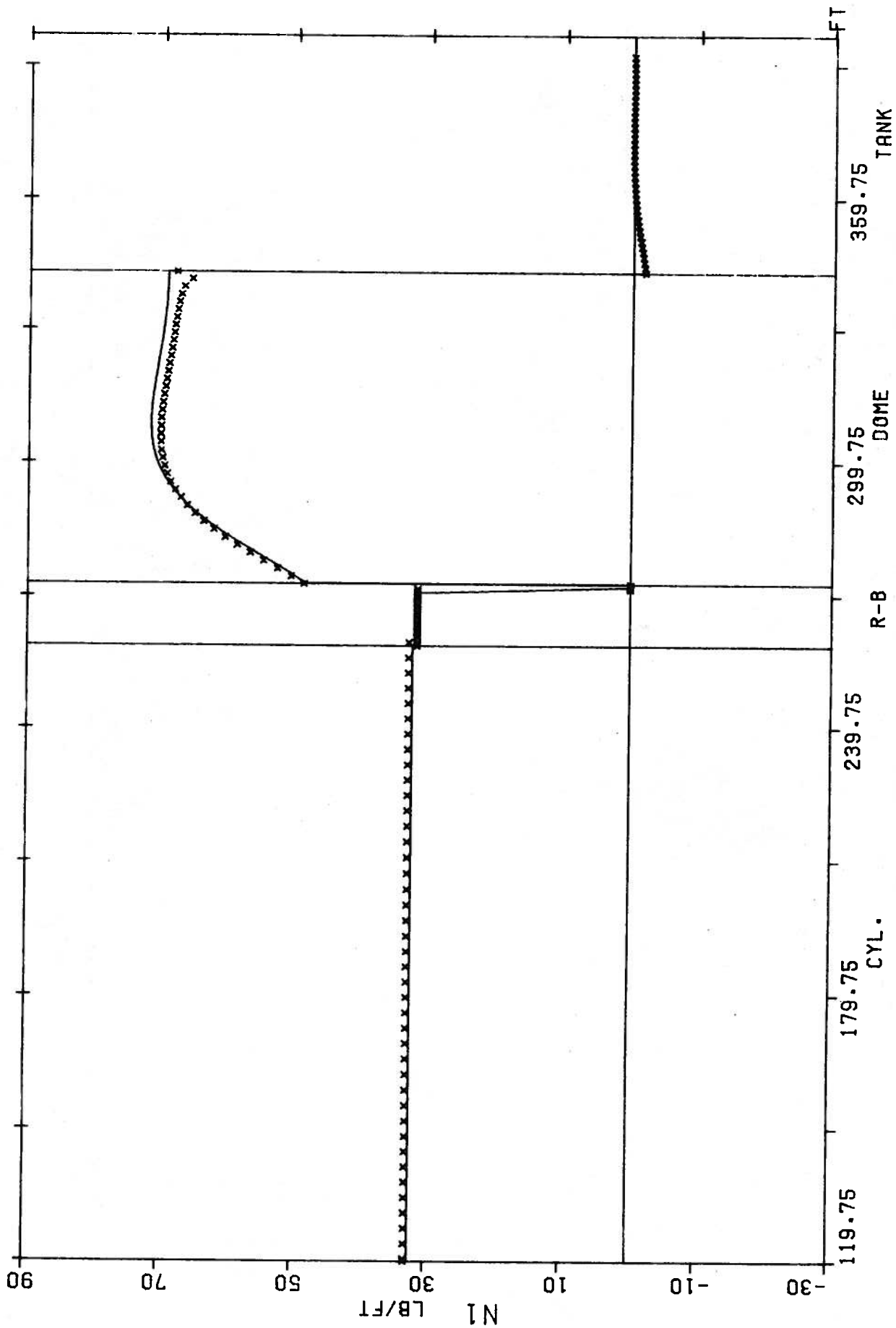


FIGURE 5.1 N1 INTERNAL PRESSURE (1LB/FT**2)

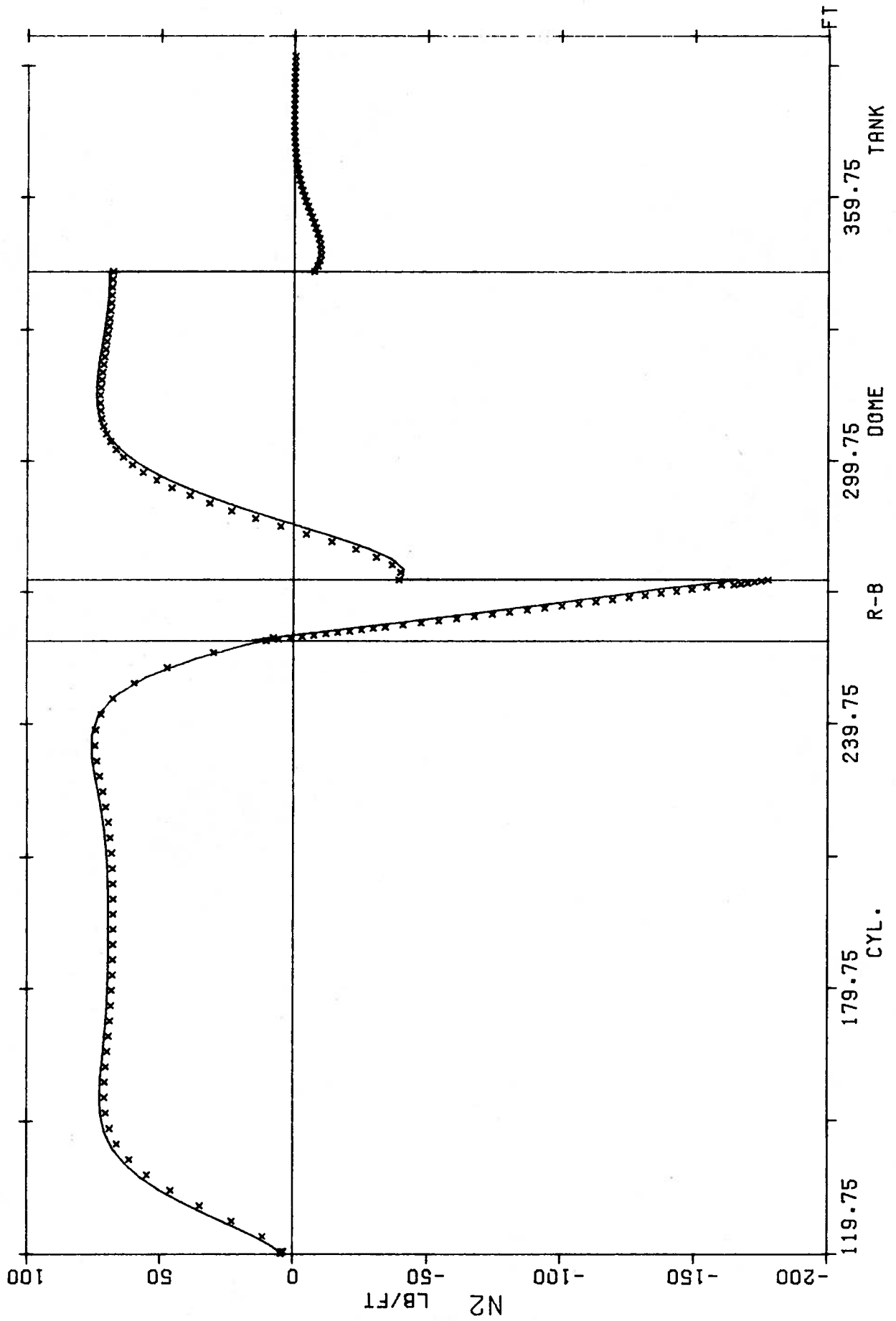


FIGURE 5.2 N2 INTERNAL PRESSURE (1LB/FT**2)

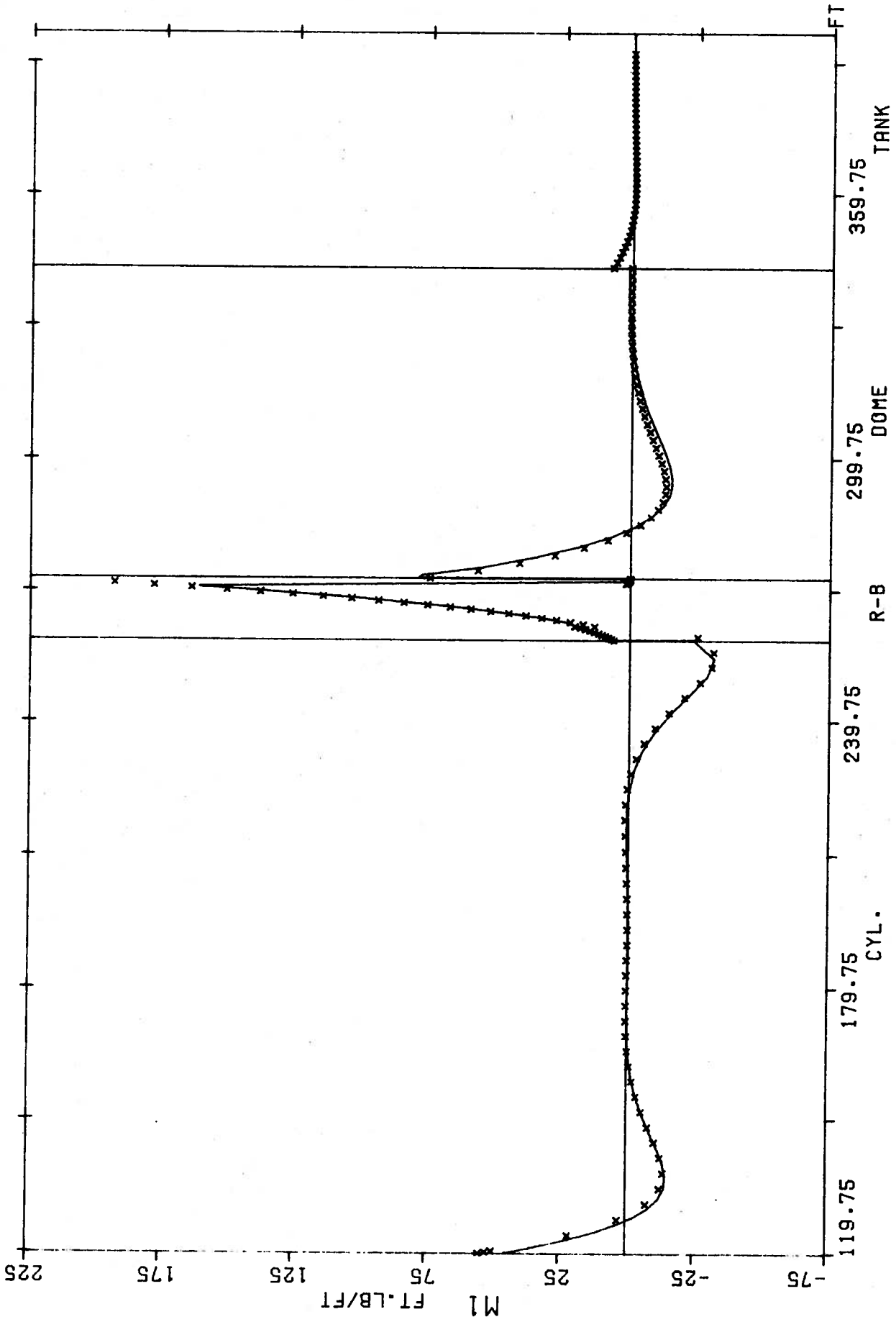


FIGURE 5.3 M1 INTERNAL PRESSURE (1LB/FT²)

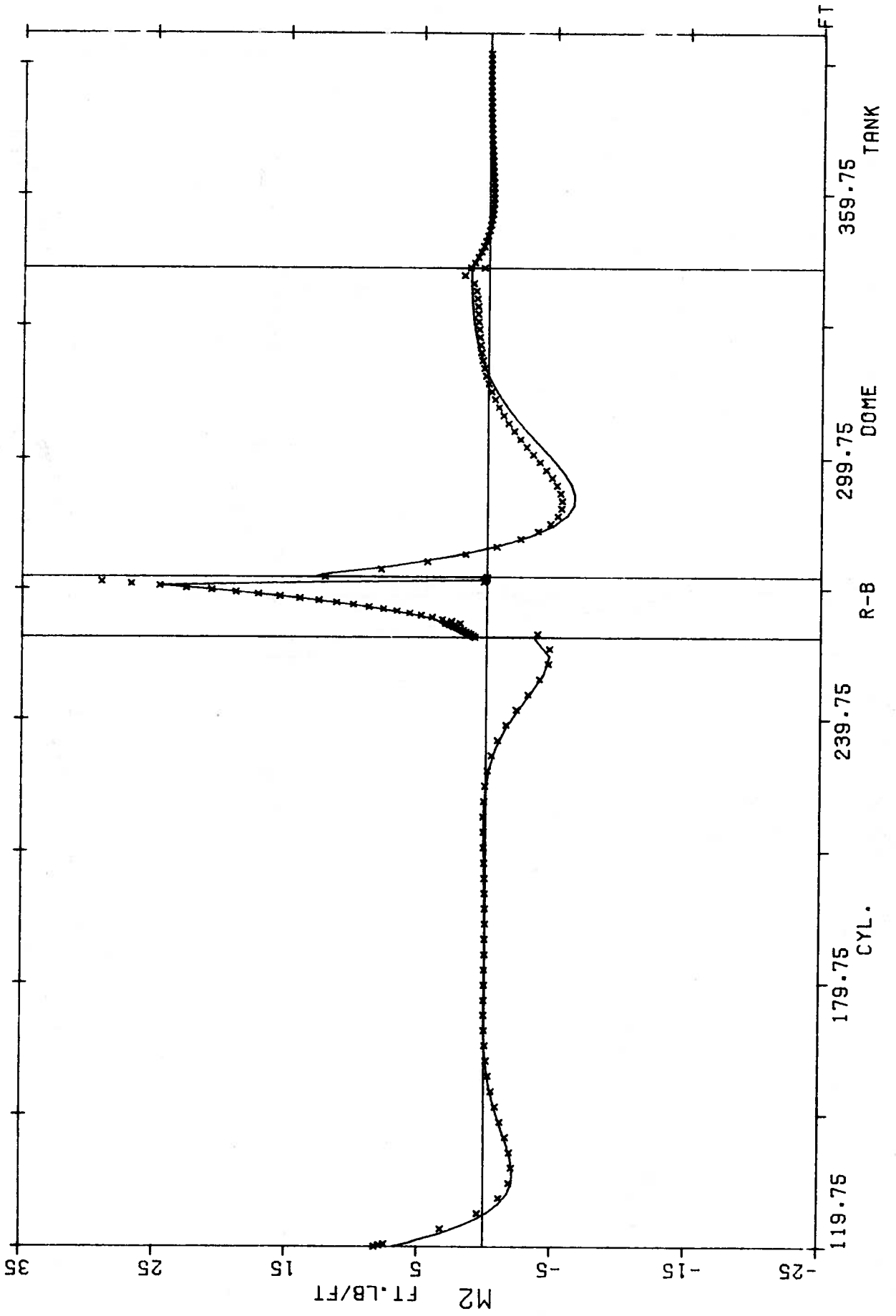


FIGURE 5.4 M2 INTERNAL PRESSURE (1LB/FT**2)

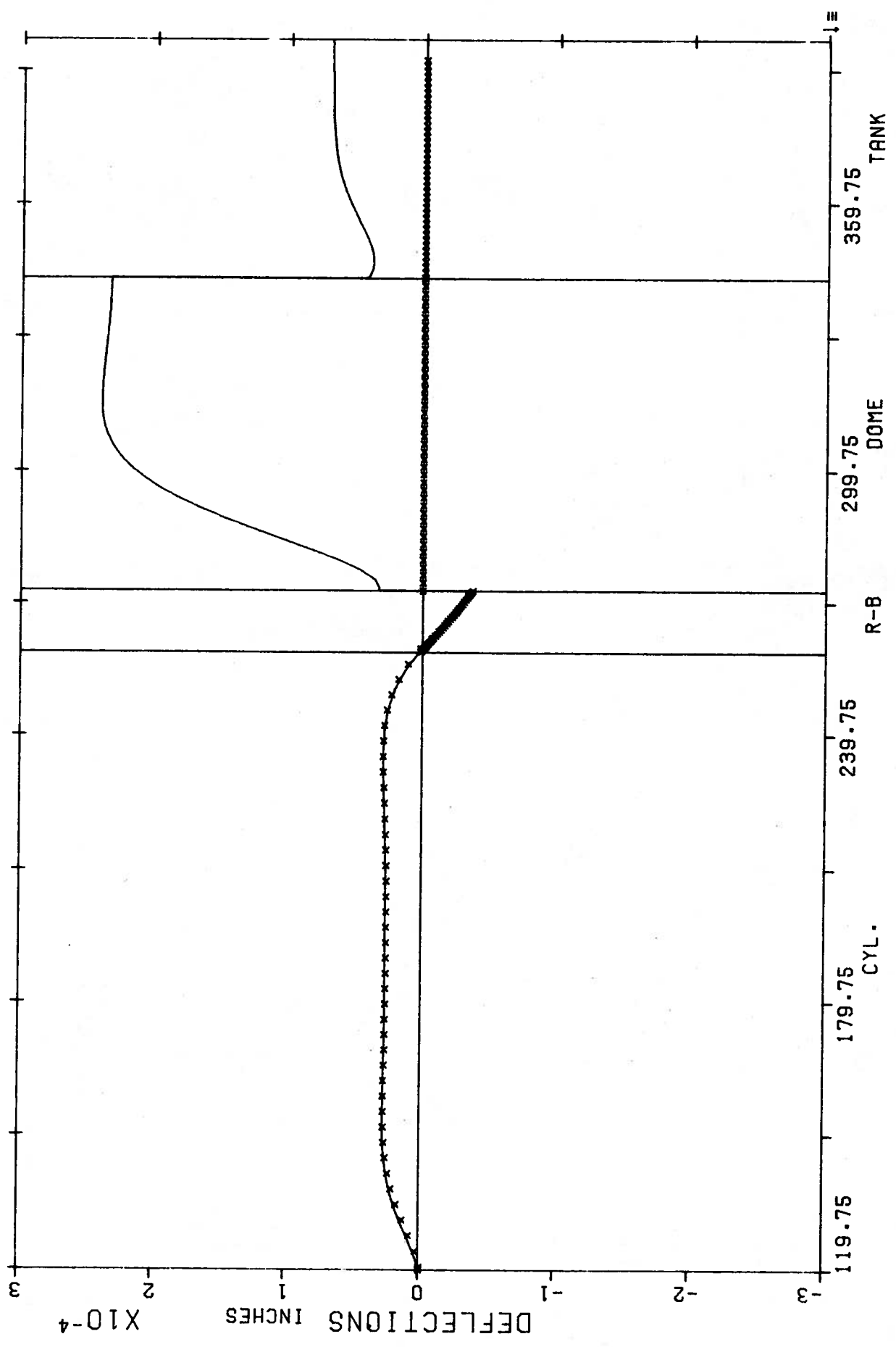


FIGURE 5.5 NORMAL DISPLACEMENTS INTERNAL PRESSURE (1LB/FT²)

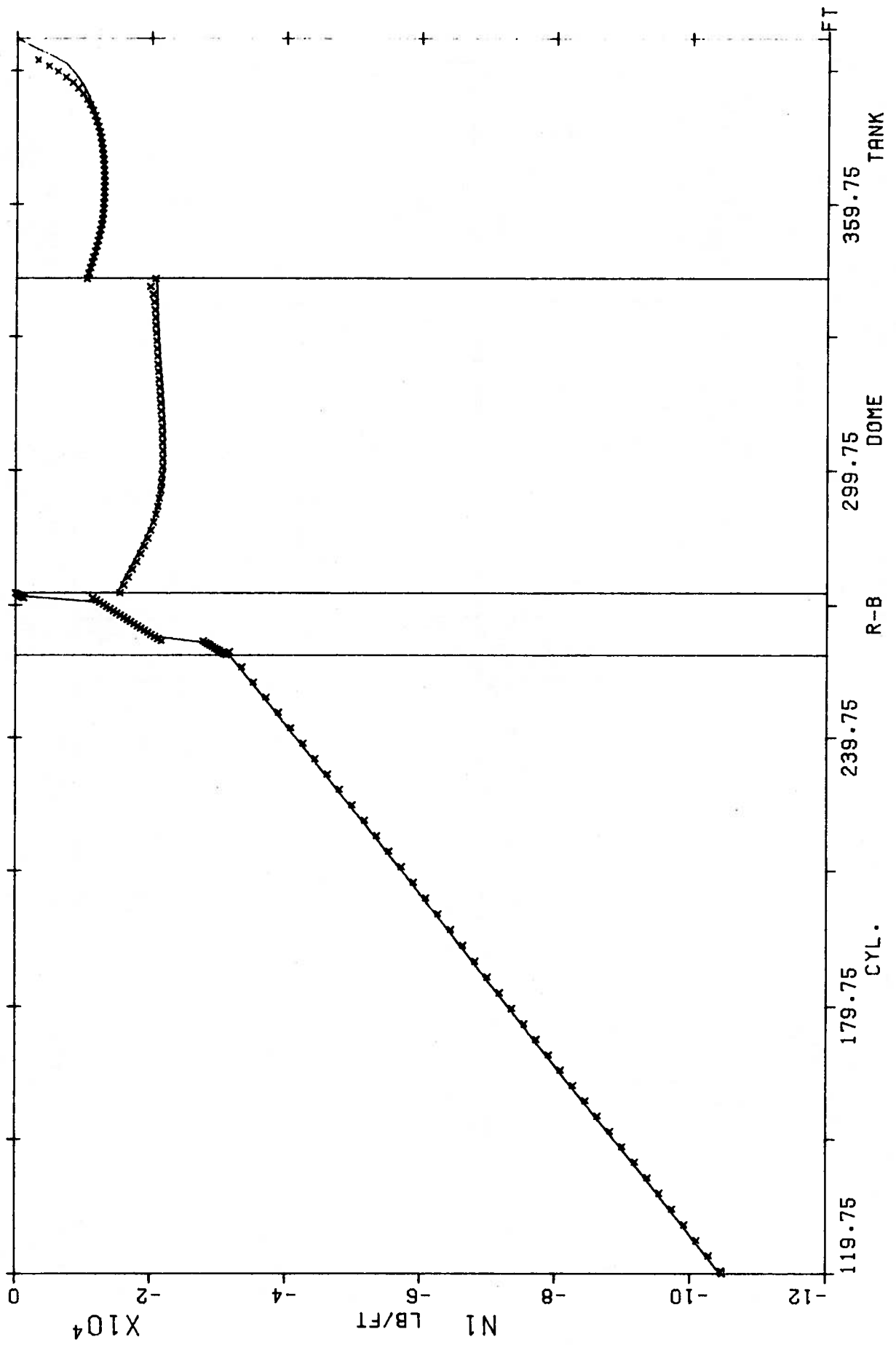


FIGURE 5.6 N1 DEAD LOAD OF 150 LB/FT

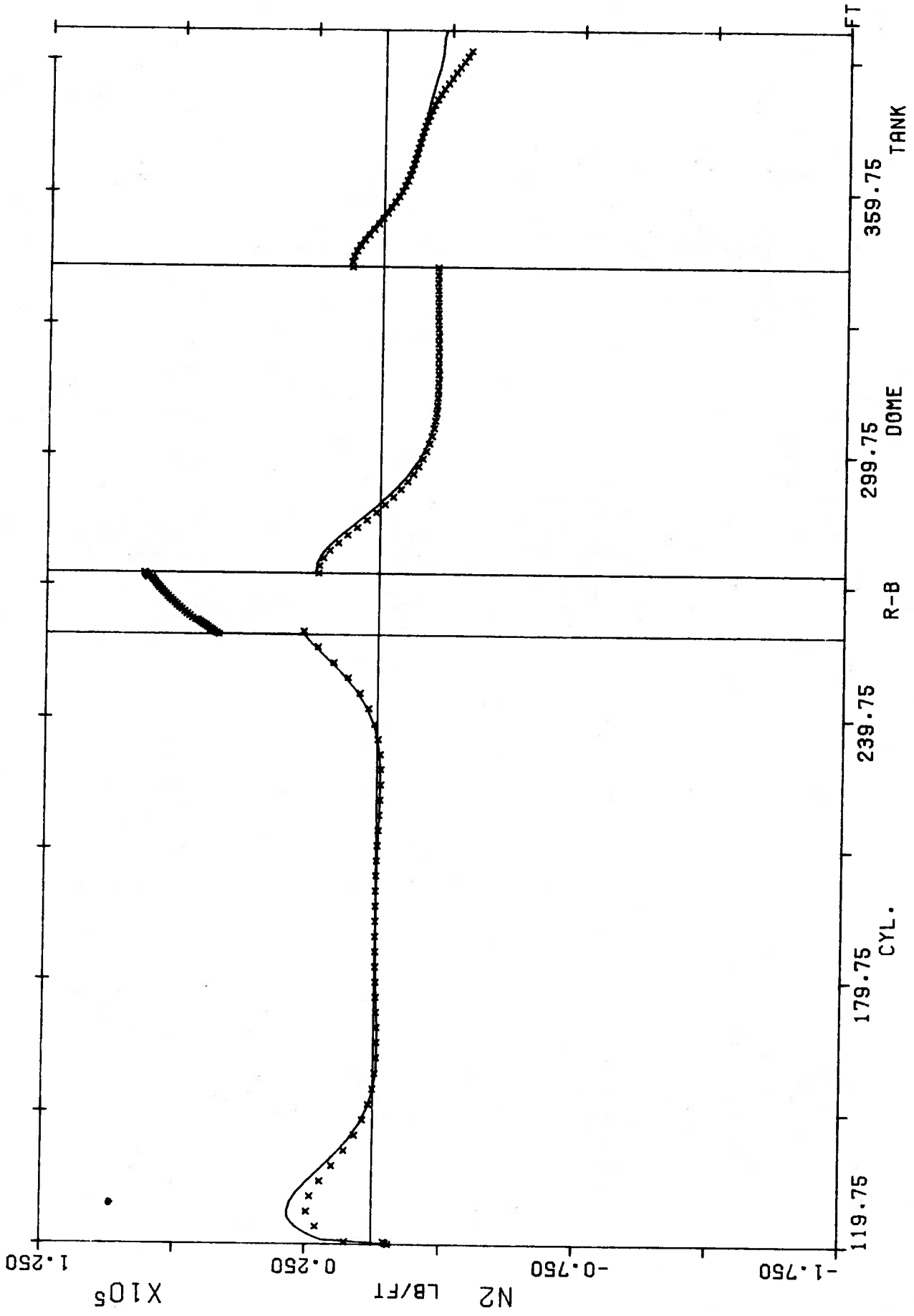


FIGURE 5.7 N2 DEAD LOAD OF 150 LB/FT#3

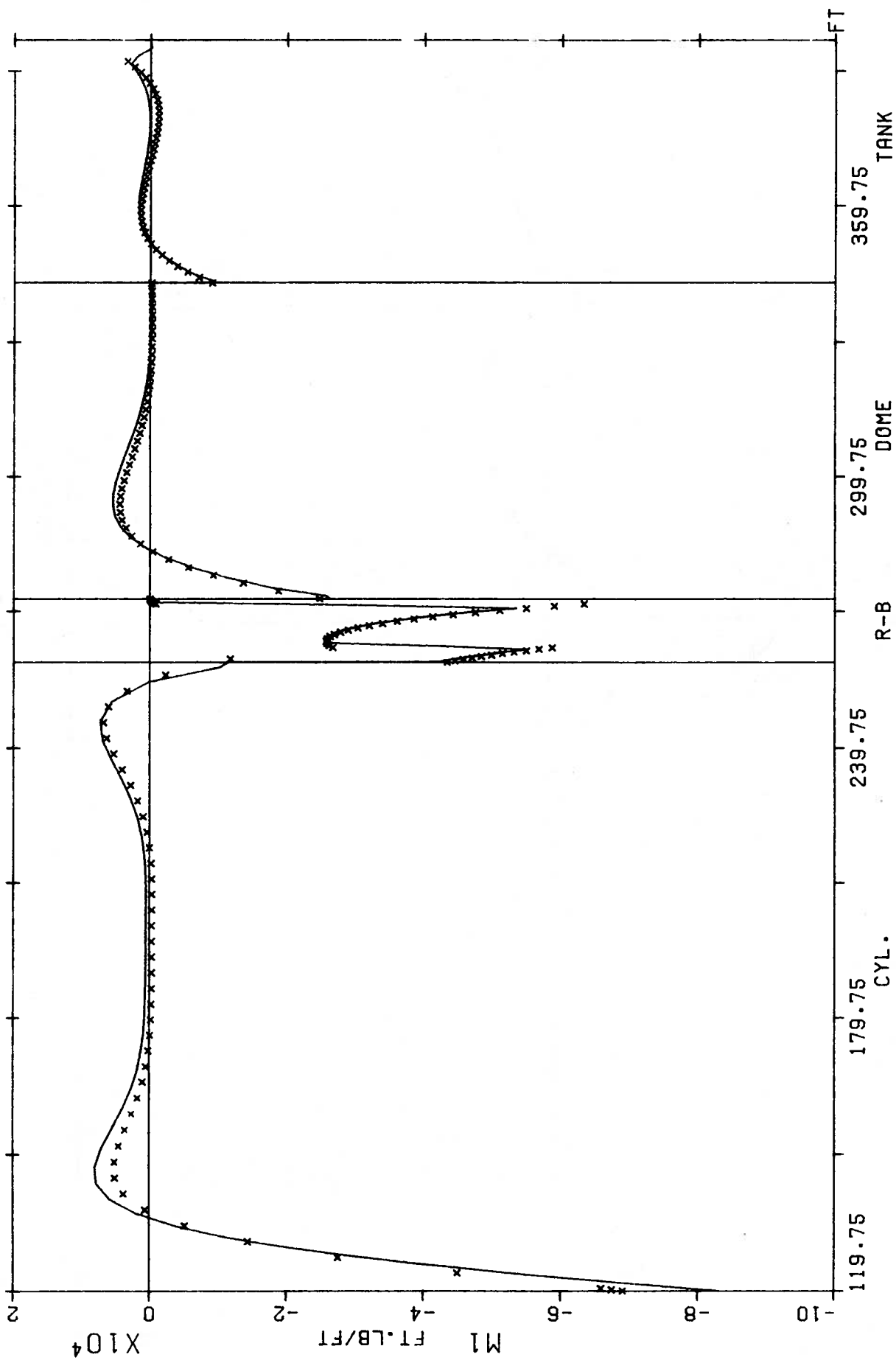


FIGURE 5.8 M1 DEAD LOAD OF 150 LB/FT#3

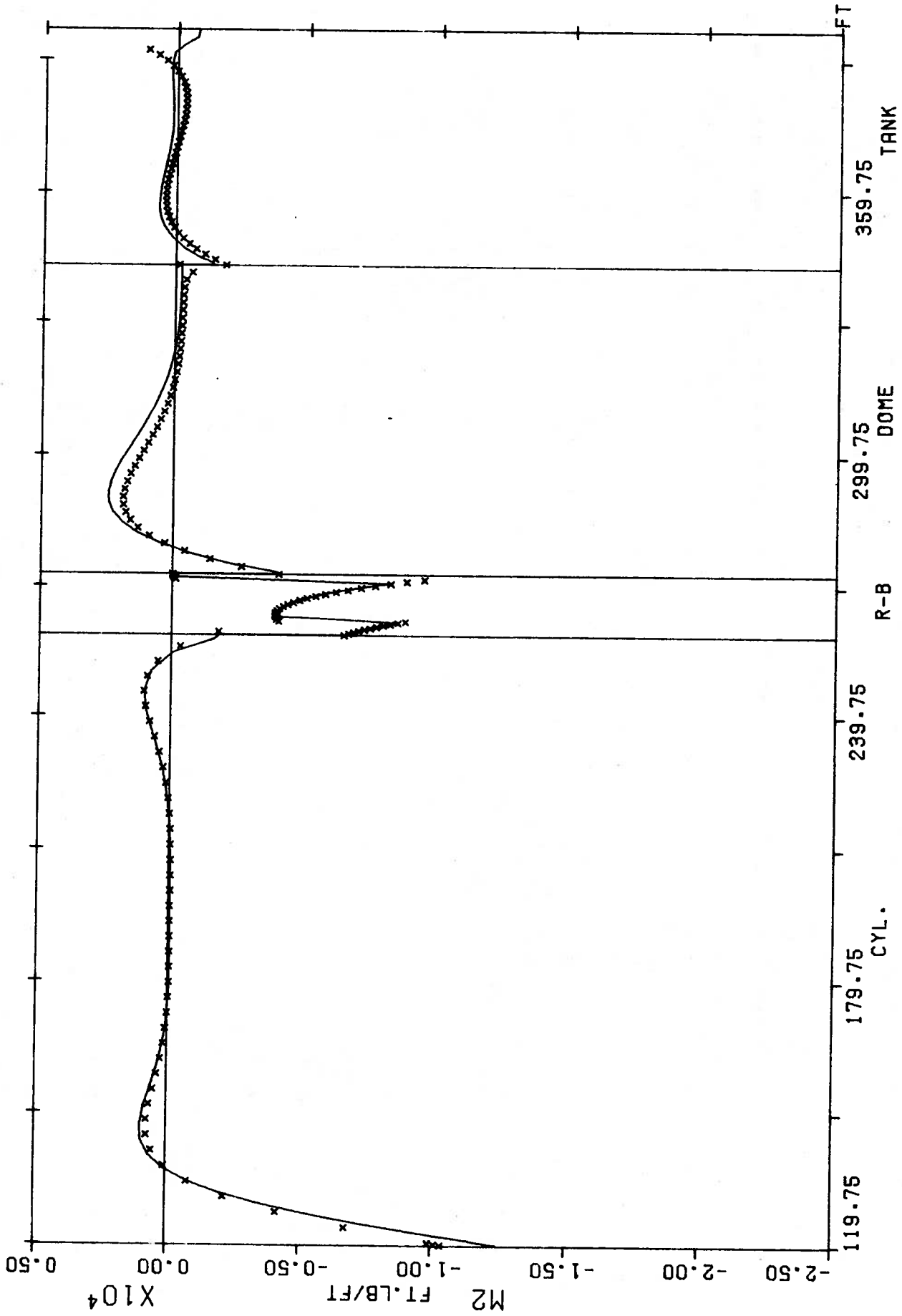


FIGURE 5.9 M2 DEAD LOAD OF 150 LB/FT³

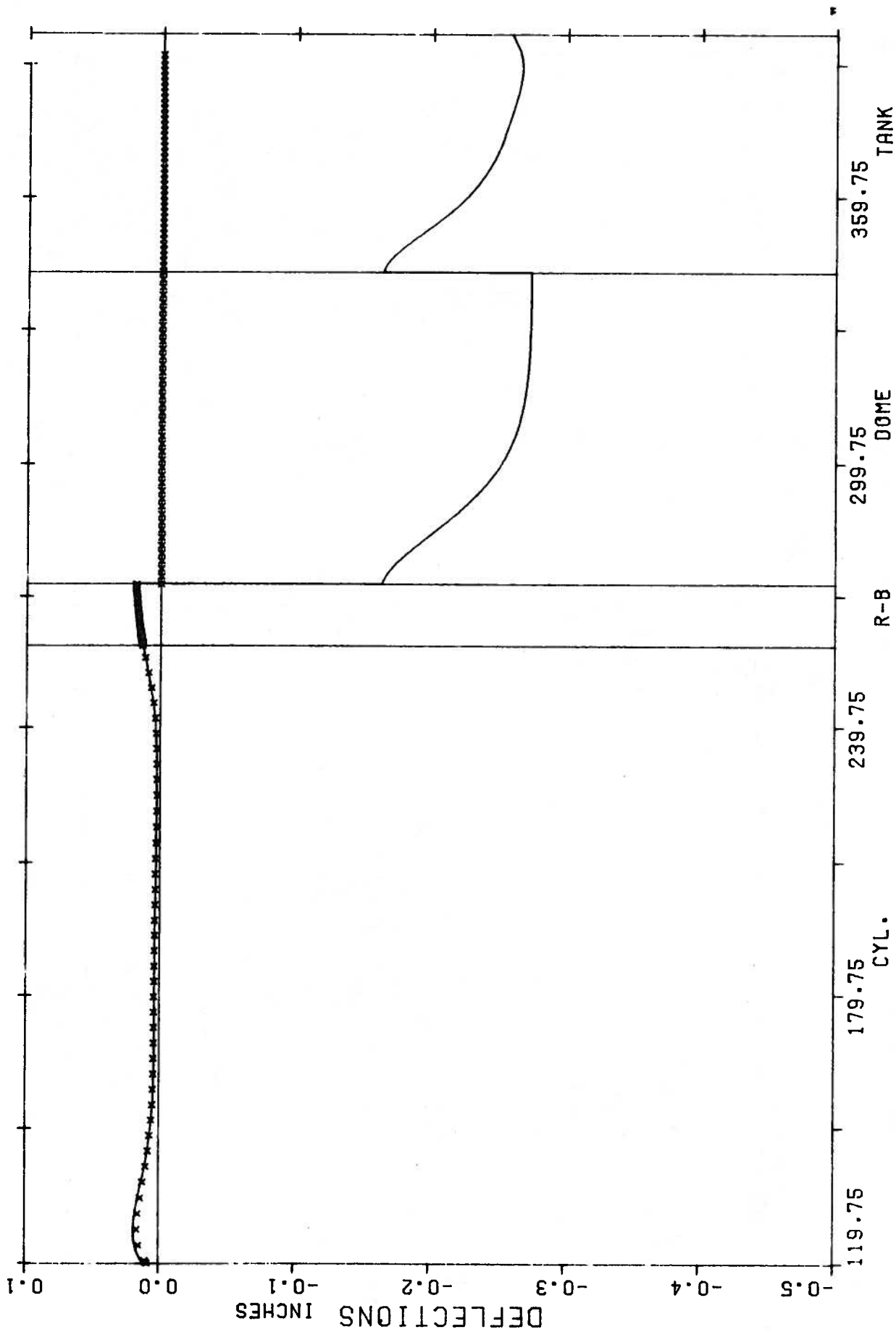


FIGURE 5.10 NORMAL DISPLACEMENTS

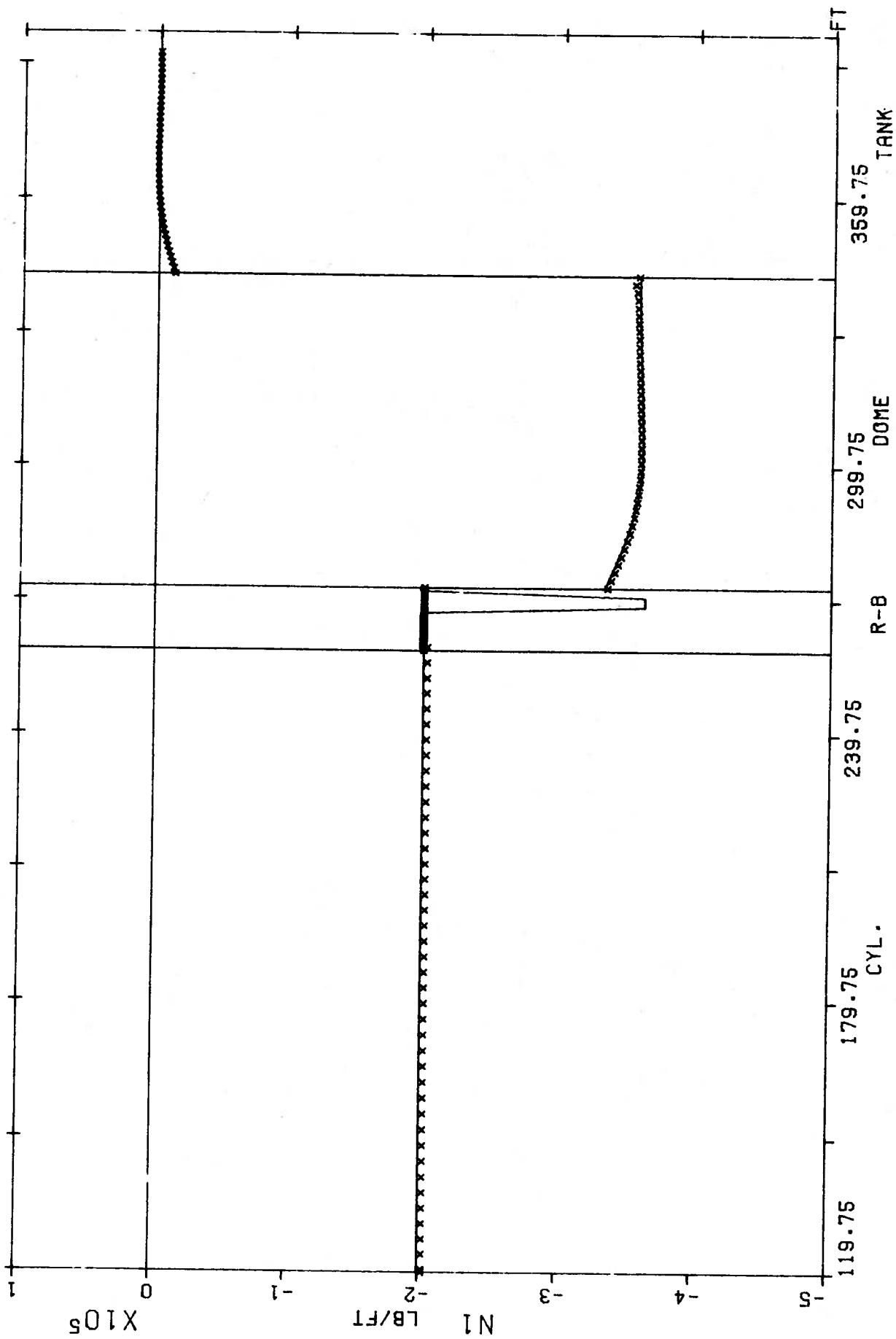


FIGURE 5.11 N1 SWITCHED-ON-PRESTRESS

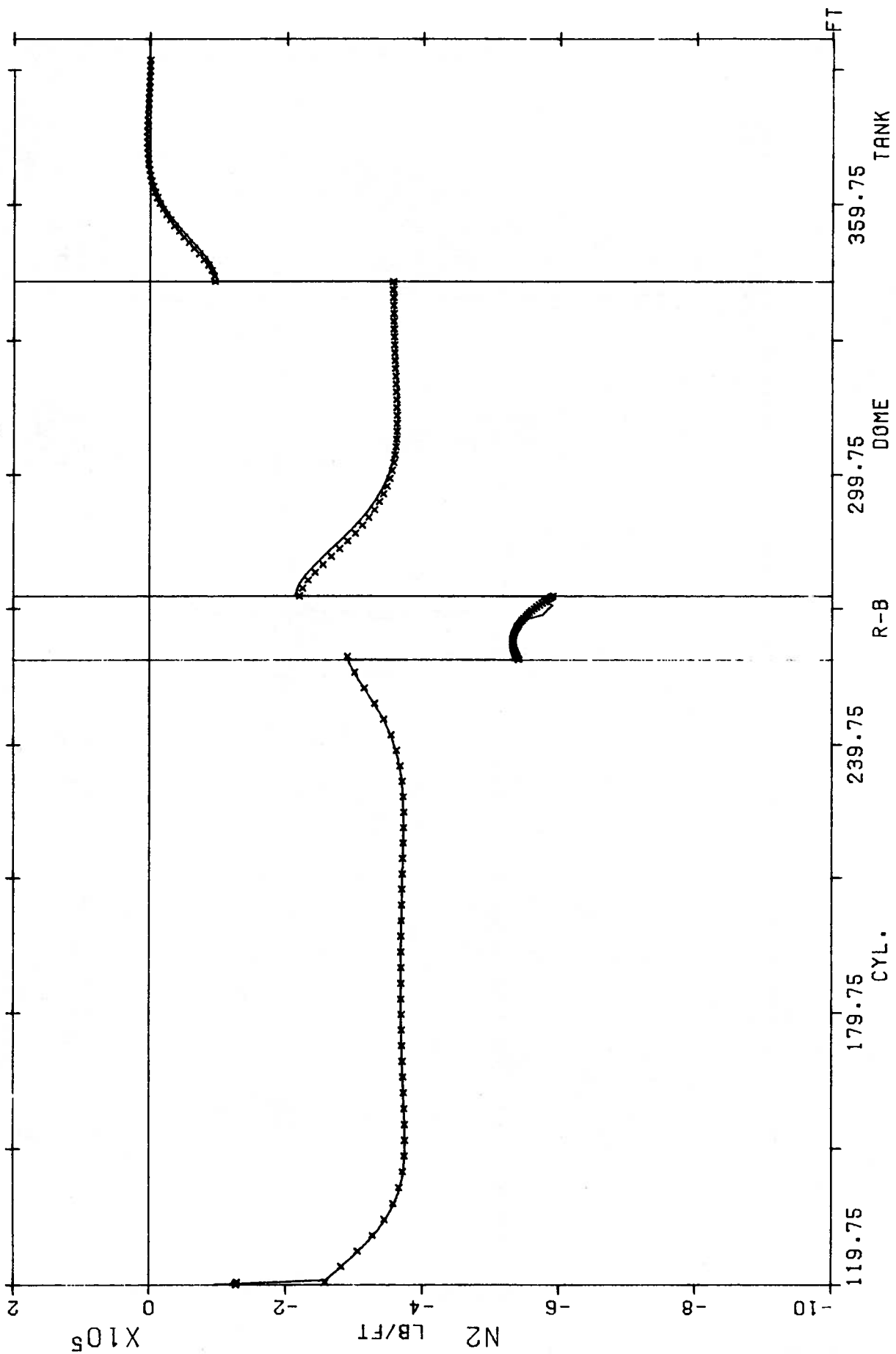


FIGURE 5.12 N2 SWITCHED-ON-PRESTRESS

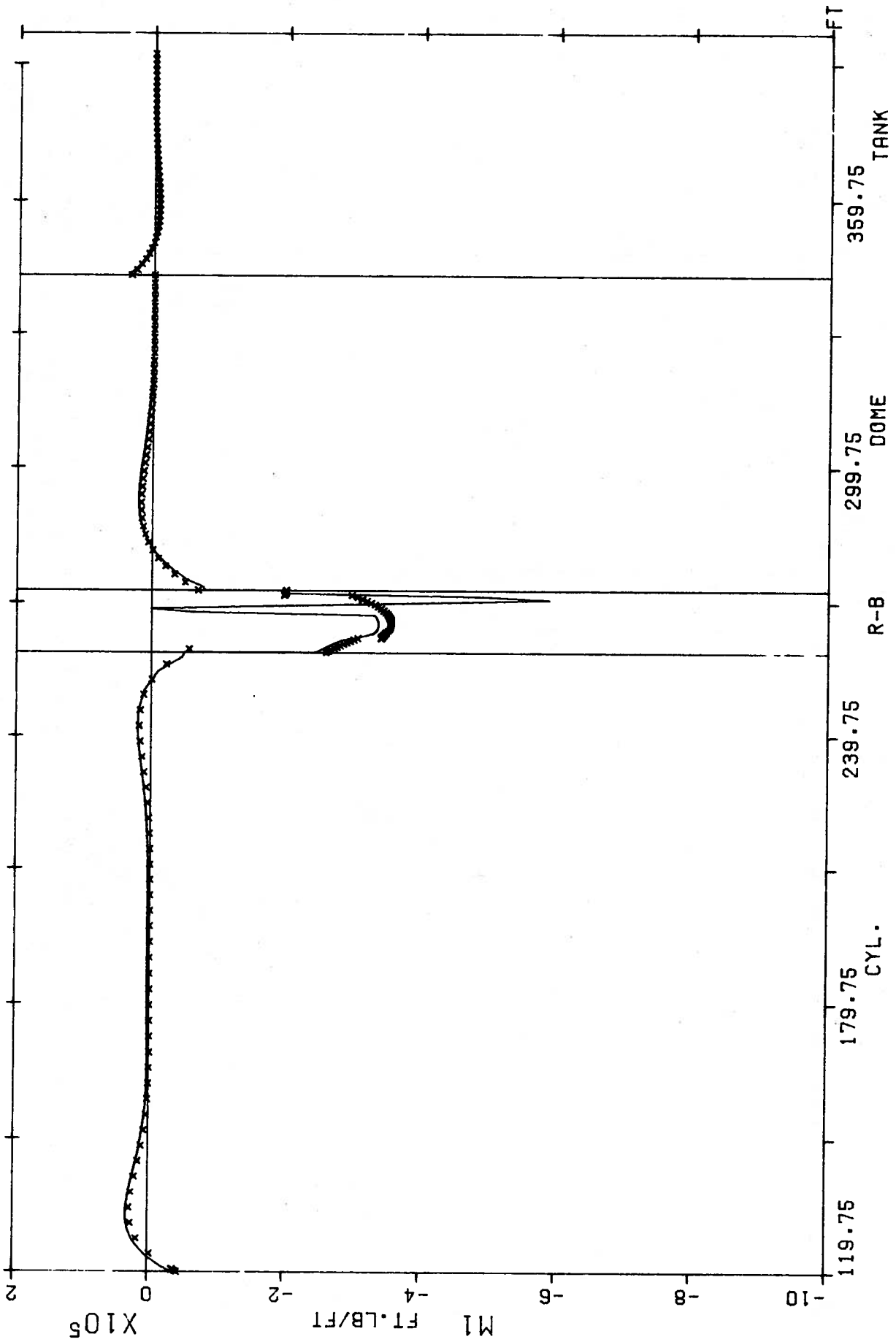


FIGURE 5.13 M1 SWITCHED-ON-PRESTRESS

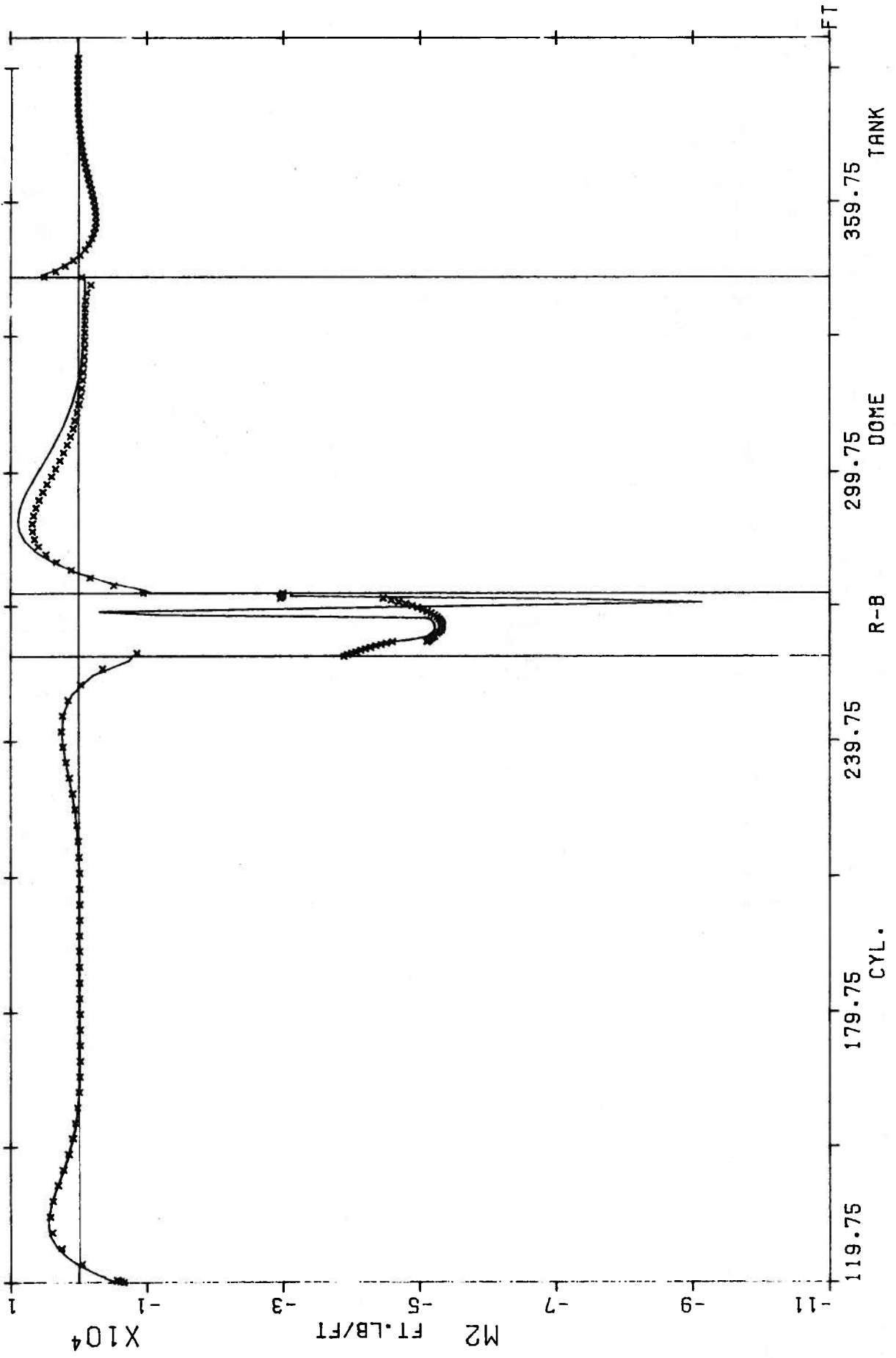


FIGURE 5.14 M2 SWITCHED-ON-PRESTRESS

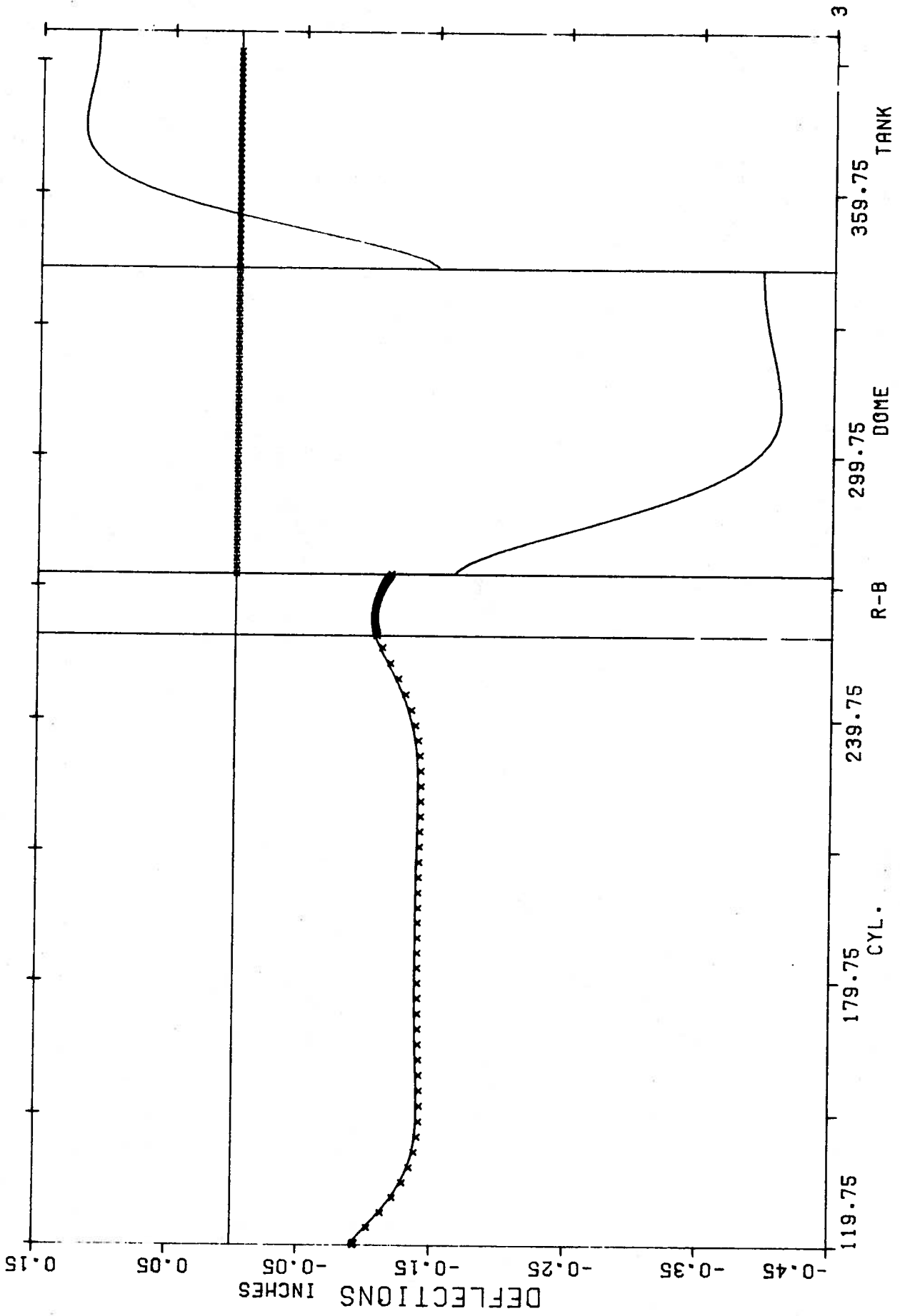


FIGURE 5.15 NORMAL DISPLACEMENTS SWITCHED-ON-PRESTRESS

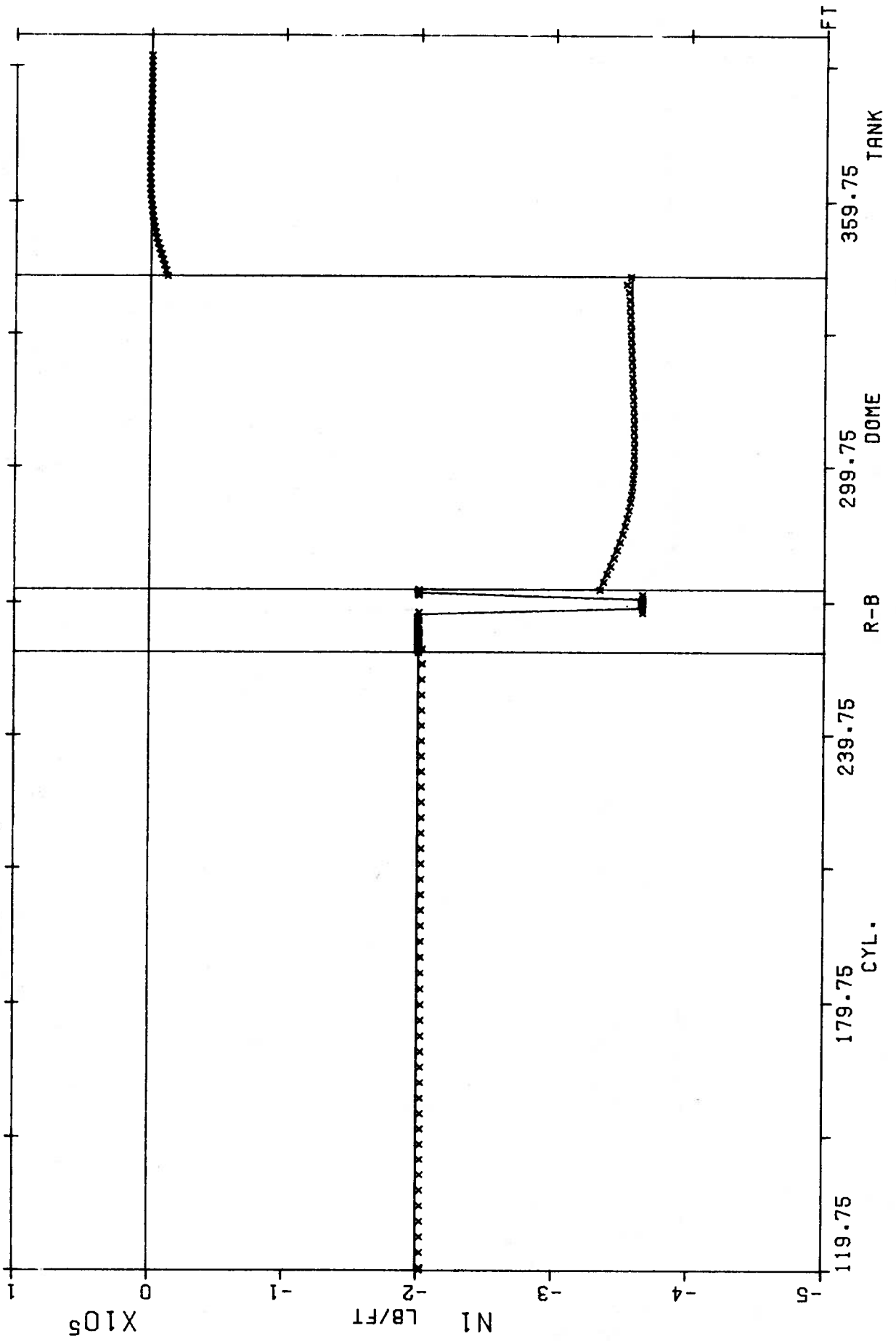


FIGURE 5.16 N1 SWITCHED-ON-PRESTRESS (BOSOR4)

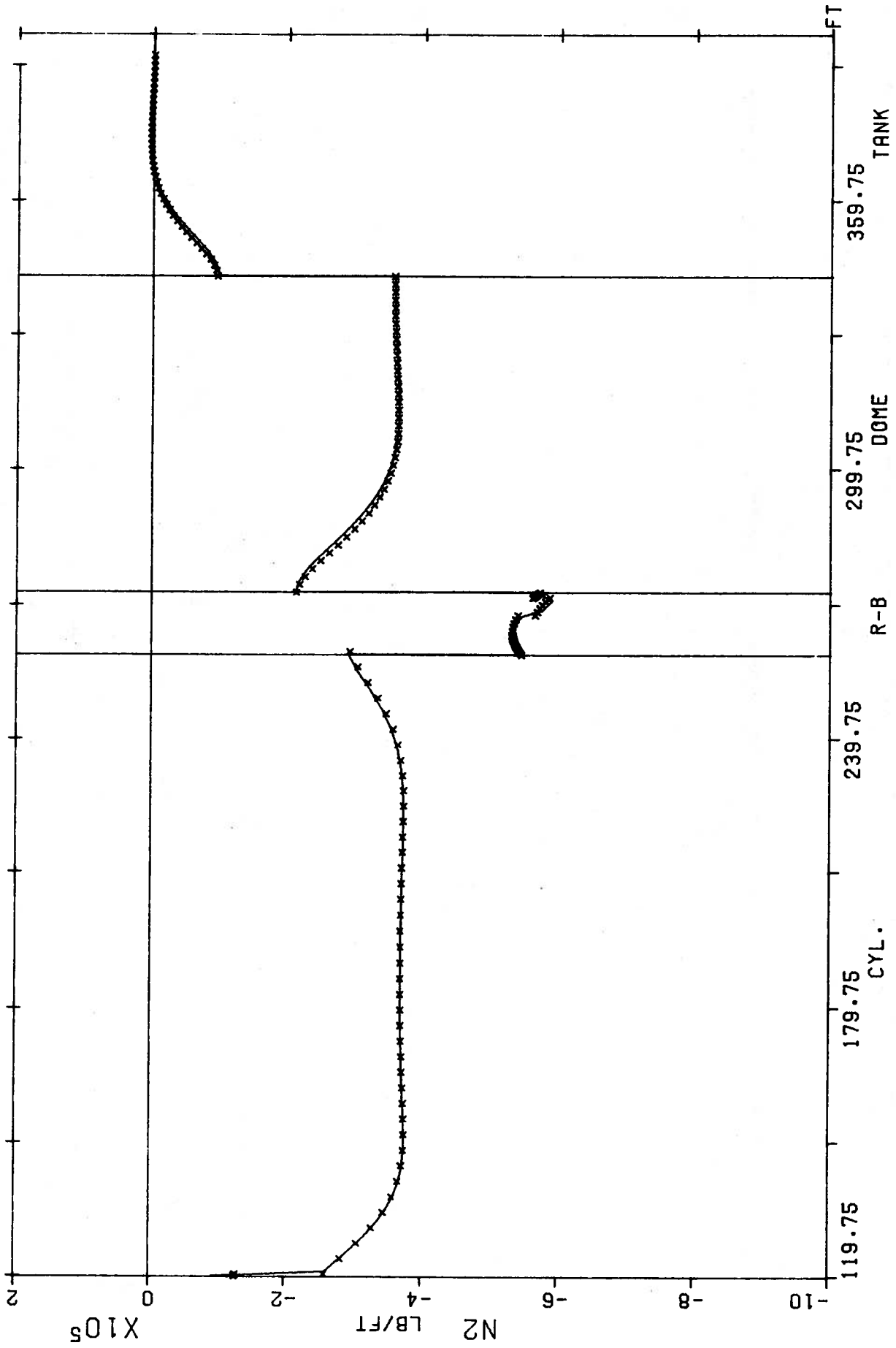


FIGURE 5.17 N2 SWITCHED-ON-PRESTRESS (BOSOR4)

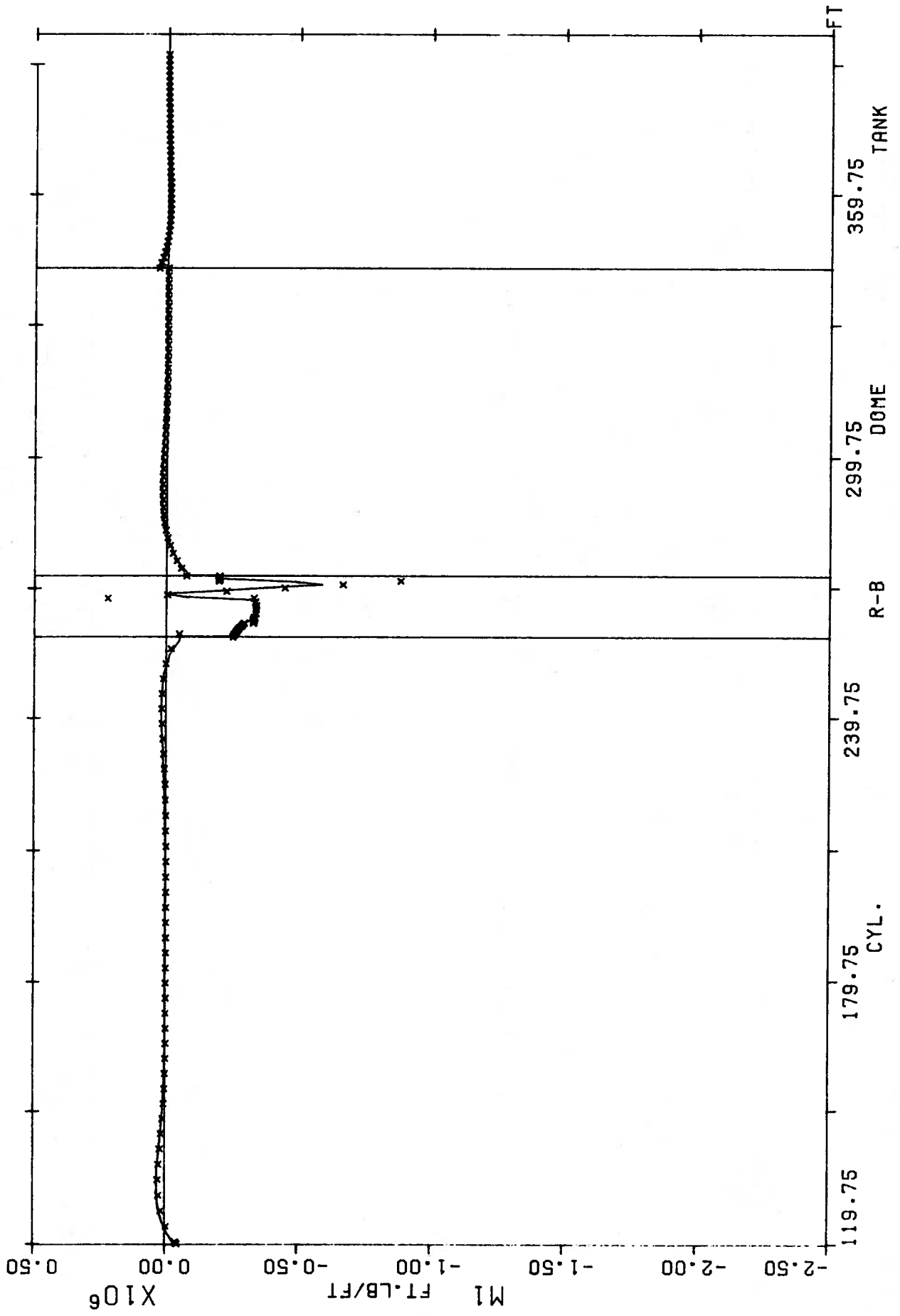


FIGURE 5.18 M1 SWITCHED-ON-PRESTRESS (BOSOR4)

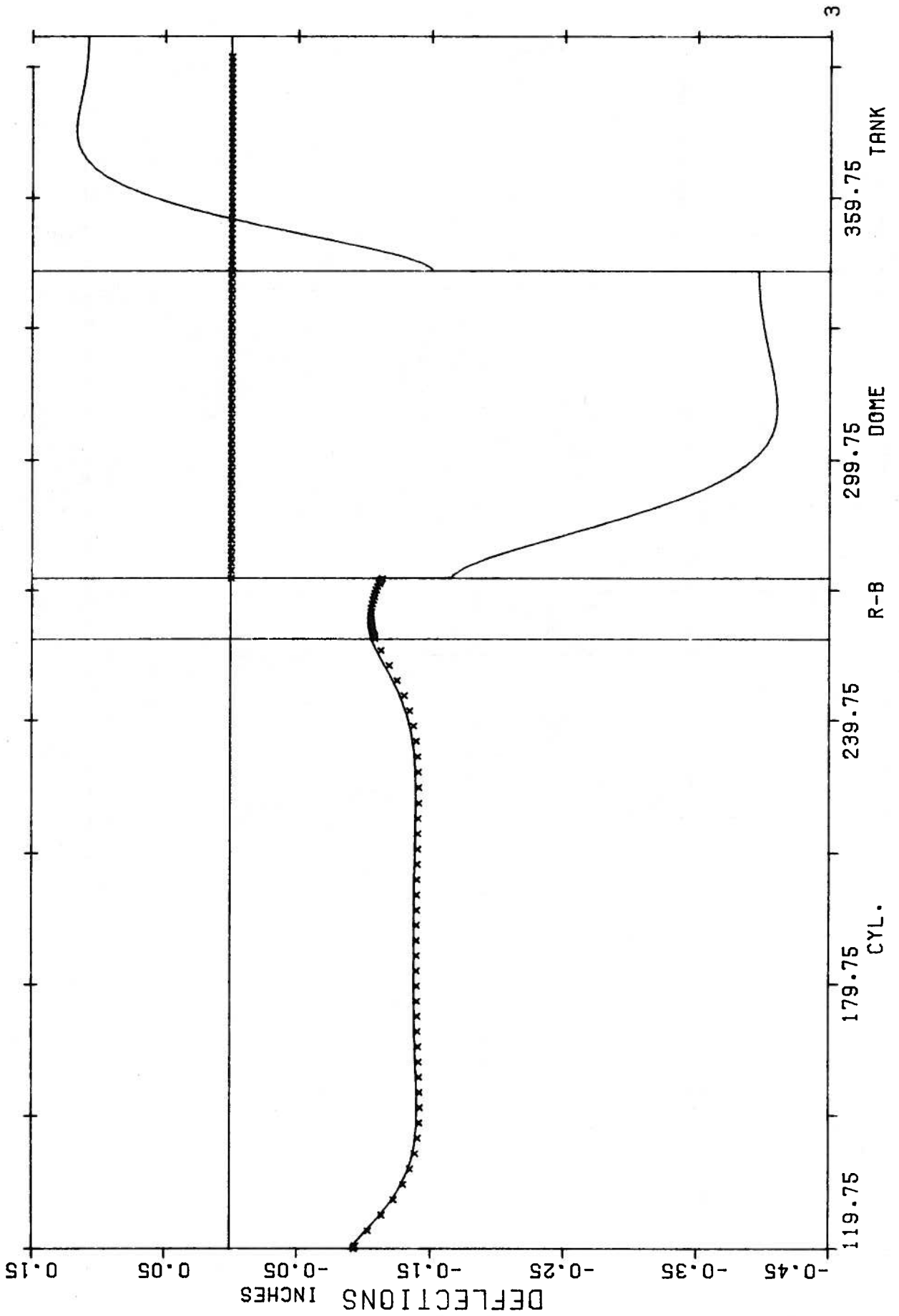


FIGURE 5.20 NORMAL DISPLACEMENTS SWITCHED-ON-PRESTRESS (BOSOR4)

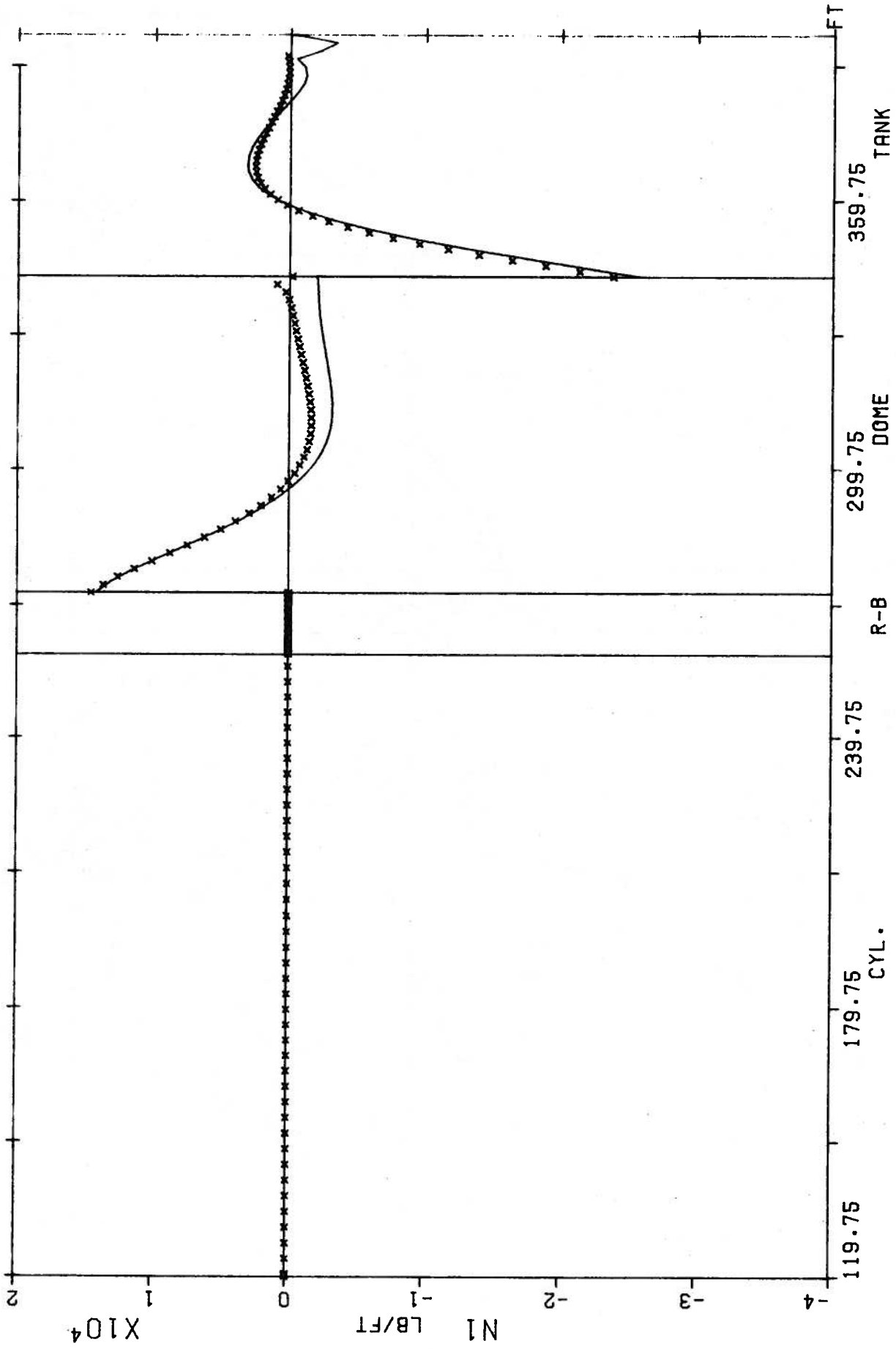


FIGURE 5.21 N_1 FOR W O T

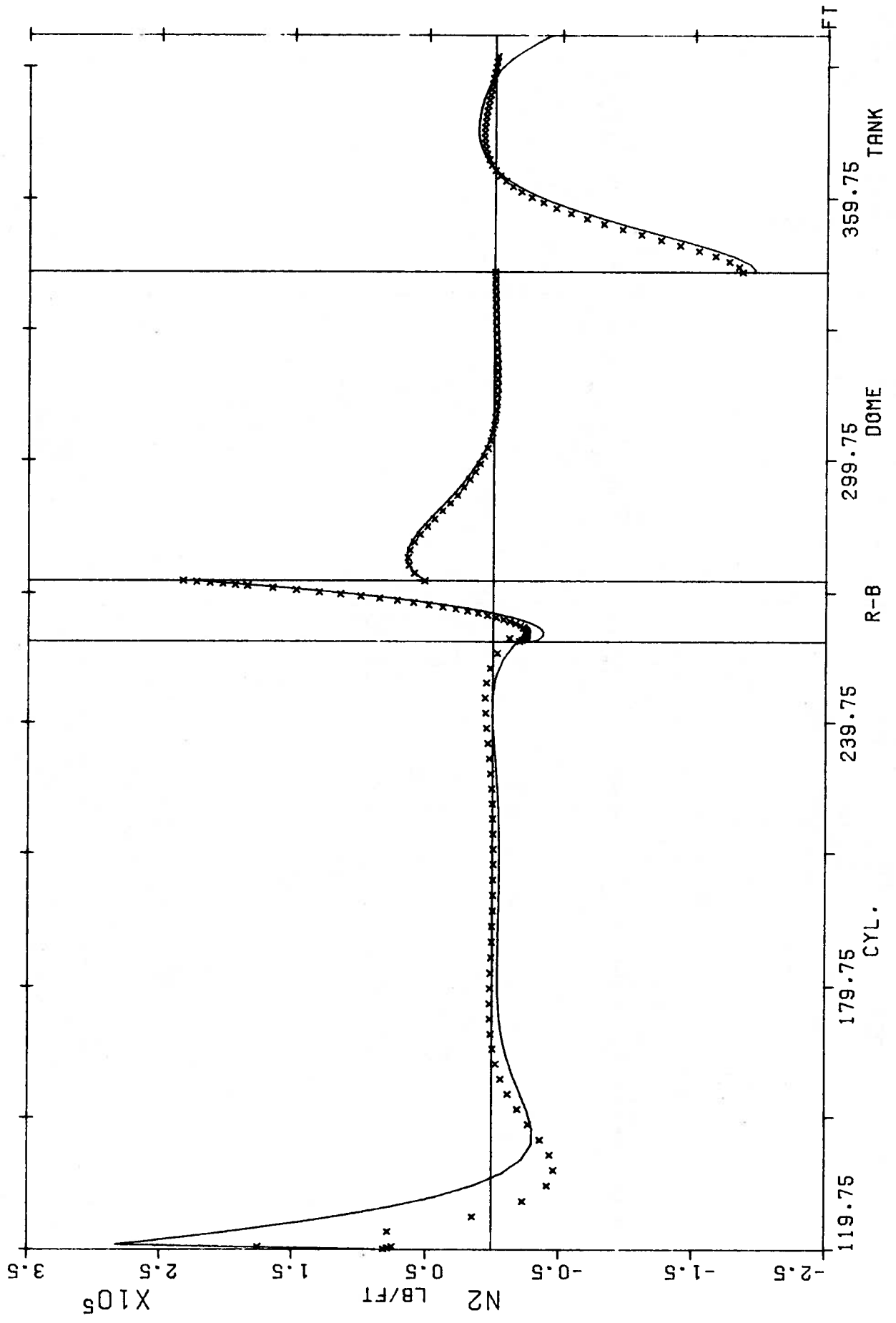


FIGURE 5.22 N2 FOR W O T

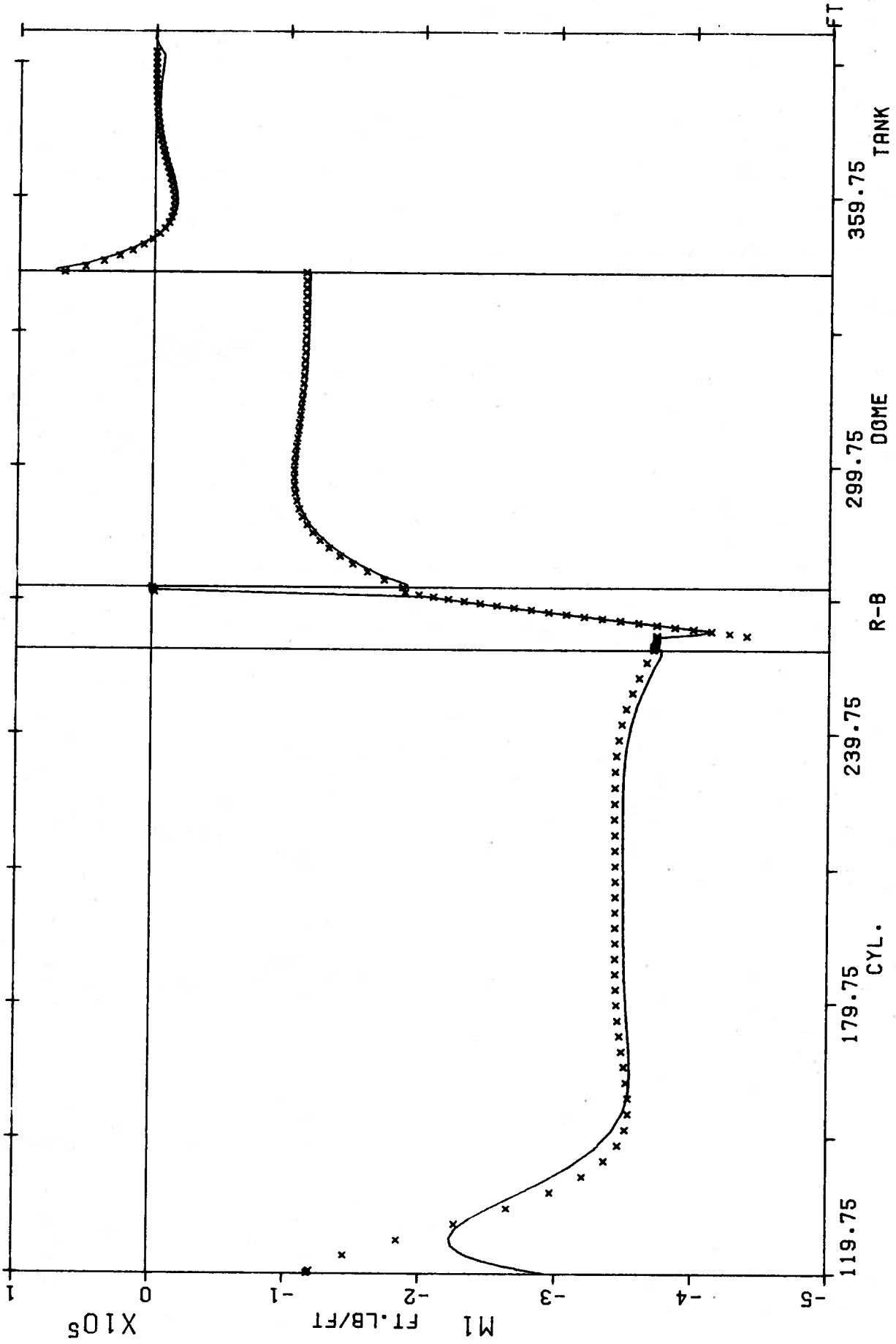


FIGURE 5.23 M1 FOR W O T

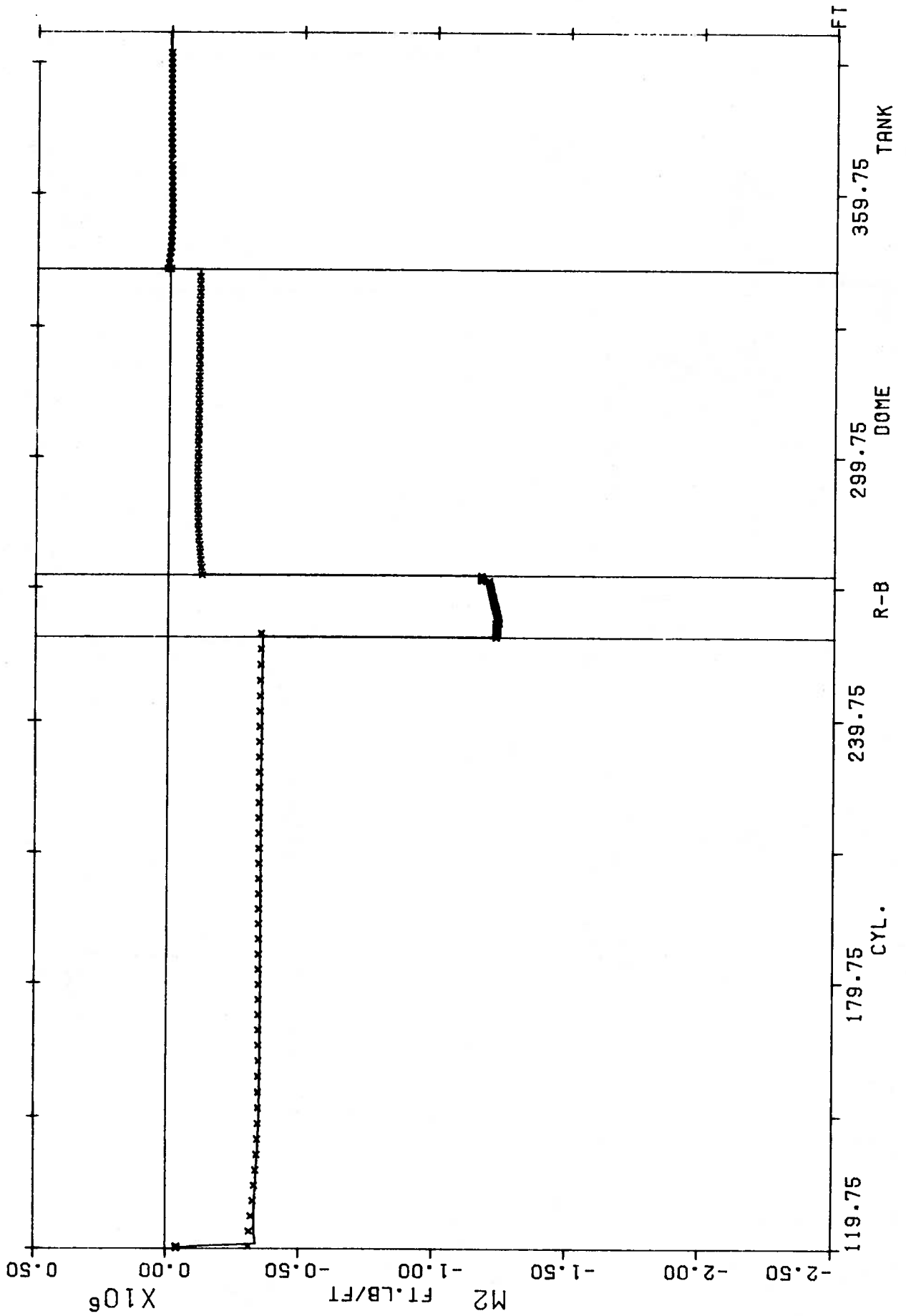


FIGURE 5.24 M2 FOR W O T

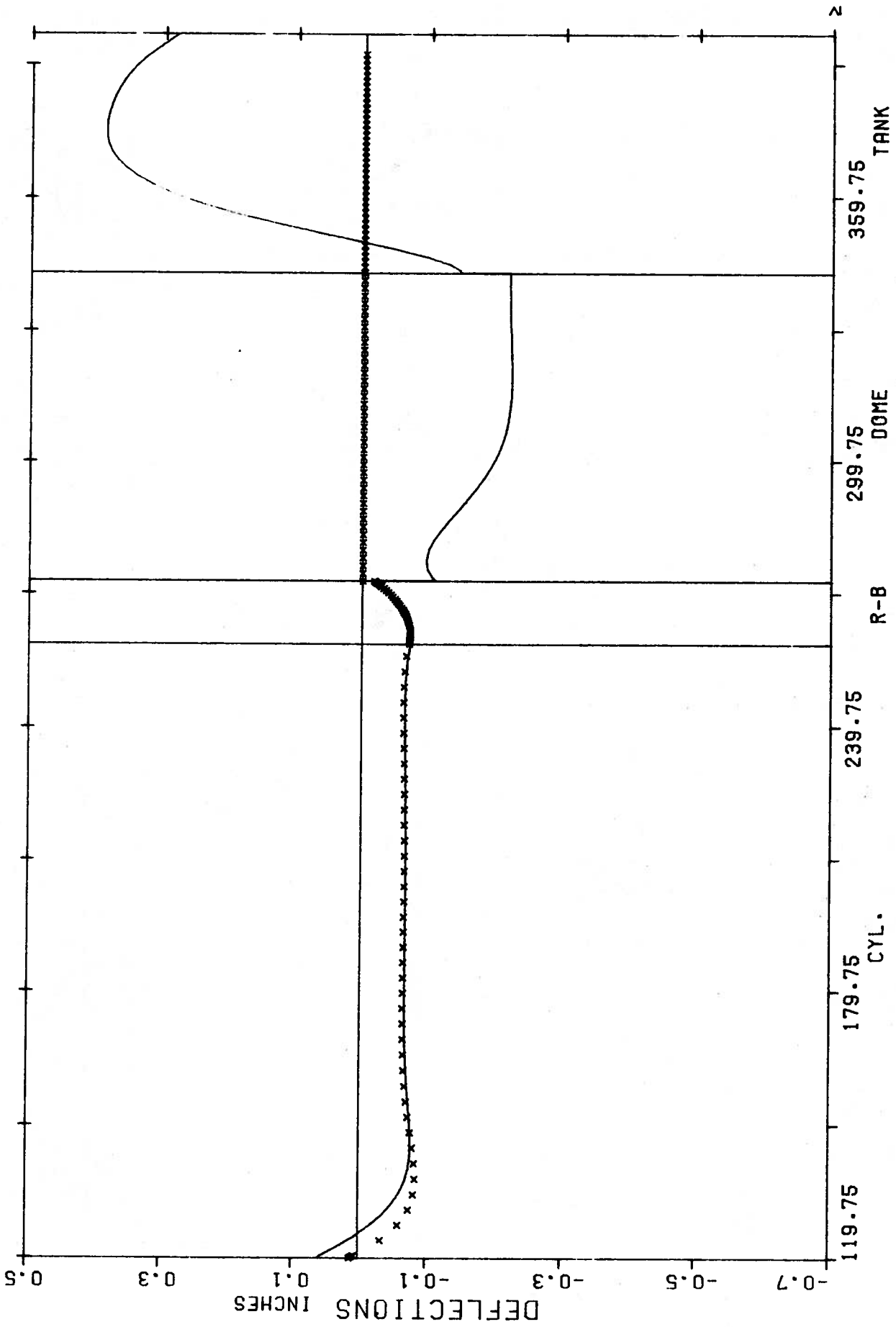


FIGURE 5.25 NORMAL DISPLACEMENTS FOR W O T

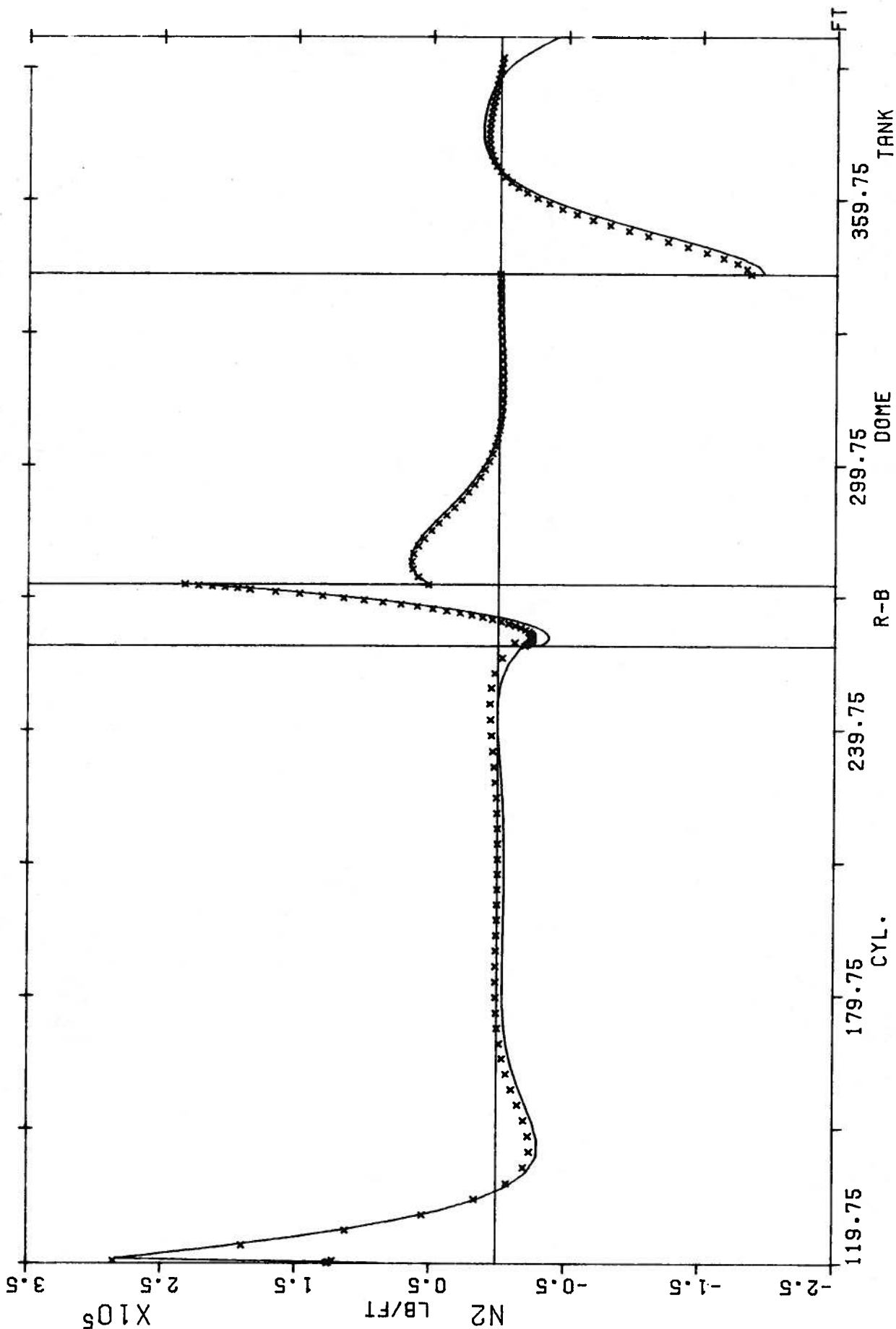


FIGURE 5.26 N2 FOR W O T (BOSOR4 - MODEL)

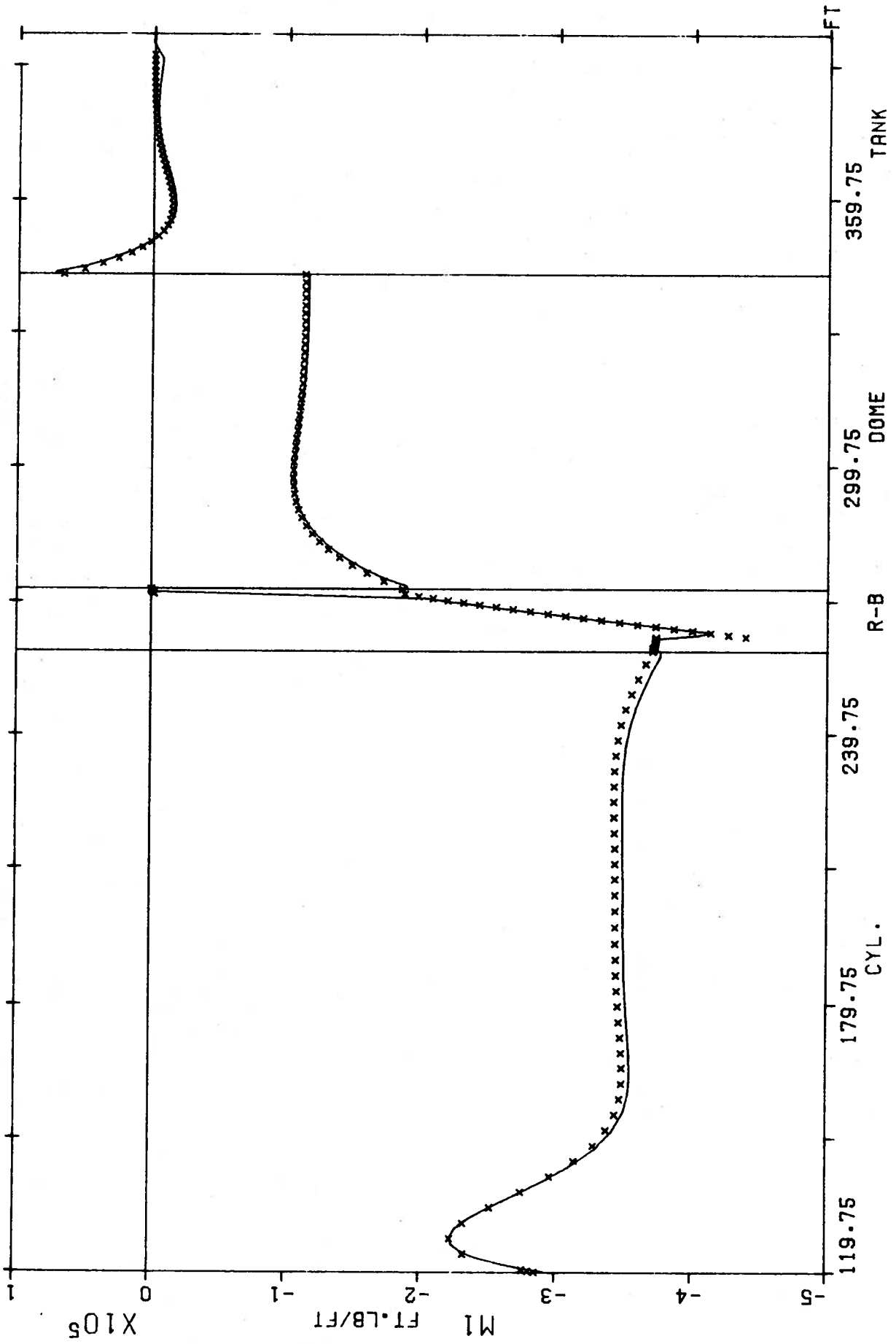


FIGURE 5.27 M1 FOR W O T (BOSOR4 - MODEL)

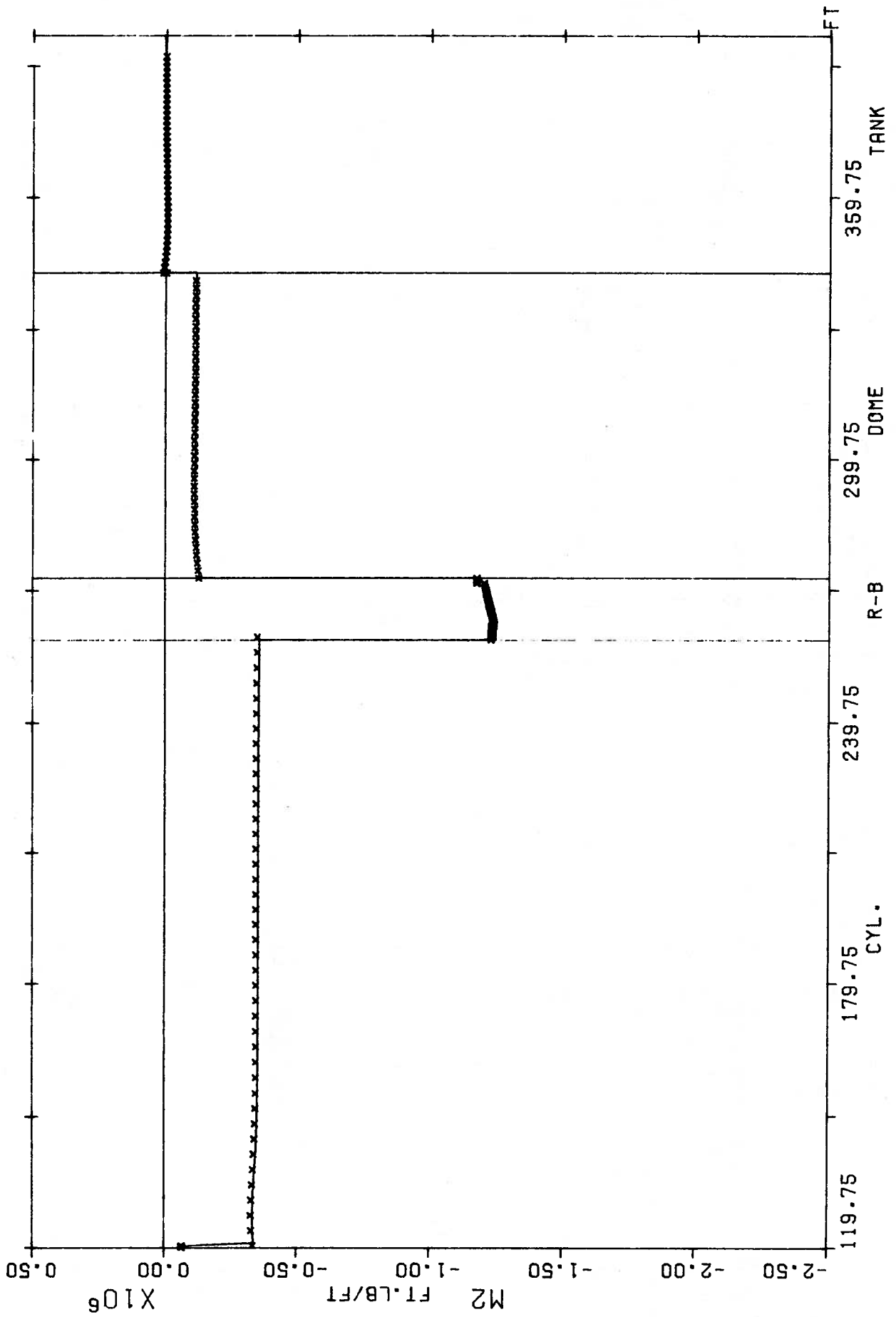


FIGURE 5.28 M2 FOR W O T (BOSOR4 - MODEL)

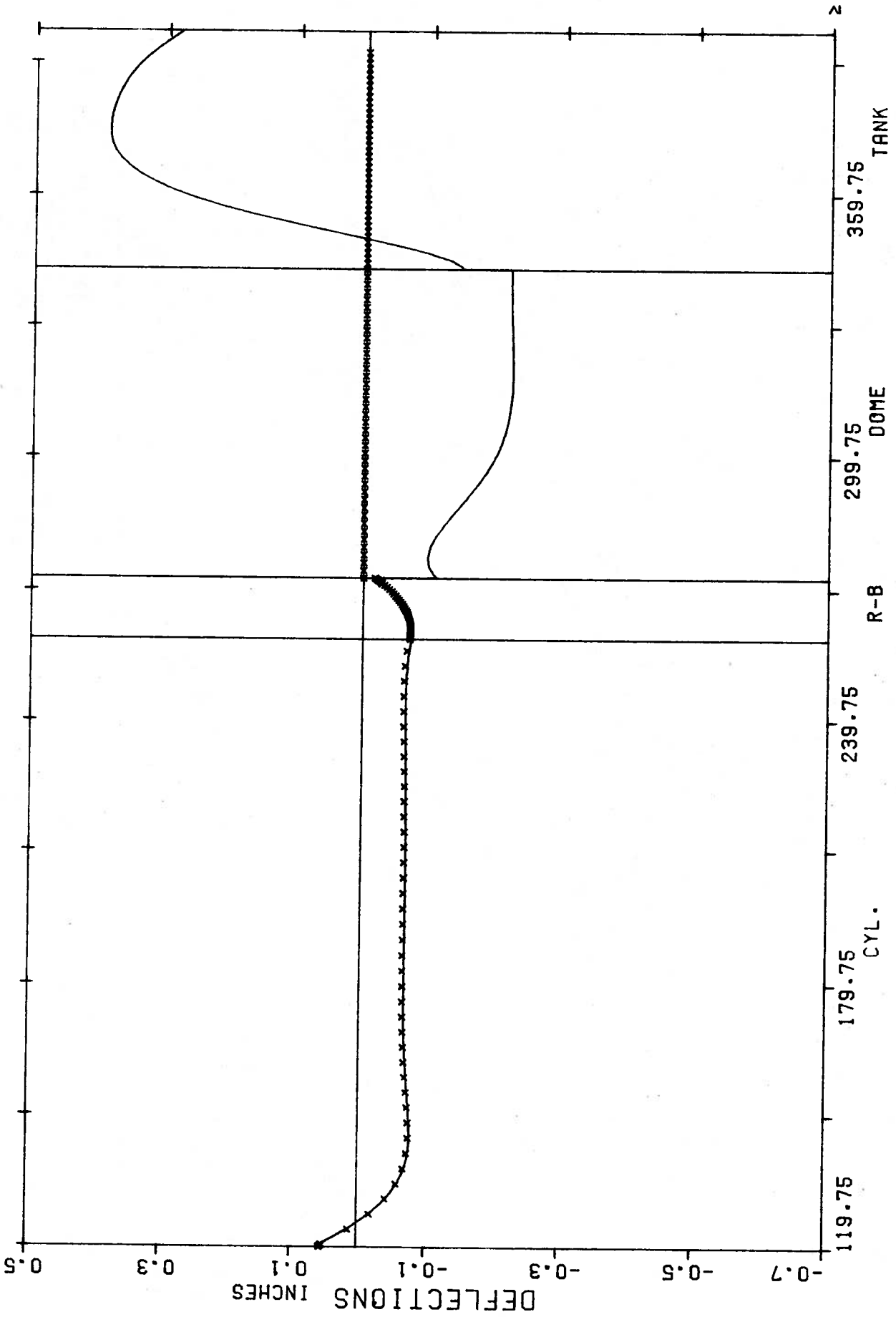


FIGURE 5.29 NORMAL DISPLACEMENTS FOR W O T (BOSOR4 - MODEL)

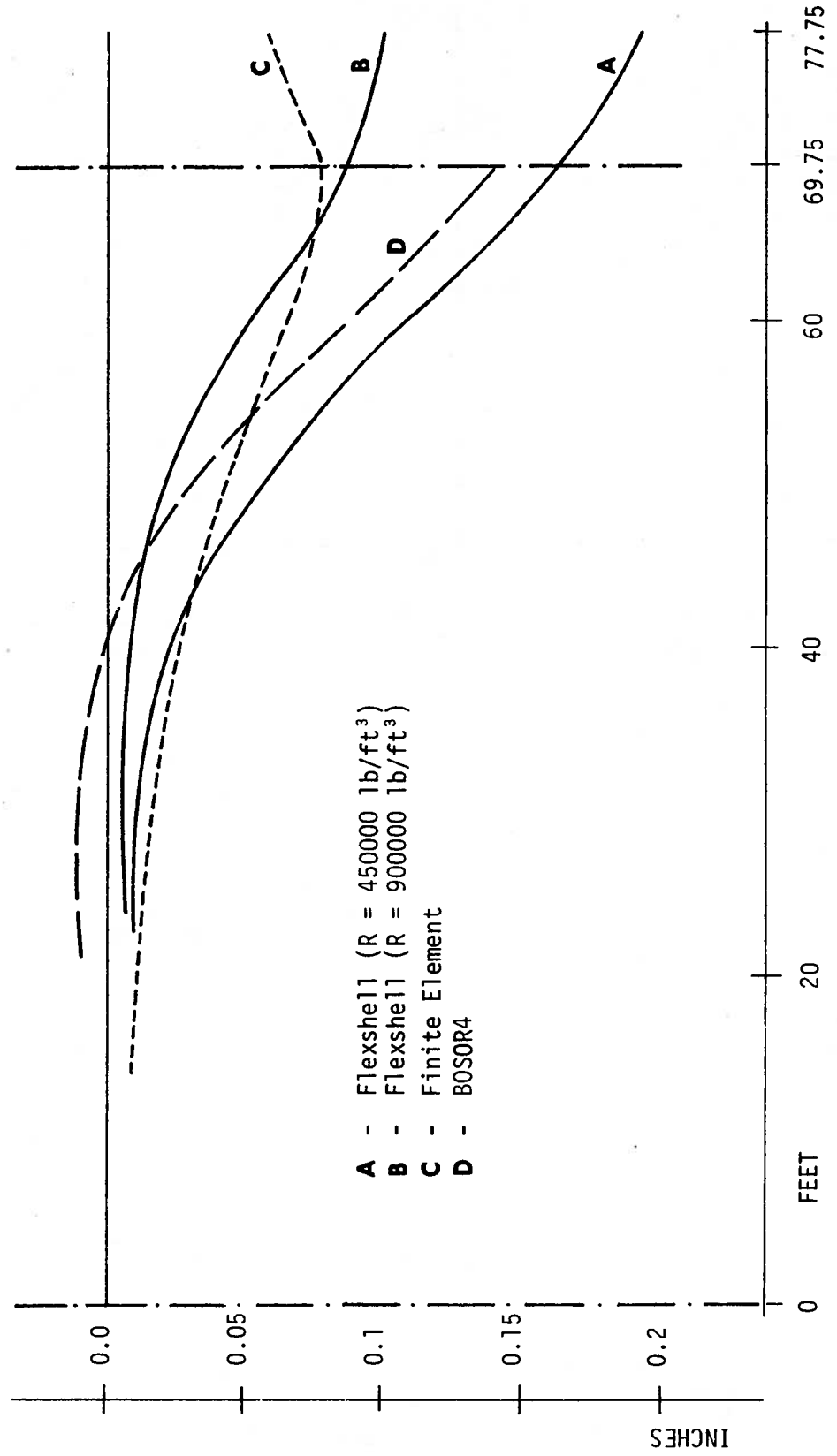


FIGURE 5.30 Dead Load Base Deflections

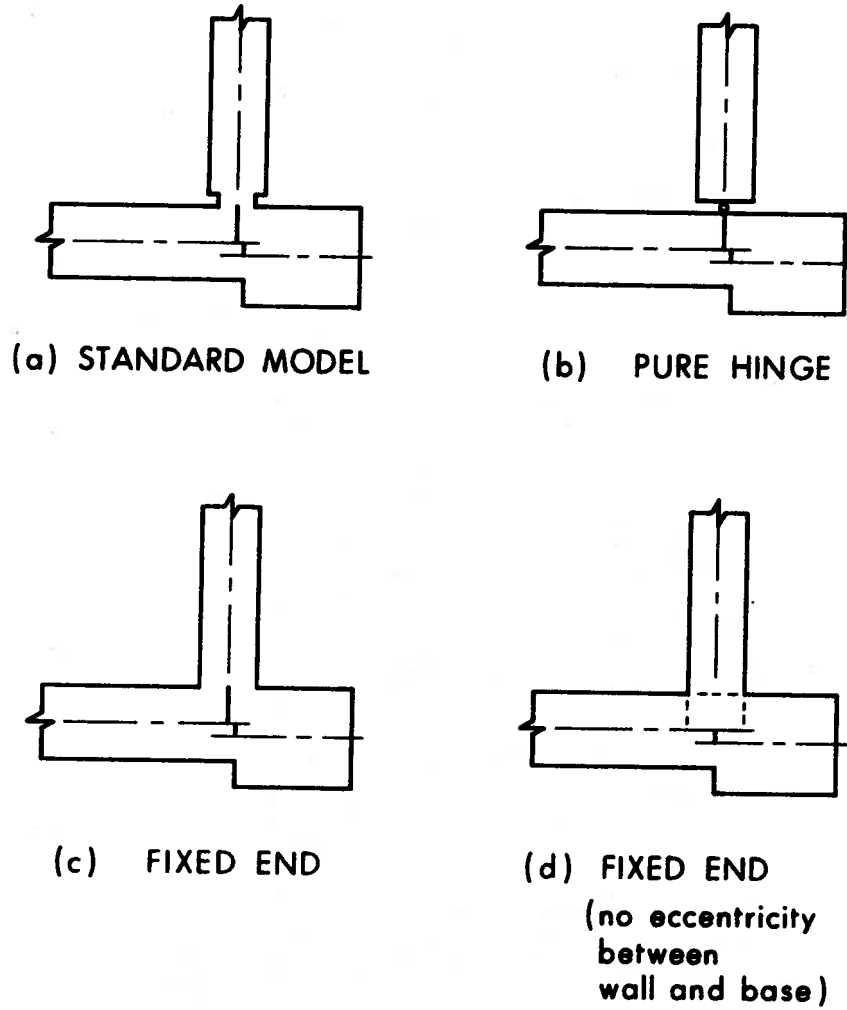
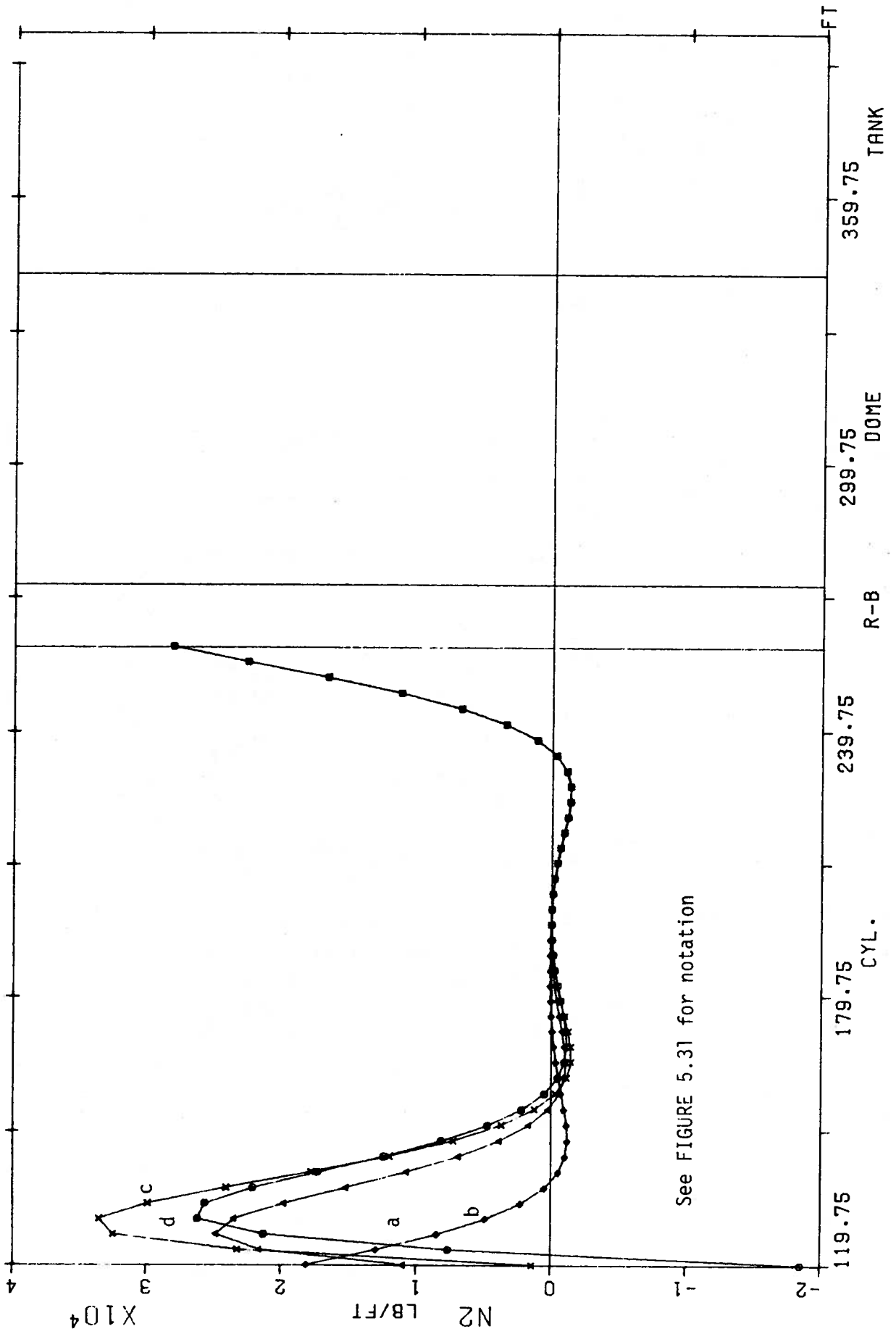
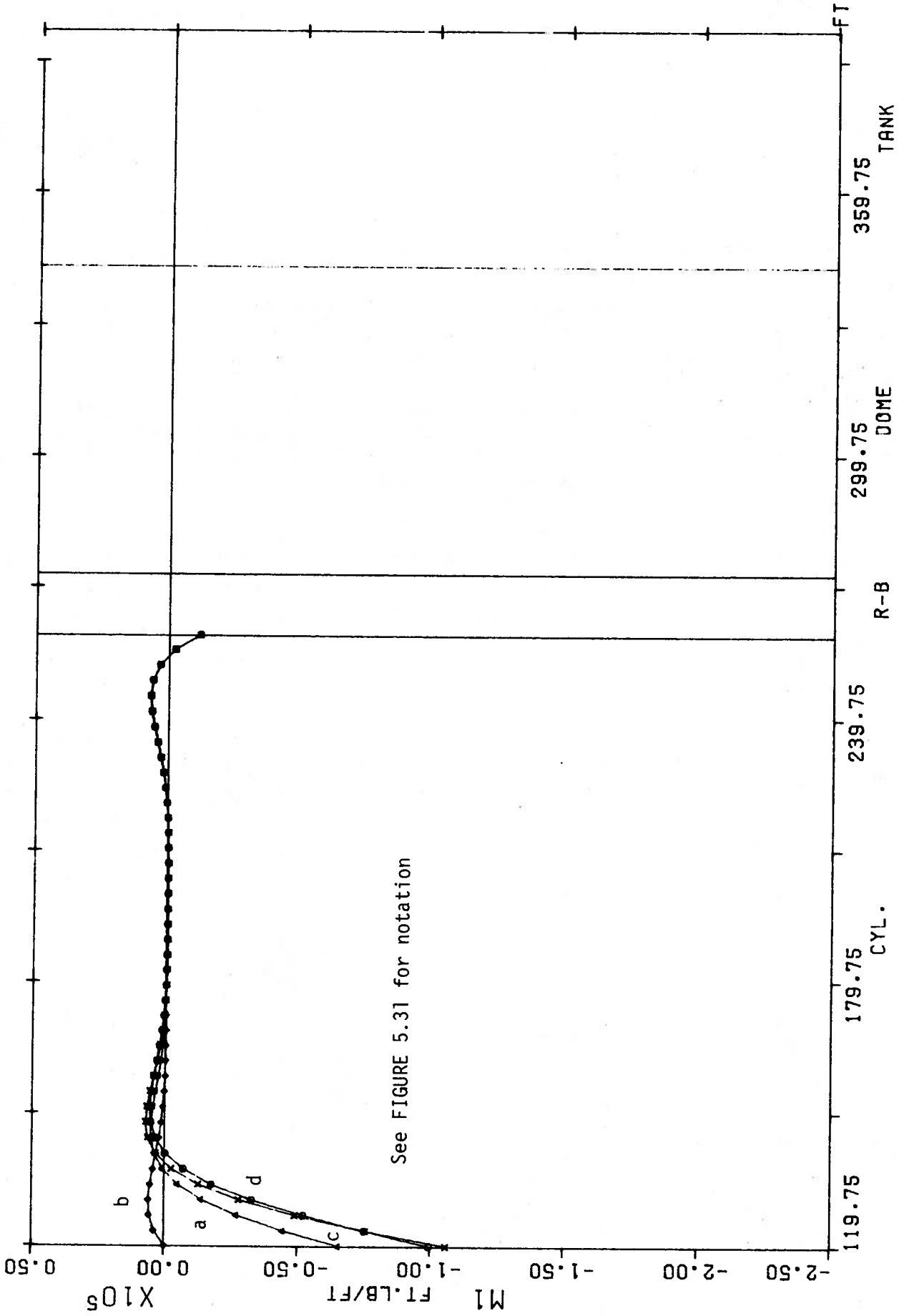


FIGURE 5.31 Variations of Base Connection Detail



See FIGURE 5.31 for notation

FIGURE 5.32 N2 BASE MODEL COMPARISON (DEAD LOAD)



See FIGURE 5.31 for notation

FIGURE 5.33 M1 BASE MODEL COMPARISON (DEAD LOAD)

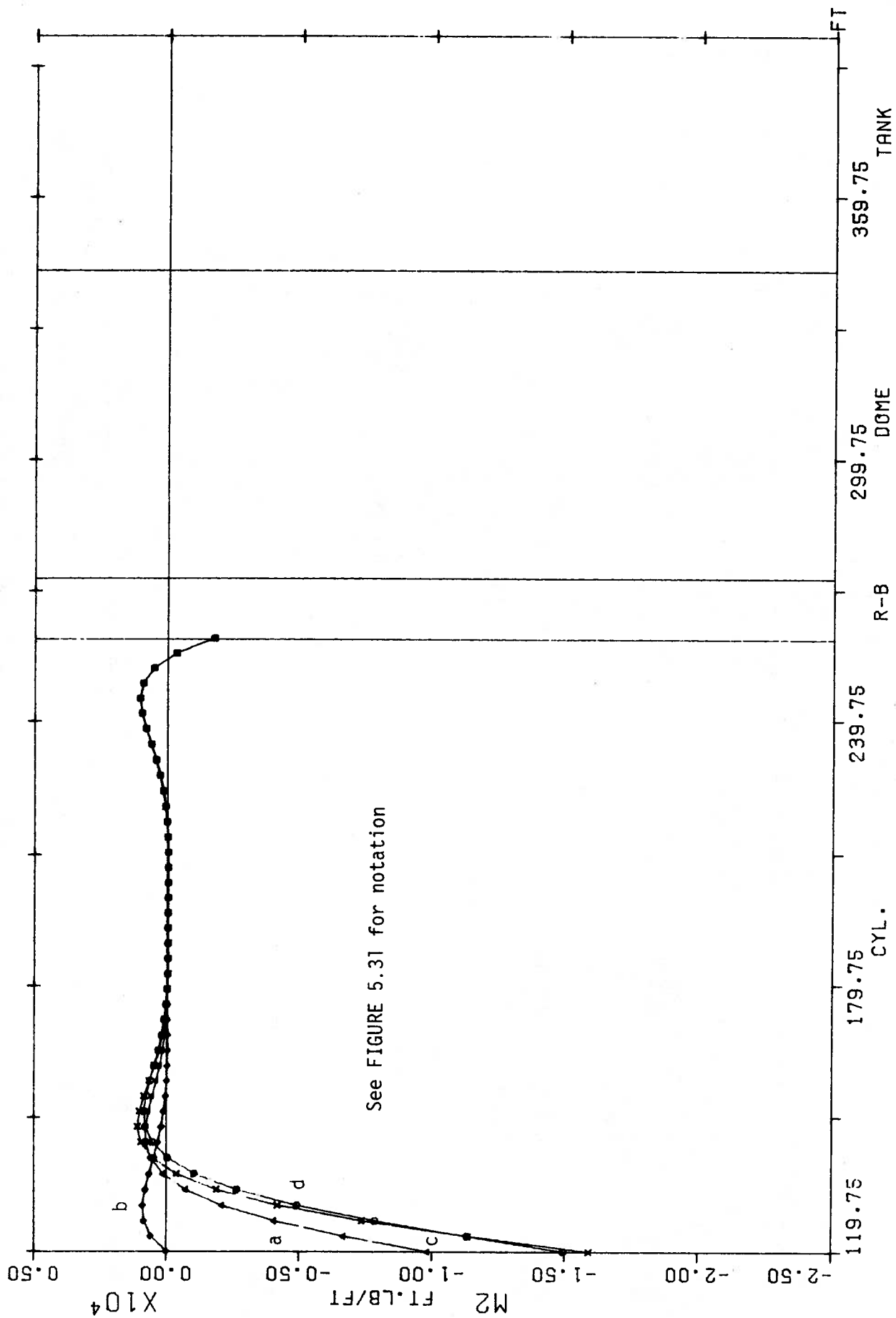


FIGURE 5.34 M2 BASE MODEL COMPARISON (DEAD LOAD)

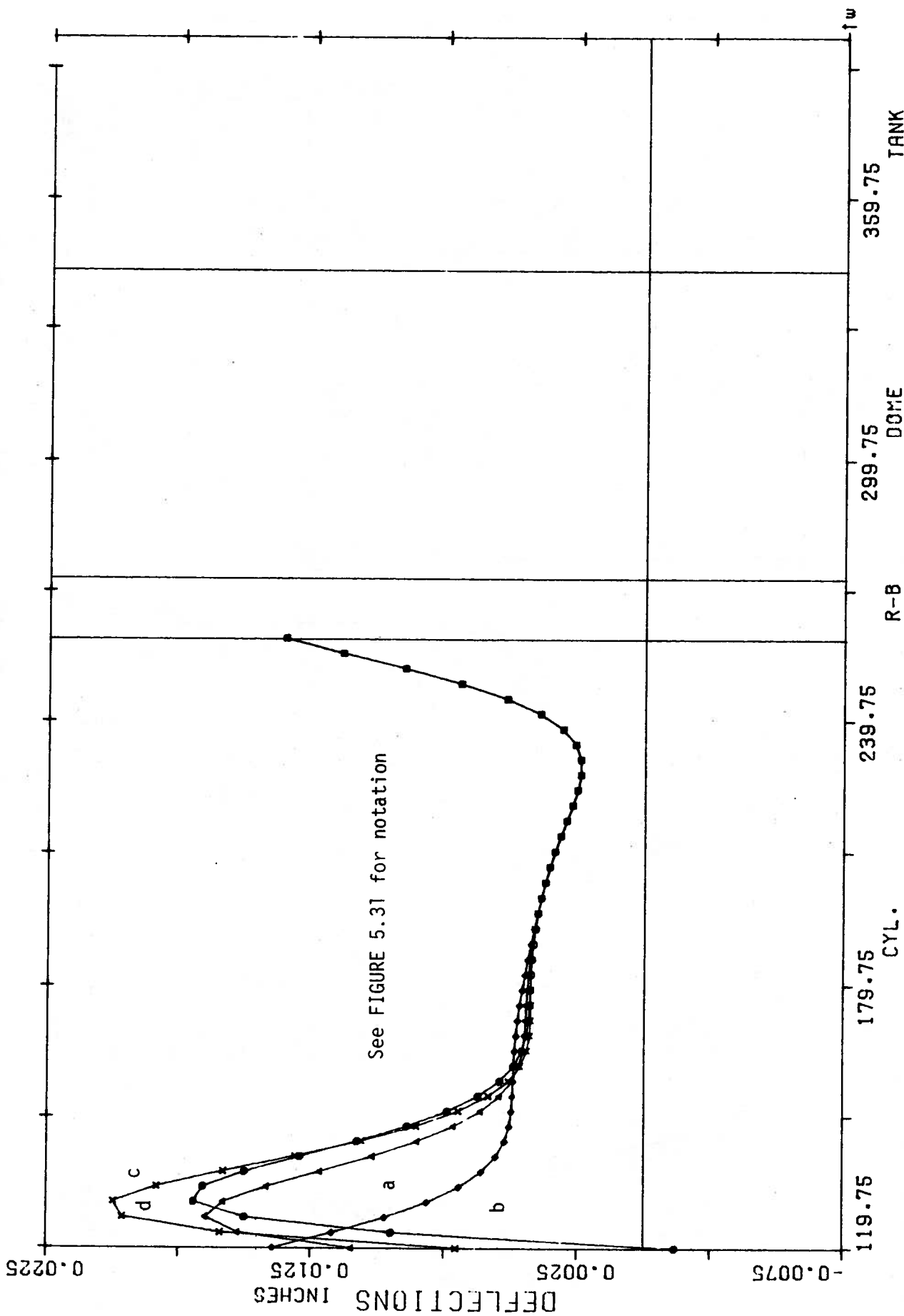


FIGURE 5.35 NORMAL DISPLACEMENTS BASE MODEL COMPARISON (DEAD LOAD)

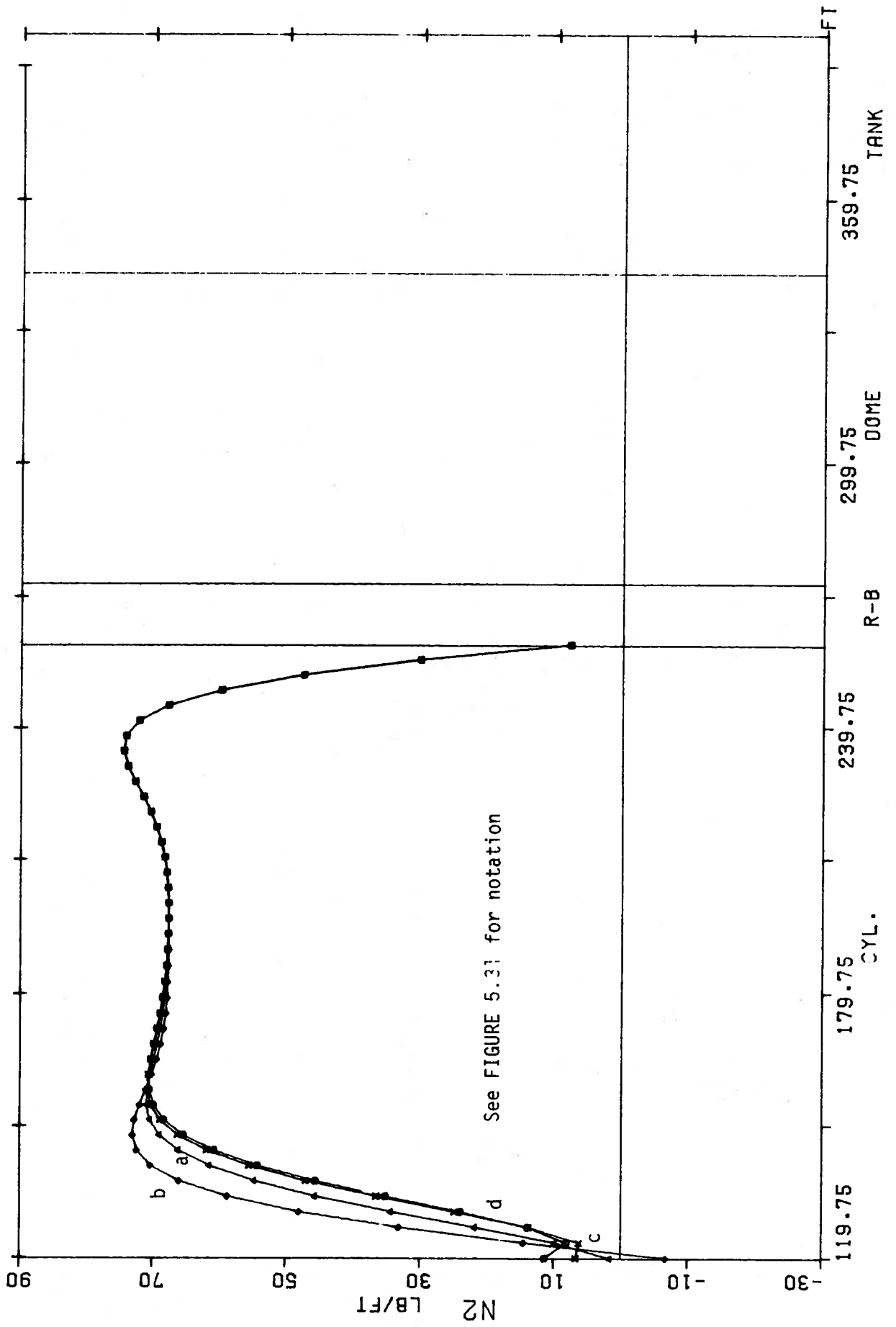


FIGURE 5.36 N2 BASE MODEL COMPARISON (INT. PRESSURE)

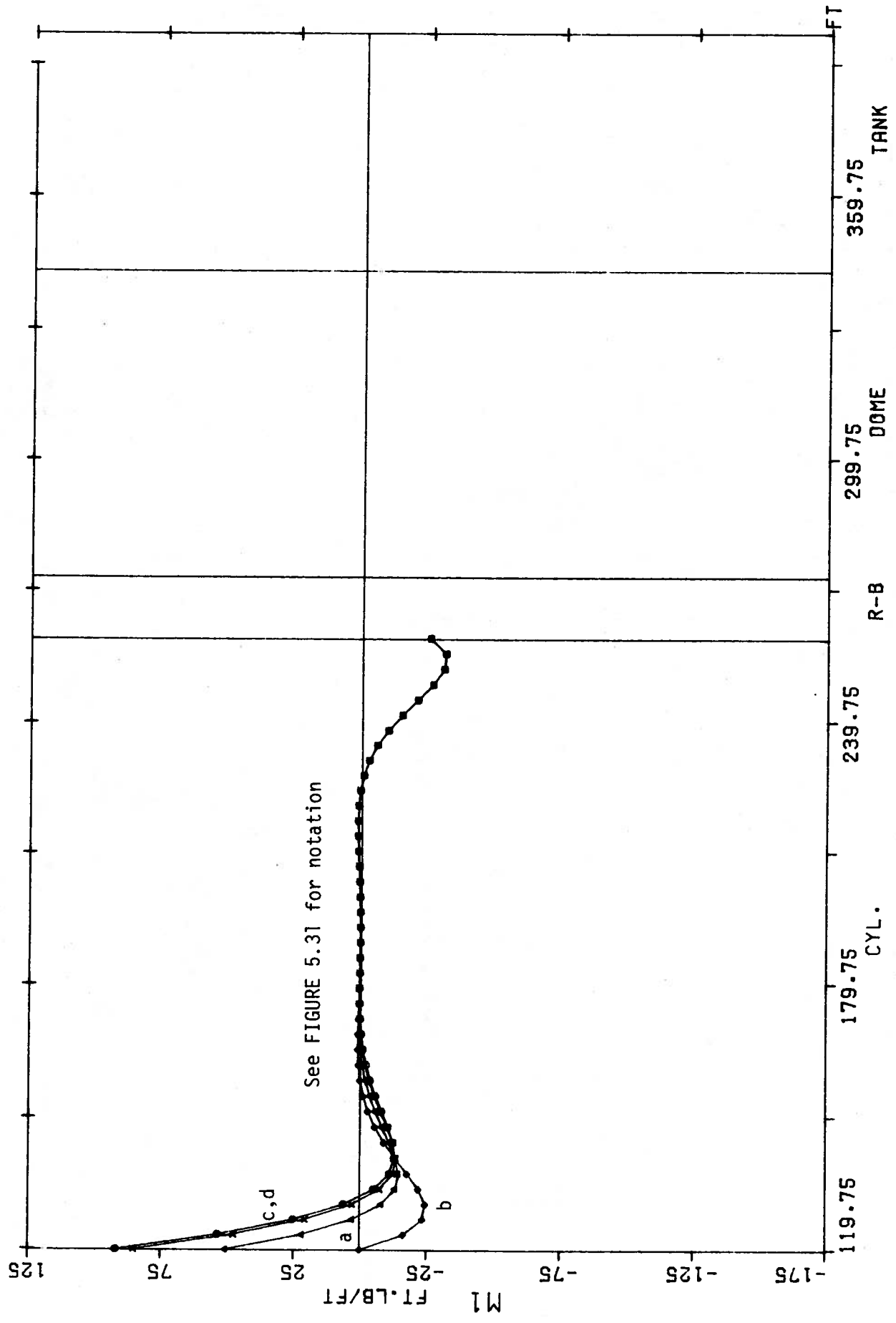


FIGURE 5.37 M1 BASE MODEL COMPARISON (INT. PRESSURE)

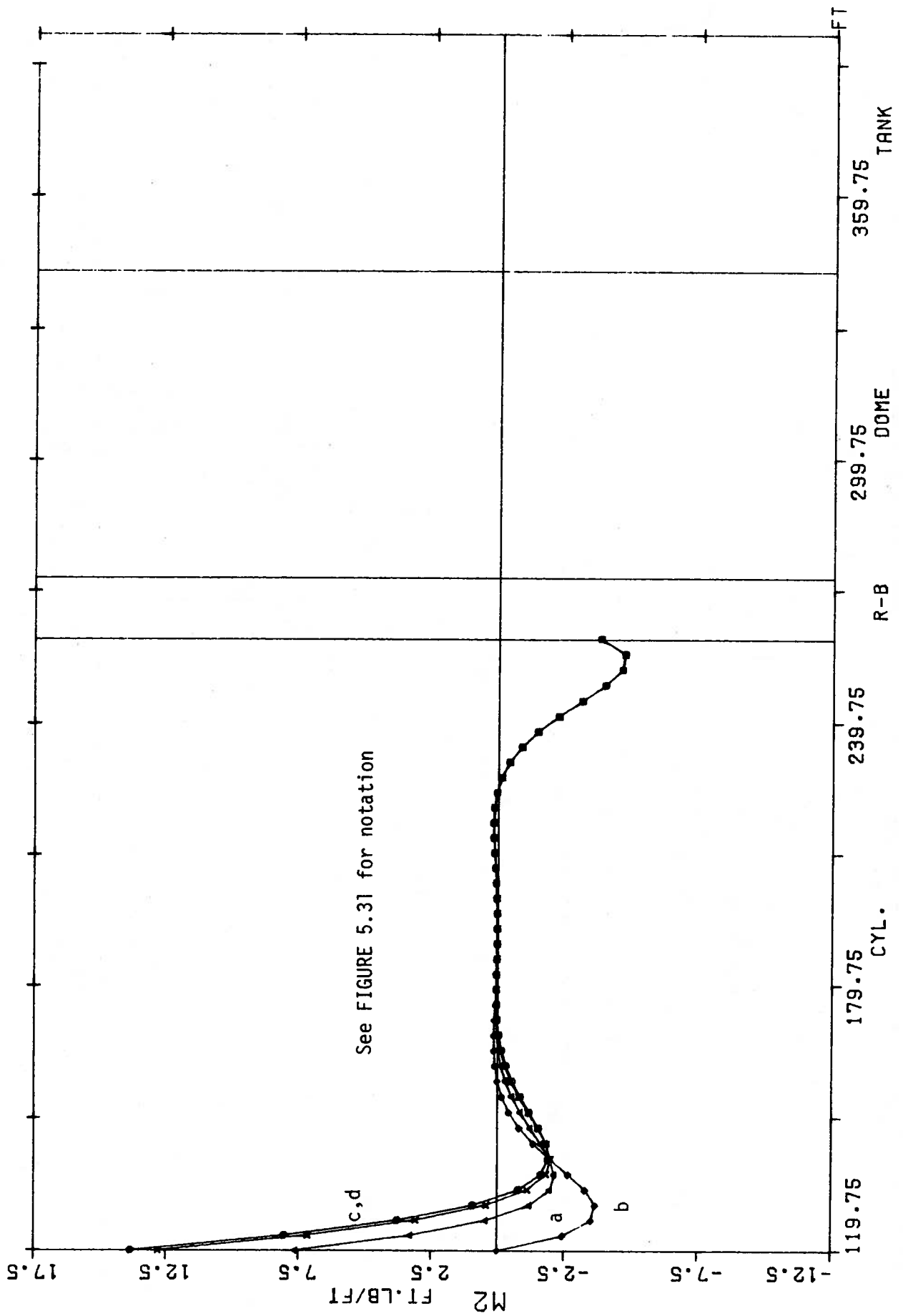


FIGURE 5.38 M2 BASE MODEL COMPARISON (INT. PRESSURE)

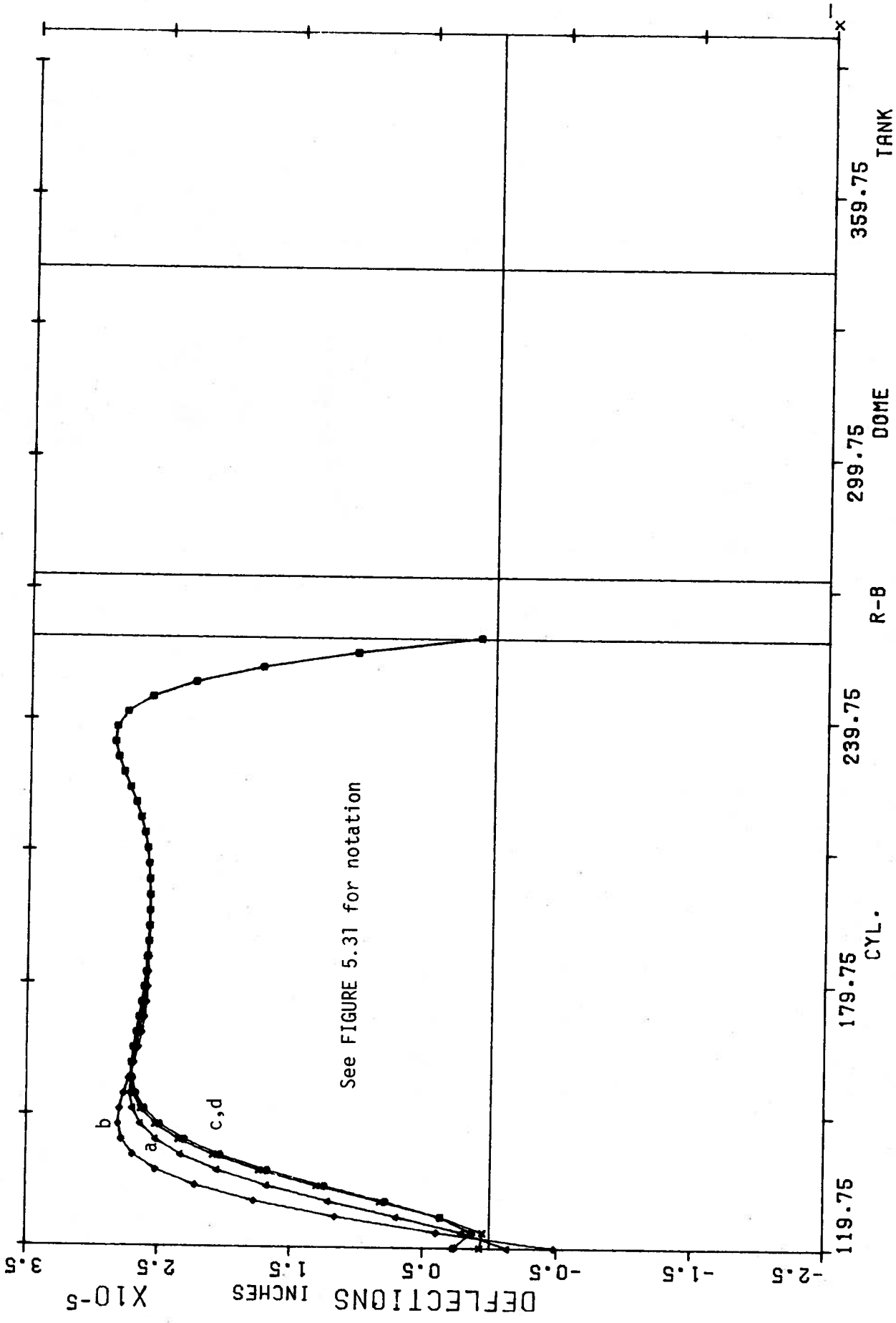


FIGURE 5.39 NORMAL DISPLACEMENTS BASE MODEL COMPARISON (INT. PRESSURE)

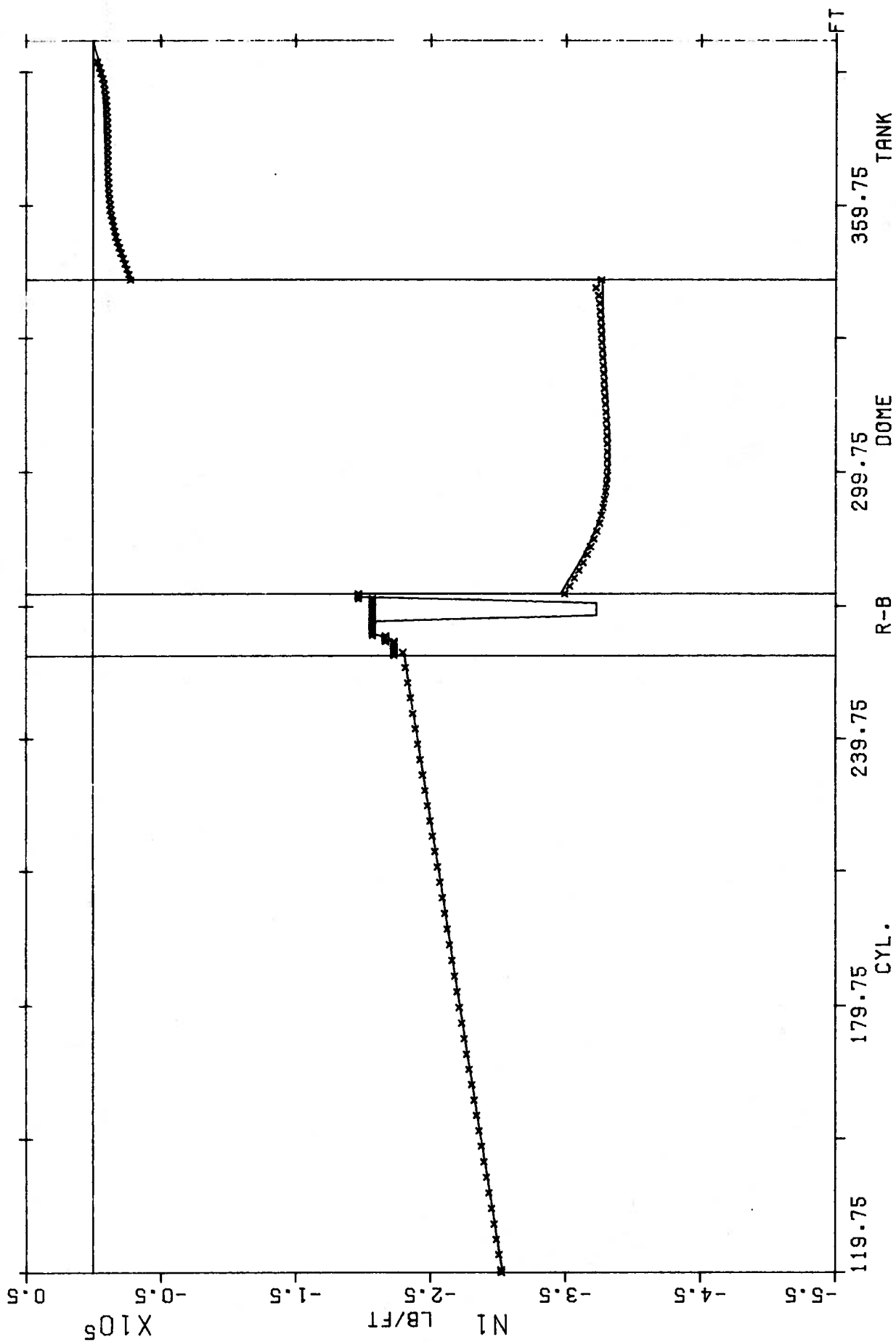


FIGURE 5.40 N1 FOR RF1

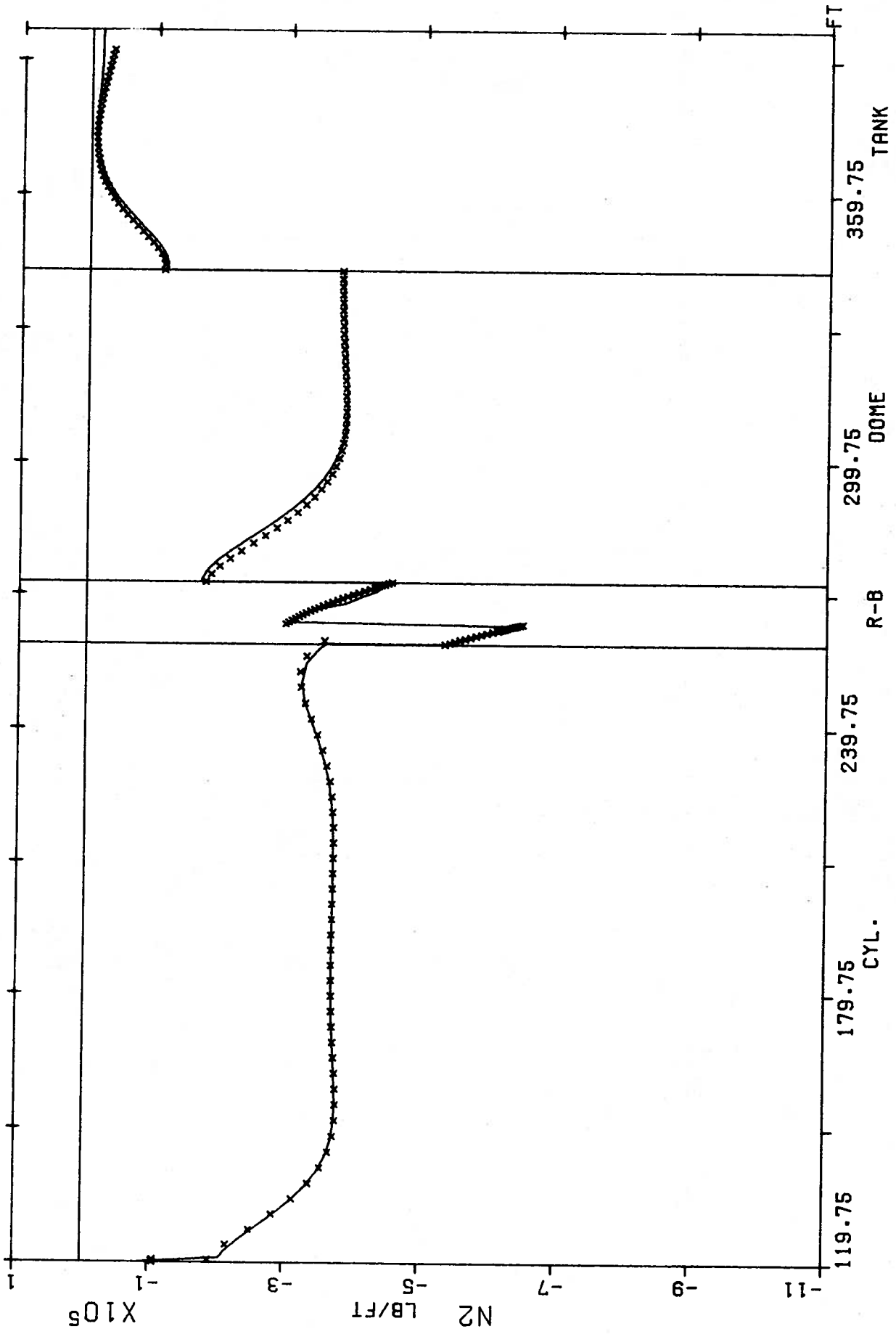


FIGURE 5.41 N₂ FOR RF1

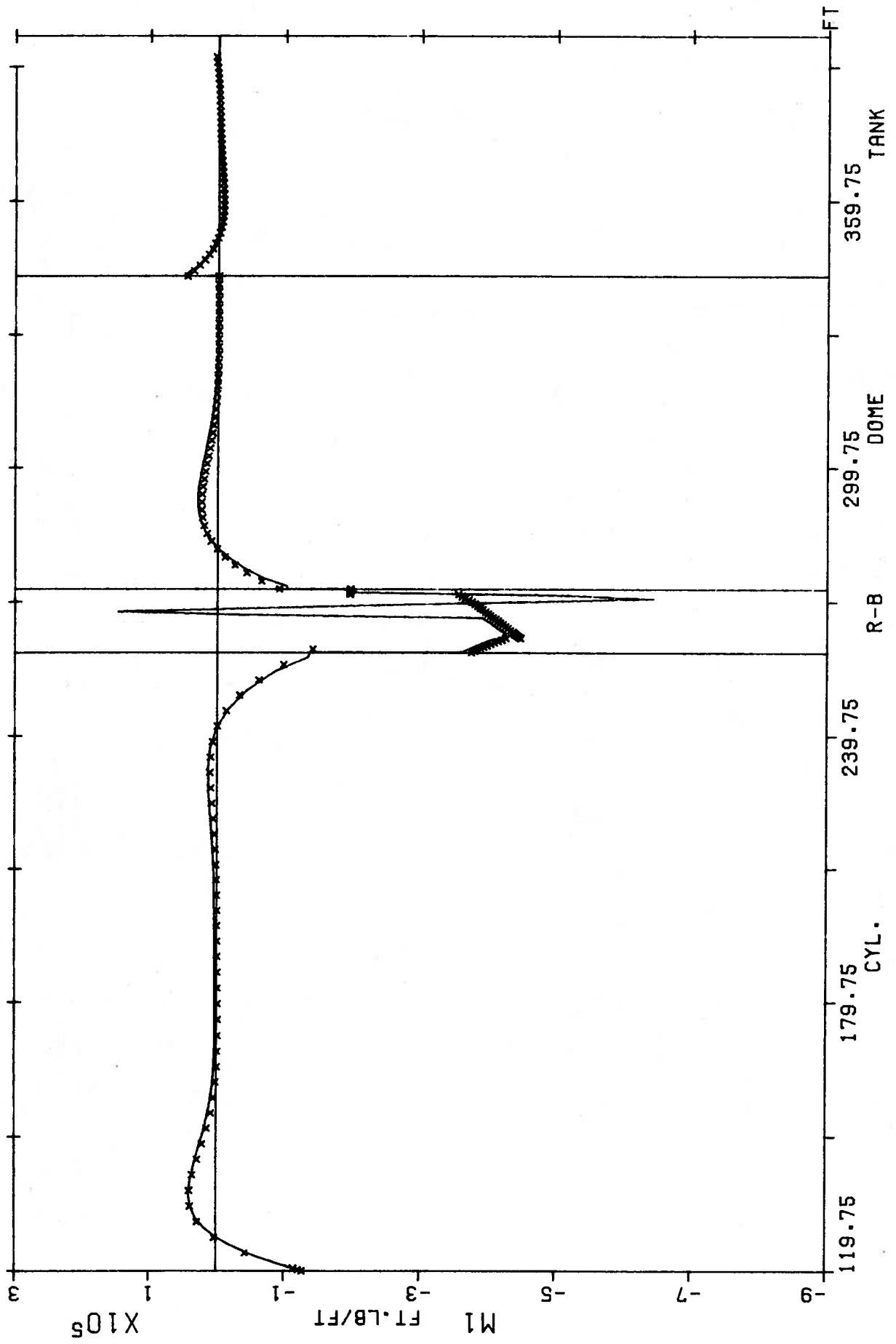


FIGURE 5.42 M1 FOR RF1

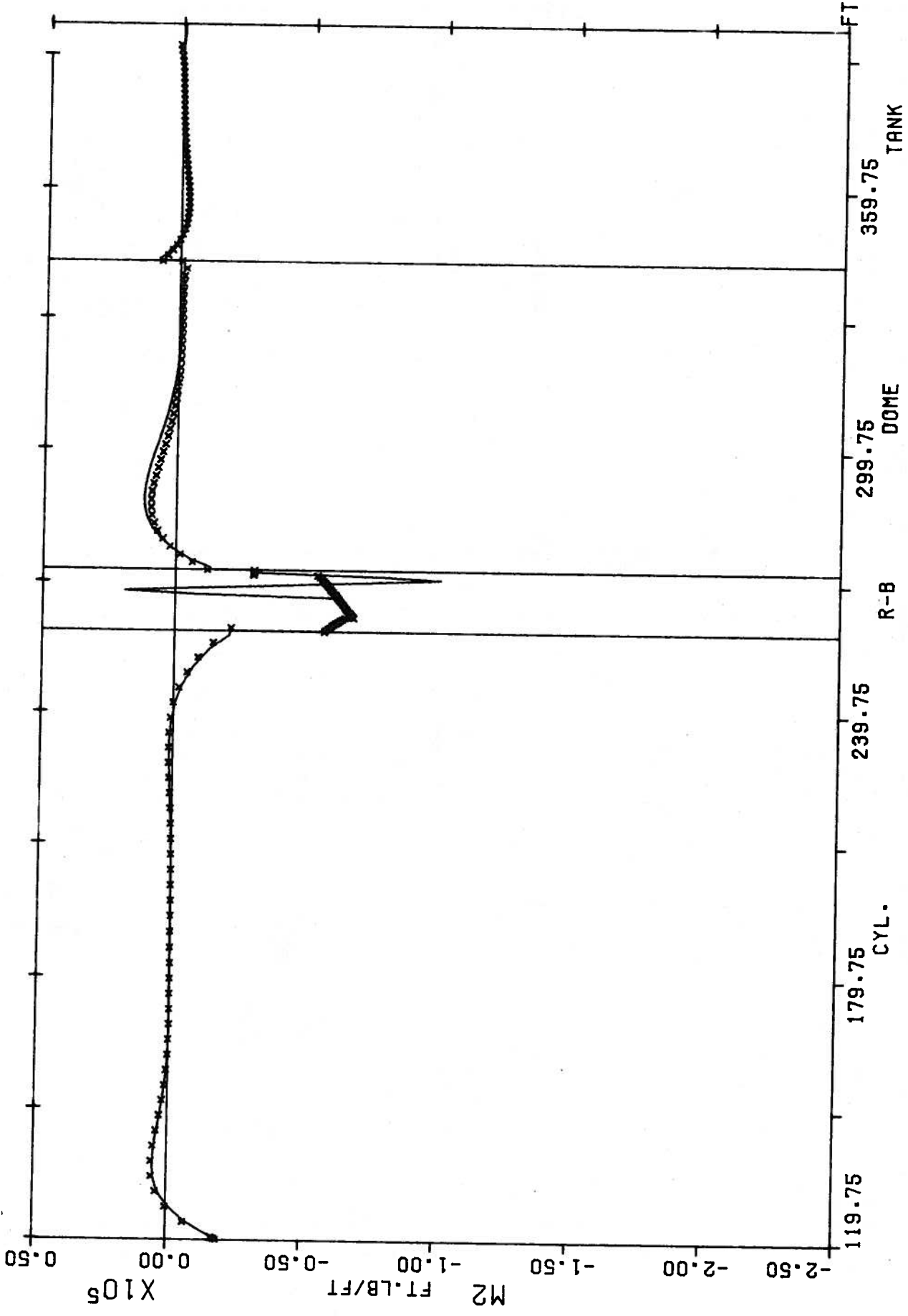


FIGURE 5.43 M2 FOR RF1

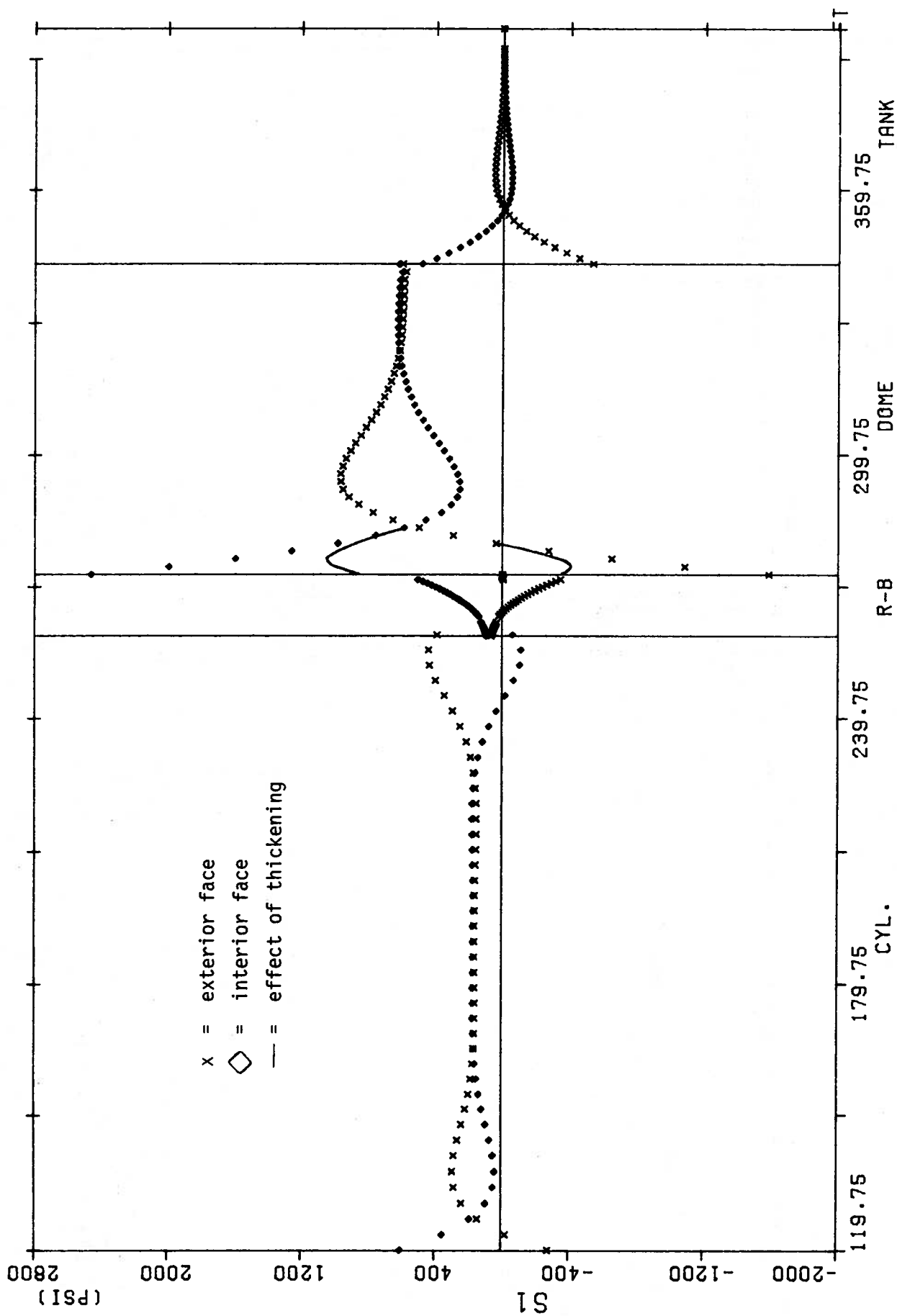


FIGURE 6.1 S1 FOR INT. PRESSURE (18PSI)

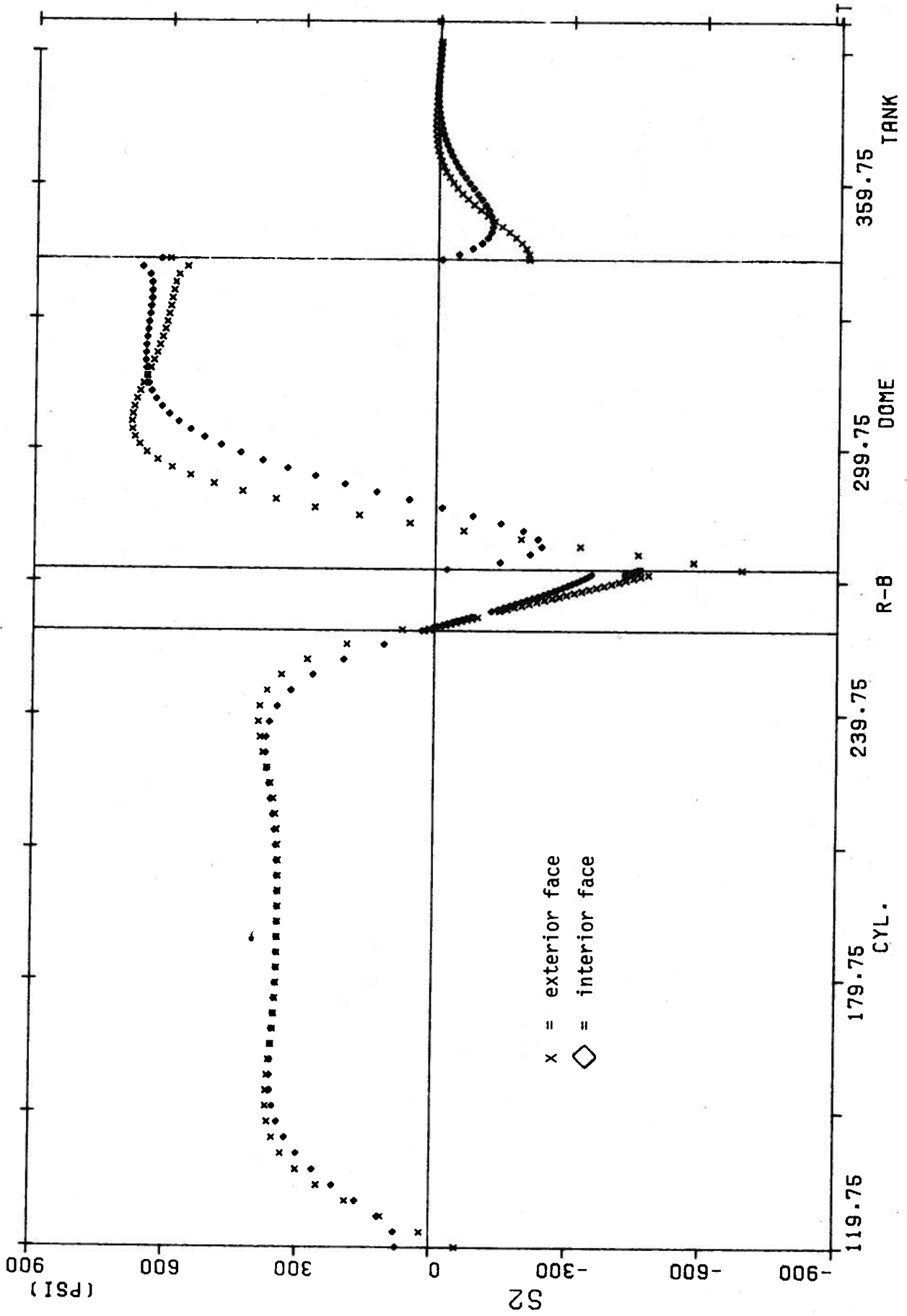


FIGURE 6.2 S2 FOR INT. PRESSURE (18PSI)

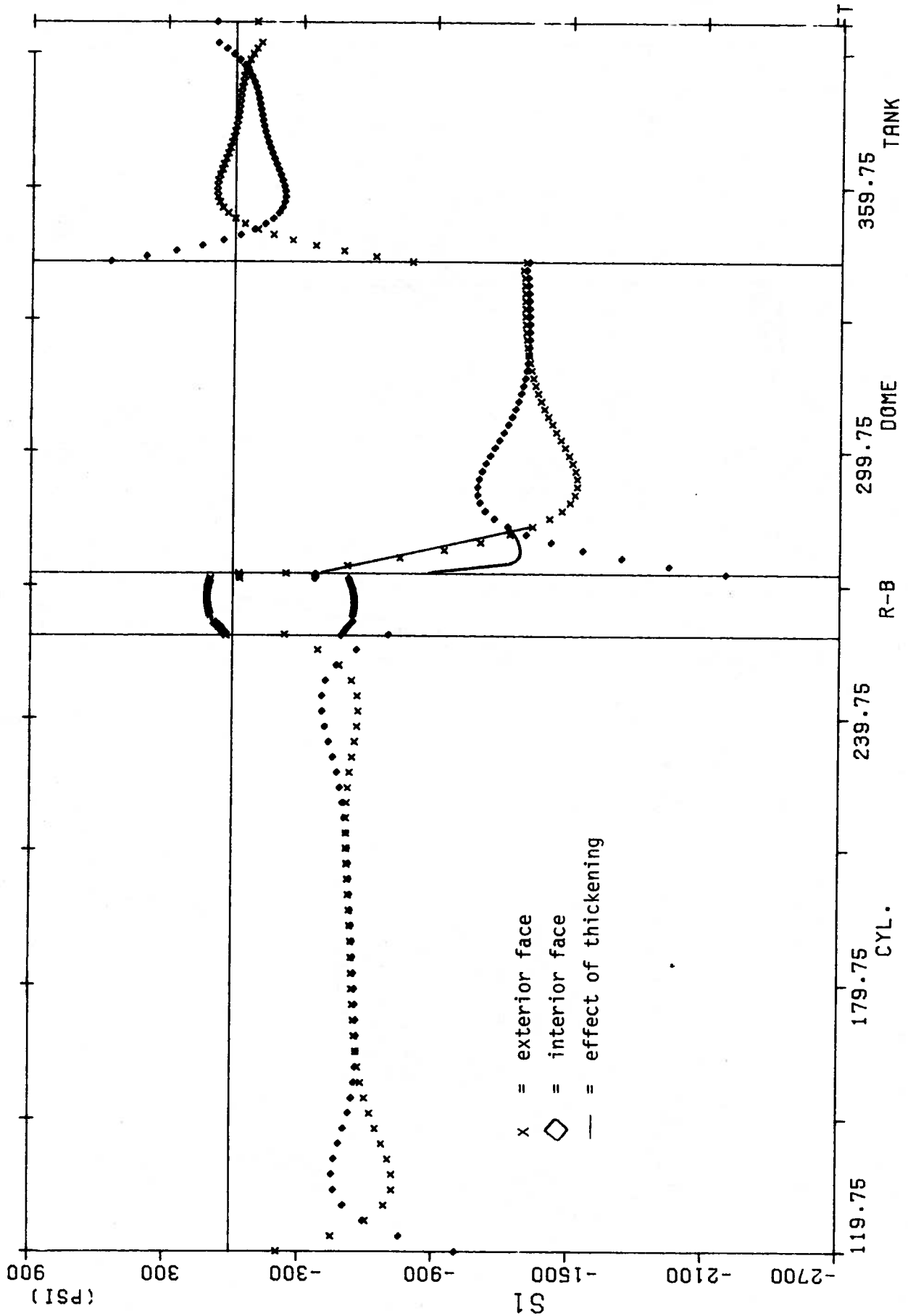


FIGURE 6.3 S1 for Switched-on Reference State

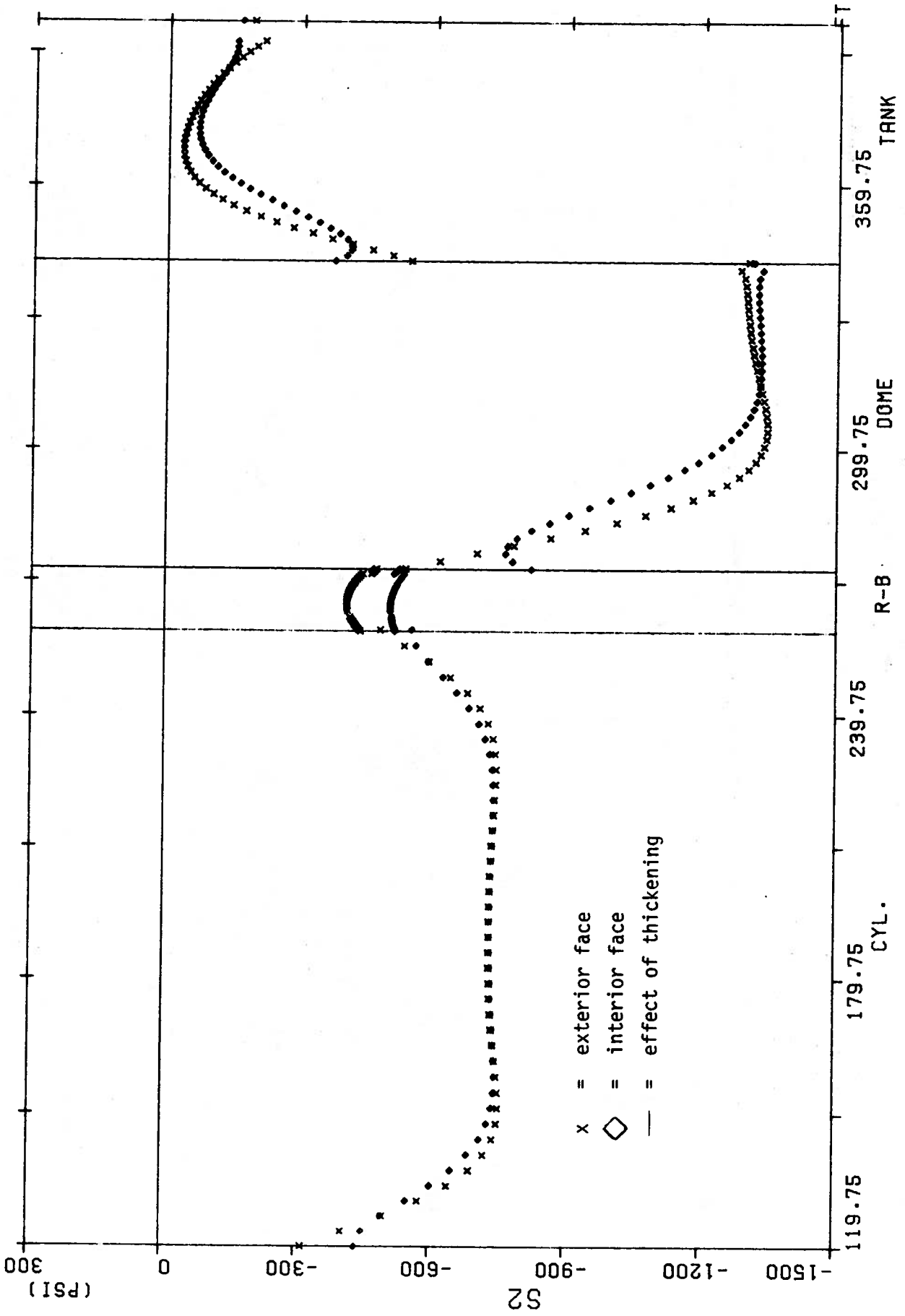


FIGURE 6.4 S2 for Switched-on Reference State

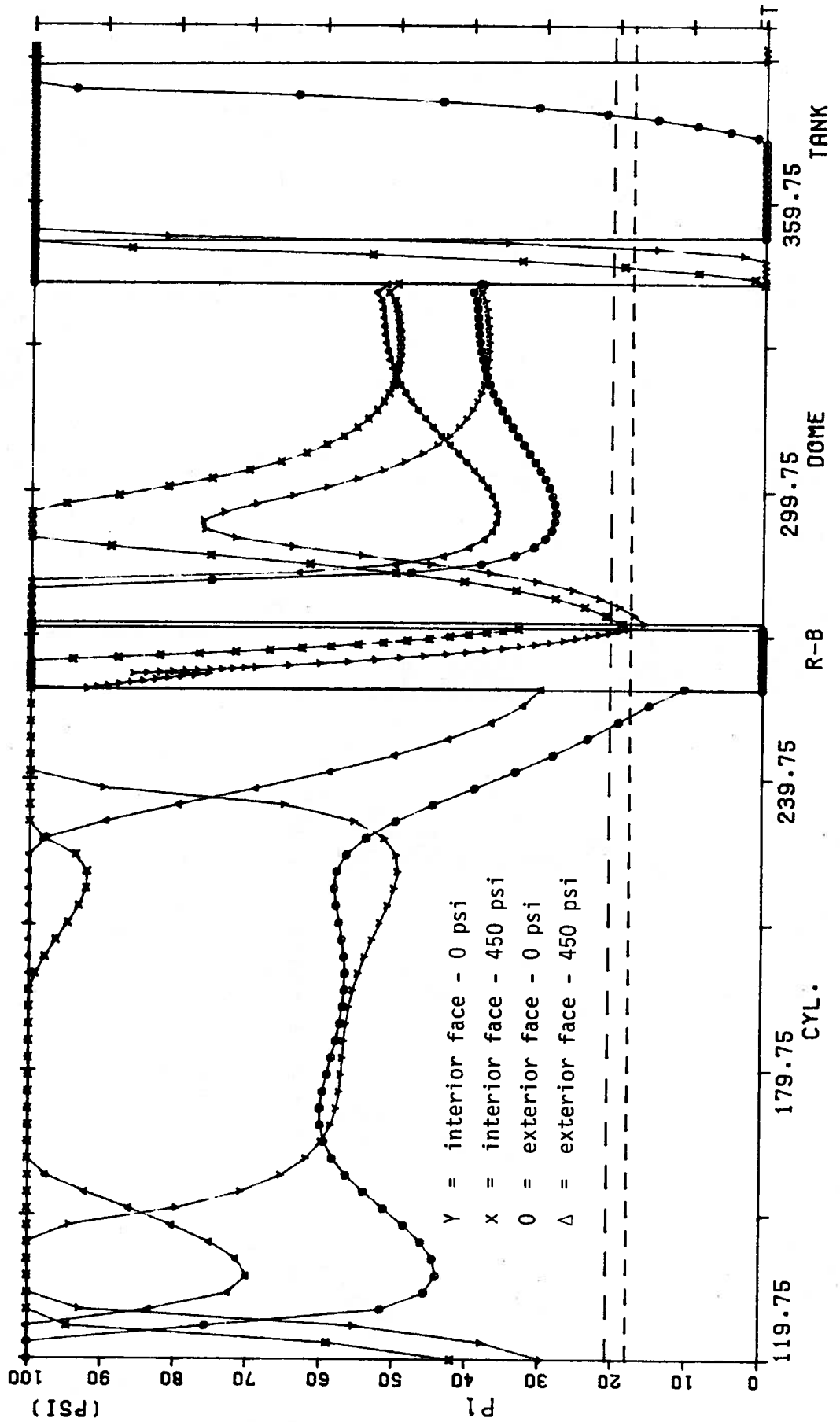
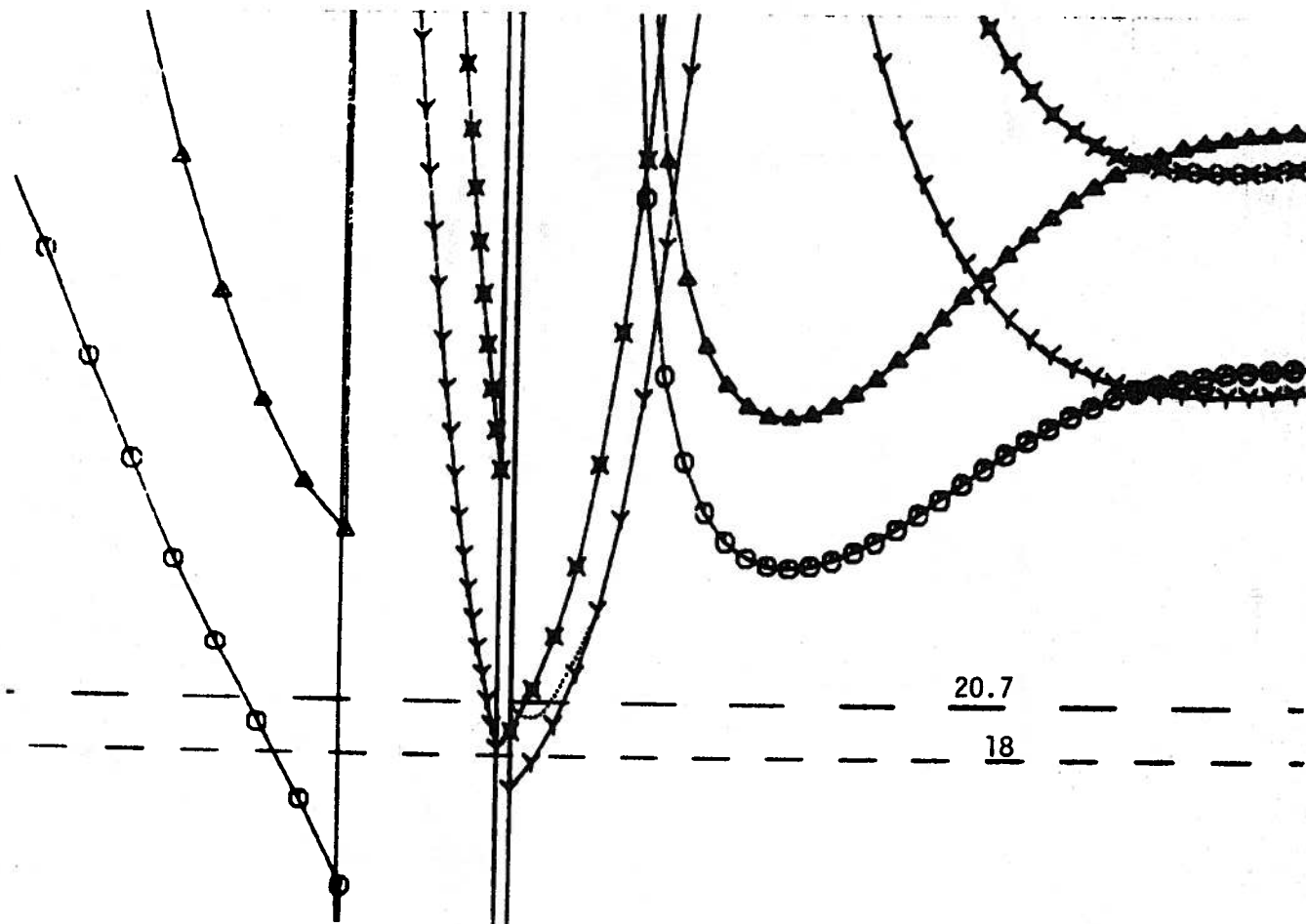


FIGURE 6.5 P1 for Switched-on Reference State



Y = interior face - 0 psi
 x = interior face - 450 psi
 O = exterior face - 0 psi
 Δ = exterior face - 450 psi
 effect of the thickening

FIGURE 6.6 P1 in Ring Beam Area for Switched-on Reference State

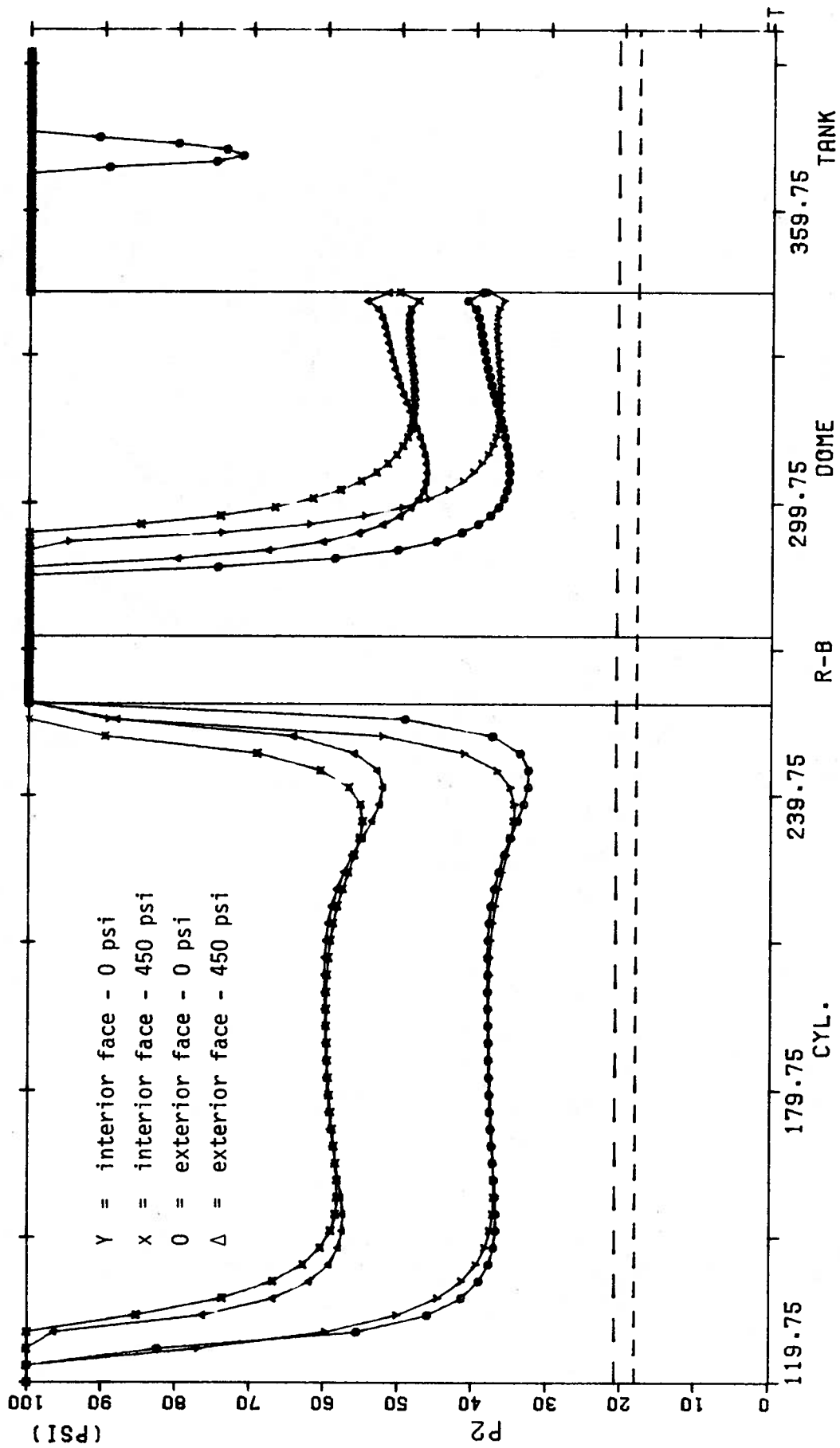


FIGURE 6.7 P2 for Switched-on Reference State

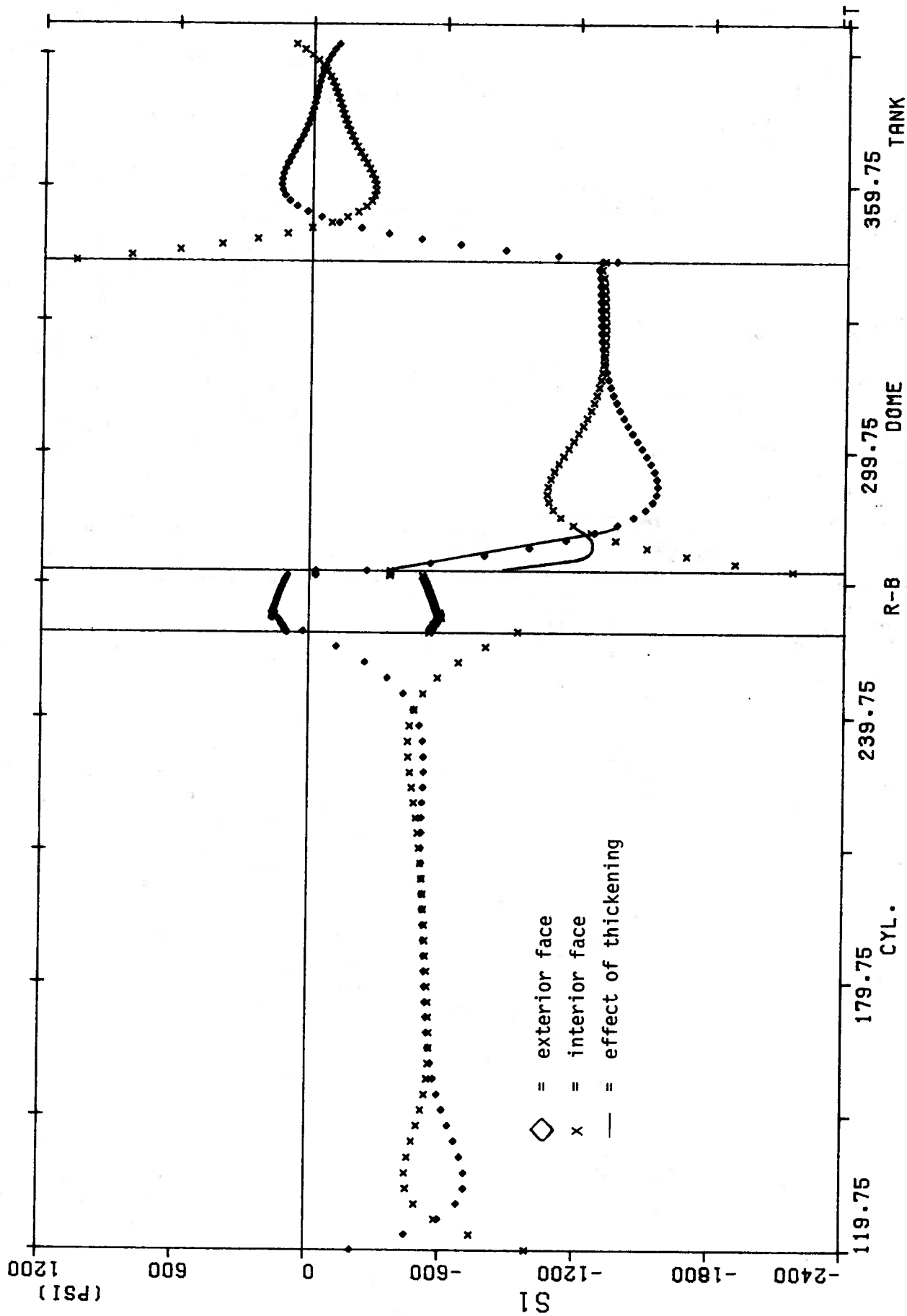


FIGURE 6.8 S1 FOR RF1

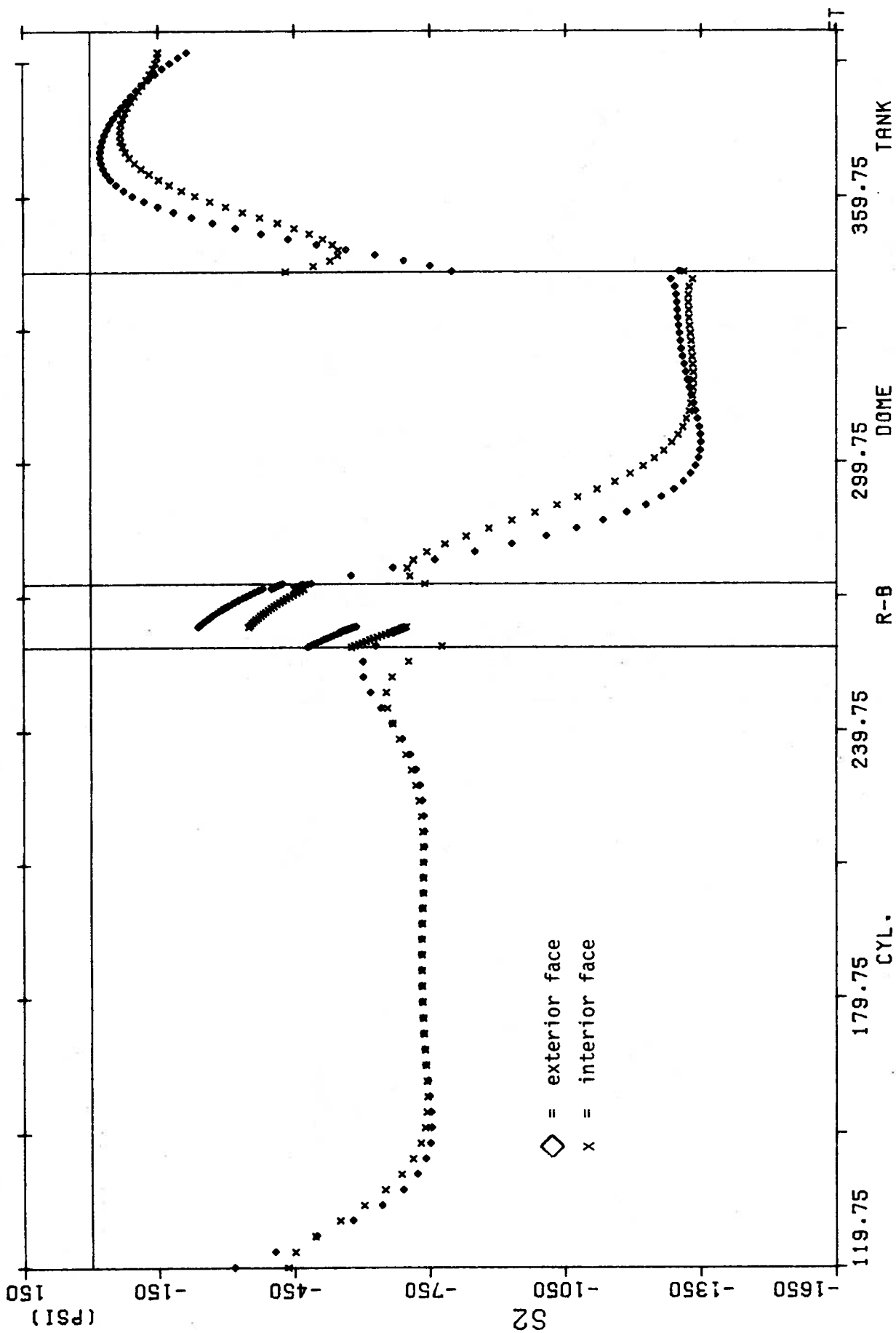


FIGURE 6.9 S2 FOR RF1

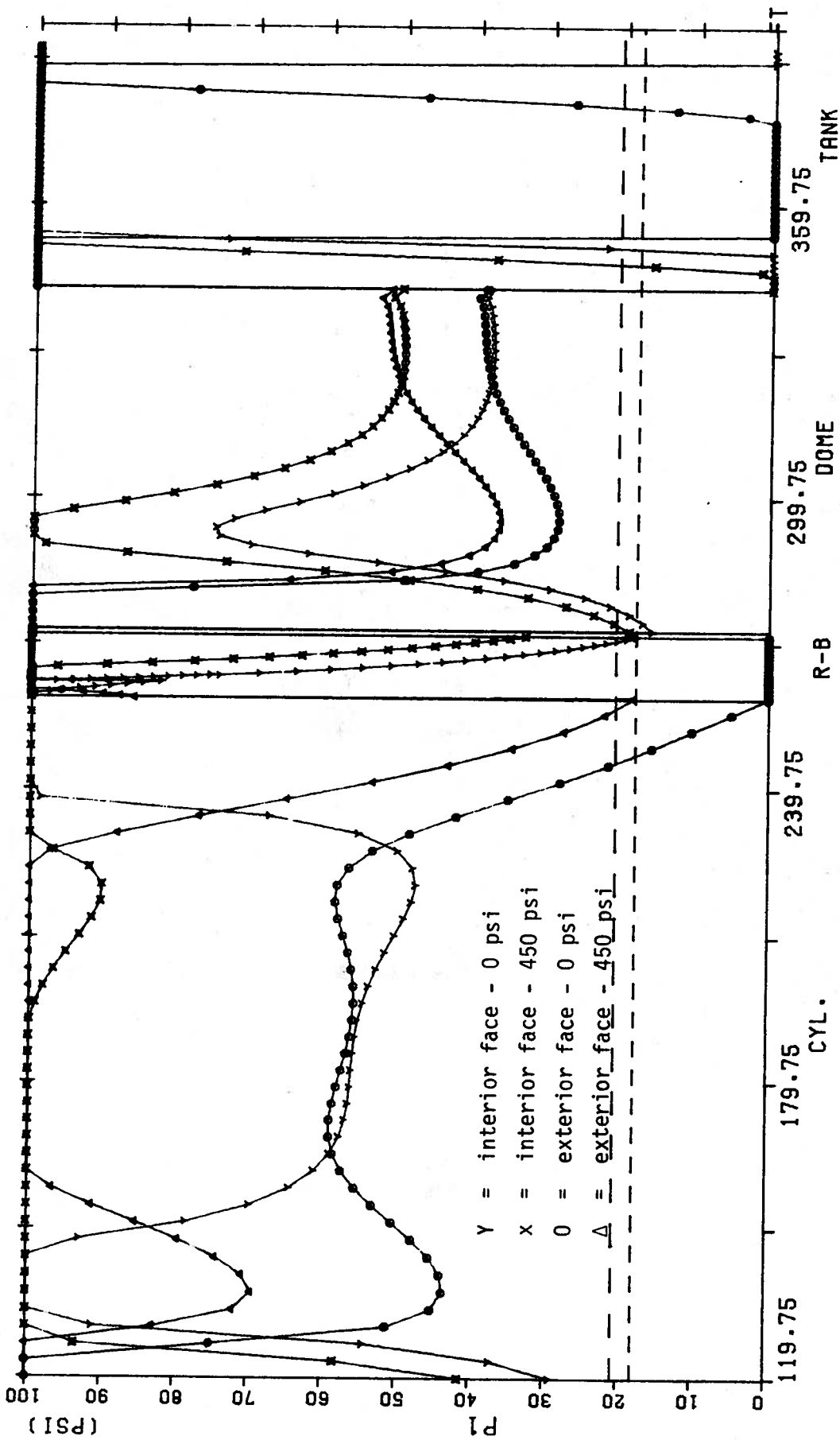


FIGURE 6.10 P1 for Reference State Rf1

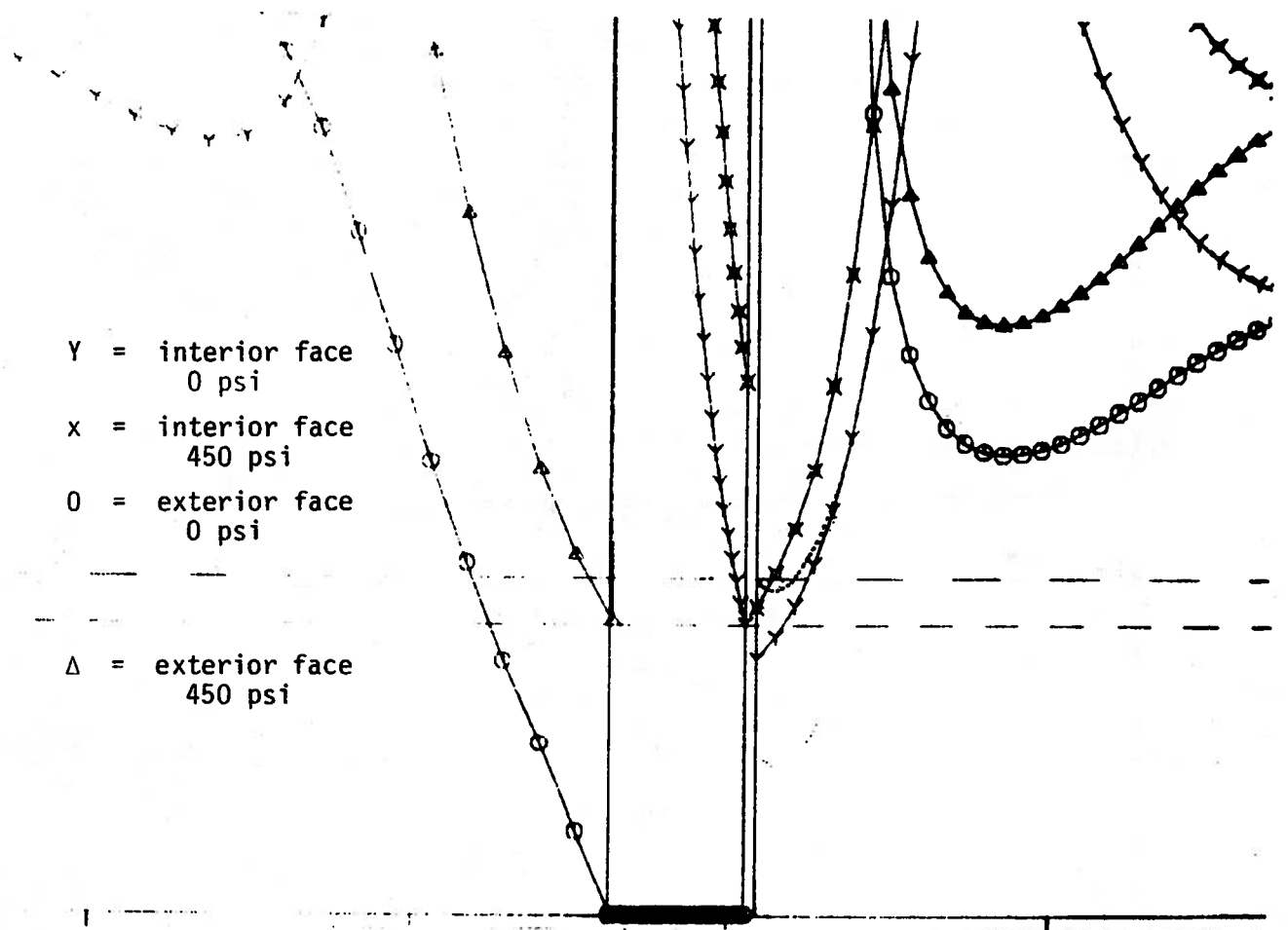


FIGURE 6.11 P1 in Ring Beam Area for Reference State Rf1

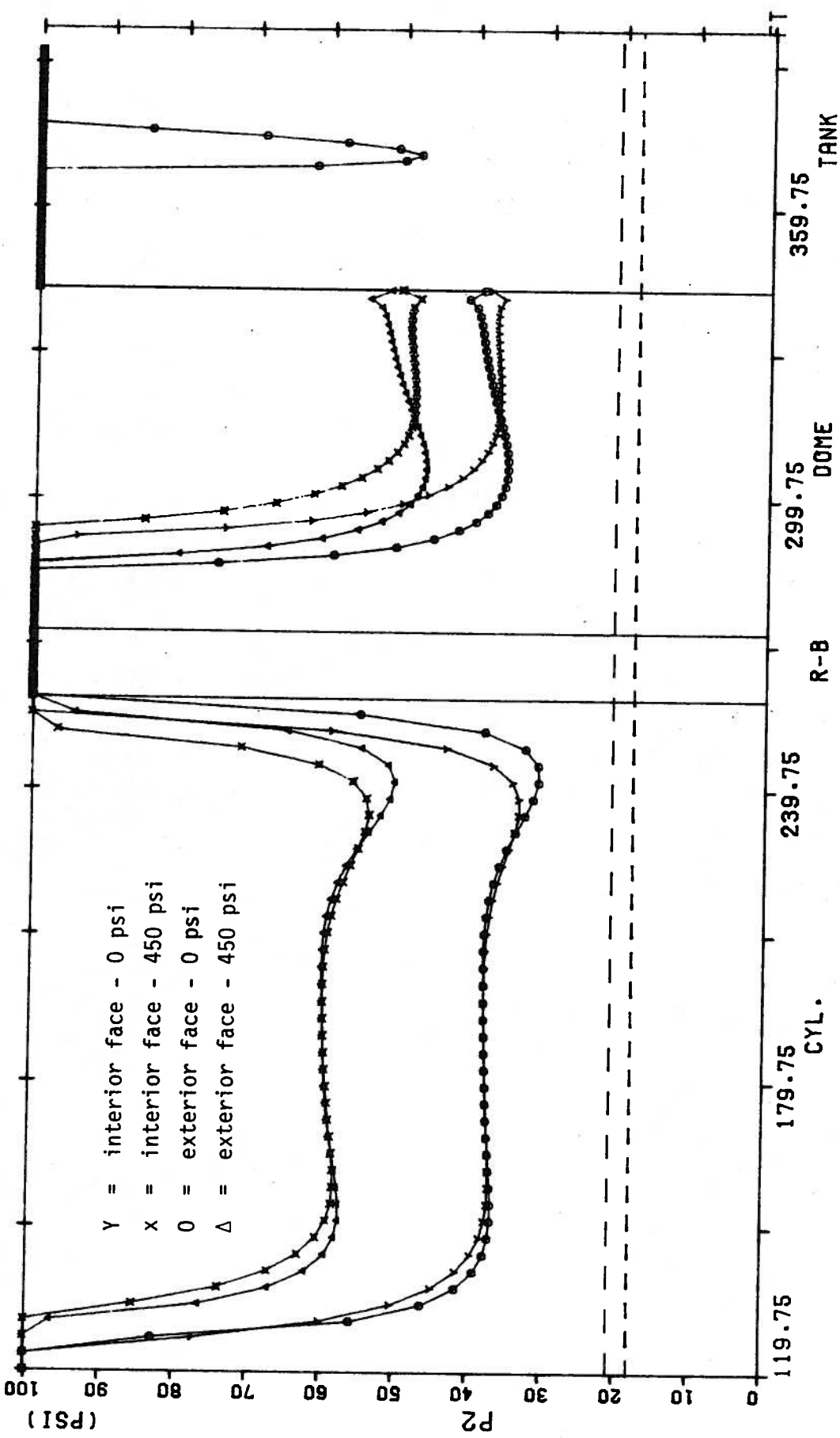


FIGURE 6.12 P2 for Reference State Rf1

APPENDIX A
FLEXSHELL USER'S MANUAL

APPENDIX A

User's Manual for Program FLEXSHELL

Program FLEXSHELL computes the in-plane forces and bending moments due to five types of loading conditions for axisymmetric branched segmented shells of revolution consisting of cylindrical and spherical shell segments and base slabs on elastic foundation. The loading conditions included are distributed pressure, self weight, prestress of segments, uniform temperature change and temperature gradient through the shell thickness. A complete listing of the program is given in Appendix B.

Solutions are obtained using the flexibility matrix method. Particular solutions are approximated using membrane solutions. Flexibility influence coefficients are obtained from bending solutions based on classical elastic shell theory. The general assembly procedure is described in detail in the report and all equations used in the program are listed in Appendix D. Examples of input are given in Appendix C and some discussion of input is contained in Chapter 4.

This Appendix is restricted to describing the input to the program.

The input to FLEXSHELL consists of multiple lines of input which may be either lines in a data file or data input cards. For convenience since each line in a data file corresponds exactly to a single input card, both will be referred to as cards.

There are six input card types each containing a separate type of data and having its own format. Certain card types may be repeated as required.

A typical explanation of a card type consists of the card type number, a descriptive name indicating the nature of the data being entered, the format for the data on that card and the number of data cards of that type required. This is followed by a symbolic line of input which, in turn, is followed by definitions of the terms and/or options available for the input variables. Examples of input for five sample problems are given in Appendix C. Throughout the input, all units have to be consistent.

TYPE 1: TITLE CARD

Format 10A8; 1 card

80
AN IDENTIFIER STRING

In order to identify the output, the user may enter any character string of up to 80 characters which will be reproduced as the first line in the output. This card is mandatory and if no title is desired on the output a blank entry card must be used which will appear as a blank line in the output.

TYPE 2: CONTROL CARD

Format 2I4; 1 card

4	8	
NSEG	IPRINT	

NSEG = number of shell segments in the structure to be analysed.

Maximum number = 20.

IPRINT = print control character

If IPRINT=0, echos input data and prints final results only.
(Usual mode of useage.)

IPRINT≠0, prints full output including intermediate values.
(Used for checking purposes only.)

TYPE 3: SEGMENT TYPE CARDS

Format 5I4, 2F10.4; 1 card for each segment,

4	8	12	16	20	30	40
I	IT(I)	IR(I,1)	IR(I,2)	NDIV(I)	EC(I,1)	EC(I,2)

I = segment number

IT = segment type

If IT = 1, segment is a cylinder segment

IT = 2, segment is a spherical segment.

IT = 3, segment is a base segment.

IR(I,1) = Top connectivity flag for segment I.

If IR(I,1) = 0, top not connected to another segment,

IR(I,1) = 1, top is connected to another segment.

IR(I,2) = Bottom connectivity flag for segment I.

If IR(I,2) = 0, bottom not connected to another segment,

IR(I,2) = 1, bottom is connected to another segment.

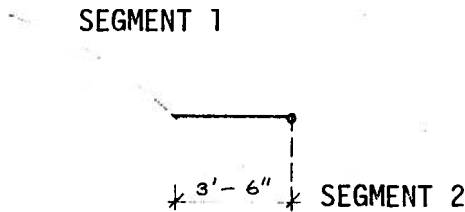
IR(I,2) = -1, bottom is connected to another segment with a
pure hinge.

NDIV(I) = number of divisions for segment I at which stress result-
ants are to be computed and printed. (NDIV(I) ≤ 100)

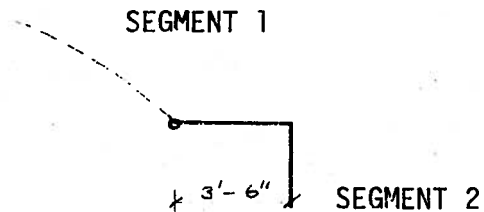
EC(I,1) = eccentricity of joint connection at the top of the segment
in feet.

EC(I,2) = eccentricity of joint connection at the bottom of the segment in feet.

NOTE: When two shell segments are connected at a given elevation but have different midsurface radii, a horizontal eccentricity equal to the differences in horizontal radii to the midsurfaces will result. This eccentricity can be applied to either shell segment and is positive when directed inwards. For the eccentricity between a spherical and cylindrical segment, EITHER of the following entries is permissible.



EC(1,2) = -3.5
 EC(2,1) = 0.0



EC(1,2) = 0.0
 EC(2,1) = +3.5

TYPE 4: CONNECTIVITY SPECIFICATION CARDS

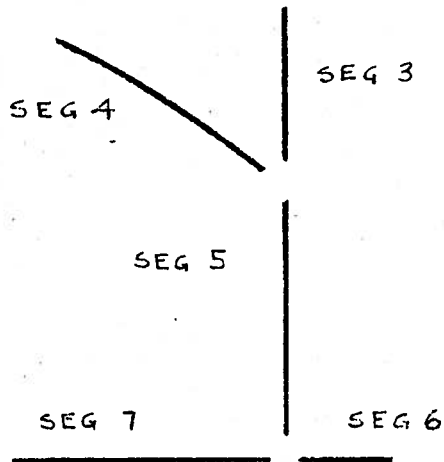
Format 2I4; 1 card for each connection between segments, (i.e.: - NSEG - 1 cards)

4	8	
IDCO(I,1)	IDCO(I,2)	

IDCO(I,1) = the number of the top segment

IDCO(I,2) = the number of the segment to which the top segment is connected

NOTE: Where three shell segments intersect at the same elevation, two connectivity specification cards are required. For the condition shown below the entries are 3 5 , on the first card, and 4 5 on the



second card. *)Note that each segment number appears precisely once in IDCO(I,1) and these numbers must be arranged consecutively in increasing order, starting with segment 1 and ending with segment NSEG.

*) For the base intersection the entries are 5 7 on the first card and 6 7 on the second.

TYPE 5: SEGMENT PROPERTIES CARDS

Format I4, F6.0, F12.0, F8.0, 5F10.0; 1 card for each segment.

4	10	20	30	40	50	60	70	80
I	T(I)	R(I)	H(I)	HO(I)	E(I)	PR(I)	ALPHA(I)	UW(I)

- I = segment number
- T(I) = segment thickness
- R(I) = radius to midsurface of segment for cylindrical and spherical segments
- = subgrade coefficient for base segments
- H(I) = the length for a cylindrical segment
- = the total angle from the axis of revolution to the outer edge in degrees, for a spherical segment
- = the outer radius of a circular base ring slab
- HO(I) = 0.0 or blank, for cylindrical segment

- = the angle in degrees measured from the axis of revolution to the inner edge of the shell, for spherical segment.
- = the inner radius of a circular base ring slab
- E(I) = modulus of elasticity for segment
- PR(I) = Poisson's ratio for segment
- ALPHA(I) = coefficient of thermal expansion
- UW(I) = unit weight of material for segment

TYPE 6: PARTICULAR SOLUTION CARDS

Format 2I4, 7F10.0; 1 card for each segment

	4	8	18	28	38	48	58	68	78
I	IP	PV(I)	PSF(I,1)	PSF(I,2)	PSF(I,3)	PSF(I,4)	PSF(I,5)	PSF(I,6)	

- I = segment number
- IP = classification of 'particular solution' according to the following code:
- 1 = uniform pressure
- 2 = self weight
- 3 = prestress loading
- 4 = uniform temperature change across section
- 5 = temperature gradient across section
- PV(I) = Numerical value of particular solution, interpreted as follows:

If IP = 1, magnitude of pressure

(Positive for internally directed pressure and negative for externally directed pressure. For a base segment positive when pressure directed downward and negative when directed upward.)

IP = 2, the value of PV is disregarded and a dead load analysis is carried out for the unit weights specified on cards of Type 5.

IP = 3, value of the distributed prestress pressure on the midsurface. Same sign convention as 1.

IP = 4, value of the uniform temperature change in degrees (positive if the temperature rises above the reference temperature.)

IP = 5, gradient of temperature across section in degrees per unit of thickness. Positive if temperature increases in a radially inward direction.

PSF(I,1) = magnitude of externally applied horizontal force at the top of the segment

PSF(I,2) = magnitude of externally applied moment at the top of the segment

PSF(I,3) = magnitude of externally applied horizontal force at the bottom of the segment

PSF(I,4) = magnitude of externally applied moment at the bottom of the segment

PSF(I,5) = magnitude of externally applied vertical force at the top of the segment

PSF(I,6) = magnitude of externally applied vertical force at the bottom of a base segment.

NOTE: (a) The PSF forces are forces and moments which, if necessary, are to be applied in addition to the distributed loading

effects identified by the PV particular solution values.

(b) Prestressing effects are generally simulated as distributed loads but cable anchorages give rise to concentrated loads which are treated as PSF forces.

APPENDIX B
PROGRAM LISTING

*** FLEXSHELL ***

THIS PROGRAM IS FOR THE FLEXIBILITY ANALYSIS OF SEGMENTED
 AXISYMMETRIC SHELLS. IT CAN HANDLE ANY COMBINATION OF DOME
 AND SHERICAL SEGMENTS CONNECTED TOGETHER AT JUNCTION POINTS.
 REDUNDANT FORCES ARE APPLIED TO THE INDIVIDUAL
 SEGMENTS TO ESTABLISH THE REQUIRED GEOMETRIC COMPATIBILITY.
 CODED BY D.W. MURRAY AND A.M.ROHARDT, DECEMBER 1976
 THE UNIVERSITY OF ALBERTA, EDMONTON, ALBERTA
 REVISED: MAY 1977

*** NOTATION ***

IT=TYPE OF SEGMENT :1=CYLINDER :2=DOME :3=BASE ON ELASTIC FOUND.
 IP=TYPE OF LOADING :1=INTERNAL PRESSURE :2=DEAD LOAD
 :3=PRESTRESS PRESSURE :4=UNIFORM THERMAL STRAIN
 :5=GRADIENT THERMAL STRAIN

GEOMETRIC VARIABLES

SEG. TYPE	CYLINDER	SHELL	BASE
T=	THICKNESS	THICKNESS	THICKNESS
R=	RADIUS	RADIUS	BASE STIFEN
H=	LNPGTH	OUTER ANGLE	OUTER RADIUS
HO=	**	INNER ANGLE	INNER RADIUS

INDECES

NF=NUMBER OF SEGMENT EDGE FORCES NR=NUMBER OF REDUNDANTS
 NSEG=NUMBER OF SEGMENTS

MAIN ARRAYS

IR(*,1)=REDUNDANT FLAG TOP OF ELEMENT
 IR(*,2)=REDUNDANT FLAG BOTTOM OF ELEMENT
 IDF=IDENTITY OF UNKNOWN FORCES AT TOP AND BOTTOM OF ELEMENTS
 PBF=PARTICULAR SOLUTION BASE FORCES
 PSD=PARTICULAR SOLUTION EDGE DISPLACEMENTS
 PARD=PARTICULAR SOLUTION INCOMPATIBLE DISPLACEMENTS
 PSF=PARTICULAR SOLUTION FORCES WHICH PRODUCE ADDITIONAL INCOMPAT
 -IBLE DISPLACEMENTS
 A=MATRIX ESTABLISHING GEOMETRIC COMPATIBILITY BETWEEN DEGREES OF
 FREEDOM

EXTERNAL FUNCTIONS AND SUBROUTINES FOLLOW THE MAIN PROGRAM
 IN THE FOLLOWING ORDER:

FUNCTIONS:	SUBROUTINES:	
1. CONST	4. PCYLIN	9. BASE
2. FN1	5. CYLIN	10. BSHAPP
3. FN2	6. PDOME	11. JINVER
	7. DOME	12. SOL
	8. PBASE	13. PFOR

IMPLICIT REAL*8 (A-H, O-Z)
 DIMENSION T (20), R (20), H (20), HO (20), F (20), PR (20), ALPHA (20), PV (20),
 * S (6,6), PSD (6), F (80,80), TT (80,80), PARD (80), PART (80), PBF (6,20),
 * FO (80), SF (6), CVEC (4), XH (101), A (80,80), TS (4,4), PSF (20,6), BB (4,4),
 * RM1 (101), PM2 (101), RN1 (101), RN2 (101), EC (20,2), UR (20), TITLE (10)
 DIMENSION IT (20), IR (20,2), TP (20), IDCO (19,2), IDF (19,6), NDIV (20)
 * , IBASE (6), IVECT (4), SR (10), M1 (100), M2 (100), V (100), HR (101), W (100)
 DATA PI/3.1415926536/, RAD/57.295779513/, IBASE/1,2,5,3,4,6/

 C READ AND ECHOCHECK DATA

```

READ (5,1001) TITLE
WRITE (6,2001) TITLE
READ (5,1000) NSEG,IPRINT
WRITE (6,2000) NSEG,IPRINT
IF (NSEG.GT.20) GO TO 999
READ (5,1000) (I,IT(I),IR(I,1),IR(I,2),NDIV(I),EC(I,1),EC(I,2),
* II=1,NSEG)
WRITE (6,2100) (I,IT(I),IR(I,1),IR(I,2),NDIV(I),EC(I,1),EC(I,2),
* I=1,NSEG)
NSEG1=NSEG-1
READ (5,1200) ((IDCO(I,J),J=1,2),I=1,NSEG1)
WRITE (6,2200) ((IDCO(I,J),J=1,2),I=1,NSEG1)
READ (5,1300) (I,T(I),R(I),H(I),HO(I),E(I),PR(I),ALPHA(I),UW(I),
* II=1,NSEG)
WRITE (6,2300) (I,T(I),R(I),H(I),HO(I),E(I),PR(I),ALPHA(I),UW(I),
* I=1,NSEG)
READ (5,1400) (I,IP(I),PV(I),(PSF(I,J),J=1,6),II=1,NSEG)
WRITE (6,2400) (I,IP(I),PV(I),(PSF(I,J),J=1,6),I=1,NSEG)
P4=PI/4
R2=2.0
R2=DSQRT(R2)
IFLAG=0

```

 C IDENTIFY DEGREES OF FREEDOM AND FORM A-MATRIX

```

C FORM IDF ARRAY
DO 30 J=1,6
DO 30 I=1,NSEG
30 IDF(I,J)=0
C
KV=0
KOUNT=0
NRH=0
DO 50 I=1,NSEG
DO 50 J=1,2
J2=2*J-1
IF (IR(I,J).EQ.0) GO TO 50
IDF(I,J2)=KOUNT+1
IF (IR(I,J).GT.0) GOTO 40
KOUNT=KOUNT+1
NRH=-1
GOTO 41
40 IDF(I,J2+1)=KOUNT+2
KOUNT=KOUNT+2
41 IF (IT(I).NE.3) GO TO 50
IF (J.EQ.1) J2=5
IF (J.EQ.2) J2=6
KOUNT=KOUNT+1
IDF(I,J2)=KOUNT
KV=KV+1
50 CONTINUE
NF=KOUNT
NR=2*NSEG1+KV/2+NRH

```

C
 FILE

```

C
  IF (IPRINT.EQ.0) GOTO 45
  WRITE (6,2435)
  DO 35 I=1,NSEG
  WRITE (6,2440) (IDF(I,J), J=1,6)
35  CONTINUE
2440  FORMAT(20I5)
2435  FORMAT(///' THE IDF MATRIX IS '/')
45  CONTINUE
C
C   FORM A MATRIX
  IO=1
  DO 180 I=1,NR
  DO 180 J=1,NF
180  A(I,J)=0.0
  DO 300 I=1,NSEG1
  K=IDCO(I,1)
  L=IDCO(I,2)
250  J1=IDF(K,3)
  J2=IDF(L,1)
  A(IO,J1)=1.
  A(IO,J2)=-1.
  IF (IDF(K,4).EQ.0.OR.IDF(L,2).EQ.0) GOTO 260
  A(IO+1,J1+1)=1.
  A(IO+1,J2+1)=-1.
C
260  IF (IT(L).EQ.3) A(IO,J2+1)=+FC(L,1)
  IF (IT(K).EQ.3.AND.IT(L).EQ.3) A(IO,J2+1)=-FC(K,2)
  IO=IO+2
  IF (IDF(K,4).EQ.0.OR.IDF(L,2).EQ.0) IO=IO-1
  IF (IT(I).NE.3.OR.IT(L).NE.3) GOTO 300
  J1=IDF(K,6)
  J2=IDF(L,5)
  A(IO,J1)=1
  A(IO,J2)=-1
  IO=IO+1
300  CONTINUE
C
  IF (IPRINT.EQ.0) GO TO 351
  WRITE (6,2450)
  DO 350 I=1,NR
  WRITE (6,2500) (A(I,J),J=1,NF)
350  CONTINUE
2450  FORMAT(///' THE A CONNECTIVITY MATRIX IS')
2500  FORMAT(20F4.1)
C-----
C  CONSTRUCT BASIC FORCES FOR PARTICULAR SOLUTIONS (PBF AND PSF ARRAYS)
C-----
351  DO 355 N=1,NSEG
  DO 355 J=1,6
355  PBF(J,N)=0.0
  DO 356 I=1,NSEG
356  PBF(5,I)=PSF(I,5)
C
  DO 385 N=1,NSEG

```

```

IF (IPRINT.EQ.0) GOTO 45
WRITE (6,2435)
DO 35 I=1,NSEG
WRITE (6,2440) (IDF(I,J), J=1,6)
35 CONTINUE
2440 FORMAT(20I5)
2435 FORMAT(///' THE IDF MATRIX IS '/')
45 CONTINUE

C
C FORM A MATRIX
IO=1
DO 180 I=1,NR
DO 180 J=1,NF
180 A(I,J)=0.0
DO 300 I=1,NSEG1
K=IDCO(I,1)
L=IDCO(I,2)
250 J1=IDF(K,3)
J2=IDF(L,1)
A(IO,J1)=1.
A(IO,J2)=-1.
IF (IDF(K,4).EQ.0.OR.IDF(L,2).EQ.0) GOTO 260
A(IO+1,J1+1)=1.
A(IO+1,J2+1)=-1.

C
260 IF (IT(L).EQ.3) A(IO,J2+1)=+EC(L,1)
IF (IT(K).EQ.3.AND.IT(L).EQ.3) A(IO,J2+1)=-EC(K,2)
IO=IO+2
IF (IDF(K,4).EQ.0.OR.IDF(L,2).EQ.0) IO=IO-1
IF (IT(I).NE.3.OR.IT(L).NE.3) GOTO 300
J1=IDF(K,6)
J2=IDF(L,5)
A(IO,J1)=1
A(IO,J2)=-1
IO=IO+1
300 CONTINUE

C
IF (IPRINT.EQ.0) GO TO 351
WRITE (6,2450)
DO 350 I=1,NR
WRITE (6,2500) (A(I,J),J=1,NF)
350 CONTINUE
2450 FORMAT(///' THE A CONNECTIVITY MATRIX IS')
2500 FORMAT(20F4.1)

C-----
C CONSTRUCT BASIC FORCES FOR PARTICULAR SOLUTIONS (PBF AND PSF ARRAYS)
C-----
351 DO 355 N=1,NSEG
DO 355 J=1,6
355 PBF(J,N)=0.0
DO 356 I=1,NSEG
356 PBF(5,I)=PSF(I,5)
C
DO 385 N=1,NSEG
C

```

```

DO 387 I=1,NSEG
387 WRITE(6,2553) (PSF(I,J),J=1,6)
2550 FORMAT(///,' *** PBF *** '/')
2551 FORMAT(6E13.4)
2552 FORMAT(///,' *** PSF *** '/')
2553 FORMAT(6E13.4)
C-----
C CONSTRUCT AND ASSEMBLE ELEMENT FLEXIBILITY MATRICES
C AND INITIAL DISPLACEMENT VECTOR
C-----
398 DO 400 I=1,NF
PARD(I)=0.0
DO 400 J=1,NF
400 F(I,J)=0.0
C
DO 500 N=1,NSEG
IF(IT(N).NE.1) GO TO 405
CALL CYLIN(T(N),R(N),H(N),HO(N),E(N),PR(N),UW(N),S,TS,D,BETA,
* IFLAG)
PBT=PBF(5,N)
CALL PCYLIN(T(N),R(N),H(N),HO(N),E(N),PR(N),UW(N),ALPHA(N),S,PSD,
* IP(N),PV(N),N,PSF,PBT)
C
IF(IPRINT.EQ.0) GO TO 420
WRITE(6,2600) N,((S(I,J),J=1,4),I=1,4)
2600 FORMAT(///' FLEXIBILITY MATRIX FOR CYLINDRICAL SEGMENT',I4/
* (4E16.5))
C
GOTO 420
405 IF(IT(N).NE.2) GO TO 410
C
C SPHERICAL SEGMENT
CALL DOME(T(N),R(N),H(N),HO(N),E(N),PR(N),UW(N),S,ANG,ANGO)
PBT=PBF(5,N)
PST=PSF(N,1)
CALL PDOME(T(N),R(N),H(N),HO(N),E(N),PR(N),UW(N),ALPHA(N),
* S,PSD,IP(N),PV(N),N,PSF,ANG,ANGO,PBT,PST)
C
IF(IPRINT.EQ.0) GO TO 420
WRITE(6,2700) N,((S(I,J),J=1,4),I=1,4)
2700 FORMAT(///' FLEXIBILITY MATRIX FOR DOME SEGMENT',I4/
* (4E16.5))
GOTO 420
C
C ELASTIC FOUNDATION SEGMENTS
410 IF(IT(N).NE.3) GO TO 999
IFLAG=0
CALL BASE(IFLAG,T(N),R(N),H(N),HO(N),E(N),PR(N),UW(N),BB,S,TS,D)
CALL PBASE(T(N),R(N),H(N),HO(N),E(N),PR(N),ALPHA(N),UW(N),S,PSD,
* IP(N),PV(N),N,PSF,PBF)

```

FILE

C SPECIAL ASSEMBLY FOR BASE ELEMENTS

```

C
  DO 415 I=1,6
  L=IDF(N,I)
  IF(L.EQ.0) GO TO 415
  PARD(L)=PSD(I)
  DO 412 J=1,6
  K=IDF(N,J)
  IF(K.EQ.0) GO TO 412
  F(L,K)=S(I,J)
412 CONTINUE
  415 CONTINUE
  IF (IPRINT.EQ.0) GO TO 500
  WRITE(6,2720) N,S
2720 FORMAT(///' FLEXIBILITY MATRIX FOR BASE SEGMENT',I4/
* (6E16.5))
  GO TO 500

```

C ASSEMBLY OF FLEXIBILITY MATRIX AND DISPLACEMENT VECTOR (PARD)

```

420 DO 460 I=1,4
  L=IDF(N,I)
  IF(L.EQ.0) GO TO 460
  PARD(L)=PSD(I)
  DO 450 J=1,4
  K=IDF(N,J)
  IF(K.EQ.0) GO TO 450
  F(L,K)=S(I,J)
450 CONTINUE
  460 CONTINUE
500 CONTINUE

```

```

C
  IF (IPRINT.EQ.0) GO TO 508
  WRITE(6,2800)
2800 FORMAT(///' ELEMENT FLEXIBILITIES AFTER ASSEMBLY')
  DO 505 I=1,NF
  WRITE(6,2850) (F(I,J),J=1,NF)
505 CONTINUE
2850 FORMAT(6E12.4)

```

C CONDENSE TO REDUNDANT FLEXIBILITY MATRIX AND DISPLACEMENT VECTOR

```

508 DO 520 I=1,NF
  DO 520 J=1,NR
  C=0.0
  DO 510 K=1,NF
510 C=C+F(I,K)*A(J,K)
520 TT(I,J)=C
C
  DO 650 I=1,NR
  C=0.0
  DO 610 K=1,NF
610 C=C+A(I,K)*PARD(K)
  PART(I)=-C

```

C

FILE

```

C
DO 630 J=1, NR
C=0.0
DO 620 K=1, NF
620 C=C+A(I, K)*TT(K, J)
630 F(I, J)=C
650 CONTINUE
C
IF (IPRINT.EQ.0) GO TO 670
WRITE(6, 2900)
2900 FORMAT(///' CONDENSED FLEXIBILITY MATRIX')
DO 660 I=1, NR
WRITE(6, 2850) (F(I, J), J=1, NR)
660 CONTINUE
WRITE(6, 3001) (I, PART(J), I=1, NR)
3001 FORMAT(///' INCOMPATIBLE DISPLACEMENTS'/' IDISP VALUE'/
* (I5, E13.5))
-----
C SOLVE FOR REDUNDANTS AND FIND SEGMENT END FORCES
-----
670 CALL SOL(F, PART, 80, NR)
C
C FIND SEGMENT FORCES
DO 700 I=1, NF
C=0.0
DO 690 J=1, NR
690 C=C+A(J, I)*PART(J)
700 FO(I)=C
C
C WRITE TOTAL VECTOR OF SEGMENT END FORCES
WRITE(6, 3100)
3100 FORMAT(///'FORCES ON ENDS OF SEGMENTS'/' SEG J IF', 6X,
* 'FORCE')
DO 706 N=1, NSEG
DO 705 J=1, 6
L=IDF(N, J)
IF(L.EQ.0) GO TO 705
WRITE(6, 3200) N, J, L, FO(L)
705 CONTINUE
706 CONTINUE
3200 FORMAT(3I4, E13.5)
-----
C FIND AND OUTPUT SEGMENT STRESS RESULTANTS
-----
C
DO 900 N=1, NSEG
IPN=IP(N)
IF(IT(N).EQ.3) GOTO 800
C
C FORM SEGMENT END FORCE CVECTOR
IF(NDIV(N).GT.100) GO TO 999
DH=(H(N)-HO(N))/DFLOAT(NDIV(N))
NDIV1=NDIV(N)+1
DO 710 I=1, 4
SF(I)=PSF(N, I)

```

FILE

```

IF (L.EQ.0) GO TO 710
SF (I)=FO (L) +SF (I)
710 CONTINUE
SF (5)=PBF (5, N)
SF (6)=PBF (6, N)
C
C WRITE INDIVIDUAL SEGMENT END FORCES
WRITE (6, 3300) N, (SF (I), I=1, 6)
3300 FORMAT (///' INDIVIDUAL END FORCES FOR SEGMENT ', I6, / (4E13.5))
C-----
C STRESS RESULTANTS FOR CYLINDRICAL SEGMENTS
C-----
IF (IT (N) .NE. 1) GO TO 750
IFLAG=1
CALL CYLIN (T (N), R (N), H (N), HO (N), E (N), PR (N), UW (N), S, TS, D, BETA,
* IFLAG)
DN1=0.0
CM1=0.0
CM2=0.0
CN1=-PBF (5, N)
WP=CN1*R (N) *PR (N) / (E (N) *T (N))
CN2=0.0
WW=0.0
RN=E (N) *T (N) /R (N)
GOTO (711, 712, 713, 714), IPN
711 CN2=-PV (N) *R (N)
WP=PV (N) *R (N) **2 / (E (N) *T (N)) +WP
GOTO 721
712 DN1=-T (N) *UW (N) *DH
WW=DN1*R (N) *PR (N) / (E (N) *T (N))
GOTO 721
713 WP=-R (N) *ALPHA (N) *PV (N) +WP
GOTO 721
714 CM1= (1. +PR (N)) *D*ALPHA (N) *PV (N)
CM2=CM1
721 D=2. *D*BETA**2
DO 730 I=1, 4
C=0.0
DO 720 J=1, 4
720 C=C+TS (I, J) *SF (J)
730 CVEC (I) =C
C
X=0.0
DO 740 L=1, NDIV1
BX=BETA*X
DC=DCOS (BX)
DS=DSIN (BX)
C
W (L) =WP+DEXP (BX) * (CVEC (1) *DC+CVEC (2) *DS) +DEXP (-BX) *
* (CVEC (3) *DC+CVEC (4) *DS) +WW*DFLOAT (L-1)
C
735 RN1 (L) =CN1+DN1*DFLOAT (L-1)
RN2 (L) =CN2- (DEXP (BX) * (CVEC (1) *DC+CVEC (2) *DS) +
*DEXP (-BX) * (CVEC (3) *DC+CVEC (4) *DS)) *RN
RM1 (L) =DEXP (BX) * (D*CVEC (2) *DC-D*CVEC (1) *DS) +DEXP (-BX) * (D*
* CVEC (3) *DS-D*CVEC (4) *DC)

```



```

RM2(L)=PR(N)*RM1(L)+CM2
RM1(L)=RM1(L)+CM1
XH(L)=X
740 X=X+DH
C
WRITE(6,4000) N,(L,XH(L),RN1(L),RN2(L),RM1(L),RM2(L),L=1,NDIV1)
WRITE(6,4005) (L,XH(L),W(L),L=1,NDIV1)
GOTO 900

```

```

C-----
C STRESS RESULTANTS FOR DOME SEGMENTS
C-----

```

```

750 IF(IT(N).NE.2) GO TO 800
   ANGO=HO(N)/RAD
   X=0.
   ANG=H(N)/RAD
   DX=DH/RAD
   C=CONST(PV(N),UW(N),R(N),T(N),IP(N))
   D=T(N)**3/(12.*(1.-PR(N)**2))
   RLAM=(3.*(1.-PR(N)**2)*(R(N)/T(N))**2)**.25
   C2=R2*SF(4)
   C1=R(N)*DSIN(ANG)*SF(3)/RLAM
   CM=0.0
   IF(IP(N).EQ.5) CM=(1.+PR(N))*D*ALPHA(N)*PV(N)*E(N)

```

```

C
DO 780 L=1,NDIV1
   PSIL=(ANG-(ANGO+X))*RLAM
   ELAM=DEXP(-PSIL)
   FAC=RLAM*X
   RN1(L)=C*FN1(IP(N),X,ANGO,ANG)

```

```

C
   CAOX=DCOS(ANGO+X)
   SAOX=DSIN(ANGO+X)
   SA=DSIN(ANG)
   CP=DCOS(PSIL)
   SP=DSIN(PSIL)
   SAO=DSIN(ANGO)
   CAO=DCOS(ANGO)
   CFA=DCOS(FAC)
   SFA=DSIN(FAC)
   EF=DEXP(-FAC)

```

```

C
   WP=0.
   WVT=0.
   WHT=0.
   WMT=0.
   WHB=0.
   WMB=0.
   IF(X.EQ.0..AND.ANGO.EQ.0.) GOTO 759

```

```

C
   IFN=IP(N)
   GOTO (752,753,752,754,755),IPN
752 WP=PV(N)*R(N)**2*SAOX*(1-PR(N)+(1+PR(N))*
*   SAO**2/SAOX**2)/(2*E(N)*T(N))
   GOTO 755
753 WP=-UW(N)*R(N)**2*SAOX*((1+PR(N))*(CAO-
*   CAOX)/SAOX**2-CAOX)/E(N)
   GOTO 755
754 WP=-ALPHA(N)*R(N)*SAOX*PV(N)
C

```

```

755  IF (ANGO.EQ.0.) GOTO 756
      WVT=-SF (5) *R (N) * ( (1+PR (N) ) *SAO/SAOX-2*SAO*
*    CAO*RLAM*EF*CFA) / (E (N) *T (N) )
      WHT=SF (1) *2*SAO**2*RLAM*R (N) *EF*CFA/(E (N) *T (N) )
      WMT=-SF (2) *2*SAO*RLAM**2*EF* (CFA-SFA)
*    / (E (N) *T (N) )
756  WHB=SF (3) *2*SA**2*R (N) *RLAM*DEXP (-PSIL) *CP
*    / (E (N) *T (N) )
      WMB=SF (4) *2*SA*RLAM**2*DEXP (-PSIL) * (CP-
*    SP) / (E (N) *T (N) )
      W (L) =WP+WVT+WHT+WMT+WHB+WMB
      GOTO 758
759  W (L) =0.

```

```

C
758  RN2 (L) =C*FN2 (IP (N) , X, ANGO, ANG)
*+2*RLAM*SA*ELAM*DSIN (PSIL-PI/2) *SF (3)
*+2*R2*RLAM**2/R (N) *ELAM*DSIN (PSIL-PI/4) *SF (4)
      IF (ANGO.EQ.0.) GOTO 761
      RN2 (L) =RN2 (L) -2*SAO*RLAM*EF*CFA*SF (1)
*+2*RLAM**2/R (N) *EF* (CFA-SFA) *SF (2)
*- (2*CAO*RLAM*EF*CFA-SAO/DSIN (X+AN
*GO)**2) * SF (5)

```

```

C
761  IF (ANGO.EQ.0.AND.X.EQ.0) GOTO 763
760  RN1 (L) =RN1 (L) +R2* (CAOX/SAOX) *SA*ELAM*DSIN (
*PSIL-PI/4) *SF (3)
*+2*RLAM/R (N) * (CAOX/SAOX) *ELAM*SP*SF (4)
      IF (ANGO.EQ.0.) GOTO 765
      RN1 (L) =RN1 (L) +SAO*EF* (CFA-SFA) * (DC
*OS (X+ANGO) /SAOX) *SF (1)
*+2*RLAM/R (N) *EF*SFA* (CAOX/SAOX)
**SF (2)
*+ (CAOX/SAOX*CAO*EF* (CFA
*-SFA) -SAO/SAOX**2) *SF (5)
      GOTO 765

```

```

763  RN1 (L) =RN2 (L)

```

```

C
765  RM1 (L) =C1*ELAM*SP+C2*ELAM*DSIN (PSIL+P4)
      IF (ANGO.EQ.0.) GOTO 770
      RM1 (L) =RM1 (L) +SAO*R (N) /RLAM*EF*SFA*SF (1)
*-EF* (CFA+SFA) *SF (2)
*+CAO*R (N) /RLAM*EF*SFA*SF (5)

```

```

C
770  IF (X.EQ.0..AND.ANGO.EQ.0.) GOTO 775
      COT=CAOX/SAOX
      RM2 (L) =PR (N) *RM1 (L) +CM+SF (3) * (COT*SA*
*R (N) *ELAM* (CP+SP) / (2*RLAM**2) )
      RM2 (L) =RM2 (L) +SF (4) *COT*ELAM*CP/RLAM
      R11=RM1 (L)
      R22=RM2 (L)
      GOTO 774

```

```

775  RM2 (L) =RM1 (L)
774  IF (ANGO.EQ.0.) GOTO 772
      RM2 (L) =RM2 (L) +SF (5) *CAO*CAOX*R (N) *
*ELAM* (CP+SP) / (2*RLAM**2)

```

```

      *-SF(1)*(R(N)*EF*SAO*CAOX*
      *(CFA+SFA)/(2*SAOX*RLAM**2))
      *-SF(2)*(EF*CFA*CAOX/(SAOX*RLAM))
772 RM1(L)=RM1(L)+CM
771 X=X+DX
      XH(L)=DFLOAT(L-1)*DH
780 CONTINUE
C
      WRITE(6,4500) N, (L,XH(L),RN1(L),RN2(L),RM1(L),RM2(L),L=1,NDIV1)
      WRITE(6,4505) (L,XH(L),W(L),L=1,NDIV1)
      GOTO 900
C-----
C STRESS RESULTANTS FOR BASE-SLAB ELEMENT
C-----
C FORM SEGMENT END FORCE VECTOR
800 IF (NDIV(N).GT.100) GOTO 999
      NDIV1=NDIV(N)+1
      DO 805 I=1,6
      SF(I)=PSF(N,I)
      L=IDF(N,I)
      IF(L.EQ.0) GOTO 805
      SF(I)=FO(L)+SF(I)
805 CONTINUE
C
C WRITE INDIVIDUAL SEGMENT END FORCES
      WRITE(6,5000) N, (SF(I),I=1,6)
5000 FORMAT(///' INDIVIDUAL END FORCES FOR',
      * ' SEGMENT',I6,/(4E13.5))
C
C COMPUTE STRESS RESULTANTS
      IFLAG=1
      CALL BASE(IFLAG,T(N),R(N),H(N),HO(N),E(N),PR(N),UW(N),BB,S,TS,D)
      DATA IVECT/2,5,4,6/
      DO 820 I=1,4
      C=0.0
      DO 815 J=1,4
      JJ=IVECT(J)
815 C=C+TS(I,J)*SF(JJ)
820 CVEC(I)=C
      HT=H(N)
C
      IFLAG=2
      DO 825 I=1,4
      DO 825 J=1,4
825 BB(I,J)=0.0
      DO 860 L=1,NDIV1
      CALL BASE(IFLAG,T(N),R(N),HT,HO(N),E(N),PR(N),UW(N),BB,S,TS,D)
      DO 830 I=1,4
      CC=0.0
      DO 835 J=1,4
835 CC=CC+BB(I,J)*CVEC(J)
830 SR(I)=CC
      HR(L)=HT
      DH=(H(N)-HO(N))/DFLOAT(NDIV(N))
      HT=HT-DH
C

```

```

RM1(L)=SR(2)
RM2(L)=SR(1)
V(L)=SR(3)
W(L)=SR(4)
GOTO (840,841,860,860,860),IPN
840 W(L)=W(L)+PV(N)/R(N)
GOTO 860
841 W(L)=W(L)+UW(N)*T(N)/R(N)
GOTO 860
860 CONTINUE
WRITE(6,5500) N,(L,HR(L),RM1(L),RM2(L),V(L),L=1,NDIV1)
5500 FORMAT(///' *** OUTPUT FOR BASE ELEMENT',I4,' ***'/
* ' POINT COORD M1',12X,'M2',12X,'V',12X,
* /(I6,F10.4,3E14.5))
WRITE(6,5505) (L,HR(L),W(L),L=1,NDIV1)
5505 FORMAT(///' *** VERTICAL DISPLACEMENT ***'/
* ' POINT COORD W'/(I6,F10.4,E14.5))
C
900 CONTINUE
STOP
999 WRITE(6,3000)
3000 FORMAT(' STOP FOR PROGRAM DIAGNOSED INPUT ERROR ')
STOP
C-----
C FORMAT STATEMENTS
C-----
1001 FORMAT(10A8)
2001 FORMAT('1',10A8//)
1000 FORMAT(5I4,2F10.4)
2000 FORMAT('1',' **** OUTPUT FOR FLEXIBILITY ANALYSIS OF SEGMENTED',
* ' SHELL ****'/,
* ' NUMBER OF SEGMENTS =',I4/
* ' IPRINT =',I4///
* ' SEG TYPE IR JR NDIV',4X,'EC1',7X,'EC2')
2100 FORMAT(I4,4I5,2F10.4)
1200 FORMAT(2I4)
2200 FORMAT(///,' CONNECTIVITY MATRIX'/(5X,2I4))
1300 FORMAT(I4,F6.0,F12.0,F8.0,5F10.0)
2300 FORMAT(///' GEOMETRIC PARAMETERS'/ SEG',4X,'THICK',3X,'RADIUS'
*,3X,'L OR ANG',4X,'ANGO',7X,'MODULUS',6X,'P RATIO',2X,'THERMCOEF',
* 3X,'WEIGHT'/(I4,F8.3,F12.3,2F10.3,E13.4,F10.3,E13.4,F10.3))
1400 FORMAT(2I4,7F10.0)
2400 FORMAT(///' PARTICULAR SOLUTION INPUT INFORMATION'/
* ' SEG TYPE VALUE',4X,'TOP SHEAR',4X,'TOP MOM',6X,'BOT SHEAR',
* 4X,'BOT MOM',4X,'TOP FORCE',4X,'VERT FORCE'/(I4,I5,F10.3,6E13.5))
4000 FORMAT(///' *** OUTPUT FOR CYLINDRICAL SEGMENT',I4,' ***'/
* ' POINT COORD N1',12X,'N2',12X,'M1',12X,'M2',/
* (I6,F10.4,4E14.5))
4005 FORMAT(///' *** HORIZONTAL DISPLACEMENT *** '/
* ' POINT COORD W'/(I6,F10.4,E14.5))
4500 FORMAT(///' *** OUTPUT FOR DOME SEGMENT',I4,' ***'/
* ' POINT ANGLE N1',12X,'N2',12X,'M1',12X,'M2',/
* (I6,F10.4,4E14.5))
4505 FORMAT(///' *** HORIZONTAL DISPLACEMENT *** '/
* ' POINT COORD W'/(I6,F10.4,E14.5))
END

```

C

FILE

```

C *****
  FUNCTION CONST (PV,UW,R,T,IP)
C THIS FUNCTION IS USED FOR THE IN-PLANE DOME STRESS RESULTANTS
  IMPLICIT REAL*8 (A-H,O-Z)
  CONST=0.0
  GOTO (10,20,10,100,100) ,IP
  10 CONST=-0.5*PV*R
  GOTO 100
  20 CONST=-UW*T*R
  100 RETURN
  END
C *****
  FUNCTION FN1 (IP,X,ANGO,ANG)
C THIS FUNCTION IS USED FOR N1 DOME STRESS RESULTANTS
  IMPLICIT REAL*8 (A-H,O-Z)
  FN1=0.0
  GOTO (10,20,10,100,100) ,IP
  10 FN1=1.0
  IF (ANGO.GT.1.0E-03) FN1=1-(DSIN (ANGO) **2/DSIN (X+ANGO) **2)
  GOTO 100
  20 IF (ANGO.NE.0.0) GOTO 21
  IF (X.NE.0.0) GOTO 21
  FN1=0.5
  GOTO 100
  21 FN1=(DCOS (ANGO) -DCOS (X+ANGO) )/DSIN (X+ANGO) **2
  100 RETURN
  END
C *****
  FUNCTION FN2 (IP,X,ANGO,ANG)
C THIS FUNCTION IS USED FOR N2 DOME STRESS RESULTANTS
  IMPLICIT REAL*8 (A-H,O-Z)
  FN2=0.0
  GOTO (10,20,10,100,100) ,IP
  10 FN2=1.0
  IF (ANGO.GT.1.0E-03) FN2=1+(DSIN (ANGO) **2/DSIN (X+ANGO) **2)
  GOTO 100
  20 IF (ANGO.NE.0.0) GOTO 21
  IF (X.NE.0.0) GOTO 21
  FN2=0.5
  GOTO 100
  21 FN2=- (DCOS (ANGO) -DCOS (X+ANGO) )/DSIN (X+ANGO) **2+DCOS (X+ANGO)
  100 RETURN
  END
C *****
  SUBROUTINE PCYLIN (T,R,H,HO,E,PR,UW,ALPHA,F,PSD,IP,PV,N,PSF,PBT)
C THIS SUBROUTINE COMPUTES CYLINDER PARTICULAR SOLUTION DISPLACEMENTS (PSD)
  IMPLICIT REAL*8 (A-H,O-Z)
  DIMENSION F (6,6) , PSD (4) , PSF (20,6)
C
  DO 10 I=1,4
  10 PSD (I) =0.0
  IF (IP.LT.1.OR.IP.GT.5) GO TO 999
  PSD (1) =-PBT*PR*R/(E*T)
  PSD (3) =PSD (1)
C

```

```

GO TO (20,30,20,40,70),IP
20 PSD(1)=PV*R**2/(E*T) +PSD(1)
   PSD(3)=PSD(1)
   GO TO 70
C
30 PSD(3)=PSD(3)-UW*T*PR*R*H/(E*T)
   C=UW*T*PR*R/(E*T)
   PSD(2)=PSD(2)-C
   PSD(4)=PSD(4)-C
   GO TO 70
C
40 C=-ALPHA*R*PV
   PSD(1)=PSD(1)+C
   PSD(3)=PSD(3)+C
C
70 DO 100 I=1,4
   C=PSD(I)
   DO 80 J=1,4
80 C=C+F(I,J)*PSF(N,J)
100 PSD(I)=C
C
   RETURN
C
999 WRITE(6,1000) IP
1000 FORMAT(' PROGRAM STOPPED FOR CYLINDER IP =',I4)
   STOP
   END
C*****
C SUBROUTINE CYLIN(T,R,H,HO,E,PR,UW,F,TT,D,BETA,IFLAG)
C THIS SUBROUTINE COMPUTES THE CYLINDER FLEXIBILITY (F) AND B MATRICES (TT)
C IMPLICIT REAL*8(A-H,O-Z)
C DIMENSION F(6,6),TT(4,4),TA(4,4)
C
D=E*T**3/(12.*(1.-PR**2))
BETA=(3.*(1.-PR**2)/(R*T)**2)**.25
X=BETA*H
C=DCOS(X)
S=DSIN(X)
EP=DEXP(X)
EM=DEXP(-X)
PHI1=EP*C
PHI2=EP*S
PHI3=EM*C
PHI4=EM*S
TH1=PHI1-PHI2
TH2=PHI1+PHI2
TH3=PHI3+PHI4
TH4=PHI3-PHI4
DENOM=DEXP(2.*X)+DEXP(-2.*X)-4.*S**2-2.
C2=1./(2.*BETA**2*D*DENOM)
C1=C2/BETA

```

C

FILE

```

TT (1,1) = (TH4*(PHI1-PHI3) - PHI4*(TH1+TH3)) *C1
TT (2,1) = (TH4*PHI2-TH2*PHI4) *C1
TT (3,1) = (TH2*(PHI1-PHI3) - PHI2*(TH1+TH3)) *C1
TT (4,1) = (TH4*PHI2 -TH2*PHI4) *C1
TT (1,2) = (PHI4*(TH1-TH3) +PHI3*(TH1-TH4) +PHI1*(TH3-TH4)) *C2
TT (2,2) = (PHI4*(TH2-TH3) +PHI3*(TH2-TH4) +PHI2*(TH3-TH4)) *C2
TT (3,2) = (PHI1*(TH3-TH2) +PHI3*(TH1-TH2) +PHI2*(TH1-TH3)) *C2
TT (4,2) = (PHI4*(TH1-TH2) +PHI1*(TH2-TH4) +PHI2*(TH4-TH1)) *C2
TT (1,3) = (PHI1-PHI3-2.*PHI4) *C1
TT (2,3) = (PHI2-PHI4) *C1
TT (3,3) = (PHI1-PHI3-2.*PHI2) *C1
TT (4,3) = (PHI2-PHI4) *C1
TT (1,4) = (TH1+TH3-2.*TH4) *C2
TT (2,4) = (TH2-TH4) *C2
TT (3,4) = (TH1+TH3-2.*TH2) *C2
TT (4,4) = (TH2-TH4) *C2

```

C

```
IF (IFLAG.NE.0) GO TO 200
```

C

```

TA (1,1) =1.0
TA (1,2) =0.0
TA (1,3) =1.0
TA (1,4) =0.0
TA (2,1) =BETA
TA (2,2) =BETA
TA (2,3) =-BETA
TA (2,4) =BETA
TA (3,1) =PHI1
TA (3,2) =PHI2
TA (3,3) =PHI3
TA (3,4) =PHI4
TA (4,1) =TH1*BETA
TA (4,2) =TH2*BETA
TA (4,3) =-TH3*BETA
TA (4,4) =TH4*BETA

```

C

```

DO 100 I=1,4
DO 100 J=1,4
C=0.0
DO 80 K=1,4
80 C=C+TA (I,K) *TT (K,J)
100 F (I,J) =C

```

C

```

200 RETURN
END

```

FILE

```

C*****
  SUBROUTINE PDOME(T,R,H,HO,E,PR,UW,ALPHA,F,PSD,IP,PV,N,PSF,ANG,
*   ANGO,PBT,PST)
C   THIS SUBROUTINE COMPUTES DOME PARTICULAR DISPLACEMENTS (PSD)
  IMPLICIT REAL*8(A-H,O-Z)
  DIMENSION F(6,6),PSD(4),PSF(20,6)

C
  IF(IP.LT.1.OR.IP.GT.5) GO TO 999
  DO 10 I=1,4
10   PSD(I)=0.0
     RLAM=(3.*(1.-PR**2)*(R/T)**2)**.25
     X=ANG-ANGO
     PSD(2)=PBT*(-DCOS(ANGO)*R**2*6*(1.-PR**2)/(2*T**3*E*RLAM**2))
*   -PST*DSIN(ANGO)*R**2*6*(1.-PR**2)/(E*T**3*RLAM**2)
     PSD(1)=PBT*(-R*((1.+PR)-2*DSIN(ANGO)*DCOS(ANGO)*RLAM)/(E*T))
*   +PST*2*DSIN(ANGO)**2*R*RLAM/(E*T)
     PSD(3)=PBT*(-R*((1.+PR)*DSIN(ANGO)/DSIN(ANG)-2.*DSIN(ANGO)*
*   DCOS(ANGO)*RLAM*DEXP(-RLAM*X)*DCOS(RLAM*X))/(E*T))
*   +PST*2*DSIN(ANGO)**2*R*RLAM*DEXP(-RLAM*X)*DCOS(RLAM*X)/(E*T)
     PSD(4)=PSD(2)*DEXP(-RLAM*X)*(DCOS(RLAM*X)+DSIN(RLAM*X))
*   -PST*DSIN(ANGO)*R**2*6*(1.-PR**2)*DEXP(-RLAM*X)*
*   (DCOS(RLAM*X)+DSIN(RLAM*X))/(E*T**3*RLAM**2)
20   GO TO (20,30,20,40,70),IP
     PSD(3)=PSD(3)+PV*R**2*(1.-PR+(1+PR)*(DSIN(ANGO)**2/
*   DSIN(ANG)**2))*DSIN(ANG)/(2.*T*E)
     IF(ANGO.EQ.0.) GOTO 70
     PSD(1)=PSD(1)+PV*R**2*DSIN(ANGO)/(T*E)
     GO TO 70

C
30   CC=-UW*R**2/E
     DSO=DSIN(ANGO)
     DCO=DCOS(ANGO)
     DS=DSIN(ANG)
     DC=DCOS(ANG)
     PSD(3)=PSD(3)+CC*((1.+PR)*(DCO-DC)/DS**2-DC)*DS
     PSD(1)=PSD(1)-CC*DCO*DSO
     CC=CC*(2.+PR)/R
     PSD(2)=PSD(2)+CC*DSO
     PSD(4)=PSD(4)+CC*DS
     GO TO 70

C
40   PSD(3)=PSD(3)-ALPHA*PV*R*DSIN(ANG)
     PSD(1)=PSD(1)-ALPHA*PV*R*DSIN(ANGO)
     GOTO 70

C
C
70   DO 100 I=1,4
     C=PSD(I)
     DO 80 J=1,4
80    C=C+F(I,J)*PSF(N,J)
100   PSD(I)=C
     RETURN

C
999  WRITE(6,1000) IP
1000 FORMAT(' PROGRAM STOPPED FOR DOME IP =',I4)
     STOP
     END

```



```

C *****
  SUBROUTINE DOME (T,R,H,HO,E,PR,UW,F,ANG,ANGO)
C THIS SUBROUTINE COMPUTES DOME FLEXIBILITY MATRICES (F)
  IMPLICIT REAL*8 (A-H,O-Z)
  DIMENSION F(6,6)
  ANG=H/57.295779513
  ANGO=HO/57.295779513
  RLAM=(3.*(1.-PR**2)*(R/T)**2)**0.25
  S=DSIN(ANG)
  SS=DCOS(ANG)
  S1=DSIN(ANGO)
  SS1=DCOS(ANGO)

C
  AN=ANG-ANGO
  EX=DEXP(-RLAM*AN)
  CO=DCOS(RLAM*AN)
  SI=DSIN(RLAM*AN)

C
  DO 100 I=1,4
  DO 100 J=1,4
100 F(I,J)=0.0
C
  F(1,3)=2*S**2*R*RLAM*EX*CO/(E*T)
  F(1,4)=2*S*RLAM**2*EX*(CO-SI)/(E*T)
  F(2,3)=S*R**2*6*(1.-PR**2)*EX*(CO-SI)/(E*T**3*RLAM**2)
  F(2,4)=R*12*(1-PR**2)*EX*CO/(E*T**3*RLAM)
  F(3,1)=F(1,3)*SI**2/S**2
  F(3,2)=-F(1,4)*SI/S
  F(4,1)=-F(2,3)*SI/S
  F(4,2)=F(2,4)

C
  F(1,2)=-2*S1*RLAM**2/(E*T)
  F(2,2)=R*12*(1-PR**2)/(E*T**3*RLAM)
  F(1,1)=2*S1**2*R*RLAM/(E*T)
  F(2,1)=-S1*R**2*6*(1-PR**2)/(E*T**3*RLAM**2)
  F(3,3)=2.*RLAM*S**2*R/(E*T)
  F(3,4)=2.*RLAM**2*S/(E*T)
  F(4,3)=F(3,4)
  F(4,4)=4.*RLAM**3/(E*T*R)

C
  RETURN
  END

```

FILE

```

C*****
C      SUBROUTINE PBASE(T,R,H,HO,E,PR,ALPHA,UW,F,PSD,IP,PV,N,PSF,PBF)
C      THIS SUBROUTINE EVALUATES THE PARTICULAR SOLUTION
C      DISPLACEMENTS FOR A BASE SEGMENT
C      IMPLICIT REAL*8(A-H,O-Z)
C      DIMENSION F(6,6),PSD(6),PSF(20,6),PBF(6,20)
C
C      DO 10 I=1,6
10     PSD(I)=0.0
C
C      SELECT LOAD TYPE
C      IF(IP.LT.1.OR.IP.GT.5) GO TO 999
C      GO TO (20,30,40,50,70),IP
C
C      INTERNAL PRESSURE
20     PSD(5)=PV/R
C      PSD(6)=PSD(5)
C      GO TO 70
C
C      DEAD LOAD
30     PSD(5)=UW*T/R
C      PSD(6)=PSD(5)
C      GO TO 70
C
C      IN-PLANE PRESTRESS
40     PSD(1)=PV*H/T
C      PSD(3)=PSD(1)*HO/H
C      GO TO 70
C
C      UNIFORM THERMAL
50     PSD(1)=-PV*ALPHA*H
C      PSD(3)=-PV*ALPHA*HO
C
70     DO 100 I=1,6
C      C=PSD(I)
C      DO 80 J=1,6
80     C=C+F(I,J)*PSF(N,J)
100    PSD(I)=C
C      RETURN
C
999    WRITE(6,1000)
1000   FORMAT('0',' ** PROGRAM STOPPED IN SUBROUTINE PBASE FOR DIAGNOSE'
*      , 'D ERROR')
C
C      STOP
C      END

```

FILE

```

C*****
C      SUBROUTINE BASE(IFLAG,T,R,H,HO,E,PR,UW,BB,S,TT,D)
C THIS SUBROUTINE COMPUTES THE FLEXIBILITY MATRIX (S)
C FOR A BASE SEGMENT ON AN ELASTIC FOUNDATION, OR
C (IF IFLAG=1) THE MATRIX BB TO DETERMINE INTERNAL
C DISPLACEMENTS AND STRESS RESULTANTS
C      IMPLICIT REAL*8 (A-H,O-Z)
C      DIMENSION S(6,6),TT(4,4),B(4,4),G(4,4),BB(4,4)
C      DIMENSION PHI(4),PHIP(4),PHIDP(4),PHITP(4),IVEC(4)
C      DATA IVEC/2,5,4,6/
C
C      FUNCTION DEFINITIONS
C      FII(RO,RI)=CM*RI/RO**2+CP/RI
C      FOI(RO,RI)=2.*C/RO
C      FOO(RO,RI)=CM*RO/RI**2+CP/RO
C      FIO(RO,RI)=2.*C/RI
C
C      LM=2
C      IF(HO.EQ.0.) LM=1
C      LN=2*LM
C      D=E*T**3/(12.*(1.-PR**2))
C      STIFL=(D/R)**0.25
C      IF(IFLAG.EQ.2) GOTO 300
C
C      SIGN=1.0
C      RD=H
C      DO 50 J=1,6
C      DO 50 I=1,6
50    S(I,J)=0.0
C      DO 51 I=1,4
C      DO 51 J=1,4
51    B(I,J)=0.0
C
C      DO 100 I=1,LM
C      I1=2*(I-1)+1
C      I2=I1+1
C      IF(I.EQ.2) RD=HO
C      IF(I.EQ.2) SIGN=-1.0
C      RDI=1./RD
C      RDI2=RDI**2
C      CALL BSHAPE(STIFL,RD,PHI,PHIP,PHIDP,PHITP)
C      DO 80 J=1,LN
C      B(I2,J)=-D*(PHITP(J)+RDI*PHIDP(J)-RDI2*PHIP(J))*SIGN
C      B(I1,J)=D*(PHIDP(J)+PR*RDI*PHIP(J))*SIGN
C      G(I2,J)=PHI(J)
C      G(I1,J)=PHIP(J)
80    CONTINUE
100   CONTINUE
C

```

FILE

```
CALL JINVER(B,TT,4,LN)
IF(IFLAG.EQ.1) GOTO 210
```

C

```
DO 200 I=1,LN
II=IVEC(I)
DO 200 J=1,LN
JJ=IVEC(J)
C=0.0
```

```
150 C=C+G(I,K)*TT(K,J)
200 S(II,JJ)=C
```

C

```
C ADD FLEXIBILITIES FOR IN PLANE STIFFNESSES
```

```
IF(LM.EQ.1) GOTO 205
C=(H*HO)**2/(T*(H**2-HO**2)*E)
CM=(1.-PR)*C
CP=(1.+PR)*C
S(1,1)=FOO(H,HO)
S(1,3)=FOI(H,HO)
S(3,1)=FIO(H,HO)
S(3,3)=FII(H,HO)
GOTO 210
```

```
205 S(1,1)=H*(1.-PR)/(E*T)
```

C

```
210 RETURN
```

C

```
300 CALL BSHAPE(STIFL,H,PHI,PHIP,PHIDP,PHITP)
DO 320 J=1,LN
BB(1,J)=D*(PR*PHIDP(J)+PHIP(J)/H)
BB(2,J)=D*(PHIDP(J)+PR*PHIP(J)/H)
BB(3,J)=-D*(PHITP(J)+PHIDP(J)/H-PHIP(J)/H**2)
BB(4,J)=PHI(J)
X=HO/STIFL
IF(X.LT.2.) X=2.0
HO=X*STIFL
320 CONTINUE
GOTO 210
END
```

C

C

ILE

```

C*****
C      SUBROUTINE BSHAPE(STIFL, RD, PHI, PHIP, PHIDP, PHITP)
C      THIS SUBROUTINE EVALUATES THE PHI VECTOR AND ITS DERIVATIVES
C      FOR A BASE ON ELASTIC FOUNDATION SEGMENT
C      IMPLICIT REAL*8 (A-H, O-Z)
C      DATA RT, PI/2.0, 3.1415926536/
C      DIMENSION PHI(4), PHIP(4), PHIDP(4), PHITP(4)

C
C      P8=PI/8.
C      CD1=1./(DSQRT(RT)*STIFL)
C      SIG=RD*CD1
C      RSIG=DSQRT(SIG)
C      COSP=DCOS(SIG+P8)
C      SINP=DSIN(SIG+P8)
C      COSM=DCOS(SIG-P8)
C      SINM=DSIN(SIG-P8)
C      ETA=RT**0.75*DSQRT(PI)
C      CPHIP=DEXP(SIG)/(ETA*RSIG)
C      CPHIM=PI*DEXP(-SIG)/(ETA*RSIG)
C      CD2=CD1**2
C      CD3=CD2*CD1

C
C      FORM PHI VECTOR
C      PHI(1)=CPHIP*COSM
C      PHI(2)=CPHIP*SINM
C      PHI(3)=CPHIM*COSP
C      PHI(4)=CPHIM*SINP

C
C      FORM PHIP VECTOR
C      SIG2I=1./(2.*SIG)
C      SIGP=1.+SIG2I
C      SIGM=1.-SIG2I
C      PHIP(1)=CD1*(SIGM*PHI(1)-PHI(2))
C      PHIP(2)=CD1*(SIGM*PHI(2)+PHI(1))
C      PHIP(3)=-CD1*(SIGP*PHI(3)+PHI(4))
C      PHIP(4)=CD1*(-SIGP*PHI(4)+PHI(3))

C
C      FORM PHIDP VECTOR
C      C2=1./(2.*SIG**2)
C      PHIDP(1)=CD2*C2*PHI(1)+(SIGM*PHIP(1)-PHIP(2))*CD1
C      PHIDP(2)=CD2*C2*PHI(2)+(SIGM*PHIP(2)+PHIP(1))*CD1
C      PHIDP(3)=CD2*C2*PHI(3)-(SIGP*PHIP(3)+PHIP(4))*CD1
C      PHIDP(4)=CD2*C2*PHI(4)-(SIGP*PHIP(4)-PHIP(3))*CD1

C
C      FORM PHITP VECTOR
C      C2=2.*C2
C      C3=-1./(SIG**3)
C      PHITP(1)=CD3*C3*PHI(1)+CD2*C2*PHIP(1)+(SIGM*PHIDP(1)-
*      PHIDP(2))*CD1
C      PHITP(2)=CD3*C3*PHI(2)+CD2*C2*PHIP(2)+(SIGM*PHIDP(2)+
*      PHIDP(1))*CD1
C      PHITP(3)=CD3*C3*PHI(3)+CD2*C2*PHIP(3)-(SIGP*PHIDP(3)+
*      PHIDP(4))*CD1
C      PHITP(4)=CD3*C3*PHI(4)+CD2*C2*PHIP(4)-(SIGP*PHIDP(4)-
*      PHIDP(3))*CD1

C
C      RETURN
C      END

```

```

C*****
C      SUBROUTINE JINVER (A, B, NDIM, NEQ)
C      THIS SUBROUTINE INVERTS THE MATRIX A BY THE JACOBI METHOD
C      AND STORES THE RESULT IN B
C      IMPLICIT REAL*8 (A-H, O-Z)
C      DIMENSION A (NDIM, 1), B (NDIM, 1)
C
C      INITIALIZE THE B MATRIX
C      DO 100 J=1, NDIM
C      DO 100 I=1, NDIM
100    B (I, J) = 0.0
C      DO 110 J=1, NEQ
110    B (J, J) = 1.0
C
C      BEGIN JACOBI REDUCTION OF MATRIX A AND ALSO OPERATE ON B
C      DO 600 N=1, NEQ
C      IF (DABS (A (N, N)) .LT. 1.0D-06) GO TO 999
C      C=1./A (N, N)
C      N1=N+1
C      IF (N.EQ.NEQ) GO TO 410
C      DO 400 J=N1, NEQ
C      AJ=A (N, J) *C
C      BJ=B (N, J) *C
C      DO 300 I=1, NEQ
C      A (I, J) = A (I, J) - AJ * A (I, N)
300    B (I, J) = B (I, J) - BJ * A (I, N)
C      A (N, J) = AJ
400    B (N, J) = BJ
C
410    DO 500 J=1, N
C      BJ=B (N, J) *C
C      DO 450 I=1, NEQ
450    B (I, J) = B (I, J) - BJ * A (I, N)
500    B (N, J) = BJ
C
600    CONTINUE
C      RETURN
C
999    WRITE (6, 1000) N
1000   FORMAT ('0', ' ** ZERO ELEMENT ON MAIN DIAGONAL FOR EQUATION',
*   I4, ' INDICATES MATRIX IS SINGULAR')
C      STOP
C      END

```

C
C

FILE

```

C*****
      SUBROUTINE SOL(A,B,NN,NEQ)
C   THIS SUBROUTINE SOLVES A SET OF LINEAR ALGEBRAIC EQUATIONS
C   OF THE FORM A*X=B BY GAUSSIAN ELIMINATION, WHERE 'A' IS A
C   SQUARE MATRIX. B IS THE RIGHT-HAND SIDE VECTOR
C   ON ENTRY. BUT IS OVERWRITTEN WITH THE SOLUTION VECTOR 'X'
C   DURING BACK SUBSTITUTION
      IMPLICIT REAL*8 (A-H,O-Z)
      DIMENSION A (NN,NN),B (NN)
      NL=NEQ-1
      DO 250 N=1,NL
      IF (A (N,N) .LE.0.)   GO TO 500
      N1=N+1
      DO 100 J=N1,NEQ
100   A (N,J)=A (N,J)/A (N,N)
      B (N)=B (N)/A (N,N)
      DO 250 I=N1,NEQ
      IF (A (I,N) .EQ.0.)   GO TO 250
      C=A (I,N)
      DO 200 J=N1,NEQ
200   A (I,J)=A (I,J)-C*A (N,J)
      B (I)=B (I)-C*B (N)
250   CONTINUE
C   BACK SUBSTITUTION
      M=NEQ
      B (M)=B (M)/A (M,M)
      DO 400 N=1,NL
      M1=M
      M=M-1
      DO 400 J=M1,NEQ
400   B (M)=B (M)-B (J)*A (M,J)
      GO TO 600
500   WRITE (6,1000)  N
      CALL EXIT
1000  FORMAT (' ZERO OR NEGATIVE ELEMENT ON MAIN DIAGONAL OF TRIANGULARIZ
1ED STIFFNESS MATRIX ' / ' FOR EQUATION NUMBER ',I4)
600   RETURN
      END

```

FILE

```

C*****
C      SUBROUTINE PFOR(IT,T,R,H,HO,E,PR,UW,ALPHA,IP,PV,PBF)
C      THIS SUBROUTINE COMPUTES PARTICULAR SOLUTION EDGE FORCES (PBF)
C      IMPLICIT REAL*8(A-H,O-Z)
C      DIMENSION PBF(6)
C      DATA RAD/57.295779513/
C
C      SELECT SEGMENT TYPE
C      GO TO (50,500,700),IT
C
C      CYLINDRICAL SEGMENTS
C      50 GO TO (900,100,900,900,200),IP
C      DEAD LOAD
C      100 PBF(6)=PBF(6)+T*UW*H
C          RETURN
C      THERMAL GRADIENT
C      200 PBF(2)=PBF(2)+E*PV*ALPHA*T**3/(12.*(1.-PR))
C          PBF(4)=-PBF(2)
C          RETURN
C
C      SPHERICAL SEGMENTS
C      500 ANG=H/RAD
C          ANGO=HO/RAD
C          GO TO (550,600,550,900,650),IP
C      PRESSURE OR PRESTRESS
C      550 C=0.5*PV*R
C          RATIO=(DSIN(ANGO)/DSIN(ANG))**2
C          PBF(6)=PBF(6)+C*DSIN(ANG)*(1.-RATIO)
C          PBF(3)=PBF(3)+C*DCOS(ANG)*(1.-RATIO)
C          RETURN
C      DEAD LOAD
C      600 C=UW*T*R*(DCOS(ANGO)-DCOS(ANG))/DSIN(ANG)**2
C          PBF(6)=C*DSIN(ANG)
C          PBF(3)=C*DCOS(ANG)
C          RETURN
C      THERMAL GRADIENT
C      650 PBF(4)=PBF(4)-E*PV*ALPHA*T**3/(12.*(1.-PR))
C          PBF(2)=-PBF(4)
C      900 RETURN
C
C      BASE ON ELASTIC FOUNDATION
C      700 GOTO (900,900,900,900,850),IP
C
C      THERMAL GRADIENT
C      850 PBF(4)=PBF(4)-E*PV*ALPHA*T**3/(12.*(1.-PR))
C          PBF(2)=-PBF(4)
C          RETURN
C
C      END
C
C
C

```

FILE

APPENDIX C
DATA FILES AND OUTPUT FOR
TYPICAL LOAD CONDITIONS

TABLE C1: INDEX OF DATA FILES

PAGE	DATA FILE	NUMBER OF SEG	REMARKS
C2	Int. Pressure	10	1 PSF
C3	Dead Load	11	} "Switched-On-Loading"
C4	Prestress	11	
C5	Const. Temp. Change	10	
C6	Temp. Gradient	10	
C7	Prestress	12	"Switched-On" (BOSOR4)
C8	Const. Temp. Change	9	} BOSOR4 Model (Without Outer Base Ring)
C9	Temp. Gradient	9	
C10	Dead Load (BW)	4	} BOSOR4 Models For Partial Structures in Order to Get RF1
C11	Dead Load (BD)	8	
C12	Dead Load (C)	11	
C13	Prestress (BW)	4	
C14	Prestress (BD)	8	
C15	Prestress (C)	11	

Line	PRESTRESS (BD)	BD	Value	Value	Value	Value	Value	Value	Value	Value	Value	Value	Value
1													
2	8	0											
3	1	1	10	0.	0.	0.	0.	0.	0.	0.	0.	0.	0.
4	2	1	10	0.	0.	0.	0.	0.	0.	0.	0.	0.	0.
5	3	2	40	0.	0.	0.	0.	0.	0.	0.	0.	0.	0.
6	4	1	10	0.	0.	0.	0.	0.	0.	0.	0.	0.	0.
7	5	1	40	0.	0.	0.	0.	0.	0.	0.	0.	0.	0.
8	6	1	2	0.	0.	0.	0.	0.	0.	0.	0.	0.	0.
9	7	3	10	0.	0.	0.	0.	0.	0.	0.	0.	0.	0.
10	8	3	20	0.	0.	0.	0.	0.	0.	0.	0.	0.	0.
11	1	4											
12	2	3											
13	3	4											
14	4	5											
15	5	6											
16	6	8											
17	7	8											
18	1	7.	70.75	1.322	0.0	0.5804E+09	0.15	.6500E-05	0.0	0.0	0.0	0.0	0.0
19	2	1.25	20.50	4.000	0.0	0.5804E+09	0.15	.6500E-05	0.0	0.0	0.0	0.0	0.0
20	3	1.25	136.625	29.487	8.88	0.5804E+09	0.15	.6500E-05	0.0	0.0	0.0	0.0	0.0
21	4	7.	70.75	3.178	0.0	0.5804E+09	0.15	.6500E-05	0.0	0.0	0.0	0.0	0.0
22	5	3.5	69.75	139.	0.0	0.5804E+09	0.15	.6500E-05	0.0	0.0	0.0	0.0	0.0
23	6	1.5	69.75	0.5	0.0	0.5804E+09	0.15	.6500E-05	0.0	0.0	0.0	0.0	0.0
24	7	6.5	450000.0	77.75	69.75	0.5804E+09	0.15	.6500E-05	0.0	0.0	0.0	0.0	0.0
25	8	5.0	450000.0	69.75	0.0	0.5804E+09	0.15	.6500E-05	0.0	0.0	0.0	0.0	0.0
26	1	3	9624.000	0.	0.	0.	0.	0.	0.	0.	0.	0.	0.
27	2	3	0.	0.	0.	0.	0.	0.	0.	0.	0.	0.	0.
28	3	3	0.	0.	0.	0.	0.	0.	0.	0.	0.	0.	0.
29	4	3	9624.000	0.	0.	0.	0.	0.	0.	0.	0.	0.	0.
30	5	3	0.000	0.	0.	0.	0.	0.	0.	0.	0.	0.	0.
31	6	3	0.	0.	0.	0.	0.	0.	0.	0.	0.	0.	0.
32	7	3	0.	0.	0.	0.	0.	0.	0.	0.	0.	0.	0.
33	8	3	0.	0.	0.	0.	0.	0.	0.	0.	0.	0.	0.

END OF FILE

1*** INTERNAL PRESSURE ***

1 **** OUTPUT FOR FLEXIBILITY ANALYSIS OF SEGMENTED SHELL ****
 NUMBER OF SEGMENTS = 10
 IPRINT = 0

SEG	TYPE	IR	JR	NDIV	EC1	EC2
1	2	0	1	40	0.0	-3.5000
2	1	0	1	5	0.0	0.0
3	1	1	1	20	0.0	0.0
4	1	0	1	10	0.0	0.0
5	2	1	1	40	0.0	-3.5000
6	1	1	1	10	0.0	0.0
7	1	1	1	40	-1.0000	0.0
8	1	1	1	2	0.0	0.0
9	3	0	1	10	0.0	0.7500
10	3	1	0	20	2.5000	0.0

CONNECTIVITY MATRIX

1	3
2	3
3	6
4	5
5	6
6	7
7	8
8	10
9	10

FORCES ON ENDS OF SEGMENTS

SEG	J	IF	FORCE
1	3	1	0.22147E+02
1	4	2	-0.19169E+03
2	3	3	0.27628E+01
2	4	4	-0.15971E+01
3	1	5	-0.24910E+02
3	2	6	0.19328E+03
3	3	7	-0.86327E+01
3	4	8	-0.13410E+02
4	3	9	-0.23545E-01
4	4	10	0.29810E-01
5	1	11	0.23545E-01
5	2	12	-0.29810E-01
5	3	13	0.20398E+01
5	4	14	-0.73587E+01
6	1	15	0.65929E+01
6	2	16	0.20768E+02
6	3	17	-0.30336E+01
6	4	18	-0.60010E+01
7	1	19	0.30336E+01
7	2	20	0.60010E+01
7	3	21	0.99191E+01
7	4	22	-0.50657E+02
8	1	23	-0.99191E+01
8	2	24	0.50657E+02
8	3	25	0.10369E+02
8	4	26	-0.55729E+02
9	3	27	-0.15201E+01
9	4	28	-0.46002E+02
9	6	29	-0.10333E+02
10	1	30	-0.88491E+01
10	2	31	0.12879E+03
10	5	32	0.10333E+02

INDIVIDUAL END FORCES FOR SEGMENT 1
 0.0 -0.0 0.22147E+02 -0.74823E+02
 0.0 -0.33389E+02

*** OUTPUT FOR DOME SEGMENT 1 ***

POINT	ANGLE	N1	N2	M1	M2
1	0.0	0.68039E+02	0.68039E+02	-0.37663E+00	-0.37663E+00
2	0.7349	0.65835E+02	0.68144E+02	-0.42687E+00	-0.18601E+01
3	1.4699	0.67022E+02	0.68278E+02	-0.47428E+00	-0.11945E+01
4	2.2048	0.67467E+02	0.68442E+02	-0.51583E+00	-0.99120E+00
5	2.9398	0.67735E+02	0.68641E+02	-0.54781E+00	-0.90036E+00
6	3.6747	0.67939E+02	0.68876E+02	-0.56574E+00	-0.85056E+00
7	4.4097	0.68117E+02	0.69148E+02	-0.56431E+00	-0.81664E+00
8	5.1446	0.68285E+02	0.69457E+02	-0.53740E+00	-0.78641E+00
9	5.8796	0.68452E+02	0.69802E+02	-0.47803E+00	-0.75239E+00
10	6.6145	0.68621E+02	0.70178E+02	-0.37845E+00	-0.70903E+00
11	7.3495	0.68795E+02	0.70579E+02	-0.23017E+00	-0.65165E+00
12	8.0844	0.68974E+02	0.70995E+02	-0.24203E-01	-0.57596E+00
13	8.8194	0.69156E+02	0.71412E+02	0.24881E+00	-0.47785E+00
14	9.5543	0.69341E+02	0.71812E+02	0.59824E+00	-0.35339E+00
15	10.2893	0.69526E+02	0.72172E+02	0.10331E+01	-0.19879E+00
16	11.0242	0.69707E+02	0.72463E+02	0.15613E+01	-0.10560E-01
17	11.7592	0.69879E+02	0.72650E+02	0.21895E+01	0.21440E+00
18	12.4941	0.70036E+02	0.72693E+02	0.29218E+01	0.47859E+00
19	13.2291	0.70172E+02	0.72541E+02	0.37591E+01	0.78366E+00
20	13.9640	0.70279E+02	0.72140E+02	0.46978E+01	0.11302E+01
21	14.6990	0.70347E+02	0.71429E+02	0.57287E+01	0.15172E+01
22	15.4339	0.70365E+02	0.70338E+02	0.68358E+01	0.19421E+01
23	16.1689	0.70324E+02	0.68795E+02	0.79943E+01	0.24000E+01
24	16.9038	0.70209E+02	0.66724E+02	0.91693E+01	0.28833E+01
25	17.6388	0.70008E+02	0.64046E+02	0.10314E+02	0.33815E+01
26	18.3737	0.69707E+02	0.60687E+02	0.11368E+02	0.38803E+01
27	19.1087	0.69292E+02	0.56578E+02	0.12255E+02	0.43615E+01
28	19.8436	0.68750E+02	0.51660E+02	0.12882E+02	0.48024E+01
29	20.5786	0.68066E+02	0.45893E+02	0.13139E+02	0.51753E+01
30	21.3135	0.67230E+02	0.39260E+02	0.12896E+02	0.54476E+01
31	22.0485	0.66232E+02	0.31777E+02	0.12003E+02	0.55810E+01
32	22.7834	0.65065E+02	0.23506E+02	0.10291E+02	0.55319E+01
33	23.5184	0.63725E+02	0.14560E+02	0.75748E+01	0.52514E+01
34	24.2533	0.62216E+02	0.51205E+01	0.36524E+01	0.46858E+01
35	24.9883	0.60545E+02	-0.45531E+01	-0.16884E+01	0.37774E+01
36	25.7232	0.58729E+02	-0.14106E+02	-0.86648E+01	0.24656E+01
37	26.4582	0.56792E+02	-0.23076E+02	-0.17492E+02	0.68836E+00
38	27.1931	0.54769E+02	-0.30878E+02	-0.28370E+02	-0.16152E+01
39	27.9281	0.52707E+02	-0.36793E+02	-0.41473E+02	-0.45025E+01
40	28.6630	0.50668E+02	-0.39953E+02	-0.56935E+02	-0.80236E+01
41	29.3980	0.48725E+02	-0.39337E+02	-0.74823E+02	-0.12217E+02

*** HORIZONTAL DISPLACEMENT ***

POINT	COORD	W
1	0.0	0.0
2	0.7349	-0.94692E-07
3	1.4699	-0.18993E-06
4	2.2048	-0.28696E-06
5	2.9398	-0.38591E-06
6	3.6747	-0.48690E-06
7	4.4097	-0.58998E-06
8	5.1446	-0.69513E-06
9	5.8796	-0.80222E-06
10	6.6145	-0.91102E-06
11	7.3495	-0.10211E-05
12	8.0844	-0.11319E-05
13	8.8194	-0.12427E-05
14	9.5543	-0.13523E-05
15	10.2893	-0.14593E-05
16	11.0242	-0.15622E-05
17	11.7592	-0.16589E-05
18	12.4941	-0.17469E-05
19	13.2291	-0.18235E-05
20	13.9640	-0.18853E-05
21	14.6990	-0.19289E-05
22	15.4339	-0.19502E-05
23	16.1689	-0.19451E-05
24	16.9038	-0.19090E-05
25	17.6388	-0.18374E-05
26	18.3737	-0.17261E-05
27	19.1087	-0.15709E-05
28	19.8436	-0.13685E-05
29	20.5786	-0.11165E-05
30	21.3135	-0.81400E-06
31	22.0485	-0.46187E-06
32	22.7834	-0.63604E-07
33	23.5184	0.37418E-06
34	24.2533	0.84104E-06
35	24.9883	0.13219E-05
36	25.7232	0.17962E-05
37	26.4582	0.22373E-05
38	27.1931	0.26112E-05
39	27.9281	0.28763E-05
40	28.6630	0.29823E-05
41	29.3980	0.28700E-05

INDIVIDUAL END FORCES FOR SEGMENT

6

0.65929E+01 0.20768E+02 -0.30336E+01 -0.60010E+01
 -0.31738E+02 0.0

*** OUTPUT FOR CYLINDRICAL SEGMENT 6 ***

POINT	COORD	N1	N2	M1	M2
1	0.0	0.31738E+02	-0.34153E+02	-0.20768E+02	-0.31153E+01
2	0.3178	0.31738E+02	-0.29729E+02	-0.18745E+02	-0.28117E+01
3	0.6356	0.31738E+02	-0.25297E+02	-0.16859E+02	-0.25289E+01
4	0.9534	0.31738E+02	-0.20861E+02	-0.15106E+02	-0.22659E+01
5	1.2712	0.31738E+02	-0.16419E+02	-0.13479E+02	-0.20218E+01
6	1.5890	0.31738E+02	-0.11972E+02	-0.11971E+02	-0.17956E+01
7	1.9068	0.31738E+02	-0.75213E+01	-0.10576E+02	-0.15864E+01
8	2.2246	0.31738E+02	-0.30670E+01	-0.92879E+01	-0.13932E+01
9	2.5424	0.31738E+02	0.13905E+01	-0.81003E+01	-0.12150E+01
10	2.8602	0.31738E+02	0.58507E+01	-0.70068E+01	-0.10510E+01
11	3.1780	0.31738E+02	0.10313E+02	-0.60010E+01	-0.90015E+00

*** HORIZONTAL DISPLACEMENT ***

POINT	COORD	W
1	0.0	0.67765E-06
2	0.3178	0.60060E-06
3	0.6356	0.52343E-06
4	0.9534	0.44617E-06
5	1.2712	0.36882E-06
6	1.5890	0.29138E-06
7	1.9068	0.21388E-06
8	2.2246	0.13631E-06
9	2.5424	0.58688E-07
10	2.8602	-0.18983E-07
11	3.1780	-0.96696E-07

INDIVIDUAL END FORCES FOR SEGMENT 9
 0.0 0.0 -0.15201E+01 -0.46002E+02
 0.0 -0.10333E+02

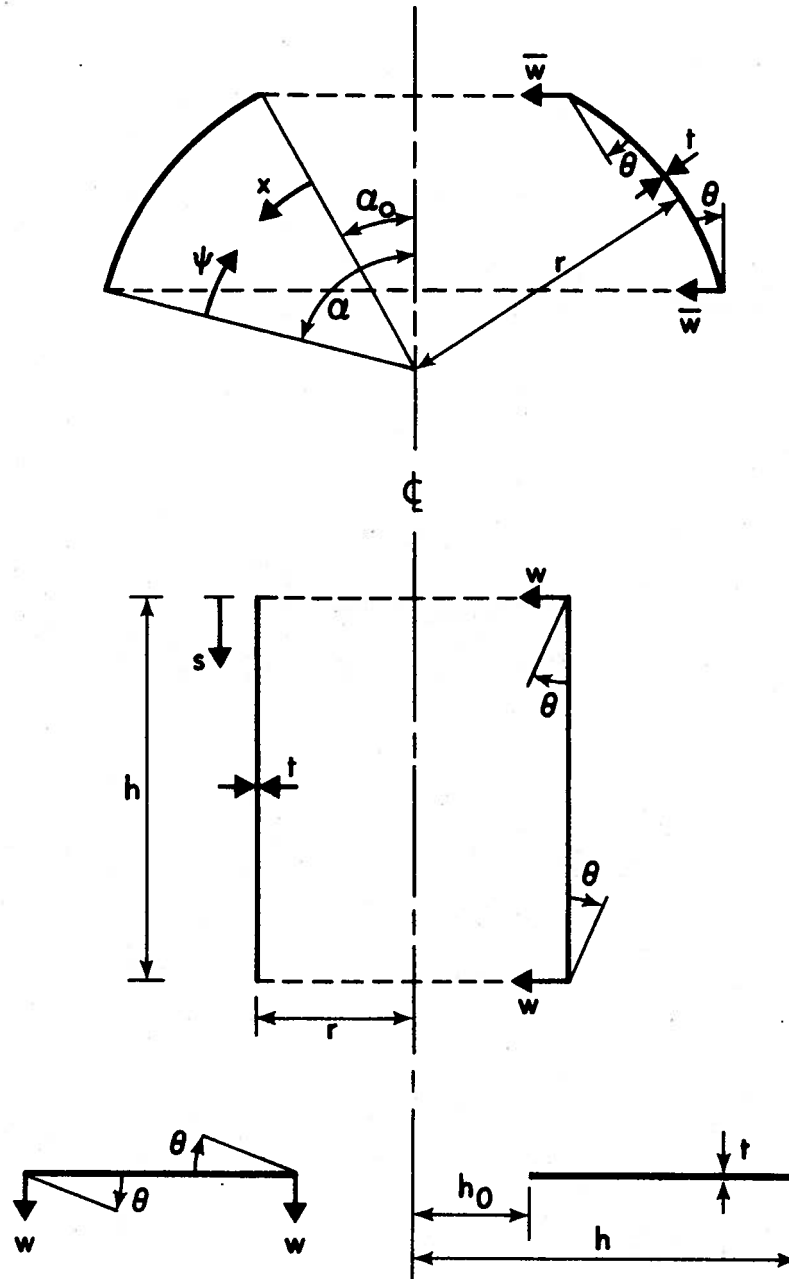
*** OUTPUT FOR BASE ELEMENT 9 ***

POINT	COORD	M1	M2	V
1	77.7500	-0.35527E-14	-0.17103E+02	0.17764E-14
2	76.9500	0.62555E+00	-0.17216E+02	0.11109E+01
3	76.1500	0.21466E+01	-0.17211E+02	0.22046E+01
4	75.3500	0.45579E+01	-0.17097E+02	0.32811E+01
5	74.5500	0.78547E+01	-0.16887E+02	0.43406E+01
6	73.7500	0.12032E+02	-0.16590E+02	0.53829E+01
7	72.9500	0.17087E+02	-0.16220E+02	0.64081E+01
8	72.1500	0.23015E+02	-0.15787E+02	0.74160E+01
9	71.3500	0.29812E+02	-0.15305E+02	0.84064E+01
10	70.5500	0.37476E+02	-0.14786E+02	0.93789E+01
11	69.7500	0.46002E+02	-0.14244E+02	0.10333E+02

*** VERTICAL DISPLACEMENT ***

POINT	COORD	W
1	77.7500	-0.31084E-05
2	76.9500	-0.30283E-05
3	76.1500	-0.29480E-05
4	75.3500	-0.28674E-05
5	74.5500	-0.27865E-05
6	73.7500	-0.27051E-05
7	72.9500	-0.26230E-05
8	72.1500	-0.25400E-05
9	71.3500	-0.24557E-05
10	70.5500	-0.23699E-05
11	69.7500	-0.22822E-05

APPENDIX D
FORMULAE FOR HOMOGENEOUS
AND PARTICULAR SOLUTIONS



E = MODULUS OF ELASTICITY

ν = POISSONS RATIO

α_t = THERMAL COEFFICIENT

$$\lambda = \sqrt[4]{3(1-\nu^2)\left(\frac{r}{t}\right)^2}$$

FIGURE D.1 Notation for Spherical, Cylindrical and Base Segments

TABLE D1: LABELING OF HOMOGENEOUS AND PARTICULAR SOLUTION EQUATIONS

(a) Homogeneous Solutions

General Form: $XH\ell.j$

XH	Interpretation
SH	Spherical segment homogeneous solution
CH	Cylindrical segment homogeneous solution
PH	Plate segment homogeneous solution
SS	Special homogeneous solutions

ℓ	Loading
1	Unit horizontal force at top of segment
2	Unit moment at top of segment
3	Unit horizontal force at bottom of segment
4	Unit moment at bottom of segment
5	Unit vertical force at top of segment

j	Effect
1	Horizontal displacement
2	Meridional rotation
3	N1 stress resultant
4	N2 stress resultant
5	M1 stress resultant
6	M2 stress resultant

TABLE D1 (continued)

(b) Particular Solutions

General Form: $XP_{\ell}.j$

XP	Interpretation
SP	Spherical segment particular solution
CP	Cylindrical segment particular solution
PP	Plate segment particular solution

ℓ	Loading
1	Pressure (1 psf)
2	Dead weight (1b/ft ³)
3	Prestress (1 psf)
4	Uniform thermal strain (+1°)
5	Gradient thermal strain (+1°/ft)

Interpretation of j is precisely as in (a)

TABLE D2 - SPHERICAL SEGMENT HOMOGENEOUS SOLUTIONS

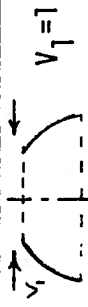

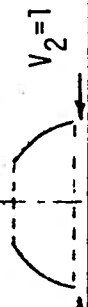

		Eq. No.			Eq. No.
$\bar{w}(x)$	$2r\lambda \sin^2\alpha_0 \cdot e^{-\lambda x} \cdot \cos \lambda x/Et$	SH1.1	$\bar{w}(x)$	$-2\sin \alpha_0 \lambda^2 e^{-\lambda x} (\cos \lambda x - \sin \lambda x)/Et$	SH2.1
$\theta(x)$	$-6r^2(1-\nu^2) \sin \alpha_0 \cdot e^{-\lambda x} (\cos \lambda x + \sin \lambda x)/Et^3 \lambda^2$	SH1.2	$\theta(x)$	$12r(1-\nu^2) e^{-\lambda x} \cos \lambda x/Et^3 \lambda$	SH2.2
N_1	$[\cos \lambda x - \sin \lambda x] e^{-\lambda x} \sin \alpha_0 \operatorname{ctg}(\alpha_0+x)$	SH1.3	N_1	$2\lambda e^{-\lambda x} \sin \lambda x \operatorname{ctg}(\alpha_0+x)/r$	SH2.3
N_2	$-2\lambda e^{-\lambda x} \sin \alpha_0 \cos \lambda x$	SH1.4	N_2	$2\lambda^2 e^{-\lambda x} [\cos \lambda x - \sin \lambda x]/r$	SH2.4
M_1	$re^{-\lambda x} \sin \alpha_0 \sin(\lambda x)/\lambda$	SH1.5	M_1	$-e^{-\lambda x} [\cos \lambda x + \sin \lambda x]$	SH2.5
M_2	$-re^{-\lambda x} \sin \alpha_0 \cos(\alpha_0+x) [\cos \lambda x + \sin \lambda x] / (2\sin(\alpha_0+x) \lambda^2) + \nu M_1$	SH1.6	M_2	$+e^{-\lambda x} \cos \lambda x \operatorname{ctg}(\alpha_0+x)/\lambda - \nu M_1$	SH2.6
		Eq. No.			Eq. No.
$\bar{w}(\psi)$	$2r\lambda \sin^2\alpha_0 \cdot e^{-\lambda\psi} \cdot \cos \lambda\psi/Et$	SH3.1	$\bar{w}(\psi)$	$2\sin \alpha_0 \lambda^2 e^{-\lambda\psi} (\cos \lambda\psi - \sin \lambda\psi)/Et$	SH4.1
$\theta(\psi)$	$6r^2(1-\nu^2) \sin \alpha_0 \cdot e^{-\lambda\psi} (\cos \lambda\psi + \sin \lambda\psi)/Et^3 \lambda^2$	SH3.2	$\theta(\psi)$	$12r(1-\nu^2) e^{-\lambda\psi} \cos \lambda\psi/Et^3 \lambda$	SH4.2
N_1	$e^{-\lambda\psi} \sqrt{2} \sin \alpha_0 \sin(\lambda\psi - \frac{\pi}{4}) \operatorname{ctg}(\alpha_0-\psi)$	SH3.3	N_1	$2 e^{-\lambda\psi} \sin \lambda\psi \operatorname{ctg}(\alpha_0-\psi)/r$	SH4.3
N_2	$e^{-\lambda\psi} 2\lambda \sin \alpha_0 \sin(\lambda\psi - \frac{\pi}{2})$	SH3.4	N_2	$2 \sqrt{2} \cdot \lambda^2 \cdot e^{-\lambda\psi} \sin(\lambda\psi - \frac{\pi}{4})/r$	SH4.4
M_1	$re^{-\lambda\psi} \sin \alpha_0 \sin \lambda\psi/\lambda$	SH3.5	M_1	$\sqrt{2} e^{-\lambda\psi} \sin(\lambda\psi + \frac{\pi}{4})$	SH4.5
M_2	$\sin \alpha_0 \cos(\alpha_0+x) re^{-\lambda\psi} [\cos \lambda\psi + \sin \lambda\psi] / (2\sin(\alpha_0+x) \lambda^2) + \nu M_1$	SH3.6	M_2	$\operatorname{ctg}(\alpha_0+x) e^{-\lambda\psi} \cos(\lambda\psi)/\lambda + \nu M_1$	SH4.6

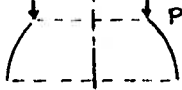
TABLE D3 - SPHERICAL SEGMENT PARTICULAR SOLUTIONS

Eq. No.	Pressure	Eq. No.	Deflect	Dead Load	Eq. No.
			$\bar{w}(x)$		
SP1.1	$pr^2 \sin(\alpha_0+x)[1-\nu+(1+\nu) \sin^2 \alpha_0 / \sin^2(\alpha_0+x)]/2Et$	SP1.1	$\bar{w}(x)$	$-pr^2 \sin(\alpha_0+x)[(1+\nu)(\cos \alpha_0 - \cos(\alpha_0+x)) / \sin^2(\alpha_0+x) - \cos(\alpha_0+x)]/Et$	SP2.1
	0	SP1.2a	$\theta(\alpha_0)$	$-pr(2+\nu) \sin \alpha_0 / Et$	SP2.2a
	0	SP1.2b	$\theta(\alpha)$	$-pr(2+\nu) \sin \alpha / Et$	SP2.2b
N_1	$-pr[1 - \sin^2 \alpha_0 / \sin^2(\alpha_0+x)]/2$	SP1.3	N_1	$-pr[\cos \alpha_0 - \cos(\alpha_0+x)] / \sin^2(\alpha_0+x)$	SP2.3
N_2	$-pr[1 + \sin^2 \alpha_0 / \sin^2(\alpha_0+x)]/2$	SP1.4	N_2	$pr[(\cos \alpha_0 - \cos(\alpha_0+x)) / \sin^2(\alpha_0+x) - \cos(\alpha_0+x)]$	SP2.4
M_1	0	SP1.5	M_1	0	SP2.5
M_2	0	SP1.6	M_2	0	SP2.6
			$\bar{w}(x)$		
	Constant Temperature Change C	Eq. No.	$\bar{w}(x)$	Temperature Gradient ΔC	Eq. No.
SP4.1	$-\alpha_t r \sin(\alpha_0+x) c$	SP4.1	\bar{w}	0	SP5.1
	0	SP4.2a	$\theta(0)$	0	SP5.2a
	0	SP4.2b	$\theta(\alpha)$	0	SP5.2b
N_1	0	SP4.3	N_1	0	SP5.3
N_2	0	SP4.4	N_2	0	SP5.4
M_1	0	SP4.5	M_1	$\Delta C \alpha_t Et^2 / 12(1-\nu)$	SP5.5
M_2	0	SP4.6	M_2	$\Delta C \alpha_t Et^2 / 12(1-\nu)$	SP5.6


TABLE D4 - CYLINDRICAL SEGMENT PARTICULAR SOLUTIONS

Effect	Pressure	Eq. No.	Effect	Dead Load	Eq. No.
w	pr^2/Et	CP1.1	w	$-pvr_s/Et$	CP2.1
θ	0	CP1.2	θ	$-pvr/Et$	CP2.2
N_1	0	CP1.3	N_1	$-ps$	CP2.3
N_2	$-pr$	CP1.4	N_2	0	CP2.4
M_1	0	CP1.5	M_1	0	CP2.5
M_2	0	CP1.6	M_2	0	CP2.6
Effect	Constant Temperature Change C	Eq. No.	Effect	Temperature Gradient ΔC	Eq. No.
w	$-\alpha_T C$	CP4.1	w	0	CP5.1
θ	0	CP4.2	θ	0	CP5.2
N_1	0	CP4.3	N_1	0	CP5.3
N_2	0	CP4.4	N_2	0	CP5.4
M_1	0	CP4.5	M_1	$\alpha_T \Delta C Et^2/12(1-\nu)$	CP5.5
M_2	0	CP4.6	M_2	$\alpha_T \Delta C Et^2/12(1-\nu)$	CP5.6

TABLE D5 - SPECIAL HOMOGENEOUS SOLUTIONS

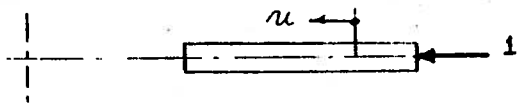
Effect	 P=1	Eq. No.
$\bar{w}(x)$	$-r[(1+\nu) \sin \alpha_0 / \sin \alpha - 2 \sin \alpha_0 \cos \alpha_0 \lambda e^{-\lambda x} \cos \lambda x] / Et$	SS2.1
$\theta(x)$	$-\cos \alpha_0 r^2 6(1-\nu^2) \cdot e^{-\lambda x} (\cos \lambda x + \sin \lambda x) / Et^3 \lambda^2$	SS2.2
N_1	$-\sin \alpha_0 / \sin^2(\alpha_0 + x) + \cos \alpha_0 e^{-\lambda x} [\cos \lambda x - \sin \lambda x] \operatorname{ctg}(\alpha_0 + x)$	SS2.3
N_2	$-2 \cos \alpha_0 \lambda e^{-\lambda x} \cos(\lambda x) + \sin \alpha_0 / \sin(\alpha_0 + x)$	SS2.4
M_1	$+\cos \alpha_0 r e^{-\lambda x} \sin \lambda x / \lambda$	SS2.5
M_2	$\cos \alpha_0 \cos(\alpha_0 + x) r e^{-\lambda x} [\cos \lambda x + \sin \lambda x] / 2 \lambda^2 \sin(\alpha_0 + x)$ $-\nu M_1$	SS2.5

(a) Effect of Top Vertical Load on Open Spherical Segment

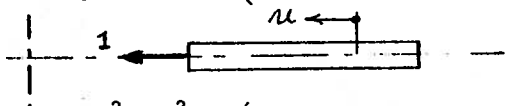
Effect	 P=1	Eq. No.
w	$-\nu \cdot r / Et$	SS1.1
θ	0	SS1.2
N_1	1	SS1.3
N_2	0	SS1.4
M_1	0	SS1.5
M_2	0	SS1.6

(b) Effect of Top Vertical Load on Cylindrical Segment

TABLE D6: PLATE ON ELASTIC FOUNDATION FORMULAE

(a) 

$$u(r) = \frac{r_o^2 r_i^2}{t(r_o^2 - r_i^2)} \left\{ \left(\frac{1 - \nu}{E} \right) \frac{r}{r_i^2} + \left(\frac{1 + \nu}{E} \right) \frac{1}{r} \right\} \quad \text{PH1.1}$$

(b) 

$$u(r) = \frac{r_o^2 r_i^2}{t(r_o^2 - r_i^2)} \left\{ \left(\frac{1 - \nu}{E} \right) \frac{r}{r_o^2} + \left(\frac{1 + \nu}{E} \right) \frac{1}{r} \right\} \quad \text{PH2.1}$$

(c) Particular Solution Displacements

$\ell =$	1,3	2	4 Const. Temp Change	5 Gradient $\Delta c(^{\circ}/\text{FT})$	
w	$\frac{p}{k}$	$\frac{\gamma t}{k}$.	.	PP ℓ .1
u	.	.	$\alpha_T r \Delta T$.	PP ℓ .1a
θ	PP ℓ .2
N_1	PP ℓ .3
N_2	PP ℓ .4
M_1	.	.	.	$\alpha_T E t^2 / 12(1 - \nu^2)$	PP ℓ .5
M_2	.	.	.	$\alpha_T E t^2 / 12(1 - \nu^2)$	PP ℓ .6

APPENDIX E

DERIVATION OF SHORT CYLINDER B MATRIX

APPENDIX E

Derivation of Short Cylinder B Matrix

The basic equations for a short cylindrical shell segment have been presented in Sect. 3.2. The displacement equation of equilibrium, Eq. 3.2.1, has the general solution displayed in Eq. 3.2.4, which can be written in vector form as indicated in Eqs. 3.2.7. To evaluate the segment flexibility matrix as defined from Eq. 3.2.11 it is necessary to invert the matrix of Eq. 3.2.10 in order to determine the [B] matrix of Eq. 3.2.11. This inversion has been carried out in closed form and the resulting [B] matrix incorporated into the coding of FLEXSHELL. The purpose of this Appendix is to provide details of this procedure.

The vector $\{\phi\}$ of Eq. 3.2.7b and expressions for $\{\phi\}'$, $\{\phi\}''$ and $\{\phi\}'''$ are given in Table E.1. Evaluating these expressions as indicated, Eq. 3.2.8 may be written as

$$\begin{Bmatrix} V_1 \\ M_1 \\ V_2 \\ M_2 \end{Bmatrix} = 2D\beta^2 \begin{bmatrix} -\beta & \beta & \beta & \beta \\ 0 & -1 & 0 & 1 \\ \beta\gamma_2 & -\beta\gamma_1 & -\beta\gamma_4 & -\beta\gamma_3 \\ -\phi_2 & \phi_1 & \phi_4 & -\phi_3 \end{bmatrix} \begin{Bmatrix} C_1 \\ C_2 \\ C_3 \\ C_4 \end{Bmatrix} \quad (\text{E.1})$$

where, in this equation and the remainder of this Appendix, it is understood that the notation ϕ_i implies the $\phi_i(y)$ functions of Table E.1 evaluated at $y=l$. With this notation the symbols γ_i appearing in Eq. E.1 are defined as

$$\gamma_1 = \phi_1 - \phi_2 \quad (\text{E.2a})$$

$$\gamma_2 = \phi_1 + \phi_2 \quad (\text{E.2b})$$

$$\gamma_3 = \phi_3 + \phi_4 \quad (\text{E.2c})$$

$$\gamma_4 = \phi_3 - \phi_4 \quad (\text{E.2d})$$

The factor β is defined in Eq. 3.2.3.

Factoring the β 's, Eq. E.1 may be written as

$$\{V^*\} = [E]\{C\} \quad (\text{E.3a})$$

where $\{C\}$ is the vector of constants, of Eq. 3.2.7c,

$$\langle V^* \rangle = \frac{1}{2D\beta^2} \langle V_1/\beta, M_1, V_2/\beta, M_2 \rangle \quad (\text{E.3b})$$

and

$$[E] = \begin{bmatrix} -1 & 1 & 1 & 1 \\ 0 & -1 & 0 & 1 \\ \gamma_2 & -\gamma_1 & -\gamma_4 & -\gamma_3 \\ -\phi_2 & \phi_1 & \phi_4 & -\phi_3 \end{bmatrix} \quad (\text{E.3c})$$

Inverting the $[E]$ matrix yields

$$c E_{11}^{-1} = \gamma_4 (\phi_1 - \phi_3) - \phi_4 (\gamma_1 + \gamma_3) = \xi B_{11}/\beta \quad (\text{E.4a})$$

$$c E_{21}^{-1} = \gamma_4 \phi_2 - \gamma_2 \phi_4 = \xi B_{21}/\beta \quad (\text{E.4b})$$

$$c E_{31}^{-1} = \gamma_2 (\phi_1 - \phi_3) - \phi_2 (\gamma_1 + \gamma_3) = \xi B_{31}/\beta \quad (E.4c)$$

$$c E_{41}^{-1} = \gamma_4 \phi_2 - \gamma_2 \phi_4 = \xi B_{41}/\beta \quad (E.4d)$$

$$c E_{12}^{-1} = \phi_4 (\gamma_1 - \gamma_3) + \phi_3 (\gamma_1 - \gamma_4) + \phi_1 (\gamma_3 - \gamma_4) = \xi B_{12} \quad (E.4e)$$

$$c E_{22}^{-1} = \phi_4 (\gamma_2 - \gamma_3) + \phi_3 (\gamma_2 - \gamma_4) + \phi_2 (\gamma_3 - \gamma_4) = \xi B_{22} \quad (E.4f)$$

$$c E_{32}^{-1} = \phi_1 (\gamma_3 - \gamma_2) + \phi_3 (\gamma_1 - \gamma_2) + \phi_2 (\gamma_1 - \gamma_3) = \xi B_{32} \quad (E.4g)$$

$$c E_{42}^{-1} = \phi_4 (\gamma_1 - \gamma_2) + \phi_1 (\gamma_2 - \gamma_4) + \phi_2 (\gamma_4 - \gamma_1) = \xi B_{42} \quad (E.4h)$$

$$c E_{13}^{-1} = \phi_1 - \phi_3 - 2\phi_4 = \xi B_{13}/\beta \quad (E.4i)$$

$$c E_{23}^{-1} = \phi_2 - \phi_4 = \xi B_{23}/\beta \quad (E.4j)$$

$$c E_{33}^{-1} = \phi_1 - \phi_3 - 2\phi_2 = \xi B_{33}/\beta \quad (E.4k)$$

$$c E_{43}^{-1} = \phi_2 - \phi_4 = \xi B_{43}/\beta \quad (E.4l)$$

$$c E_{14}^{-1} = \gamma_1 + \gamma_3 - 2\gamma_4 = \xi B_{14} \quad (E.4m)$$

$$c E_{24}^{-1} = \gamma_2 - \gamma_4 = \xi B_{24} \quad (E.4n)$$

$$c E_{34}^{-1} = \gamma_1 + \gamma_3 - 2\gamma_2 = \xi B_{34} \quad (E.4o)$$

$$c E_{44}^{-1} = \gamma_2 - \gamma_4 = \xi B_{44} \quad (E.4p)$$

where

$$c = \gamma_1 (\phi_4 - \phi_2) + \gamma_2 (\phi_1 + \phi_3 - 2\phi_4) + \gamma_3 (\phi_2 + \phi_4) - \gamma_4 (\phi_1 + 2\phi_2 + \phi_3) \quad (E.4q)$$

and

$$\xi = \frac{c}{2D\beta^2} \quad (E.4r)$$

Eqs. E.4 define the elements of the [B] matrix of Eq. 3.2.11, which permits the numerical evaluation of the short cylindrical shell flexibility matrix of Eq. 3.2.12.

$\{\phi\}$	$\{\phi\}'$	$\{\phi\}''$	$\{\phi\}'''$
$e^{\beta y} \cos \beta y$	$\beta e^{\beta y} (\cos \beta y - \sin \beta y)$	$-2\beta^2 e^{\beta y} \sin \beta y$	$-2\beta^3 e^{\beta y} (\sin \beta y + \cos \beta y)$
$e^{\beta y} \sin \beta y$	$\beta e^{\beta y} (\sin \beta y + \cos \beta y)$	$2\beta^2 e^{\beta y} \cos \beta y$	$2\beta^3 e^{\beta y} (\cos \beta y - \sin \beta y)$
$e^{-\beta y} \cos \beta y$	$-\beta e^{-\beta y} (\cos \beta y + \sin \beta y)$	$2\beta^2 e^{-\beta y} \sin \beta y$	$2\beta^3 e^{-\beta y} (\cos \beta y - \sin \beta y)$
$e^{-\beta y} \sin \beta y$	$-\beta e^{-\beta y} (\sin \beta y - \cos \beta y)$	$-2\beta^2 e^{-\beta y} \cos \beta y$	$2\beta^3 e^{-\beta y} (\cos \beta y + \sin \beta y)$

TABLE E.1 - Functions for Short Cylinder Displacements

APPENDIX F
SPHERICAL SHELL M_2 STRESS RESULTANT

APPENDIX F

Spherical Shell M_2 Stress Resultant

Pflüger [10, pg. 63] gives an 'exact' expression for the meridional curvature of an arbitrary shell of revolution as

$$\chi = (\epsilon_\phi - \epsilon_\theta) \cot\phi - \frac{r_\theta}{r_\phi} \frac{d\epsilon_\theta}{d\epsilon_\phi} \quad (\text{F.1})$$

where ϕ is the meridional (angular) coordinate and θ is the circumferential (angular) coordinate. In order to formulate the governing equation of a shell it is necessary to differentiate this curvature. For a cylinder, $\cot\phi = 0$, the first term of Eq. F.1 drops out, and the derivatives of Eq. F.1 take on a simple form for which the relation $M_2 = \nu M_1$ is valid. This is also true at the edge of a hemispherical shell where $\phi = 90^\circ$. However, the first term of Eq. F.1 cannot, in general, be discarded for a spherical shell.

The results for 'long' non-cylindrical shells of revolution show a remarkable similarity to the results obtained for a 'long' cylinder. Boundary disturbance vanish rapidly in the form of damped oscillations. In differentiation of damped oscillations with large damping factors, the magnitude of the derivative is always larger by this factor than the oscillation itself. Therefore, it is a good approximation to consider only the terms involving the highest derivative when formulating the governing equations. This method is normally referred to as 'Geckler's approximation'.

A visual interpretation of this method is given by Pflüger [10, pg. 65]. The rotation of the meridional tangent of the real shell is approximated by the corresponding rotation of the tangent of a 'substitute cylinder' which has a radius equal to the radius of curvature of the real shell. In this approximation $M_2 = \nu M_1$, for the substitute cylinder. The usefulness of the method becomes questionable, however, when the central angle ϕ reduces below about 30° . The term $(\epsilon_\phi - \epsilon_\theta) \cot\phi$ in Eq. F.1 can then no longer be neglected. In this case the term can be reintroduced into the expression for evaluating the stress resultant arising from Eq. F.1, to yield [10, p. 66].

$$M_2 = D \cot\phi e^{-\lambda x} (C_1 \cos \lambda x + C_2 \sin \lambda x)/r - \nu M_1 \quad (\text{F.2})$$

This, however, is still not 'exact' because the curvature, from which M_2 is evaluated through Eq. F.2, has been determined from a solution to the simplified Geckler equation.

Eq. F.2 forms the basis for the computation of the M_2 stress resultants for spherical segments as tabulated in Appendix D.

APPENDIX G
ASYMPTOTIC APPROXIMATION FOR BASE SEGMENT

APPENDIX G

Asymptotic Approximation For Base Segment

It was pointed out in Sect. 3.4 that the shape functions $\langle \phi \rangle$ employed in Eq. 3.4.4b are asymptotic approximations of the Thomson functions which exactly satisfy the governing differential equation. They are, therefore, valid only for 'large' values of the argument σ defined in Eq. 3.4.3a. This usually does not present a problem since the stresses in the base slab near the central axis are not of significant interest and the connection to the cylinder wall usually occurs at reasonably large values of the argument.

A numerical comparison of the asymptotic approximations and the exact functions indicates that good accuracy is obtained whenever the argument $x = r/\ell \geq 2$. (ℓ is defined by Eq. 3.4.3b).

FLEXSHELL checks the value of the argument x against this value and computes a (hypothetical) inner radius for the base segment below which output of values for base displacements and stress resultants is deleted. The radius r , the thickness of the slab t , and the subgrade modulus k are limited by the lower bound on the value of x as follows:

$$r \geq 2 \sqrt[4]{Et^3/12(1 - \nu^2)k} \quad (G.1)$$

$$k \geq 4 Et^3/(3(1 - \nu^2)r^4) \quad (G.2)$$

$$t \leq \sqrt[3]{12 r k (1 - \nu)/16E} \quad (G.3)$$

In the case of a very thick base element the radii used to define the problem should be checked manually with Eq. G.1 to make sure that at least the outer radius in the input data stays within the program computed limit for FLEXSHELL output.